

AD-A115 184

LOCKHEED-CALIFORNIA CO BURBANK

F/G 11/4

ADVANCED RESIDUAL STRENGTH DEGRADATION RATE MODELING FOR ADVANC--ETC(U)

JUL 81 K N LAURAITIS, J T RYDER, D E PETTIT

F33615-77-C-3084

LR-28360-19

AFWAL-TR-79-3095-VOL-2

NL

UNCLASSIFIED

1 of 4
23 A
118184



A

5184

1.0

2.8 2.5

2.2

1.1

2.0

1.8

1.25

1.4

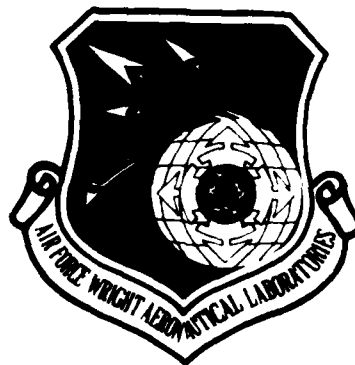
1.6

Microcopy Resolution Test Chart
ANSI #1

2

AFWAL-TR-79-3095
VOLUME II

ADVANCED RESIDUAL STRENGTH DEGRADATION RATE
MODELING FOR ADVANCED COMPOSITE STRUCTURES
VOLUME II - TASKS II AND III



K. N. Lauraitis
J. T. Ryder
D. E. Pettit

Lockheed-California Company
Burbank, California

July 1981
Final Report for 1 July 1979 to 29 May 1981

DTIC
JUN 7 1982
H

Approved for public release; distribution unlimited

DTIC FILE COPY

FLIGHT DYNAMICS LABORATORY
AIR FORCE WRIGHT AERONAUTICAL LABORATORIES
AIR FORCE SYSTEMS COMMAND
WRIGHT-PATTERSON AIR FORCE BASE, OHIO 45433

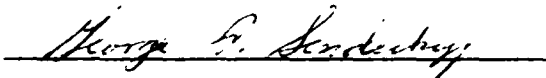
82 06 07 021


NOTICE

When Government drawings, specifications, or other data are used for any purpose other than in connection with a definitely related Government procurement operation, the United States Government thereby incurs no responsibility nor any obligation whatsoever; and the fact that the government may have formulated, furnished, or in any way supplied the said drawings, specifications, or other data, is not to be regarded by implication or otherwise as in any manner licensing the holder or any other person or corporation, or conveying any rights or permission to manufacture use, or sell any patented invention that may in any way be related thereto.

This report has been reviewed by the Office of Public Affairs (ASD/PA) and is releasable to the National Technical Information Service (NTIS). At NTIS, it will be available to the general public, including foreign nations.

This technical report has been reviewed and is approved for publication.


GEORGE P. SENDECKYJ, Aerospace Engineer
Fatigue, Fracture & Reliability Group


DAVEY L. SMITH, Chief
Structural Integrity Branch

FOR THE COMMANDER



"If your address has changed, if you wish to be removed from our mailing list, or if the addressee is no longer employed by your organization please notify AFWAL/FIBEC W-PAFB, OH 45433 to help us maintain a current mailing list".

Copies of this report should not be returned unless return is required by security considerations, contractual obligations, or notice on a specific document.

SECURITY CLASSIFICATION OF THIS PAGE (When Data Entered)

REPORT DOCUMENTATION PAGE		READ INSTRUCTIONS BEFORE COMPLETING FORM
1. REPORT NUMBER AFWAL-TR-79-3095 Volume II	2. GOVT ACCESSION NO. AD-A115184	3. RECIPIENT'S CATALOG NUMBER
4. TITLE (and Subtitle) Advanced Residual Strength Degradation Rate Modeling for Advanced Composite Structures Vol II - Task II and III	5. TYPE OF REPORT & PERIOD COVERED Final Report 1 July 1979 to 29 May 1981	
7. AUTHOR(s) K. N. Lauraitis J. T. Ryder D. E. Pettit	6. PERFORMING ORG. REPORT NUMBER LR 28360-19	
9. PERFORMING ORGANIZATION NAME AND ADDRESS Lockheed-California Company Division of Lockheed Aircraft Corporation Burbank, California 91520	8. CONTRACT OR GRANT NUMBER(s) F33615-77-C-3084	
11. CONTROLLING OFFICE NAME AND ADDRESS Flight Dynamics Laboratory Air Force Wright Aeronautics Laboratory, Air Force Systems Command, Wright-Patterson AFB, Ohio, 45433	10. PROGRAM ELEMENT, PROJECT, TASK AREA & WORK UNIT NUMBERS Project No. 2401 Work Unit 24010117	
14. MONITORING AGENCY NAME & ADDRESS (if different from Controlling Office)	12. REPORT DATE July 1981	
	13. NUMBER OF PAGES	
	15. SECURITY CLASS. (of this report) Unclassified	
	15a. DECLASSIFICATION/DOWNGRADING SCHEDULE	
16. DISTRIBUTION STATEMENT (of this Report) Approved for public release: distribution unlimited		
17. DISTRIBUTION STATEMENT (of the abstract entered in Block 20, if different from Report)		
18. SUPPLEMENTARY NOTES		
19. KEY WORDS (Continue on reverse side if necessary and identify by block number) composites, graphite/epoxy, impact damage, damaged holes, fatigue, damage propagation, residual strength, NDI		
20. ABSTRACT (Continue on reverse side if necessary and identify by block number) This report presents the results of the last two tasks of a three task program focusing on the study of relationship between damage propagation and residual strength of graphite/epoxy laminates. Specimens of two laminate types, a 32- ply quasi-isotropic and 24-ply 67%-0, containing a centered poorly drilled hole were evaluated in this study. Baseline static tension and compression tests were conducted at high and low strain rates and at elevated temperature. Com- pression tests were conducted for two restraint conditions, the full platen fatigue supports with 2.15 in. (55mm) window and 4-bar buckling supports.		

DD FORM 1 JAN 73 1473

EDITION OF 1 NOV 65 IS OBSOLETE

Continued on next page

SECURITY CLASSIFICATION OF THIS PAGE (When Data Entered)

DTIC
SELECTED
JUN 7 1982
H

Stress vs. life (S-N) fatigue data were generated at a stress ratio of $R = -1$ for each of the damaged laminates. Twenty replicate specimens for each laminate were fatigue tested to failure at a single stress level ($R = -1$) with the damage growth for each specimen monitored a minimum of ten times during its life to determine the fatigue life and damage growth distributions and pertinent statistical parameters. Based on these results, five cycle levels were selected for the residual strength study. Twenty-three specimens of each laminate were inspected, cycled to one of the five preselected N values and Holscaned again. Three of the replicates were destructively analyzed while the other surviving specimens were tested in static tension or compression. This sequence was repeated for each of the five N values.

Results indicated significant reduction in initial static tension and compression strengths due to the damaged hole condition and a further decrease in strength at the higher loading rate with a larger drop in compression than in tension. Fatigue cycling of the 24-ply specimens at ± 35 ksi (241 MPa) ($R = -1$) produced data which were dispersed over more than two orders of magnitude while data scatter was slightly more than one order of magnitude for the 32-ply coupons tested at a stress level of ± 22 ksi (152 MPa). As expected from the life data, damage growth for the 32-ply specimens was more well-behaved than for the 24-ply. However, large scatter in damage size was evident for both laminates and so no useful relationship between damage size and life could be established. Residual static properties of either laminate were not adversely affected by $R = -1$ fatigue cycling up to the 80% probability of survival life. Slight but insignificant increases (6-11%) in tensile residual strength and similar decreases in compression were noted for the 32-ply laminate. Both tension and compression residual strength tended to increase slightly as the number of cycles completed increased for the 24-ply laminate. Residual strength could not be related to damage size, not only due to the data dispersion but also because no definitive change in residual strength was observed.

A limited test program was conducted to assess the effect of different fatigue and environmental test conditions on residual strength and damage growth. The variables evaluated were: A) Specimen restraint (4-bar support); B) stress ratio, $R = -0.3$; and C) elevated temperature, 180°F (82°C). The Case A loading produced lives which were within the scatter band of tests conducted with the platen supports and very similar damage growth and residual strength behavior. Under the $R = -0.3$ loading both laminates completed 2 million cycles without failure. Most notable was the change in damage development, especially for the 24-ply laminate for which essentially no growth in the width direction was evident with extensive growth in the length direction. This longitudinal damage growth reduced the notch acuity resulting in significant increases in tensile residual strength with increasing number of cycles completed. Damage growth for the 32-ply laminate at $R = -0.3$ was also greater in the length direction, but growth in both directions did occur. For Case C, there appeared to be an order of magnitude decrease in life due to the elevated temperature exposure during cycling with more rapid initial growth for the 24-ply laminate. The life of the 32-ply laminate appeared to be shortened also but not as severely.

PREFACE



Accession For	✓
DTIC CR&I	
DTIC #19	
Unannounced	
Justification	
By	
Distribution/	
Availability	
Dist Avail and	
Special	

This report has been issued in three volumes. Volume I details the work completed under Task I, Preliminary Screening. Volumes II and III encompass the last two tasks of the investigation into the delamination growth and residual strength behavior of initially damaged graphite/epoxy laminates. This volume includes the results of Task II - Damage Growth and Residual Strength Degradation Prediction and Task III - Effect of Fatigue Loading/Environment Perturbations. The tabulated data for these tasks are available in Volume III - Appendixes.

The work reported herein was accomplished under Contract F33615-77-C-3084, Project 2401, Work Unit 24010117, sponsored by the Flight Dynamics Laboratory of the Air Force Wright Aeronautical Laboratories, Air Force Systems Command, Wright-Patterson AFB, Ohio 45433. Dr. G. P. Sendeckyj, AFWAL/FIBE, was the Air Force Program Monitor.

The program which was conducted by the Structures and Materials Department of the Lockheed-California Company, was directed by the Co-Principal Investigators, Ms. K. N. Lauraitis and Mr. D. E. Pettit of the Fatigue and Fracture Mechanics Laboratory. Analytical and conceptual assistance was provided by Dr. J. T. Ryder of the same laboratory. The support and contributions of the Materials Laboratory personnel, Mr. W. E. Krupp, Group Engineer, Mr. R. C. Young, Specimen Fabrication, Mr. S. Krystkowiak, Fractography, and the Fatigue and Fracture Mechanics Laboratory Personnel, Mr. J. M. Cox, Data Reduction, Mr. D. Diggs, Mr. P. Mohr, Mr. F. Pickel, Mr. W. Renslen, Mr. L. Silvas and Mr. C. Spratt in the area of Mechanical Testing are gratefully acknowledged.

TABLE OF CONTENTS

Volume I

<u>Section</u>		<u>Page No.</u>
1	INTRODUCTION	1
	1.1 Technical Background	1
	1.2 Program Overview	1
2	TASK I OVERVIEW	5
	2.1 Material/Laminate Selection	5
	2.2 Specimen Design	6
	2.3 Selection of Damage Type	9
	2.4 Evaluation and Selection of NDI Method for damage Monitoring	11
	2.5 Task I Test Plan	15
3	SPECIMEN FABRICATION AND QUALITY CONTROL	19
	3.1 Material Quality Control Results	19
	3.2 Panel Fabrication	22
	3.3 Preliminary Damage Development Study	22
	3.3.1 Impact Damage Study	22
	3.3.1.1 Evaluation of Impact Damaged 32-Ply Quasi- Isotropic Laminates	28
	3.3.1.2 Evaluation of Impact Damaged 24-Ply 67% 0° Fiber Laminates	33

PRECEDING PAGE BLANK-NOT FILMED

TABLE OF CONTENTS - Continued

Volume I

<u>Section</u>	<u>Page No.</u>
3.3.1.3 Final Selection of Impact Conditions	41
3.3.2 Damaged Hole Drilling Study Results	41
3.4 Specimen Randomization and Fabrication	53
4 EXPERIMENTAL PROCEDURES	65
4.1 Static Tension Test Procedures	65
4.2 Static Compression Test Procedures	65
4.3 Fatigue Test Procedures	68
5 STATIC TEST RESULTS	71
5.1 Static Tension Test Results	71
5.1.1 Quality Control Tensile Test Results	71
5.1.2 Static Tension Test Results for 24-Ply 67% 0° Fiber, T300/5208 Laminate Specimens Containing Impact Damage	75
5.1.3 Static Tension Test Results for 24-Ply 67% 0° Fiber T300/5208 Laminate Specimens Containing Damaged Holes	84
5.1.4 Static Tension Test Results for 32-Ply Quasi-Isotropic T300/5208 Laminate Specimens Containing Impact Damage	88
5.1.5 Static Tension Test Results for 32-Ply Quasi-Isotropic T300/5208 Laminate Specimens Containing a Damaged Hole	98

TABLE OF CONTENTS - Continued

Volume I

<u>Section</u>	<u>Page No.</u>
5.2 Column Buckling Test Results	98
5.2.1 24-Ply 67% 0° Fiber Laminate Results	102
5.2.2 32-Ply Quasi-Isotropic Laminate Results	102
5.3 Static Compression Test Results with Fatigue Supports	102
5.3.1 Compression Test Results for Impact Damaged 24-Ply Laminates	107
5.3.2 Compression Test Results for Damaged Hole 24-Ply Laminates	107
5.3.3 Comparison of the Compression Test Results for the 24-Ply Laminate	111
5.3.4 Compression Test Results for Impact Damaged 32-Ply Laminates	111
5.3.5 Compression Test Results for Damaged Hole 32-Ply Laminates	117
5.3.6 Comparison of the Compression Test Results for the 32-Ply Laminate	117
5.3.7 Summary of Compression Results	123
6 FATIGUE TEST RESULTS	127
6.1 Fatigue Results for the 24-Ply 67% 0° Fiber Laminate	127
6.2 Fatigue Results for the 32-Ply Quasi-Isotropic Laminate	127

TABLE OF CONTENTS - Continued

Volume I

<u>Section</u>		<u>Page No.</u>
7	DAMAGE GROWTH RESULTS	141
	7.1 Buckling Guide Considerations	141
	7.2 Recorded Data Available for Analysis	142
	7.3 System Calibration and Area Measurement Procedures	145
	7.4 Damage Growth in 24-Ply Laminates with a Damaged Hole	148
	7.5 Damaged Growth in 24-Ply Laminates with an Impact Damage	153
	7.6 Damage Growth in the 32-Ply Laminate with a Damaged Hole	168
8	EVALUATION OF THE EFFECT OF TBE	189
	8.1 X-Ray Procedures	189
	8.2 Static Compression Test Results	190
	8.3 Fatigue Test Results	194
	8.4 Effect of TBE on Compression Strength and Fatigue Life	194
	8.5 Damage as Indicated by Two Methods	197
	8.6 The Effect of TBE on Fatigue Damage Growth	214
9	SUMMARY OF TASK I RESULTS	221
	9.1 Initial Static Tension Results	221
	9.2 Initial Static Compression Results	221

TABLE OF CONTENTS - Continued

Volume I

Section

Page No.

9.3	Fatigue Results	222
9.4	Damage Growth Results	222
9.5	NDI Comparison Results	223
9.6	Concluding Observations	224
10	TASK II TEST MATRIX OVERVIEW	225
	APPENDIX A QUALITY CONTROL TEST RESULTS	A-1
	APPENDIX B INITIAL DAMAGE DIMENSIONS	B-1
	APPENDIX C TYPICAL DAMAGE GROWTH RESULTS	C-1
	REFERENCES	R-1

TABLE OF CONTENTS

Volume II

<u>Section</u>		<u>Page No.</u>
1	INTRODUCTION	1
	1.1 Program Overview	4
	1.2 Summary of Task I - Preliminary Screening	5
	1.2.1 Summary of Task I Static Test Results	6
	1.2.2 Summary of Task I Fatigue Results	12
	1.2.3 Summary of The Damage Growth Results	12
	1.2.4 Summary of TBE Enhanced X-Ray Results	18
2	OVERVIEW OF TASKS II AND III	27
	2.1 Material Selection and Specimen Design	27
	2.2 Selection of Damage type and NDI Method	30
	2.3 Procedure for Random Specimen Selection	31
	2.4 Task II Experimental Program	33
	2.5 Task III Experimental Program	36
3	MATERIAL AND SPECIMEN CHARACTERIZATION -- TASKS II AND III	39
	3.1 Prepreg Quality Control Results	39
	3.2 Panel and Specimen Fabrication	45

TABLE OF CONTENTS - Continued

Volume II

<u>Section</u>	<u>Page No.</u>
4 EXPERIMENTAL PROCEDURES	51
4.1 Static and Compression Test Procedures	51
4.2 Fatigue Test Procedures	52
4.3 Damage monitoring Method	54
4.4 Damage measurement Procedures	60
4.4.1 Recorded Data Available For Analysis	60
4.4.2 System Calibration and Area Measurement Procedures	63
4.5 Destructive Inspection Procedures	65
4.5.1 Resin Burn-Out (Deply) Procedure	65
4.5.2 Metallographic Specimen Preparation	67
5 STATIC TENSION AND COMPRESSION RESULTS	69
5.1 Quality Control Tension Test Results -- Tasks II and III	75
5.2 Static Tension and Compression Results For Damaged 24-Ply Laminate Specimens	82
5.3 Static Tension and Compression Results For Damagaed 32-Ply Laminate Specimens	87

TABLE OF CONTENTS - Continued

Volume II

<u>Section</u>	<u>Page No.</u>
5.4 Damage Growth Under Static Loading	94
5.5 Static Test Results for Damaged Laminates At Elevated Temperature	94
5.6 Static Test Results for Damaged Laminates At Elevated Temperature	101
5.7 Comparison of Task I and Task II Data	112
6 TASK II FATIGUE RESULTS	123
6.1 Fatigue Life Results	123
6.1.1 Fatigue Life Distribution for the 24-Ply Laminate	123
6.1.2 Fatigue Life Distribution for the 32-Ply Laminates	128
6.2 Damage Growth Under Fatigue Loading	134
6.2.1 24-Ply Damage Growth Results	135
6.2.2 Damage Growth Results for the 32-Ply Laminates	153
6.3 Residual Strength Results	170
6.3.1 Residual Strength Results for the 24-Ply Laminate	178
6.3.2 Residual Strength Results for the 32-Ply Laminate	183
7 TASK III FATIGUE RESULTS	201
7.1 Fatigue Test Parameter Selection For	201

TABLE OF CONTENTS - Continued

Volume II

<u>Section</u>	<u>Page No.</u>
7.1.1 Case A	201
7.1.2 Case B	203
7.1.3 Case C	205
7.2 Fatigue and Damage Growth Behavior	205
7.3 Residual Strength Results	218
8 — DAMAGE CHARACTERIZATION, ...	237
8.1 Metallographic Examination	238
8.2 Examination by Burn-Out and Deploying	238
9 ANALYSIS OF RESULTS . . .	257
9.1 Data Assessment	257
9.1.1 Mechanics of Fracture in Notched Coupons	259
9.1.2 Assessment of Damage	261
9.2 Analysis/Correlative Methodology	263
9.2.1 Methodology for Relating Damage to Residual Strength and Fatigue Life	266
10 SUMMARY AND CONCLUSIONS	269
REFERENCES	279

TABLE OF CONTENTS

Volume III

<u>Section</u>	<u>Page No.</u>
APPENDIX A QUALITY CONTROL PLAN	A-1
APPENDIX B SPECIMEN WEIGHT MEASUREMENTS	B-1
APPENDIX C STATIC TEST DATA	C-1
APPENDIX D DAMAGE GROWTH CHARACTERISTICS UNDER FATIGUE LOADING	D-1
APPENDIX E DAMAGE CHARACTERISTICS OF SPECIMENS TESTED FOR RESIDUAL STRENGTH	E-1
APPENDIX F DAMAGE MEASUREMENTS OF SPECIMENS TESTED FOR RESIDUAL STRENGTH	F-1
APPENDIX G DAMAGE AS DETERMINED BY METALLOGRAPHIC SECTIONING	G-1
APPENDIX H COMPARISON OF DAMAGE AS DETERMINED BY HOLSCAN ULTRASONIC C-SCAN AND DIB ENHANCED X-RAY	H-1
APPENDIX I DAMAGE ON INDIVIDUAL LAYERS OF SPECIMENS DEPLIED AFTER FATIGUE CYCLING	I-1
APPENDIX J STATISTICAL ANALYSIS OF PANEL VARIABILITY	J-1
APPENDIX K DISCUSSION OF WEIBULL FUNCTION AND PARAMETER ESTIMATION PROCEDURES	K-1

LIST OF ILLUSTRATIONS

<u>Figure No.</u>		<u>Page No.</u>
1	3-Inch Wide Specimen Configuration, Drawing TL1038	8
2	Typical Metallographic Sections of Panel 1SY1156, 24-ply T300/5208	20
3	Typical Metallographic Sections of Panel 2SY1156, 32-ply T300/5208	21
4	Typical Tool Drop Simulation Set Up	29
5	Ultrasonic C-Scan Results of the Preliminary Impact Damage Study of the 32-Ply Quasi-Isotropic Laminate	32
6	Site No. 4 Viewed from Impact Side, 32-Ply Panel No. 2TY-1222	34
7	Site No. 4 Viewed from Back Side, 32-Ply Panel No. 2TY-1222	35
8	Site No. 15 Viewed from Back Side, 32-Ply Panel No. 2TY-1222	36
9	Site No. 15 Viewed from Impact Side, 32-Ply Panel No. 2TY-1222	37
10	Site No. 22 Viewed from Impact Side, 32-Ply Panel No. 2TY-1222	38
11	Site No. 22 Viewed from Back Side, 32-Ply Panel No. 2TY-1222	39
12	Ultrasonic C-Scan Results of the Preliminary Impact Damage Study on the 24-Ply 67% 0° Fiber Laminate	40
13	Site No. 6 Viewed from Back Side, 24-Ply Panel No. 1TY-1222	42
14	Site No. 6 Viewed from Impact Side, 24-Ply Panel No. 1TY-1222	43
15	Site No. 13 Viewed from Impact Side, 24-Ply Panel No. 1TY-1222	44
16	Site No. 13 Viewed from Back, 24-Ply Panel No. 1TY-1222	45
17	Site No. 17 Viewed from Impact Side, 24-Ply Panel No. 1TY-1222	46
18	Site No. 17 Viewed from Back Side, 24-Ply Panel No. 1TY-1222	47
19	Site No. 24 Viewed from Impact Side, 24-Ply Panel No. 1TY-1222	48
20	Site No. 24 Viewed from Back Side, 24-Ply Panel No. 1TY-1222	49
21	Ultrasonic C-Scan Results for 32-Ply Laminate Hole Study	51
22	Ultrasonic C-Scan Results for 24-Ply Laminate Hole Study	52
23	Variability of Hole Damage for Drilling Method No. 1 in 32-Ply Laminate	54
24	Variability of Hole Damage for Drilling Method No. 3 for 32-Ply Laminate	55
25	Variability of Hole Damage for Drilling Method No. 5 for 32-Ply Laminate	56
26	Variability of Hole Damage for Drilling Method No. 1 for 24-Ply Laminate	57

LIST OF ILLUSTRATIONS - Continued

Volume I Figure No.		Page No.
27	Variability of Hole Damage for Drilling Method No. 3 for 24-Ply Laminate	58
28	Variability of Hole Damage for Drilling Method No. 5 for 24-Ply Laminate	59
29	Typical Master Panel Layout Prepared for Each Panel	60
30	Composite Specimen Column Test Fixture	67
31	Fatigue Buckling Guide Design	69
32	Typical Stress-Strain Curve Measured for the 32-Ply Quasi-Isotropic Laminate	74
33	Schematic of the Typical Stress Strain Curve Measured for the 24-Ply 67% 0° Fiber Laminate	76
34	Typical Impact Damage, 24-Ply 67% 0° Fiber T300/5208 Laminate	80
35	Typical Type 1 Tension Failure of Impact Damaged 24-Ply 67% 0° Fiber Laminate	83
36	Typical Type 2 Tension Failure Mode of Impact Damaged 24-Ply 67% 0° Fiber Laminates	83
37	Type 3 Failure Modes observed in Low Strength Tension Failures of Impact Damaged 24-Ply 67% 0° Fiber Laminates	85
38	Typical C-Scan Hole Damage Sizes in Tension Test Specimens of the 24-Ply 67% 0° Fiber Laminate	87
39	Comparison of the 2-Parameter Weibull Distributions for Tension Test Results of Undamaged, Impact Damaged, and Damaged Hole 24-Ply Laminates	89
40	Typical Fracture Characteristics of Damaged Hole 24-Ply Laminates Tested in Tension	90
41	Correlation of Fracture Strength with Damage Size for Impact Damaged 32-Ply Laminates	93
42	Damage Size Correlation with Static Tensile Strength for Impact Damaged 32-Ply Quasi-Isotropic Laminates	94
43	Typical Fracture Features of Impact Damaged 32-Ply Laminate Tension Test Failures	96
44	Two Parameter Weibull Curve Fit for Undamaged and Damaged Hole Specimens of 32-Ply Laminates	100

LIST OF ILLUSTRATIONS - Continued

Volume I

<u>Figure No.</u>		<u>Page No.</u>
45	Typical Fracture Features of Damaged Hole 32-Ply Laminate Tested in Tension	101
46	Column Buckling Failures, 24-Ply Laminate	104
47	Column Buckling Failures, 32-Ply Laminate	106
48	Typical Fracture Features of Damaged 24-Ply Laminate Tested in Compression with the Fatigue Support	109
49	Comparison of the Two Parameter Weibull Curve Fit for Damaged 24-Ply Laminates	112
50	Comparison of Damaged 24-Ply Laminate Column Buckling Results with Compression Test Results Using the Fatigue Support	114
51	Typical Load vs Deflection Compression Test Curve for Impact Damaged 32-Ply Laminate	116
52	Typical Fracture Features of Impact Damaged 32-Ply Laminate Specimens	118
53	Typical Fracture Features of Damaged Hole 32-Ply Laminate Specimens	120
54	Two Parameter Weibull Data Fits for Damaged 32-Ply Laminate Specimens	121
55	Comparison of Compression Results obtained with the Fatigue Support with the Column Buckling Behavior of Damaged 32-Ply Laminates	122
56	Fatigue Life Data for Damaged Hole 24-Ply, 67% 0° Fiber Laminates, R = -1, 5 Hz	128
57	Fatigue Life Data for Impact Damaged 24-Ply, 67% 0° Laminates	129
58	Fatigue Fracture Appearance of Damaged Hole 24-Ply 67% 0° Fiber, Specimens	132
59	Fracture Appearance of Impact Damaged 24-Ply 67% 0° Fiber Laminates Fatigue Tested at ± 36.8 ksi (254 MPa)	133
60	Fatigue Life Data for Damaged Hole 32-Ply Quasi-Isotropic Laminates, R = -1, 5 Hz	134
61	Fatigue Life Data for Impact Damaged 32-Ply Quasi-Isotropic Laminates, R = 1, 5 Hz	135

LIST OF ILLUSTRATIONS - Continued

Volume I

<u>Figure No.</u>		<u>Page No.</u>
62	Typical Failures in Damaged Hole 32-Ply Quasi-Isotropic Specimens	139
63	Typical Failures in Impact Damage 32-Ply Quasi-Isotropic Specimens	140
64	Typical Set of Holscan Data for Each Damage Growth Interval	143
65	Typical Data Set Showing Single Pass B-Scan Results at Selected Locations Through the Damage	144
66	Illustration of the Damage Zone Size Parameters Evaluated	146
67	C-Scan Photos of Calibration Block Used	147
68	Damage Growth Behavior of Damaged Hole 24-Ply 67% 0° Fiber Specimens, $R = -1$, $\sigma_{max} = 41$ ksi (283 MPa)	149
69	Damage Growth Behavior of Damaged Hole 24-Ply 67% 0° Fiber Specimens, $R = -1$, $\sigma_{max} = 41$ ksi (283 MPa)	150
70	Damage Growth Behavior of Damaged Hole 24-Ply 67% 0° Fiber Specimens, $R = -1$, $\sigma_{max} = 38$ ksi (262 MPa)	151
71	Comparison of the Damage Growth Characteristics of HA-1 with other Typical Specimens, $R = -1$, $\sigma_{max} = 38$ ksi (262 MPa)	152
72	Damage Growth Behavior of Damaged Hole 24-Ply 67% 0° Fiber Specimens, $R = -1$, $\sigma_{max} = 38$ ksi (262 MPa)	154
73	Damage Growth Behavior of Damaged Hole 24-Ply 67% 0° Fiber Specimens, $R = -1$, $\sigma_{max} = 34$ ksi (234 MPa)	155
74	Damage Growth Behavior of Damaged Hole 24-Ply 67% 0° Fiber Specimens, $R = -1$, $\sigma_{max} = 34$ ksi (234 MPa)	156
75	Typical Damage Growth Characteristics of Damaged Hole 24-Ply 67% 0° Fiber Specimens. Specimen JA-8, $\sigma_{max} = 34$ (234 MPa)	157
76	Typical Damage Growth Characteristics of Damaged Hole 24-Ply 67% 0° Fiber Specimens. Specimen IA-7, $\sigma_{max} = 41$ ksi (283 MPa)	159
77	Area Damage Growth Behavior of Damaged Hole 24-Ply 67% 0° Fiber Specimens, $R = -1$, $\sigma_{max} = 44$ ksi (303 MPa)	161

LIST OF ILLUSTRATIONS - Continued

Volume I

<u>Figure No.</u>		<u>Page No.</u>
78	Area Damage Growth Behavior of Damaged Hole 24-Ply 67% 0° Fiber Specimens, $R = -1$, $\sigma_{max} = 30$ ksi (207 MPa)	162
79	Area Damage Growth Behavior of Damaged Hole 24-Ply 67% 0° Fiber Specimens, $R = -1$, $\sigma_{max} = 26$ ksi (179 MPa)	163
80	Damage Growth Behavior of Impact Damaged 24-Ply 67% 0° Fiber Specimens, $R = -1$, $\sigma_{max} = 42.75$ ksi (295 MPa)	164
81	Damage Growth Behavior of Impact Damaged 24-Ply 67% 0° Fiber Specimens, $R = -1$, $\sigma_{max} = 36.8$ ksi (254 MPa)	165
82	Damage Growth Behavior of Impact Damaged 67% 0° Fiber Specimens, $R = -1$, $\sigma_{max} = 31.5$ ksi (217 MPa)	167
83	Damage Growth Characteristics of Impact Damaged Specimen JA-7, 24-Ply 67% 0° Laminate, $R = -1$, $\sigma_{max} = 42.75$ ksi (295 MPa)	169
84	Damage Growth Characteristics of Impact Damaged Specimen LC-22, 24-Ply 67% 0° Laminate, $R = -1$	170
85	Damage Growth Characteristics of Impact Damaged Specimen JU-22, 24-Ply 67% 0° Laminate, $R = -1$, $\sigma_{max} = 31.5$ ksi (217 MPa)	173
86	Damage Growth Characteristics of Impact Damaged 24-ply Laminates, $R = -1$, $\sigma_{max} = 27.6$ ksi (199 MPa)	174
87	Typical Change in Maximum Damage Height, Y, vs Fatigue Cycles for Damaged Hole 32-Ply Quasi-Isotropic Laminates, $R = -1$	175
88	Comparison of Change in Damage Area and Damage Width for Damaged Hole 32-Ply Quasi-Isotropic Specimens $r = -1$, $\sigma_{max} = 30$ ksi (207 MPa)	176
89	Comparison of Change in Damage Area and Damage Width for Damaged Hole 32-Ply Quasi-Isotropic Specimens, $R = -1$, $\sigma_{max} = 26$ ksi (179 MPa)	177
90	Comparison of Change in Damage Area and Damage Width for Damaged Hole 32 Ply Quasi-Isotropic Specimens, $R = -1$, $\sigma_{max} = 20$ ksi (138 MPa)	178
91	Damage Growth Characteristics of Damaged Hole Specimen DA-5, 32-Ply Quasi-Isotropic Laminate, $R = -1$, $\sigma_{max} = 26$ ksi (179 MPa)	180

LIST OF ILLUSTRATIONS - Continued

Volume I

<u>Figure No.</u>		<u>Page No.</u>
92	Damage Growth Characteristics of Damaged Hole Specimen BC-28, 32-Ply Quasi-Isotropic Laminate, $R = -1$, $\sigma_{max} = 23$ ksi (158 MPa)	182
93	Damage Growth Characteristics of Damaged Hole Specimen CA-5, 32 Ply Quasi-Isotropic T300/5208 Laminate, $R = -1$, $\sigma_{max} = 20$ ksi (138 MPa)	186
94	Effect of Delay in X-Ray Exposure after TBE Soak, Damage Hole Specimen LA-1, 24-Ply 67% 0° T300/5208 Laminate, Specimen Preloaded to 28 ksi, $\sigma_u = 47.9$ ksi	190
95	Effect of Delay in X-Ray Exposure after TBE Soak, Damage Hole Specimen BA-9, 32-Ply Quasi-Isotropic T300/5208 Laminate, $R = -1$, $\sigma_{max} = 30$ ksi (207 MPa), $N_f = 1,709$ Cycles	191
96	Schematic of Typical TBE X-Ray Damage Size Result	197
97	Comparison of Baseline and TBE Exposed Specimen Fatigue Results, $R = -1$, 5 Hz	198
98	X-Ray Examination of Static Compression Specimens, 24-Ply 67% 0° T300/5208 Laminate, Specimens HA-5, KC-24, and HA-3	199
99	X-Ray Examination of Static Compression Specimens, 32-Ply Quasi-Isotropic T300/5208 Laminate; Specimens CA-8, AC-30 and EC-29	200
100	Fatigue Damage as Detected by Holscan and X-Ray for Specimen MB-13, 24-Ply 67% 0° Laminate, $R = -1$, $\sigma_{max} = 41$ ksi (283 MPa), $N_f = 3420$ Cycles	201
101	Fatigue Damage as Detected by Holscan and X-Ray for Specimen KB-16, 24-Ply 67% 0° Laminate, $R = -1$, $\sigma_{max} = 38$ ksi (262 MPa), $N_f = 162,717$ Cycles	202
102	Fatigue Damage as Detected by Holscan and X-Ray for Specimen LA-4, 24-Ply 67% 0° Laminate, $R = -1$, $\sigma_{max} = 34$ ksi (234 MPa), $N_f = 226,390$ Cycles	203
103	Fatigue Damage as Detected by Holscan and X-Ray for Specimen BA-9, 32-Ply Quasi-Isotropic Laminate $R = -1$, $\sigma_{max} = 30$ ksi (207 MPa), $N_f = 1,709$ Cycles	204
104	Fatigue Damage as Detected by Holscan and X-Ray for Specimen AA-3, 32-Ply Quasi-Isotropic Laminate $R = -1$, $\sigma_{max} = 26$ ksi (179 MPa), $N_f = 10,565$ Cycles	205

LIST OF ILLUSTRATIONS - Continued

Volume I

<u>Figure No.</u>		<u>Page No.</u>
105	Fatigue Damage as Detected by Holscan and X-Ray for Specimen EB-13, 32-Ply Quasi-Isotropic Laminate, $R = -1$, $\sigma_{\max} = 20$ ksi (138 MPa), $N_f = 392,584$	206
106	Damage Size Comparison from X-Ray and Holscan Results, 24-Ply 67% 0° Fiber Laminate $\sigma_{\max} = 41$ ksi (282 MPa)	208
107	Damage Size Comparison from X-Ray and Holscan Results, 24-Ply 67T 0° Fiber Laminate, $\sigma_{\max} = 38$ ksi (261 MPa)	209
108	Damage Size Comparison from X-Ray and Holscan Results, 24-Ply 67% 0° Fiber Laminate, $\sigma_{\max} = 34$ ksi (234 MPa)	210
109	Damage Size Comparison from X-Ray and Holscan Results, 32-Ply Quasi-Isotropic Laminate, $\sigma_{\max} = 30$ ksi (206 MPa)	211
110	Damage Size Comparison from X-Ray and Holscan Results, 32-Ply Quasi-Isotropic Laminate, $\sigma_{\max} = 26$ ksi (179 MPa)	212
111	Damage Size Comparison from X-Ray and Holscan Results, 32-Ply Quasi-Isotropic Laminate, $\sigma_{\max} = 20$ ksi (138 MPa)	213
112	Comparison of Holscan Damage Size for Baseline Specimens and Specimens Exposed to TBE X-Ray Procedures, 24-Ply 67% 0° Fiber Laminate, $\sigma_{\max} = 41$ ksi (283 MPa)	215
113	Comparison of Holscan Damage Size for Baseline Specimens and Specimens Exposed to TBE X-Ray Procedures, 24-Ply 67% 0° Fiber Laminate, $\sigma_{\max} = 38$ ksi (262 MPa)	216
114	Comparison of Holscan Damage Size for Baseline Specimens and Specimens Exposed to TBE X-Ray Procedures, 24-Ply 67% 0° Fiber Laminate, $\sigma_{\max} = 34$ ksi (234 MPa)	217
115	Comparison of Holscan Damage Size for Baseline Specimens and Specimens Exposed to TBE X-Ray Procedures, 32-Ply Quasi-Isotropic Laminate, $\sigma_{\max} = 30$ ksi (207 MPa)	218
116	Comparison of Holscan Damage Size for Baseline Specimens and Specimens Exposed to TBE X-Ray Procedures, 32-Ply Quasi-Isotropic Laminate, $\sigma_{\max} = 26$ ksi (179 MPa)	219
117	Comparison of Holscan Damage Size for Baseline Specimens and Specimens Exposed to TBE X-Ray Procedures, 32-Ply Quasi-Isotropic Laminate, $\sigma_{\max} = 20$ ksi (138 MPa)	220

LIST OF ILLUSTRATIONS

Volume II

Figure No.

Page No

1	Comparison of the Two Parameter Weibull Distribution for Tension Test Results of Undamaged, Impact Damaged, and Damaged Hole 24-Ply Laminates	7
2	Comparison of the Two Parameter Weibull Curve Fit for Damaged 24-Ply Laminates	8
3	Correlation of Tension Strength with Damage Size for Impact Damaged 32-ply Laminates	9
4	Two Parameter Weibull Data Fits for Damaged 32-Ply Laminate Specimens	10
5	Two Parameter Weibull Curve Fit for Undamaged and Damaged Hole Specimens of 32-Ply Laminate	11
6	Fatigue Life Data for Damaged Hole Specimens of 24 Ply, 67% 0° Laminates, R = -1, 5 Hz	13
7	Fatigue Life Data for Impact Damaged 24 Ply, 67% 0° Laminates, R = -1, 5 Hz	14
8	Fatigue Life Data for Damaged Hole 32-Ply Quasi-Isotropic Laminates, R = -1, 5 Hz	15
9	Fatigue Life Data for Impact Damaged Specimens of 32-Ply Quasi-Isotropic Laminates, R = -1, 5 Hz	16
10	Damage Growth Characteristics of Impact Damaged 24-Ply 67% 0° Laminate Specimens, 72° F (21° C), R = -1, Max Stress = 36.8 ksi (254 MPa)	17

LIST OF ILLUSTRATIONS - continued

Volume II

Figure No.

Page No.

11	Damage Growth Characteristics of 24-Ply 67% 0° Laminate Specimens Containing a Damaged Hole. 72° F (21°C), R = -1, Max Stress = 34 ksi (234 MPa)	19
12	Damage Growth Characteristics of 32-Ply Quasi-Isotropic Laminate Specimens Containing a Damaged Hole. 72° F (21°C), R = -1, Max Stress = 26 ksi (179 MPa)	20
13	Damage Growth Characteristics of 32-Ply Quasi-Isotropic Laminate Specimens Containing a Damaged Hole. 72° F (21°C), R = -1, Max Stress = 20 ksi (138 MPa)	21
14	Damage Growth Characteristics of 32-Ply Quasi-Isotropic Laminate Specimens Containing a Damaged Hole. 72° F (22°C), R = -1, Max Stress = 17 ksi (117 MPa)	22
15	Damage Growth Characteristics of 32-Ply Quasi-Isotropic Laminate Specimens Containing Impact Damage. 72° F (22°C), R = -1, Max Stress = 40 ksi (276 MPa)	23
16	Comparison of Baseline and TBE Exposed Specimen Fatigue Results, R = -1, 5 Hz	25
17	Three Inch Wide Specimen Configuration, Drawing TL 1038	29
18	Typical Master Panel Specimen Layout	32
19	Specimen Supported by Restraining Fix- tures Used in Static Compression and Fatigue Tests	53
20	Fatigue Buckling Guide Design	55

LIST OF ILLUSTRATIONS - continued

Volume II

Figure No.

Page No.

21	Four-Bar Buckling Support (Constraint #2) Design	56
22	Digital Mechanical Scanner with Vertical Mounting in Place for Panel Examination	58
23	Modified Holosonic System 400 with Digital Mechanical Scanner, Vertical Mounting System and Digital Memory	59
24	Typical Holscan Data Available for Each Damage Growth Interval	61
25	Typical Data Set Illustrating Single Pass B-Scan Results at Selected Locations Through the Damage	62
26	Illustration of the Damage Zone Size Parameters Evaluated	64
27	C-Scan Photos of Calibration Block	66
28	Typical Load vs. Deflection Curve for High Strain Rate Tests of 32-Ply Laminate	70
29	Typical Deflection vs. Number of Scans Curve for High Strain Rate Tests of 32-Ply Laminate	71
30	Stress-Strain Curve for Quasi-Isotropic Specimen NA-5 Derived from Strain Gage Measurements Yielding $E = 7.5 \times 10^6$ psi (52 GPa)	76
31	Stress-Strain Curve for Quasi-Isotropic Specimen NA-5 Derived from Stroke Measurements Yielding $E = 5.2 \times 10^6$ psi (36 GPa)	77

LIST OF ILLUSTRATIONS - continued

Volume II

<u>Figure No.</u>		<u>Page No.</u>
32	Typical Stress-Strain Curve Measured for the 24-Ply 67% 0° Laminate	79
33	Typical Stress-Strain Curve Measured for the 32-Ply Quasi-Isotropic Laminate	81
34	Typical Initial C-Scans of Damaged Holes in Compression and Tension Test Specimens of 24-Ply 67% 0° Laminate	83
35	Effect of Loading Rate and Pre-Loading on the Static Strength of 24-Ply Laminate Specimens Containing a Damaged Hole	86
36	Fracture Features Typical of Both Strain Rates for Damaged 24-Ply Specimens Tested in Tension	88
37	Typical Fractures of Damaged 24-Ply Specimens Tested in Compression with 4-Bar Buckling Supports at Standard Strain Rate	88
38	Typical Fractures of Damaged 24-Ply Specimens Tested in Compression with Fatigue Guides	89
39	Typical Initial C-Scans of Damaged Holes in Compression and Tension Test Specimens of 32-Ply Quasi-Isotropic Laminate	90
40	Effect of Loading Rate and Pre-Loading on the Static Strength of 32-Ply Laminate Specimens Containing a Damaged Hole	93
41	Fracture Features Typical of High and Low Strain Rate Tests for Damaged 32-Ply Specimens	95
42	Typical Fractures of Damaged Laminates Tested in Compression at 180°F (82°C)	102

LIST OF ILLUSTRATIONS - continued

Volume II

Figure No.

Page No.

43	Typical Fractures of Damaged Laminates Tested in Tension at 180°F (82°)	103
44	Effect of Specimen Width and Loading Rate on the Tensile Strength of Undamaged, 32-Ply Laminate Specimens	106
45	Effect of Specimen Width and Loading Rate on the Tensile Strength of Undamaged, 24-Ply Laminate Specimens	107
46	Typical Fractures of Undamaged 24-Ply Laminate Specimens Tested in Tension at Room Temperature	109
47	Typical Fractures of Undamaged 32-Ply Laminate Specimens Tested in Tension at Room Temperature	110
48	Typical Fractures of Undamaged One-Inch (25 mm) Wide Q.C. Specimens Tested in Tension at Standard Strain Rate	111
49	Typical Fractures of Undamaged Specimens Tested in Compression at Room Temperature	113
50	Comparison of Two Parameter Weibull Curve Fit for Undamaged Task I and II 24-Ply Tension Data	114
51	Comparison of Two Parameter Weibull Curve Fit for Undamaged and Damaged Task II 24-Ply Tension Data	115
52	Comparison of Two Parameter Weibull Curve Fit for Damaged Task I and II 24-Ply Tension Data	116

LIST OF ILLUSTRATIONS - continued

Volume II

<u>Figure No.</u>		<u>Page No.</u>
53	Comparison of Two Parameter Weibull Curve Fit for Damaged Task I and II 24-Ply Compression Data	117
54	Comparison of Two Parameter Weibull Curve Fit for Task I and Task II 32-Ply Tension Data	118
55	Comparison of Two Parameter Weibull Curve Fit for Task I and Task II 32-Ply Compression Data	119
56	Fatigue Scatter Results for 24-Ply Damaged Hole Specimens	125
57	Two Parameter Weibull Curve Fit for Task II 24-Ply Fatigue Data, max = 35 ksi (241 MPa), R = -1	126
58	Three Parameter Weibull Curve Fit for Task II 24-Ply Fatigue Data, max = 35 ksi (241 MPa), R = -1	127
59	Fatigue Fracture Appearance of Damaged 24-Ply 67% - 0° Fiber Specimens Tested at 35 ksi (241 MPa), R = -1	129
60	Fatigue Scatter Results for 32-Ply Damaged Hole Specimens	130
61	Two Parameter Weibull Curve Fit for Task II, 32-Ply Fatigue Data, max = 22 ksi (152 MPa), R = -1	131
62	Three Parameter Weibull Curve Fit for Task II, 32-Ply Fatigue Data, max = 22 ksi (152 MPa), R = -1	132
63	Fatigue Fracture Appearances of Damaged 32-Ply Quasi-Isotropic Specimens Tested at 22 ksi (152 MPa), R = -1	133

LIST OF ILLUSTRATIONS - continued

Volume II

Figure No.

Page No.

64a	Area Damage Growth for the 24-Ply Fatigue Distribution Specimens (Specimens 1 - 10)	142
64b	Area Damage Growth for the 24-Ply Fatigue Distribution Specimens (Specimens 11 - 20)	143
65a	Damage Growth in Width Dimension for the 24-Ply Fatigue Distribution Specimens (Specimens 1 - 10)	144
65b	Damage Growth in Width Dimension for the 24-Ply Fatigue Distribution Specimens (Specimens 11 - 20)	145
66a	Damage Growth in Height Dimension for the 24-Ply Fatigue Distribution Specimens (Specimens 1 - 10)	146
66b	Damage Growth in Height Dimension for the 24-Ply Fatigue Distribution Specimens (Specimens 11 - 20)	147
67	Damage Growth Behavior of Typical Longer Lived 24-Ply Laminate Specimens	148
68	Damage Growth Behavior of Typical Shorter Lived 24-Ply Laminate Specimens	149
69	Damage Size at 30,000 Cycles vs. Life for the 24-Ply Laminate	151
70	Last Recorded Damage Size Prior to Failure vs. Remaining Life for the 24-Ply Laminate	152
71a	Typical Damage Growth Characteristics of Initially Damaged 24-Ply, 67% 0° Fiber Specimens (Specimen EA-6, $N_f = 166,600$)	154

LIST OF ILLUSTRATIONS - continued

Volume II

Figure No.

Page No.

71b	Typical Damage Growth Characteristics of Initially Damaged 24-Ply, 67% 0° Fiber Specimens (Specimen EA-6, $N_f = 166,600$)	155
72	Damage Growth Characteristics of Initially Damaged 24-Ply Specimen HC-27 Which Exhibited Rapid Growth ($N_f = 27,800$)	156
73a	Area Damage Growth for the 32-Ply Fatigue Distribution Specimens (Specimens 1 - 10)	163
73b	Area Damage Growth for the 32-Ply Fatigue Distribution Specimens (Specimens 11 - 20)	164
74a	Damage Growth in the Width Direction for the 32-Ply Fatigue Distribution Specimens (Specimens 1 - 10)	165
74b	Damage Growth in the Width Direction for the 32-Ply Fatigue Distribution Specimens (Specimens 11 - 20)	166
75a	Damage Growth in the Height Direction for the 32-Ply Fatigue Distribution Specimens (Specimens 1 - 10)	167
75b	Damage Growth in the Height Direction for the 32-Ply Fatigue Distribution Specimens (specimens 11 - 20)	168
76	Typical Damage Growth of 32-Ply Laminate Specimens	169
77	Damage Size at 20,000 Cycles vs. Life for the 32-Ply Laminate	171
78	Last Recorded Damage Size Prior to Failure vs. Remaining Life for the 32-Ply Laminate	172

LIST OF ILLUSTRATIONS - continued

<u>Figure No.</u>		<u>Page No.</u>
Volume II		
79a	Typical Damage Growth Characteristics of Initially Damaged 32-Ply Quasi-Isotropic Specimens (Specimen RB-14, $N_f = 51,400$)	173
79b	Typical Damage Growth Characteristics of Initially Damaged 32-Ply Quasi-Isotropic Specimens (Specimen RB-14, $N_f = 51,400$)	174
80a	Typical Damage Growth Characteristics of Initially Damaged 32-Ply Quasi-Isotropic Specimens (Specimen QA-5, $N_f = 234,200$)	175
80b	Typical Damage Growth Characteristics of Initially Damaged 32-Ply Quasi-Isotropic Specimens (Specimen QA-5, $N_f = 234,200$)	176
81	Relationship of Tension Residual Strength to Damage Area as Detected by the Holskan Ultrasonic C-Scan for 24-Ply Laminate Specimens	188
82	Relationship of Compression Residual Strength to Damage Area as Detected by the Holskan Ultrasonic C-Scan for 24-Ply Laminate Specimens	189
83	Typical Damage Characteristics of 24-Ply Specimens Fatigue Cycled at ± 35 ksi (± 241 MPa) for Residual Strength Determination	190
84	Typical Fracture Appearances of 24-Ply Specimens Tested for Residual Strength After Fatigue Cycling	191

LIST OF ILLUSTRATIONS - continued

<u>Figure No.</u>		<u>Page No.</u>
Volume II		
85	Relationship of Tension Residual Strength to Damage Area as Detected by the olscan Ultrasonic C-Scan for 32-Ply Laminate Specimens	196
86	Relationship of Compression Residual Strength to Damage Area as Detected by the Holscan Ultrasonic C-Scan for 32-Ply Laminate Specimens	197
87a	Typical Damage Characteristics of 32-Ply Specimens Fatigue Cycled at ± 22 ksi (± 152 MPa) for Residual Strength Determination	198
87b	Typical Damage Characteristics of 32-Ply Specimens Fatigue Cycled at ± 22 ksi (± 152 MPa) for Residual Strength Determination	199
88	Typical Fracture Appearances of 32-Ply Specimens Tested for Residual Strength After Fatigue Cycling	200
89	Column Buckling Results from Task I	204
90	Fatigue Life Data for 24 and 32-Ply Laminates for Variations in Constraint Condition, Range Ratio and Temperature Summarized in Table XXXV	206
91	Area Damage Growth Behavior for 24-Ply Specimens, Case A (4-Bar)	207
92	Area Damage Growth Behavior for 24-Ply Specimens, Case B ($R = -0.3$)	208
93	Area Damage Growth Behavior for 24-Ply Specimens, Case C (180°F)	209
94	Area Damage Growth Behavior for 32-Ply Specimens, Case A (4-Bar)	210

LIST OF ILLUSTRATIONS - continued

<u>Figure No.</u>		<u>Page No.</u>
Volume II		
95	Area Damage Growth Behavior for 32-Ply Specimens, Case B ($R = -0.3$)	211
96	Area Damage Growth Behavior for 32-Ply Specimens, Case C (180°F)	212
97	Fracture Appearances of 24-Ply Specimens Tested in Fatigue with Constraint # 2, Case A	214
98	Fracture Appearances of 32-Ply Specimens Tested in Fatigue with Constraint #2, Case A	215
99	Fracture Appearances of 24-Ply Specimens Tested in Fatigue at 180°F (82°C), Case C	216
100	Fracture Appearances of 32-Ply Specimens Tested in Fatigue at 180°F (82°C), Case C	217
101a	Damage Growth Characteristics of the 24-Ply Laminate for Fatigue Condition A, 4-Bar Support (Table XXXV) (Specimen BC-23, $N_f = 62,710$)	222
101b	Damage Growth Characteristics of the 24-Ply Laminate for Fatigue Condition A, 4-Bar Support (Table XXXV) (Specimen BC-23, $N_f = 62,710$)	223
102a	Damage Growth Characteristics of the 24-Ply Laminate for Fatigue Condition B, $R = -0.3$ (Table XXXV) (Specimen BC-24 completed 2×10^6 without failure)	224
102b	Damage Growth Characteristics of the 24-Ply Laminate for Fatigue Condition B, $R = -0.3$ (Table XXXV) (specimen BC-24 completed 2×10^6 without failure)	225

LIST OF ILLUSTRATIONS - continued

<u>Figure No.</u>		<u>Page No.</u>
Volume II		
103	Damage Growth Characteristics of the 24-Ply Laminate for Fatigue Condition C, 180°F (82°C) (Table XXXV) (Specimen AA-4, $N_f = 2,060$)	226
104a	Damage Growth Characteristics of the 32-Ply Laminate for Fatigue Condition A, 4-Bar Support (Table XXXV) (specimen FA-8, $N_f = 48,789$)	227
104b	Damage Growth Characteristics of the 32-Ply Laminate for Fatigue Condition A, 4-Bar Support (Table XXXV) (Specimen FA-8, $N_f = 48,789$)	228
105a	Damage Growth Characteristics of the 32-Ply Laminate for Fatigue Condition B, $R = -0.3$ (Table XXXV) (Specimen FC-30 completed 2×10^6 without failure)	229
105b	Damage Growth Characteristics of the 32-Ply laminate for Fatigue Condition B, $R = -0.3$ (Table XXXV) (Specimen FC-30 completed 2×10^6 without failure)	230
106a	Damage Growth Characteristics of the 32-Ply Laminate for Fatigue Condition C, 180°F (82°C) (Table XXXV) (Specimen EB-15, $N_f = 50,198$)	231
106b	Damage Growth Characteristics of the 32-Ply Laminate for Fatigue Condition C, 180°F (82°C) (Table XXXV) (Specimen EB-15, $N_f = 50,198$)	232
107	Typical Residual Tension Fracture Appearances for 24-Ply Laminate Specimens Tested Under Fatigue Condition A, B, or C of Table XXXV	233
108	Typical Residual Compression Fracture Appearances for 24-Ply Laminate Specimens Tested Under Fatigue Condition A, B, or C of Table XXXV	234

LIST OF ILLUSTRATIONS - continued

<u>Figure No.</u>		<u>Page No.</u>
Volume II		
109	Typical Residual Tension Fracture Appearances for 32-Ply Laminate Specimens Tested Under Fatigue Conditions A, B, or C of Table XXXV	235
110	Typical Residual Compression Fracture Appearances for 32-Ply Laminate Specimens Tested Under Fatigue Conditions A, B, or C of Table XXXV	236
111	Damage as Recorded by Holscan Indicating Locations at Which B-scans Were Obtained	239
112	Comparison of Damage as Determined by Metallographic Sectioning and Holscan Ultrasonic B-Scan at Location No. 1 (See Figure 111)	240
113	Comparison of Damage as Determined by Metallographic Sectioning and Holscan Ultrasonic B-scan at Location No. 2 (See Figure 111)	241
114	Comparison of Damage as Determined by Holscan Ultrasonic C-scan and DIB Penetrant Enhanced X-ray for Specimen JB-14	243
115	Comparison of Damage as Determined by Holscan Ultrasonic C-scan and DIB Penetrant Enhanced X-ray for Specimen KA-2	244
116	Comparison of Damage as Determined by Holscan Ultrasonic C-scan and DIB Penetrant Enhanced X-ray for Specimen SC-22	245
117a	Deplied 24-ply Specimen BB-15 After 40,000 Fatigue Cycles (Plies 1 - 13)	248
117b	Deplied 24-Ply Specimen BB-15 After 40,000 Fatigue Cycles (Plies 14 - 19)	249

LIST OF ILLUSTRATIONS - continued

<u>Figure No.</u>		<u>Page No.</u>
Volume II		
117c	Deplied 24-Ply Specimens BB-15 After 40,000 Fatigue Cycles (Plies 20 - 24)	250
118a	Deplied 32-Ply Specimen SC-31 After 28,000 Fatigue Cycles (Plies 1 - 7)	251
118b	Deplied 32-Ply Specimen SC-31 After 28,000 Fatigue Cycles (Plies 8 - 19)	252
118c	Deplied 32-Ply Specimen SC-31 After 28,000 Fatigue Cycles (Plies 20 - 27)	253
118d	Deplied 32-Ply specimen SC-31 After 28,000 Fatigue Cycles (Plies 28 - 32)	254
119	Comparison of Damage as Determined by Holscan Ultrasonic C-scan and DIB Penetrant Enhanced X-ray for Specimen BB-15	255
120	Comparison of Damage as Determined by Holscan Ultrasonic C-Scan and DIB Penetrant Enhanced X-Ray for Specimen SC-31.	256

LIST OF TABLES

Volume I

<u>TABLE</u>		<u>PAGE NO.</u>
I	Interlaminar Normal Stresses at Free Edges of Test Coupons	7
II	Scores of Flaws in Graphite/Epoxy in Response to Questionare 1	10
III	Proposed Task I Test Matrix	16
IV	Summary of Narmco Quality Control Tests for Rigidite 5208/T300	23
V	Summary of Lockheed Quality Control Tests for Narmco Rigidite 5208/T300 Material, Batch 1079(22)	24
VI	Summary of Panel Identification Codes	27
VII	Impact Parameters for 32 Ply Quasi-Isotropic Laminate	30
VIII	Impact Parameters for 24 Ply 67% 0° Fiber Laminate	31
IX	Preliminary Damaged Hole Drilling Parameters	50
X	Typical Randomization of Specimen Sequences	61
XI	Illustration of Randomization of Panels by Test	62
XII	Tension Test Results for 32 Ply Quasi-Isotropic T300/5208 Undamaged 1-Inch (24.4mm) Wide	72
XIII	Tension Test Results for 24-Ply Quasi-Isotropic T300/5208 Undamaged 1-Inch (25.4mm) Wide	73
XIV	Tension Test Results for 24-Ply 67% 0° Fiber T300/5208, Containing Impact Damage	77
XV	Comparison of Strain Results from Extensometers Located Across the Impact Damage Site & Across Undamaged Material in 24-Ply 67% 0° Fiber T300/5208	79
XVI	24-Ply 67% 0° Fiber T300/5208 Damaged Hole Tension Test Results	86
XVII	Tension Test Results for 32-Ply Quasi-Isotropic Specimens Containing Impact Damage	91
XVIII	Comparison of Extensometer Results from the 32-Ply Quasi-Isotropic Material.	97
XIX	32-Ply Quasi-Isotropic T300/5208 Damaged Hole Tension Test Results	99
XX	24-Ply Column Buckling Test Results	103
XXI	32-Ply Column Buckling Test Results	105
XXII	24-Ply Impact Damage Laminate Compression Test Results (with Fatigue Support)	108
XXIII	24-Ply Damaged Hole Compression Results (with Fatigue Support)	110
XXIV	Two Parameter Weibull Data Fit Parameters	113

LIST OF TABLES - Continued

Volume I

<u>TABLE</u>	<u>PAGE NO.</u>
XXV 32-Ply Impact Damaged Laminate Compression Test Results (with Fatigue Supports)	115
XXVI 32-Ply Damaged Hole Compression Results (with Fatigue Supports)	119
XXVII Summary of the Failure Stress Values for Various Test Conditions	124
XXVIII Summary of the Apparent Modulus Values for Various Test Conditions	125
XXIX Fatigue Test Results for Damaged Hole Specimens of 24-Ply 67% 0° Fiber T300/5208 Laminate	130
XXX Fatigue Test Results for Impact Damaged 24-Ply 67% 0° Fiber T300/5208 Laminate	131
XXXI Fatigue Test Results for Impact Damaged and Damaged Hole Specimens of 32-Ply Quasi-Isotropic T300/5208 Laminate	136
XXXII Fatigue Test Results for Impact Damaged Specimens of 32-Ply Quasi-Isotropic T300/5208 Laminate	137
XXXIII Static Compression Failure Stress Levels for Damaged Hole Specimens Which Had Been Previously Exposed to TBE	191
XXXIV Fatigue History for TBE Exposed X-Ray Study Specimens, R = -1	192
XXXV Task II Test Matrix	196

LIST OF TABLES

Volume II

<u>Table No.</u>		<u>Page No.</u>
I	Illustration of Randomization of Panels by Test	34
II	Task II Test Matrix	35
III	Task III Test Matrix	37
IV	Properties of T300 Fibers Used in Tasks I, II and III	40
V	Summary of the Narmco Quality Control Tests for Rigidite 5208-T300 Certified Test Report No- 35952	41
VI	Summary of Lockheed Quality Control Tests for Narmco Rigidite 5208-T300 Material Batch #1295	42
VII	Panel Identification Codes	46
VIII	Resin, Fiber, and Void Analysis Results	48
IX	Static Test Matrix Summary	73
X	Comparison of Modulus and Failure Strain Values Derived from Extensometer and Cross-Head Displacement Measurements	74
XI	Comparison of Average Q.C. Tension Data for Tasks I, II and III	78
XII	Summary of Tension and Compression Results for Damaged 24-Ply Laminate	85
XIII	Summary of Tension and Compression Results for Damaged 32-Ply Laminate	92
XIVa	Task II Residual Strength Static Damage Growth	96

LIST OF TABLES - continued

Volume II

<u>Table No.</u>		<u>Page No.</u>
XIVb	Task II Residual Strength Static Damage Growth	97
XVa	24 and 32-Ply Damaged Hole Static Damage Growth Results	98
XVb	24 and 32-Ply Damaged Hole Static Damage Growth Results	99
XVI	Comparison of Elevated and Room Temperature Strength Data at Two Strain Rates	100
XVII	Tension Strength Data for Unnotched Specimens	104
XVIII	Compression Strength Data for Unnotched Specimens	105
XIX	Comparison of Two Parameter Weibull Data Fit Parameters for Task I and Task II	120
XXa	Area Damage Growth (inches ²) for Damaged Hole 24-Ply Laminates Fatigue Cycled at \pm 35 ksi	136
XXb	Area Damage Growth (mm ²) for Damaged Hole 24-Ply Laminates Fatigue Cycled at \pm 241 MPa	137
XXIa	Damage Growth in X (Width) Direction (inches) For Damaged Hole 24-Ply Laminates Fatigue Cycled at \pm 35 ksi	138
XXIb	Damage Growth in X (Width) Direction (mm) For Damaged Hole 24-Ply Laminates Fatigue Cycled at \pm 241 MPa	139
XXIIa	Damage Growth in Y (Height) Direction (inches) For Damaged Hole 24-Ply Laminates Fatigue Cycled at \pm 35 ksi	140

LIST OF TABLES - continued

Volume II

<u>Table No.</u>		<u>Page No.</u>
XXIIb	Damage Growth in Y (Height) Direction (mm) For Damaged Hole 24-Ply Laminates Fatigue Cycled at ± 241 MPa	141
XXIIIa	Area Damage Growth (inches ²) For Damaged Hole 32-Ply laminates Fatigue Cycled at ± 22 ksi	157
XXIIIb	Area Damage Growth (mm ²) For Damaged Hole 32-Ply laminates Fatigue Cycled at ± 152 MPa	158
XXIVa	Damage Growth in X (Width) Direction (inches) For Damaged Hole 32-Ply Laminates Fatigue Cycled at ± 22 ksi	159
XXIVb	Damage Growth in X (Width) Direction (mm) For Damaged Hole 32-Ply Laminates Fatigue Cycled at ± 152 MPa	160
XXVa	Damage Growth in Y (Height) Direction (inches) For Damaged Hole 32-Ply Laminates Fatigue Cycled at ± 22 ksi	161
XXVb	Damage Growth in Y (Height) Direction (mm) for Damaged Hole 32-Ply Laminates Fatigue Cycled at 152 MPa	162
XXVI	Fatigue Results for Specimens Tested for Tension and Compression Residual Strength	180
XXVII	Baseline Fatigue Life Distribution by Machine	181
XXVIII	Failure Distribution by Test Machine for 24-Ply Laminate Specimens Fatigue Tested to $N_1 - N_5$ for Residual Strength Determination	184
XXIX	Tension Residual Strength Data Summary 24-Ply, 67% 0° Fiber Laminate	185

LIST OF TABLES - continued

Volume II

<u>Table No.</u>		<u>Page No.</u>
XXX	Compression Residual Strength Data Summary 24-Ply, 67% 0° Fiber Laminate	186
XXXI	Summary of Damage Measurements for 24-Ply Laminate Specimens	187
XXXII	Tension Residual Strength Data Summary 32-Ply Quasi-Isotropic Laminate	193
XXXIII	Compression Residual Strength Data Summary 32-Ply Quasi-Isotropic Laminate	194
XXXIV	Summary of Damage Measurements for 32-Ply Laminate Specimens	195
XXXV	Summary of Test Conditions for Variations in Fatigue Loading/Environment	202
XXXVI	Residual Strength Results	219
XXXVII	Residual Strength Data Summary	221
XXXVIII	Comparison of Damage Lengths as Determined by Holscan and Metallography	242
XXXIX	Plies Containing Damage in Deplied 24 and 32-Ply Specimens	246

SECTION 1

INTRODUCTION

Accelerated use of advanced composite materials in aircraft structural applications has turned attention towards the development of analytical methodologies to assure the same level of structural reliability found in comparable metal structures. Composite materials have thus far resisted the desired application of simple modifications or extensions of analysis methods used for metals. Significant differences in scale and structure between composites and metals have prevented such an approach. The anisotropic laminated characteristics of composites confuse attempts at defining defects or damage in composites. Delaminations, matrix cracking, fiber breakage and matrix voids readily occur in composite laminates. But, to what extent these are detrimental, necessary, or perhaps beneficial is dependent upon the loading conditions and laminate type. Not necessarily the same type of anomaly will be of major concern under various loading conditions, unlike in metals where many defect types can be conservatively considered as cracks.

Despite these differences between composite and metallic materials, it still may be possible for specific cases to express damage in terms of a parameter which is relatable to the strength degradation. Such an approach has been viewed as desirable because it quantifies the design process, thus removing the element of judgement from the role of the individual designer. This is in part due to an illusion of the part played by fracture mechanics in present day aircraft design. Fracture mechanics primarily, and usually rightly, serves as an after the fact analysis providing that "warm feeling"

that the structure was properly designed, but then, that is the aim of standards and regulations. Their role is passive, not active, and intended to provide checks, safeguards and hopefully guarantees for structural reliability. The structural design life problem is, simply stated twofold; how to design for durability and damage tolerance and how to regulate it. The single dominant flaw approach is extremely attractive for the purposes of quantification and regulation, since then initial flaw sizes can be defined, growth limits established and residual strength determined. This attractiveness is the basis for the ongoing attempt of the technical community to critically examine the feasibility of such approaches to establish whether continued effort in this direction could prove fruitful for composites. This formed the basis for this program.

The goal for this study was to establish relationships between observable damage growth parameters, residual strength and life capacity of the structure through the development of a methodology which could predict: a) damage growth as a function of fatigue loading; b) residual strength as a function of damage size; c) mechanisms of fatigue induced damage formation and d) threshold levels of damage. The aim was to be accomplished by generating statistically significant data sets so that the behavior could be well established. The range of validity of the methodology was to be defined by comparing predicted results with those from a set of tests wherein various test parameters were to be altered. The logic for the design of the test program follows directly from these objectives.

However, increasingly throughout the study, there was an awareness that these goals may not be in concert with the manifested material behavior. Thus, a set of "working objectives" was formulated which was intended to increase the probability that the data would have a positive influence on subsequent ideas, approaches, and directions. These objectives resulted from the reshaping and expansion of the original goals and can best be expressed in the following questions:

- o Is there a change in the material associated with the application of repetitive load cycles?
- o Can this change be tolerated or altered?
- o Can this change be termed "damage"?
- o Can it be related to the mechanical response of the material?
- o How strong is the relationship?
- o Is it dependent upon laminate type, loading and environmental conditions?

The first three questions are concerned with a major difficulty associated with the use of composite materials; that of the definition of damage. This program and others have shown that there is a change in the state of the material resulting from the application of cyclic loads. One of the manifesting changes was delamination which did not behave in a manner similar to cracks in a metal, but rather more as an inelastic energy dissipation zone which tended to relieve notch acuity producing an increase in residual strength. Thus, in a sense, delamination can be related to a mechanical response of the material. Moreover, the general shape of the delamination growth curve could be anticipated and within broad limits might be related to life. Although delaminations did extend, residual strength in tension or compression for the laminates investigated did not degrade, this despite the fact that in some cases numerous fatigue failures occurred.

The last three questions are concerned with establishing relationships based upon observed material interactions. They were formulated to address the problem in a manner which was open to the different possibilities which did indeed occur. The fact that strong correlations between delamination development and mechanical response were not apparent provided an insight into the mechanics of the failure process. This coupled with the observation that strength degradation was sudden and catastrophic indicated that the problem might be considered from the standpoint of the stability of the energy state of the system which is dependent upon the sequence and location of the various probabilistic events (matrix cracking, fiber breakage, delamination, etc.) occurring within the material system. This postulation as well as the data and observations are analyzed in greater detail in Section 9.

1.1 PROGRAM OVERVIEW

This program was composed of three major phases: Task I - Preliminary Screening was designed to screen the static and fatigue induced damage growth characteristics of two damage types for two distinct laminates employing two NDI methods. Based on these results a single damage condition and NDI method were selected for further study in Tasks II and III; Task II - Damage Growth and Residual Strength Degradation Prediction was devised to generate statistically significant data sets for the static and fatigue life behavior and the fatigue induced damage growth and residual strength behavior from which a relationship between the mechanical response of the material and damage may be determined; Task III - Effect of Fatigue Loading/Environment Perturbations included the study of three variations in the loading/environmental parameters to evaluate the extent

to which the proposed relationship is dependent upon laminate type, loading and environmental conditions.

All three tasks have been completed. Task I has been recorded in AFWAL-TR-79-3095, Volume I. This report contains the efforts of Tasks II and III.

1.2 SUMMARY OF TASK I - PRELIMINARY SCREENING

Two laminates of T300/5208 graphite/epoxy material were selected for this study: 1) a 24-ply, 67% $\sim 0^\circ$ fiber, $(0/45/0_2/-45/0_2/45/0_2/-45/0)_s$ and 2) a 32-ply quasi-isotropic $(0/45/90/-45_2/90/45/0)_{2s}$. These complied with the requirements that one laminate be delamination prone (32-ply) while the other would not (24-ply) under fully reversed tension-compression fatigue loading. In addition, these particular stacking sequences were chosen since results from this program could then contribute to a comprehensive static and fatigue data base being developed for these laminates of the same materials under Contracts F33615-77-C-5140 and F33615-78-C-5090 and previously developed for a different material (T300/934) under AFML Contracts F33615-75-C-5118 and F33615-77-C-5045.

A three-inch wide by fourteen-inch long specimen with a nine-inch gage section was used for both fatigue and static tests. Two damage types were included in the study: 1) a poorly drilled hole with multiple delaminations surrounding the hole; and 2) low velocity impact damage produced by dropping an impactor on the panel.

Static tension and compression properties were determined for both laminates with ten replicates per condition. Compression tests were conducted using both the fatigue supports which were full platen restraints with a 2.15 in. (55 mm) square window and 4-bar buckling guides to evaluate the inherent local buckling characteristics of the damaged laminate.

Fatigue tests conducted to obtain the $R = -1$ S-N characteristics for each of the four laminate/damage conditions also provided the basic fatigue induced damage growth characteristics. Damage growth was monitored using a Holosonics Series 400 Holscan Ultrasonic unit. A subset of both static compression and fatigue tests was conducted to provide a statistically based answer as to the effect of TBE on subsequent material behavior. The following sections present a brief summary of the results of these tests.

1.2.1 Summary of Task I Static Test Results

For the 24 ply 67% 0° fiber laminate specimens, the impact damage had no significant effect on the static tension strength as shown in Figure 1 even though failure always occurred through the damage region. However, the damaged hole condition had a major influence on both the tension strength (Figure 1) and the static compression strength as shown in Figure 2. Impact damaged specimens exhibited a static compression strength reduction comparable to that of the damaged hole specimens (Figure 2).

For the 32 ply quasi-isotropic laminate specimens, the inflicted impact damage was near the threshold size necessary to produce failure through the damage region. Failure typically occurred through regions away from the damage for the lower range of existing damage sizes as evident in Figure 3. For the upper range of impact damage sizes, the tension strength appeared to be very sensitive to the damage size. Under compression loading, the impact damage effected an approximately 30% reduction in static compression strength compared to undamaged tension as displayed in Figure 4. However, the damaged hole produced a more severe drop in the static compression strength (approximately 54%) than the impact damage. Damaged hole static tension data were extremely consistent (low scatter) and well below (approximately 50%) strengths obtained for the undamaged laminate (Figure 5).

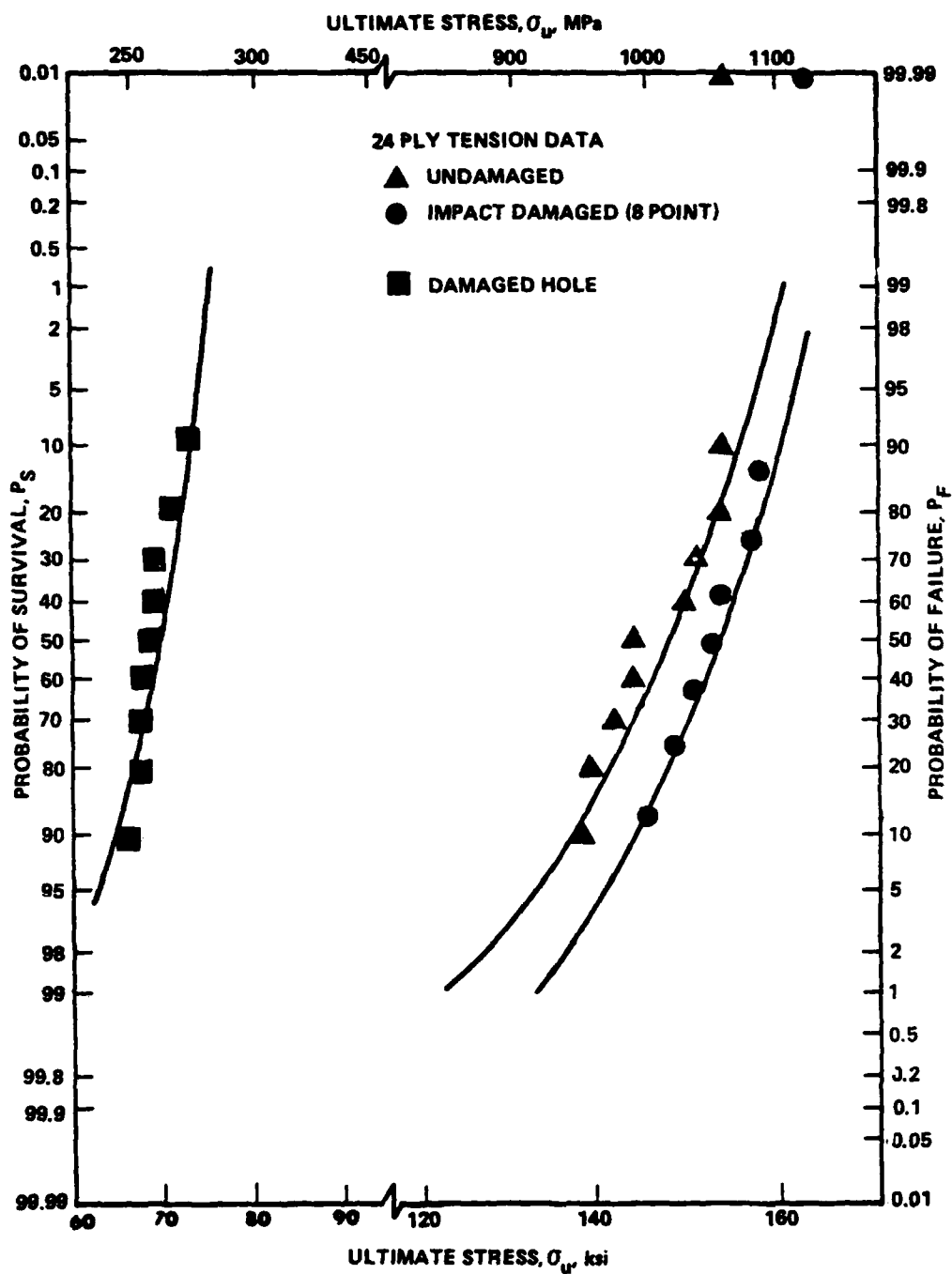


Figure 1: Comparison of the Two-Parameter Weibull Distributions for Tension Test Results of Undamaged, Impact Damaged, and Damaged Hole 24-Ply Laminates

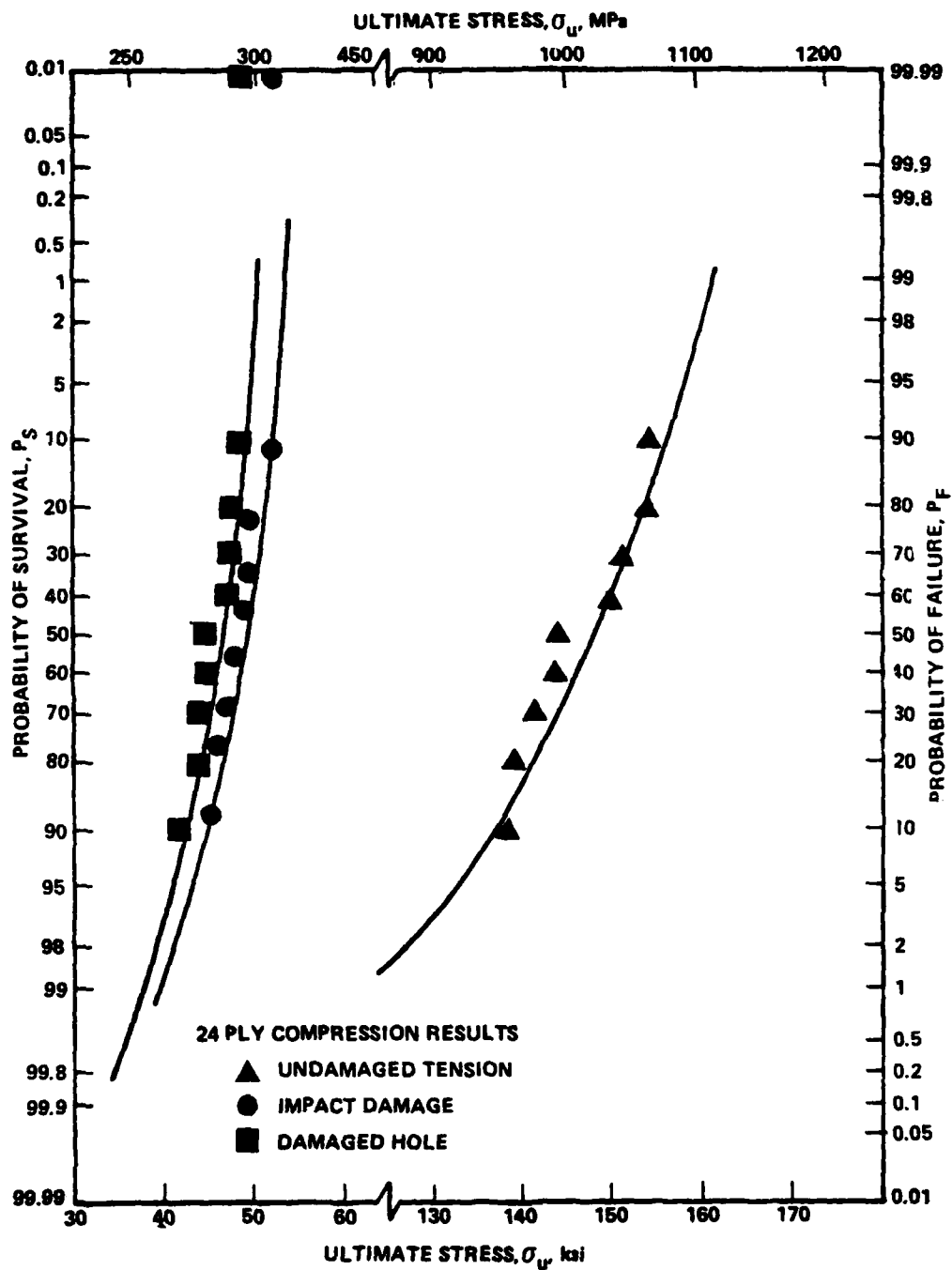


Figure 2: Comparison of the Two Parameter Weibull Curve Fit for Damaged 24-Ply Laminates

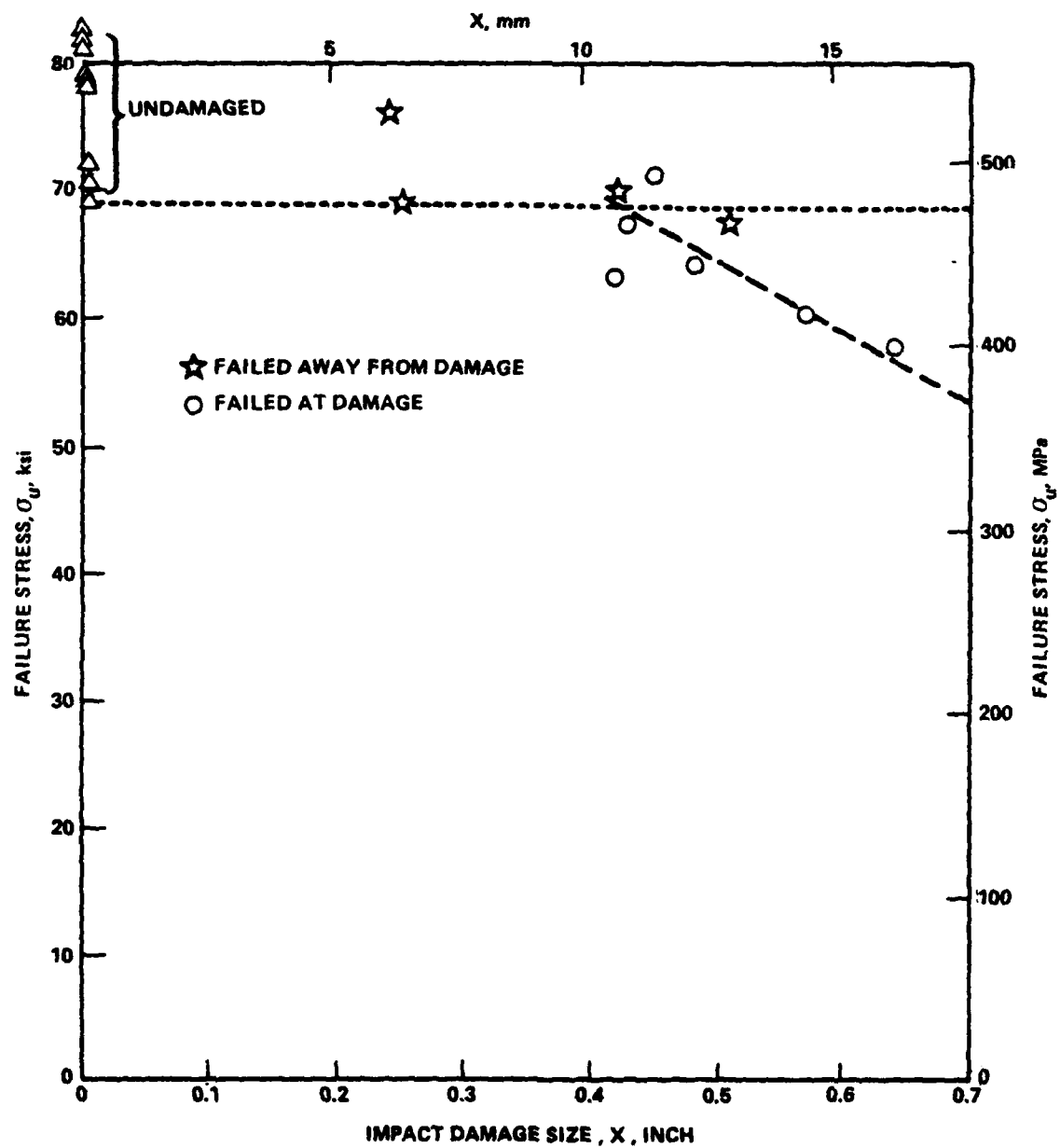


Figure 3: Correlation of Tension Strength with Damage Size for Impact Damaged 32-Ply Laminates.

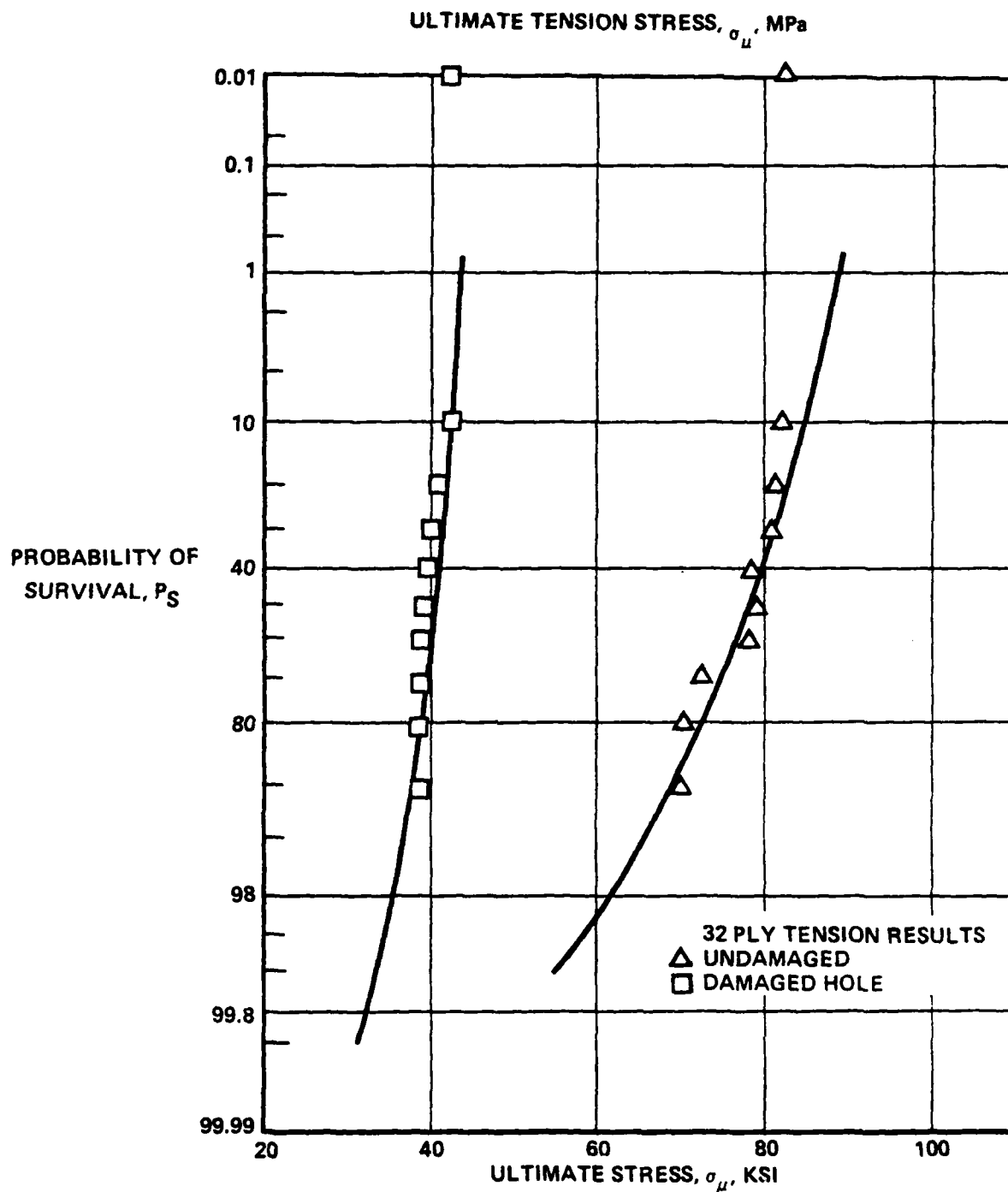


Figure 5: Two Parameter Weibull Curve Fit for Undamaged and Damaged Hole Specimens of 32 Ply Laminate

1.2.2 Summary of Task I Fatigue Results

Stress-life data for the T300/5208 24-ply 67% 0° fiber damaged hole and impact damaged specimens at $R = -1$ are presented in Figures 6 and 7. A distinct similarity in the shape of the curves for the two damage types is indicated which may be due to the nearly identical compression strength reduction produced by the two damage types. However, additional data would be required to do more than suggest possible trends.

Fatigue test results for the 32-ply quasi-isotropic specimens containing damaged holes and impact damage at $R = -1$ are presented in Figures 8 and 9 respectively. Specimens containing a single damaged hole again exhibit a typical S-N fatigue curve with what appears to be small data dispersion (i.e., less than an order of magnitude for any of three sets of triplicate specimens). However, impact damaged 32-ply quasi-isotropic specimens did not display consistent damage growth or S-N behavior. As shown in Figure 9, a large number of the failures in the 32-ply impacted specimens occurred away from the damage region, indicating that this damage was too near the threshold size to act as the dominant cause of failure under fatigue loading. Due to these findings, testing of the 32-ply impact damaged specimens was discontinued.

1.2.3 Summary of the Damage Growth Results

Impact damage in the 24-ply, 67%-0° fiber laminate specimens initially extended very slowly (if at all) for the first 60% to 70% of the specimen life. Growth then proceeded at an increasing rate during the later stages of the specimen life as indicated in Figure 10, which is typical of the behavior.

The 24-ply, 67%-0° fiber laminate specimens containing a damaged hole exhibited somewhat different behavior. Damage extended at a substantial

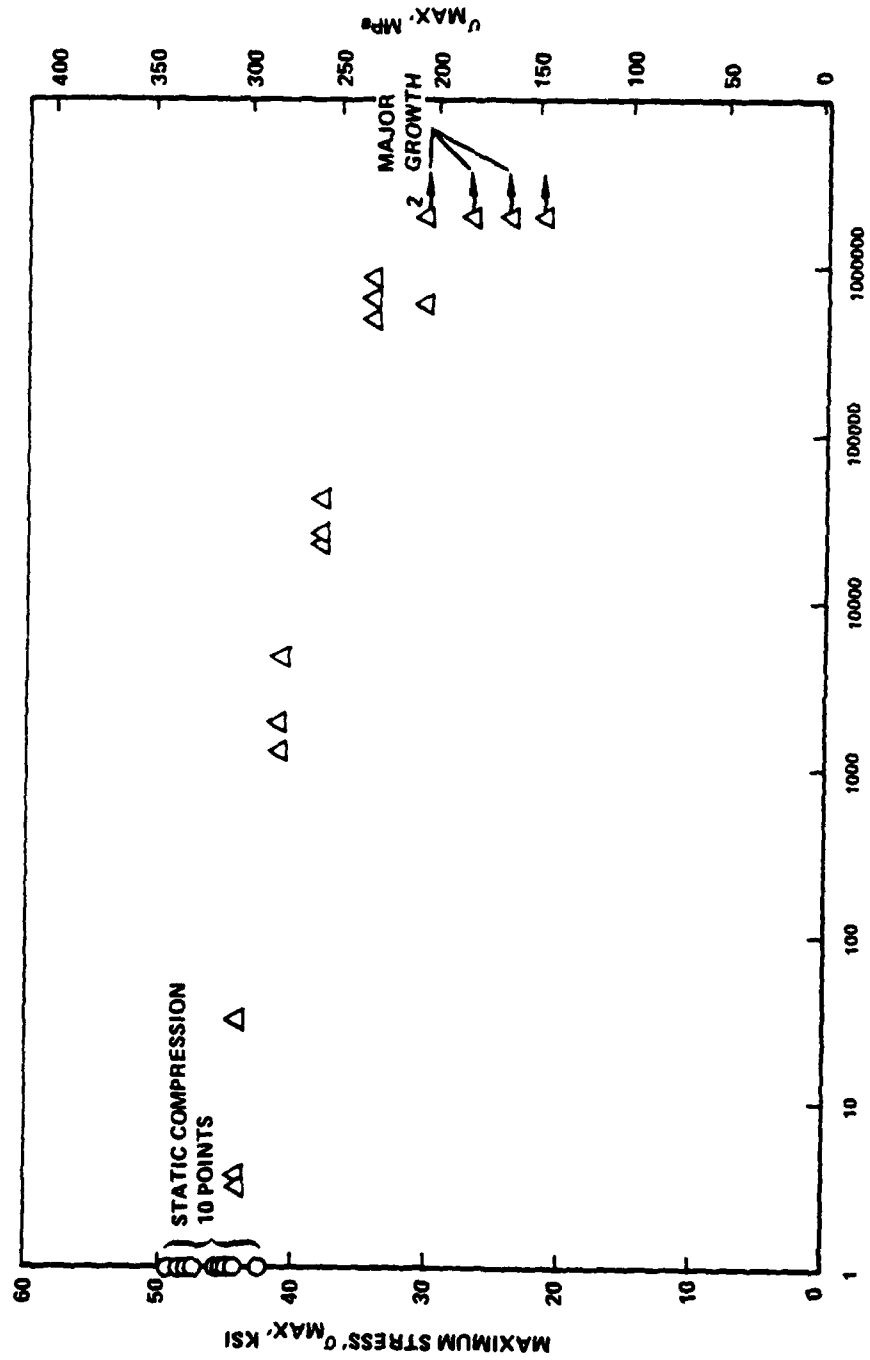


Figure 6: Fatigue Life Data for Damaged Hole Specimens of 24 Ply, 67% 0° Laminate, $R = -1$, 5 Hz

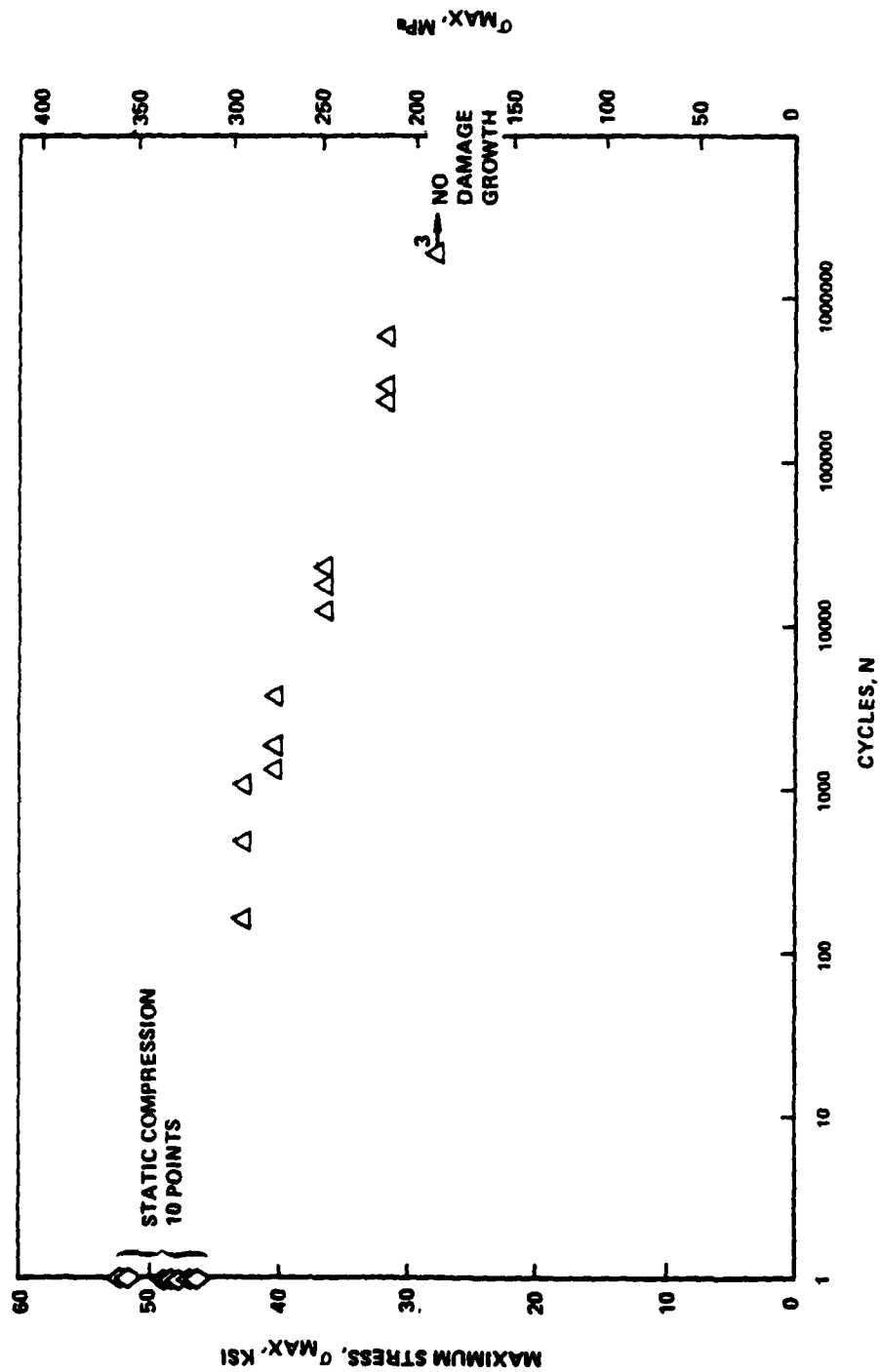


Figure 7: Fatigue Life Data for Impact Damaged 24-Ply, 67% 0° Laminates, $R = -1$, 5 Hz

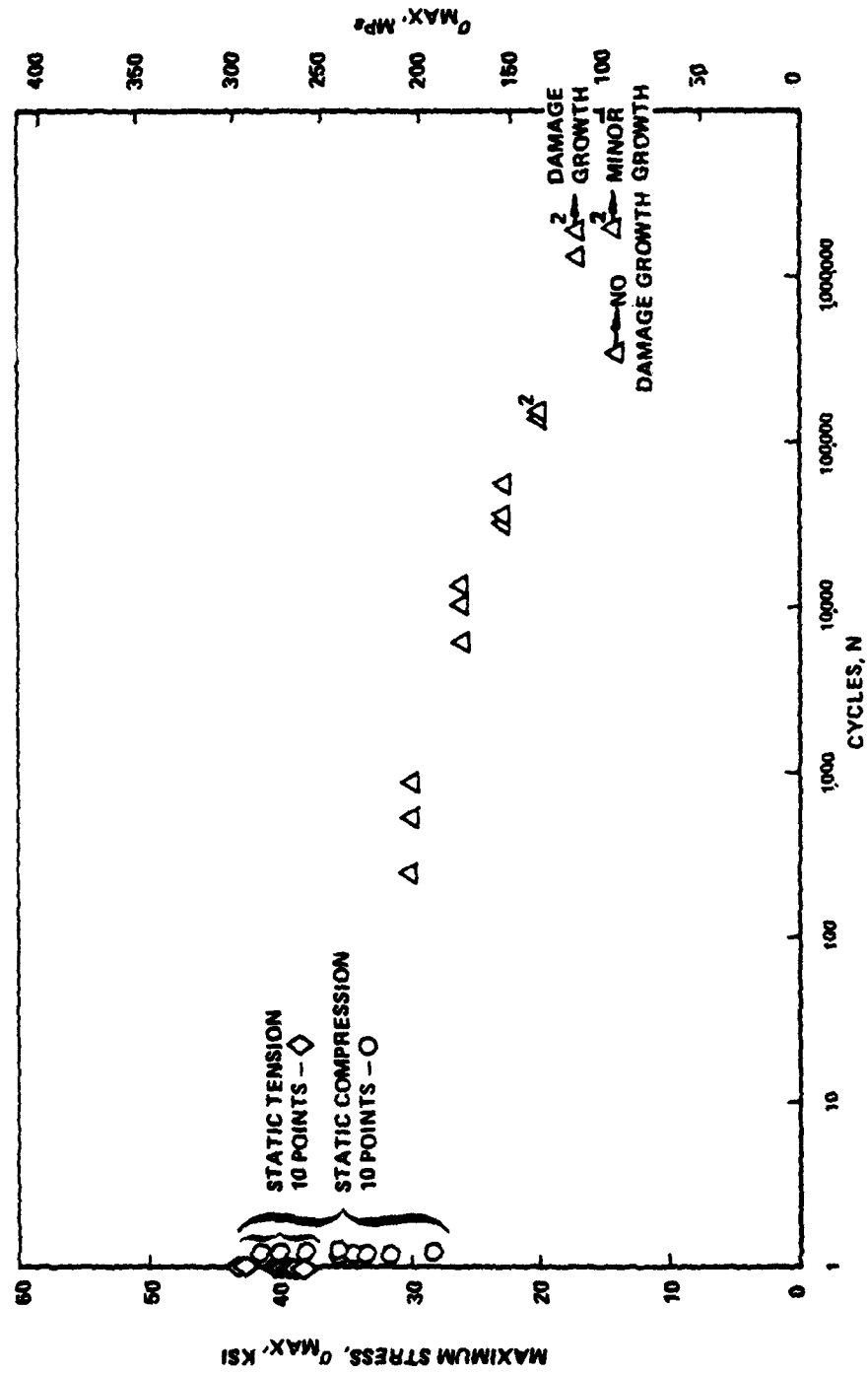


Figure 8: Fatigue Life Data for Damaged Hole 32-Ply Quasi-Isotropic Laminates, $R \approx -1$, 5 Hz

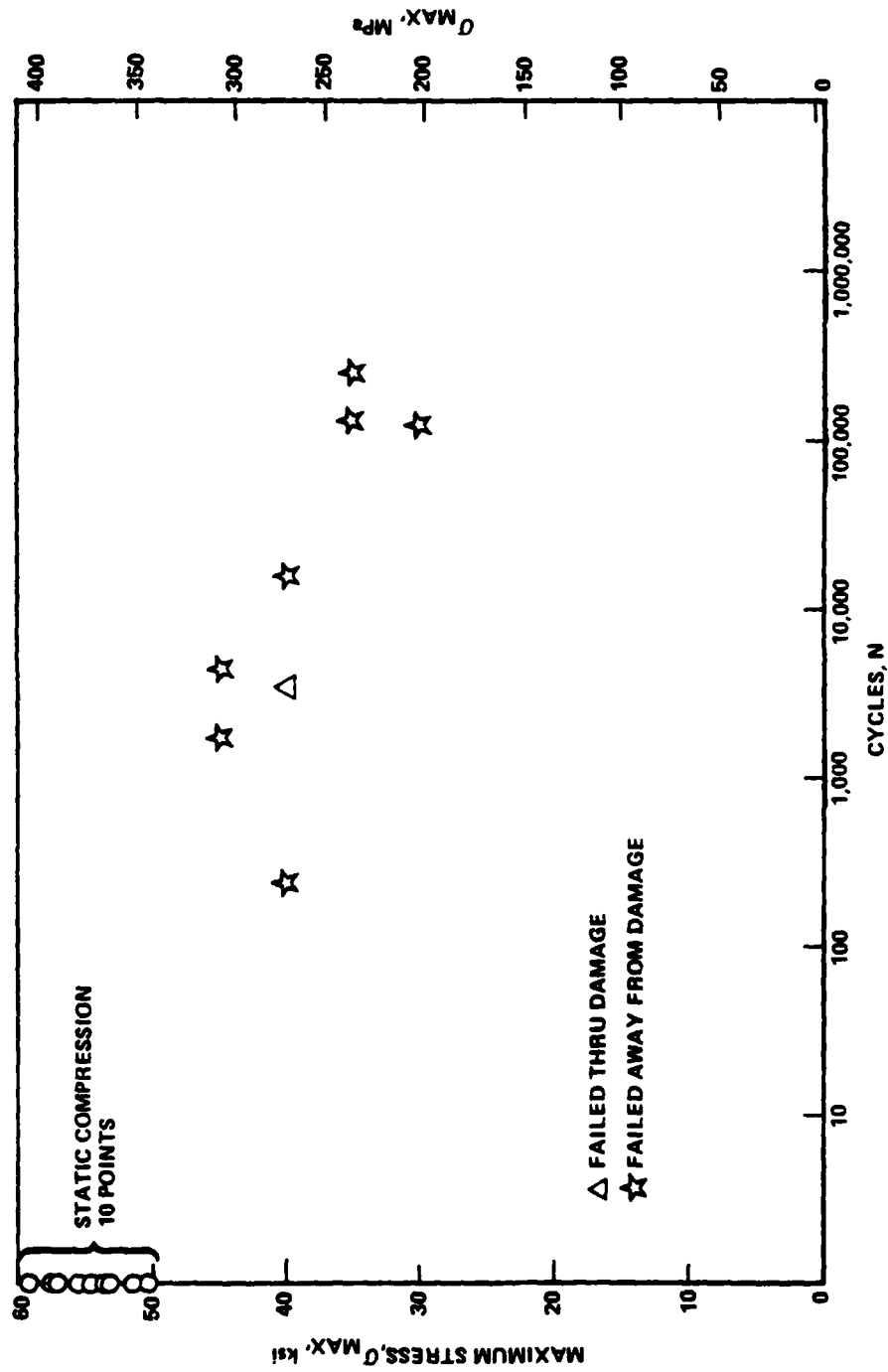


Figure 9: Fatigue Life Data for Impact Damaged Specimens of 32-Ply Quasi-Isotropic Laminates, $R = -1,5$ Hz

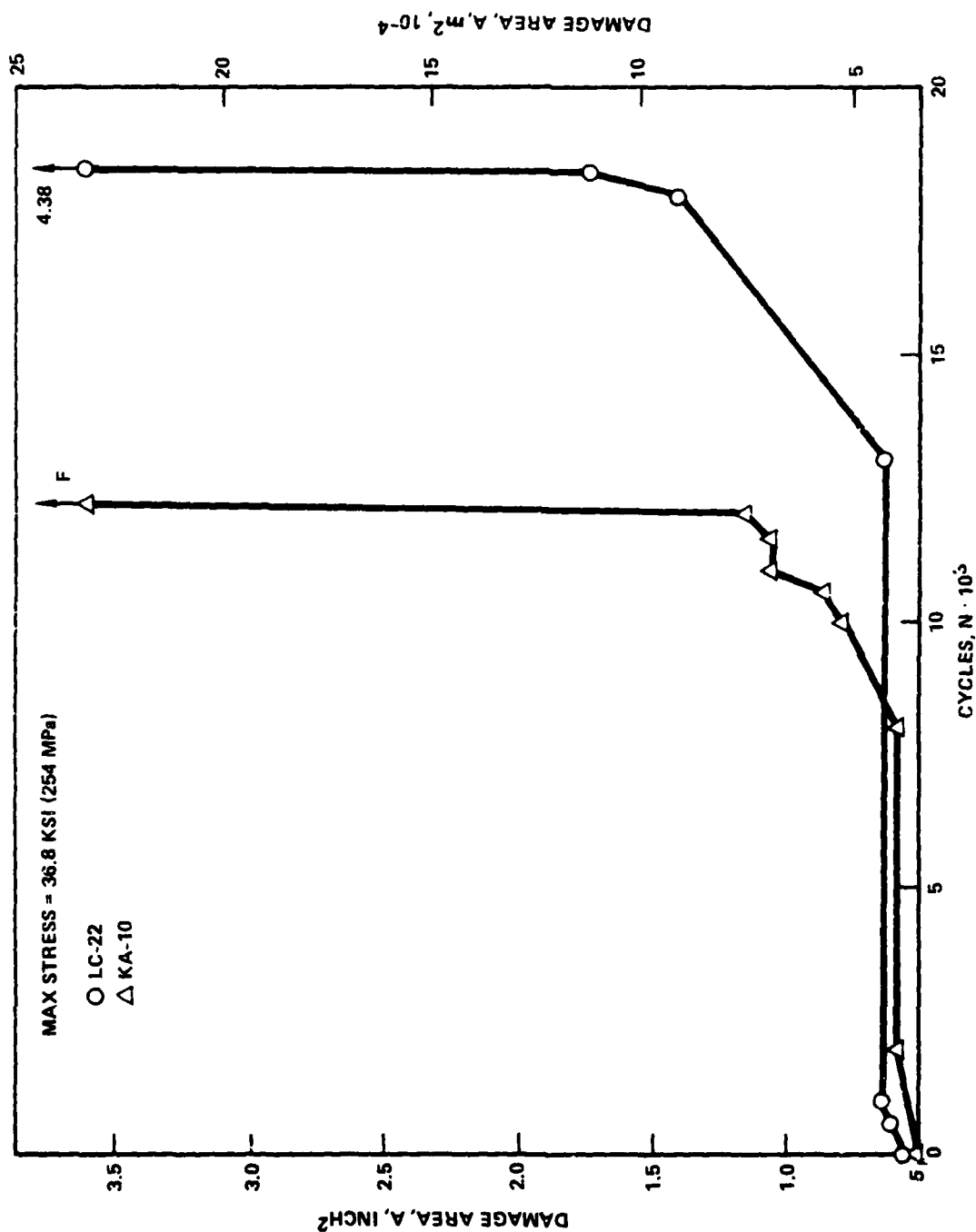


Figure 10: Damage Growth Characteristics of Impact Damaged 24-ply 0° Laminates Specimens, 72°F (21°C), R = -1, Max Stress = 36.8 ksi (254 MPa)

rate during the initial 20% to 30% of specimen life, then slowed to a significantly lower value until near the end of the specimen life where the rate of growth again accelerated until failure occurred. Typical damage growth characteristics are illustrated in Figure 11.

Typical damage growth characteristics of the 32-ply quasi-isotropic laminate specimens containing a damaged hole are presented in Figures 12 through 14. At higher stress levels, the damage growth characteristics (as measured in terms of total damage area) were similar to those observed for the 24-ply damaged hole specimens. After initially rapid damage extension, growth proceeded at a slower rate until near failure when the rate again accelerated. At lower stresses (Figures 13 and 14), the growth rates were more constant over the entire life of the specimen.

While only one apparently valid failure for the 32-ply impact damaged laminate was obtained, the results, shown in Figures 15 indicate a growth pattern similar to that observed for the 24-ply impact damaged specimens.

An important observation which is a factor in the consideration of the significance of the damage growth data is the constraining effect of the anti-buckling guides. Results appeared to indicate that for certain load ranges and laminate/damage conditions damage may extend at a stable rate to the boundary of the anti-buckling guide opening, but at this point may be stopped or slowed due to the clamping forces exerted by the guides which limits the validity of data beyond the window size.

1.2.4 Summary of TBE Enhanced X-Ray Results

A comparison of the TBE enhanced x-ray and Holskan ultrasonic damage data revealed similar damage sizes for the subset of fatigue test coupons. No significant change in static compression strength following TBE examination was discovered. Periodic TBE inspection also appeared to have no

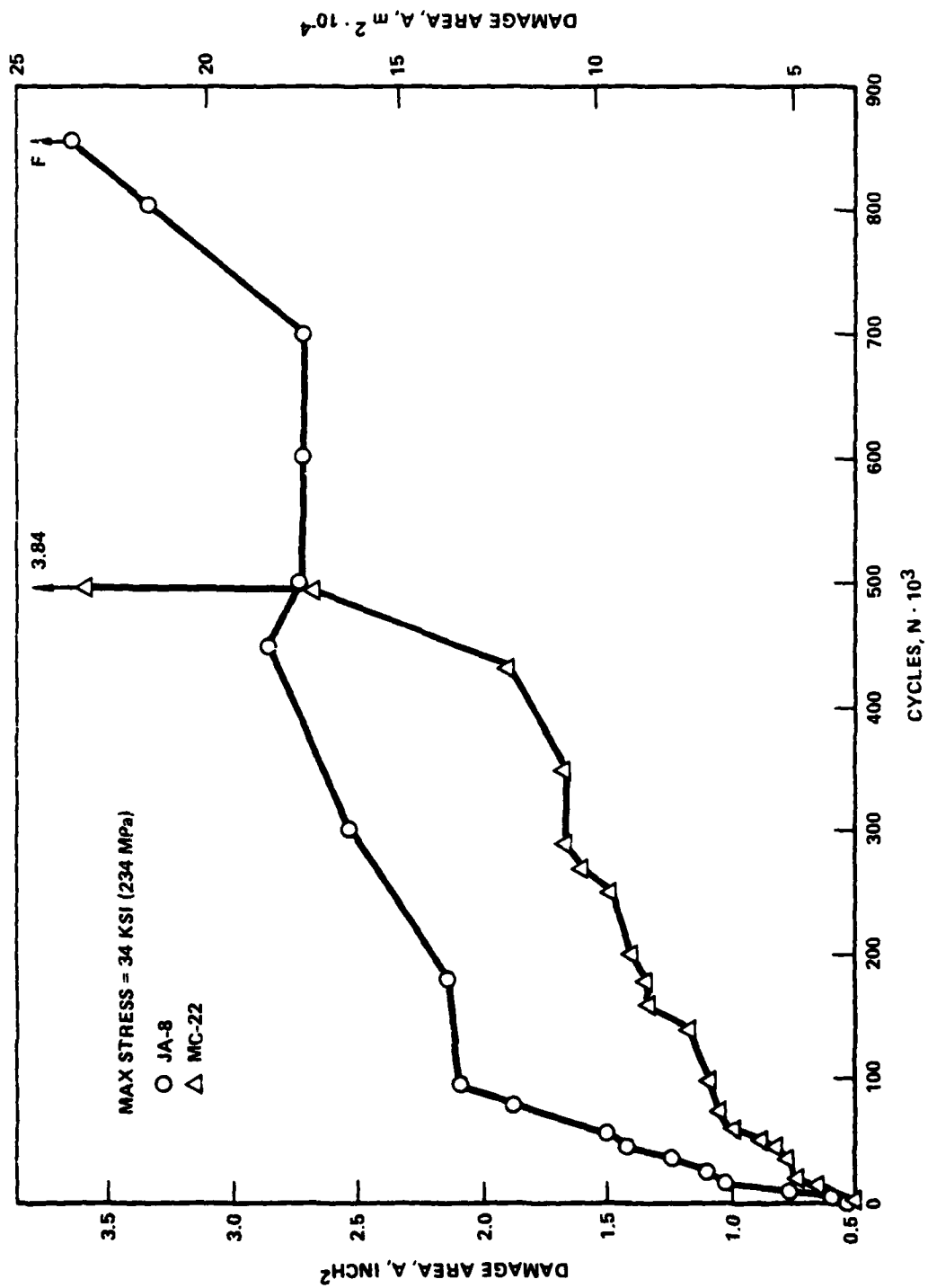


Figure 11: Damage Growth Characteristics of 24-ply 67% 0° Laminate Specimen Containing a Damaged Hole. 72°F (21°C), R = -1, Max Stress = 34 ksi (234 MPa)

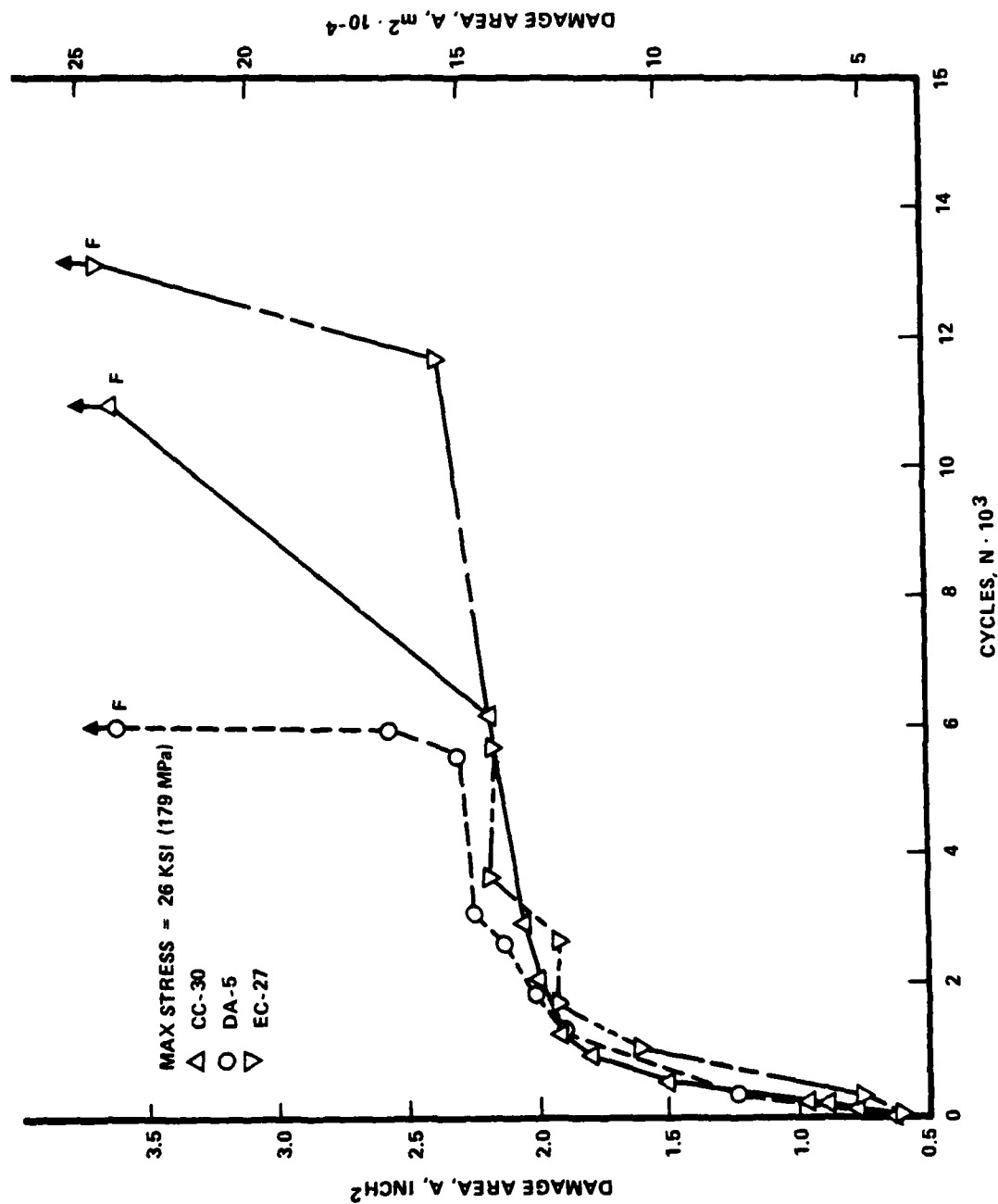


Figure 12: Damage Growth Characteristics of 32-Ply Quasi-Isotropic Laminate Specimens Containing a Damaged Hole. 72°F (22°C), R = -1, Max Stress = 26 ksi (179 MPa)

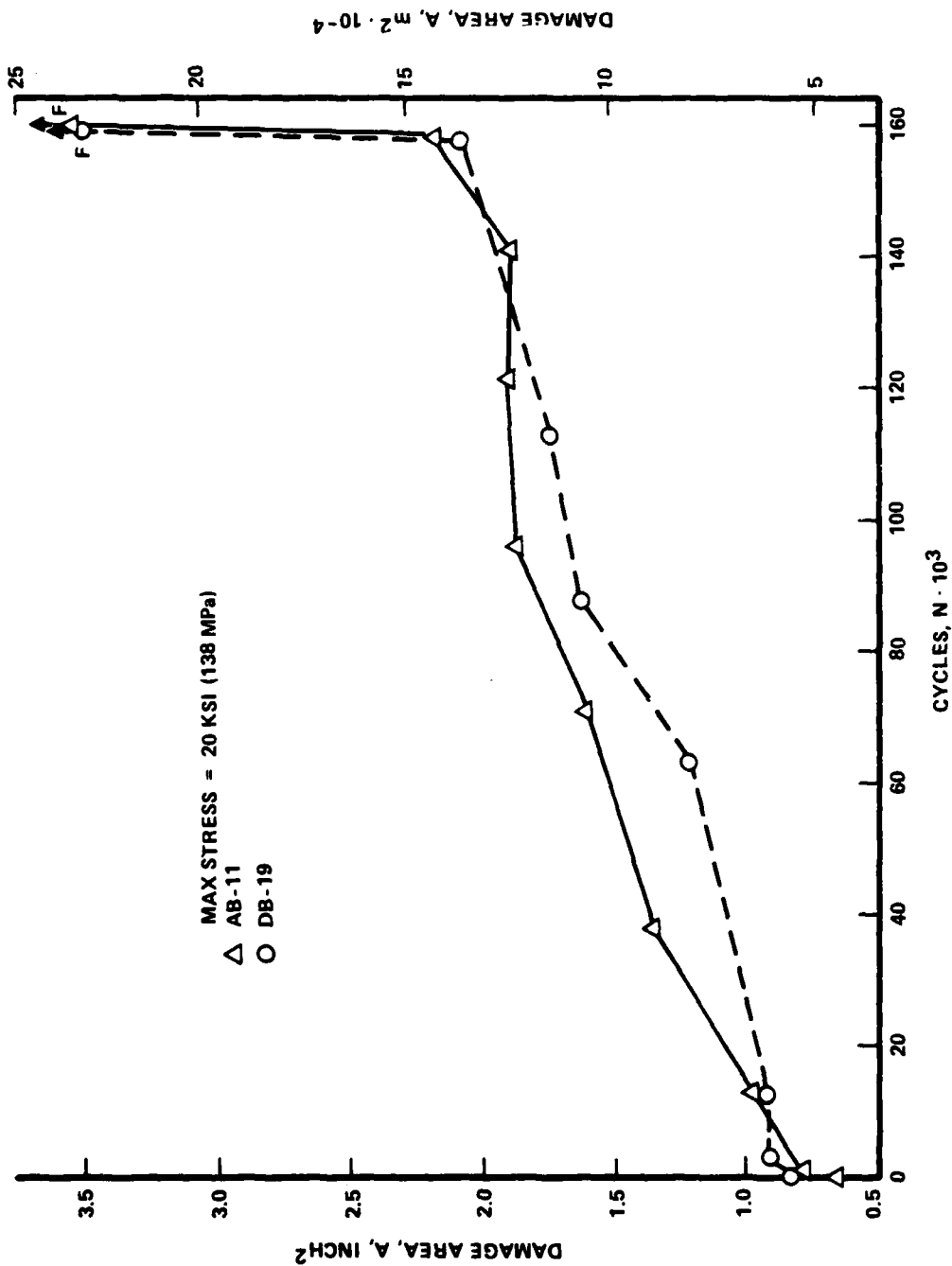


Figure 13: Damage Growth Characteristics of 32-Ply Quasi-Isotropic T300/5208 Laminate Specimens Containing a Damaged Hole. 72°F (22°C), R = -1, Max Stress = 20 ksi (138 MPa)

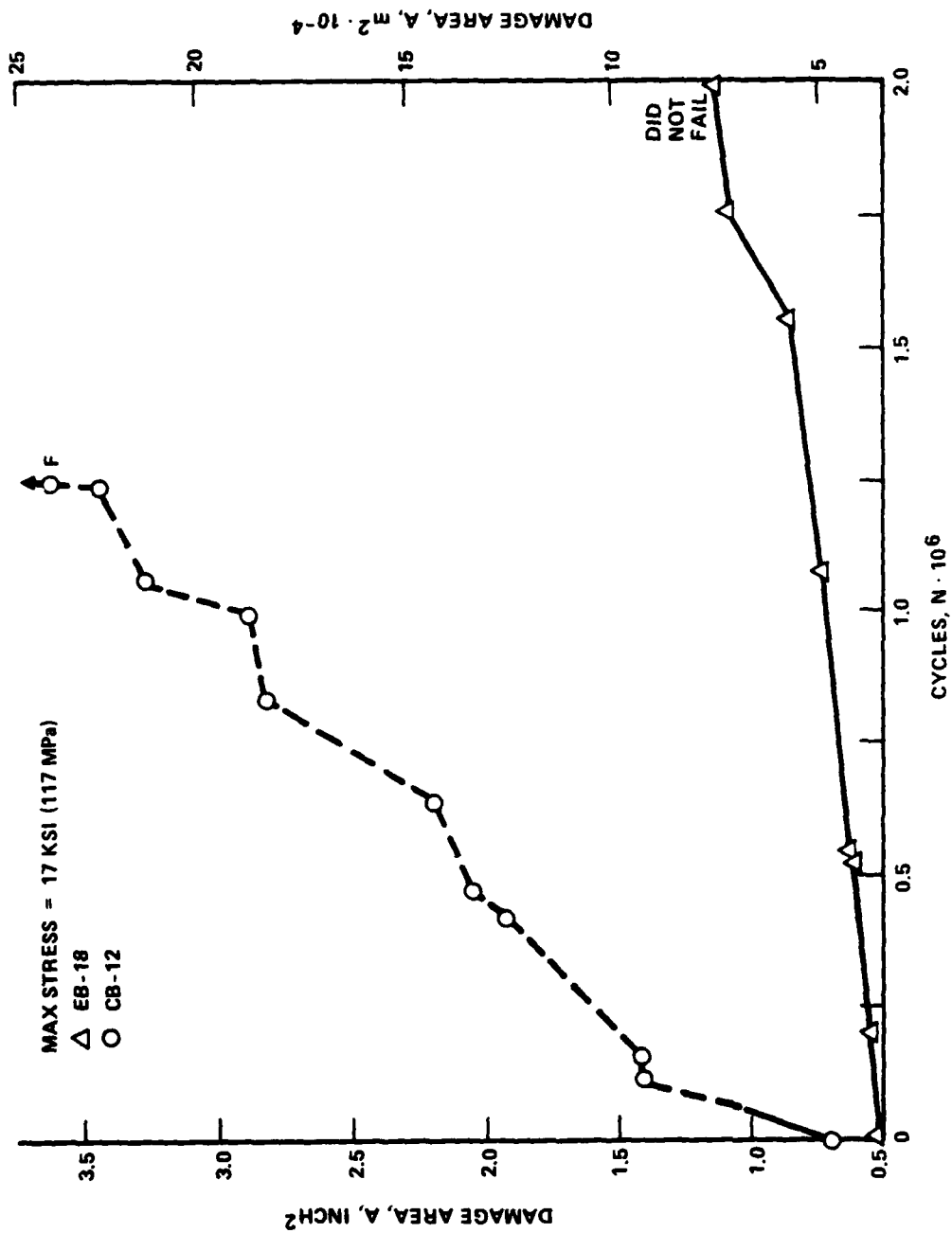


Figure 14: Damage Growth Characteristics of 32-ply Quasi-Isotropic Laminate Specimens Containing a Damaged Hole. 72°F (22°C), R = -1, Max Stress = 17 ksi (117 MPa)

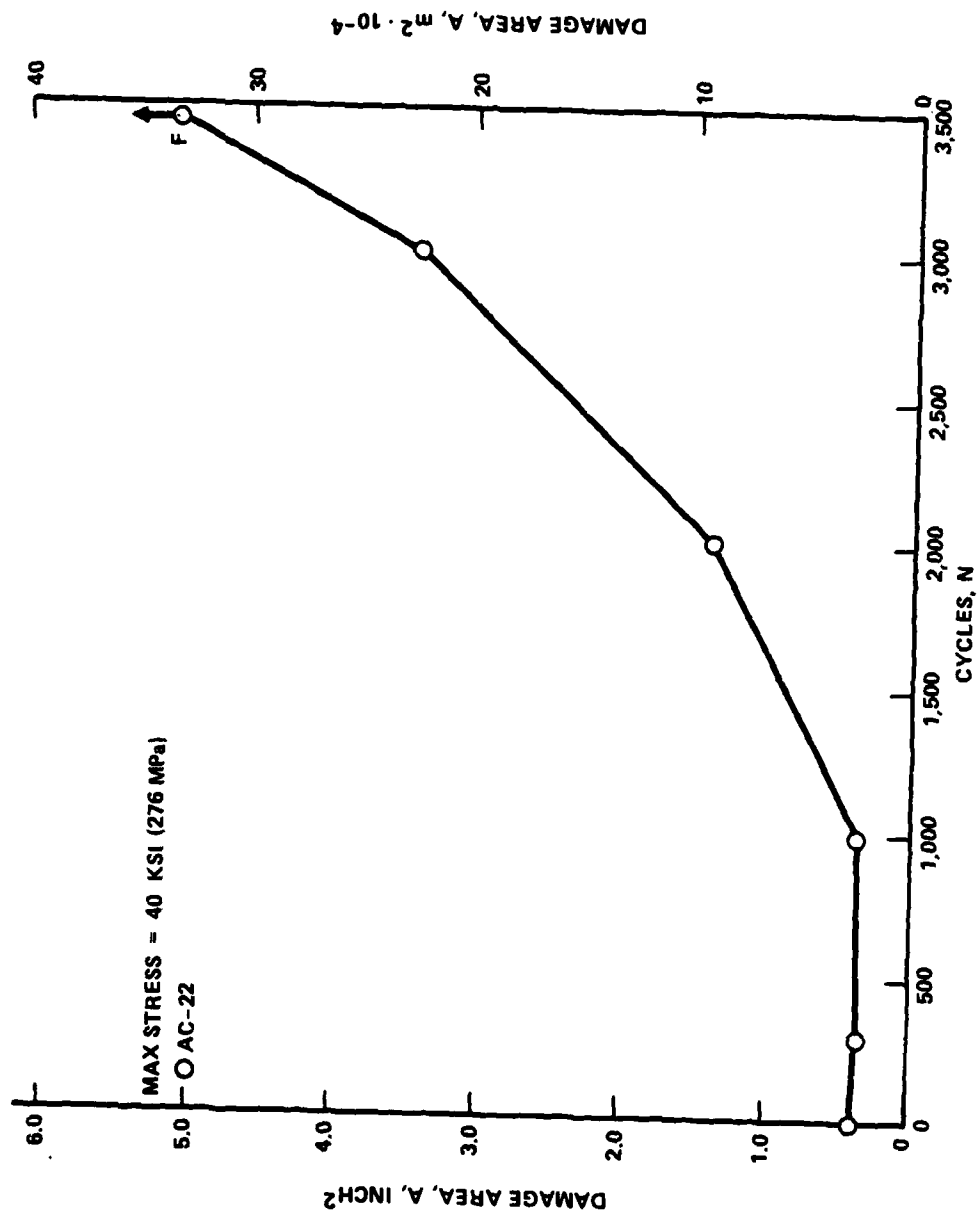


Figure 15: Damage Growth Characteristics of 32-Ply Quasi-Isotropic Laminate Specimens Containing Impact Damage 72°F (20°C), R = -1, Max Stress = 40 ksi (276 MPa)

measurable effect on the subsequent fatigue behavior of the 32-ply laminate, but results were less definitive for the 24-ply laminate where there is a slight indication of a possible shortening of the fatigue life at lower stresses. However, the limited sample size is small enough that the apparent reduction probably results from the inherent scatter under fatigue loading. A comparison of baseline and TBE exposed specimen fatigue results is presented in Figure 16.

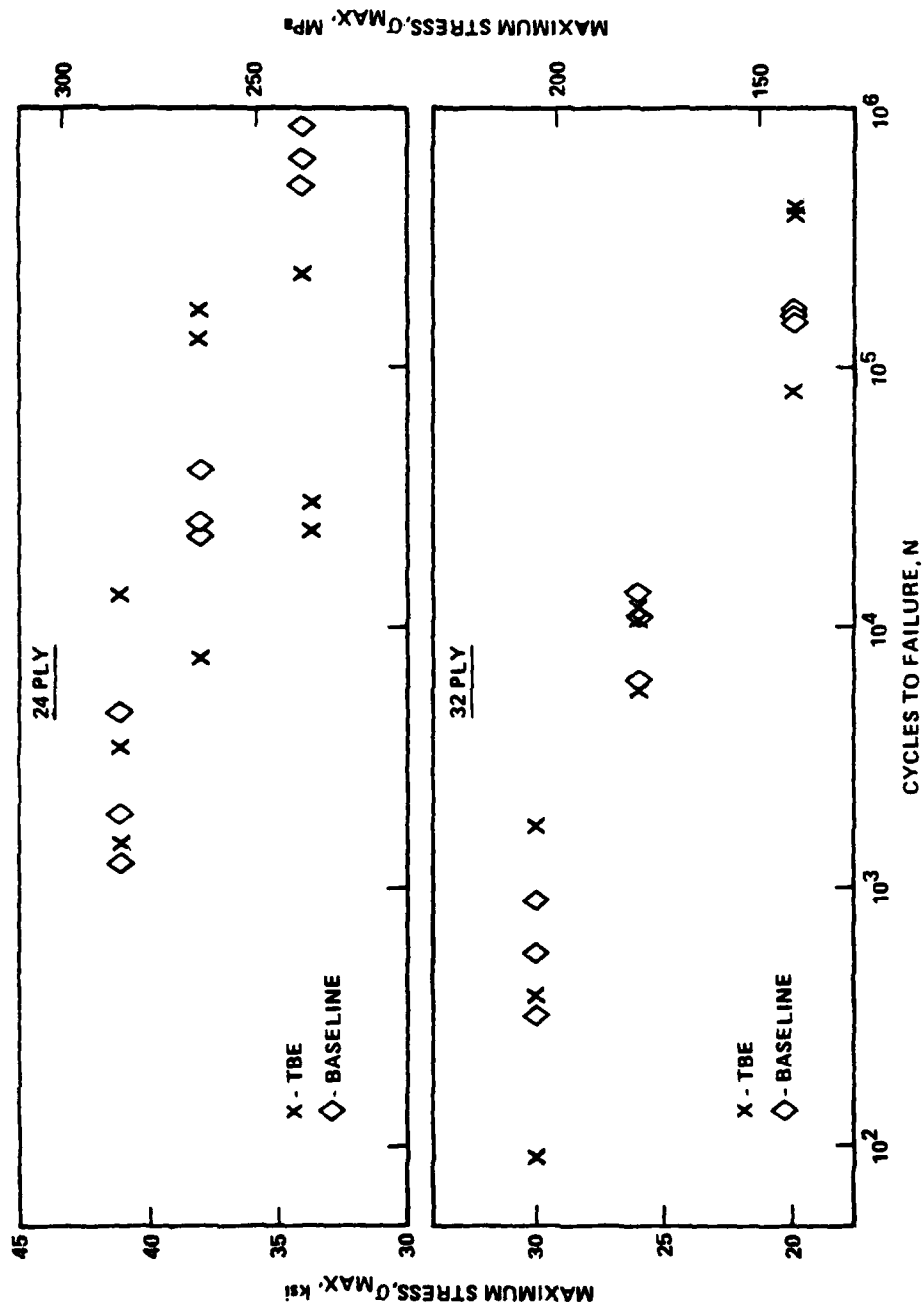


Figure 16: Comparison of Baseline and TBE Exposed Specimen Fatigue Results, $R = -1$, 5 Hz

SECTION 2

OVERVIEW OF TASKS II AND III

This section presents a discussion of the rationale for selection of material, specimen design and damage type, describes the specimen randomization procedure and outlines the test matrices for Tasks II and III.

2.1 MATERIAL SELECTION AND SPECIMEN DESIGN

The Task II and III investigations continued with the use of the same material, laminate and specimen design studied in Task I. A detailed discussion concerning their selection is available in the Task I Final Report ⁽¹⁾.

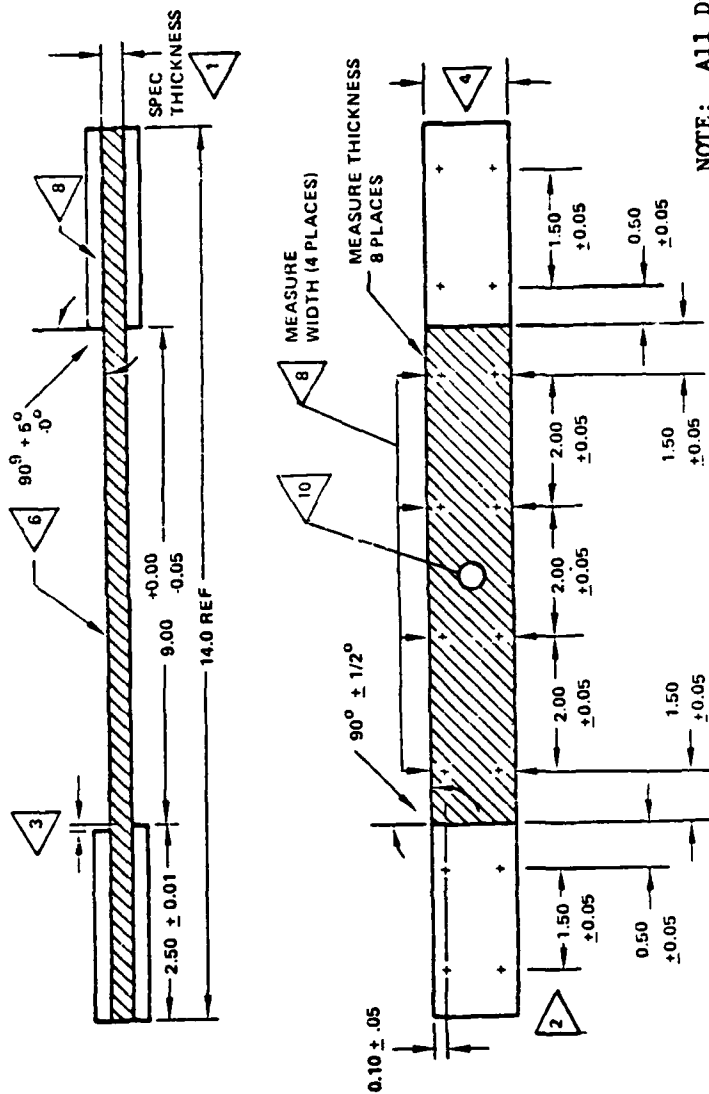
Primarily due to the extensive data base and generally large usage of the material, the selected fiber/resin system was Narmco's Rigidite T300/5208. Two laminate types were used throughout the study, a 24-ply, 67%-0° fiber laminate and 32-ply quasi-isotropic laminate having the following stacking sequences, respectively:

- o $(0/45/0_2/-45/0_2/45/0_2/-45/0)_s$
- o $(0/45/90/-45_2/90/45/0)_s$

Selection of these laminate stacking sequences was governed by many considerations including symmetry, tab bond strength requirements, free-edge stresses, adequate thickness for R = -1 loading, the requirement that one laminate be delamination prone (32-ply) while the other not (24-ply) and the extensive data base available for these laminates at the Lockheed-California Company.

Details of the specimen design for this program are presented in Figure 17. Features of this configuration leading to its selection are outlined below.

- o The geometry can be used for static tension and compression tests as well as for either tension-tension or tension-compression fatigue tests.
- o Adequate specimen length is important in composite specimens in order to obtain uniform stress conditions within the test section. Additionally, the selected length aids in minimizing end effects which could affect the damage propagation behavior without making the length too long to be able to control buckling in compression.
- o The specimen size is sufficient to provide a good probability of including point-to-point variations in material and layup properties, as well as large enough to be more representative of aircraft structures.
- o Variations in test results due to the discontinuity at the specimen edge will vary with laminate, material, and fabrication practice, but in general, will diminish as width is increased. The 3-inch (76 mm) width was chosen to minimize the free edge effects which are usually on the order of a laminate thickness (2, 3) so that these do not influence the damage propagation behavior.



NOTE: All Dimensions in Inches
(1 inch = 25.4 mm)

CENTERED HOLE, SEE SECTION 3.2

SPECIMENS TO BE FLAT OVER THE ENTIRE 14.0-INCH LENGTH WITHIN 0.01 INCHES. MEASURE AND RECORD ACTUAL FOR ALL SPECIMENS.

TAB EDGES TO BE PARALLEL TO SIDES OF SPECIMEN WITHIN 0.02 INCHES. OVERHANG NOT TO EXCEED 0.15

THE TAB AND SPECIMEN BONDING SURFACES TO BE THOROUGHLY SOLVENT CLEANED USING METHYL-ETHYL-KETONE PRIOR TO BONDING. A 350°F CURING ADHESIVE IS TO BE USED AND MUST COVER ENTIRE SURFACE UNIFORMLY.

WATER SPRAY MIST TO BE USED DURING SAWING OPERATIONS AND SOLUBLE OIL DURING GRINDING. MACHINED SURFACES TO BE RMS 50 OR BETTER. NO EDGE DAMAGE OR FIBER SEPARATION SHOULD BE VISIBLE

MEASURE SPECIMEN WIDTH 4 PLACES. WIDTH MUST NOT VARY BY MORE THAN 0.004 INCHES.

SPECIMEN WIDTH TO BE 3.00 ± 0.00 INCHES.

MISMATCH OF TABS FROM SIDE TO SIDE NOT TO EXCEED 0.01 INCHES.

TABS TO BE CUT FROM AN 8 PLY LAYUP FABRICATED FROM PREPREG OF 1581 GLASS FABRIC IN A 350°F CURING EPOXY. TAB PLUS ADHESIVE THICKNESS MUST NOT VARY SIDE TO SIDE OR END TO END BY MORE THAN 0.01 INCH AS MEASURED 8 PLACES.

SPECIMEN THICKNESS TO BE WITHIN ± 0.003 INCHES OF THE AVERAGE OF 8 THICKNESS MEASUREMENTS.

NOTE: ALL MEASUREMENTS TO BE MADE
USING A FLAT-HEADED MICROMETER

Figure 17: Three-Inch Wide Specimen Configuration, Drawing TL 1038

- o The specimen is wide enough such that a region exists where the stress distribution is not greatly influenced by the initial damage zone size at several flaw diameters away from the damage (4, 5).
- o Dimensions are convenient for fabrication and machining; tolerances required to obtain the necessary precision in test results are achievable without extraordinary measures.

The same specimen size and configuration were used for all tests including the static tension and compression tests in order to avoid any effects due to width or length differences.

2.2 SELECTION OF DAMAGE TYPE AND NDI METHOD

The preliminary considerations which led to the reduction of the many possibilities to two damage types and two NDI methods for investigation in Task I are detailed in the final report for that Task ⁽¹⁾. Based upon the Task I investigation a single damage type and NDI method were selected for further study in Tasks II and III. As outlined in Section 1.1 the effects of the two damage types upon subsequent static and fatigue behavior can be condensed in the following statements:

- Impact damage condition produced
 - o No consistent reduction in static tension strength for either of the two laminates.
 - o Consistent reduction in static compression strength for both laminates.
 - o Consistent S-N fatigue behavior for the 24-ply laminate only.
 - o Consistent damage growth characteristics for the 24-ply laminate only.

- Damaged hole condition produced
 - o Consistent reduction in static tension and compression strength for both laminates.
 - o Consistent fatigue and damage growth behavior for both laminates.

The impact damage size was apparently too near the threshold to consistently act as the primary cause of fracture in the 32-ply laminate with failures usually occurring away from the damage area which eliminated this condition as a viable candidate for further study. Therefore, the damage hole condition was selected for the efforts of Tasks II and III. The drilling procedure for introducing the damage is detailed in Section 3.2. The Holosonics System 400 ultrasonic inspection method described in Section 4.3 was selected for damage tracking in Tasks II and III since this system offered comparable results to the TBE-enhanced x-ray in Task I, was a more efficient system for this laboratory, had little potential for affecting the results as TBE enhanced x-ray might and offered B-scan as well as C-scan information so that location of delaminations through the thickness could be obtained.

2.3 PROCEDURE FOR RANDOM SPECIMEN SELECTION

Nine panels were available for each of the two laminate types in Task II and three for each laminate in Task III. Each panel contained 30 specimens as shown in Figure 18. Random selection was accomplished using software programs developed at the Lockheed-California Company and based upon unbiased, Monte Carlo random number generators. A listing of all of the tests to be performed in both tasks was prepared which included the number of specimens required for each test. For each task a random number table was generated for panel selection which consisted of repetitive groups of random numbers between one and the total number of panels per laminate type. These numbers were then listed alongside the test conditions thus assigning a panel number to each specimen required. Next, for each task a

Subpanel A										
A1	A2	A3	A4	A5	A6	QC TENSION RESIN CONT.	A7	A8	A9	A10
Subpanel B										
A11	A12	A13	QC TENSION RESIN CONT.	A14	A15	A16	A17	A18	A19	A20
Subpanel C										
A21	A22	A23	A24	A25	A26	A27	A28	A29	A30	BLANK

Figure 18: Typical Master Panel Specimen Layout

specimen number selection table was generated consisting of groups of random numbers between one and thirty. Each group was assigned a panel identification letter. The specimen numbers were then selected sequentially from the list corresponding to the designated panel. Thus, as illustrated in Table I, for the first test condition the first specimen would be from panel 9 which is I. The first specimen number from the list of 30 random numbers corresponding to panel I is 18. Since specimen 18 is from subpanel B, the specimen code is IB-18. The next time a specimen was selected from Panel I the second number from the list of 30 corresponding to "I" was used. In this manner all test panels were equally represented in a test type to eliminate any local variations that would bias the sample in terms of a single panel. An analysis of possible panel bias was performed and is available in Appendix J.

2.4 TASK II EXPERIMENTAL PROGRAM

The Task II test matrix is presented in Table II. Item 1 consisted of basic panel Q.C. tension tests to assure panel quality. Items 2 and 4 were designed to provide the static tension and compression strength distributions of the damaged specimens. For both items 2 and 4, fifteen replicates per test type/laminate were loaded to various percentages of ultimate and examined using ultrasonic Holscanning to define the damage zone growth characteristics. Item 3 tests were designed to provide additional information on the effect of higher strain rates on the fracture stress of the damaged laminates, since such rates are encountered in fatigue testing.

Twenty replicate specimens for each laminate were fatigue tested to failure to determine the fatigue life distribution statistical parameters (Item 5). A Holscan ultrasonic unit was used to monitor the damage growth of each specimen a minimum of ten times during its life. From these results a statistically based fatigue life distribution and damage growth rate distribution were obtained. Also, five cycle levels were selected for the

TABLE I
ILLUSTRATION OF RANDOMIZATION OF PANELS BY TEST

TASK II
LAMINATE: 24-PLY
PANEL DESIGNATION: CODE A (1) F (6)
B (2) G (7)
C (3) H (8)
D (4) I (9)
E (5)

Test Type	No. of Specimens	Panel	Corresponding Spec. Number	
Undamaged Low Strain Rate Tension	4	9	I-18	1st spec. from panel I
		5	E-28	1st spec. from panel E
		2	B-11	1st spec. from panel B
		8	H-14	1st spec. from panel H
Undamaged High Strain Rate Tension	4	1	A-22	1st spec. from panel A
		7	G-13	1st spec. from panel G
		6	F-22	1st spec. from panel F
		4	D-9	1st spec. from panel D
Undamaged Low Strain Rate Compression	4	3	C-13	1st spec. from panel C
		3	C-29	2nd spec. from panel C
		6	F-28	2nd spec. from panel F
		5	E-2	2nd spec. from panel E
Undamaged High Strain Rate Compression	4	2	B-3	2nd spec. from panel B
		etc.	etc.	etc.
Damaged Low Strain Rate Tension	15	4	D-23	2nd spec. from panel D
		etc.	etc.	etc.
Damaged Low Strain Rate Compression	15	1	A-4	4th spec. from panel A
		etc.	etc.	etc.
Fatigue Life Distribution etc.	20	8	H-8	5th spec. from panel H
		etc.	etc.	etc.

TABLE II
TASK II TEST MATRIX

Item	Type of Test	Test Conditions	Replicate Per Condition	Data Required	Total Tests
1.	QA Tension Tests	2 Laminates, no damage = 2	2 per panel x 8 panels x 2 conditions	Basic Tensile Data	32
2.	A. Static Tension Strength Distribution	2 Laminates x 1 damage = 2	15 replicates x 2 conditions = 30	Damaged Tension Strength Distribution	30
	B.		Plus 3 x 2 conditions = 6	Static Loading Damage Growth Characteristics	6
3.	A. Static Tension and B. Compression	2 Laminates x 1 damage = 2	5 replicates x 1 high strain rate x 2 tests x 2 conditions = 20	Strain rate effect	20
4.	A. Static Compression Strength Distribution	2 Laminates x 1 damage = 2	15 replicates x 2 conditions = 30 plus 3 x 2 conditions = 6	Damaged Compression Strength Distribution Static Load Damage Growth Characteristics	30 6
5.	Fatigue Life Distribution	2 Laminates x 1 damage = 2	20 replicates x 2 conditions = 40	Fatigue Life Distribution and Damage Growth Characteristics	40
6.	Tension Residual Strength	2 Laminates x 1 damage = 2	10 replicates x 5 cycles x 2 conditions = 100	Residual Strength at Five N Levels. Damage Zone Growth in Interval	100
7.	Compression Residual Strength	2 Laminates x 1 damage = 2	10 replicates x 5 cycles x 2 conditions = 100	Residual Compressive Strength at five N Levels. Damage Growth in Interval	100
8.	Destructive Inspection	2 Laminates x 1 damage = 2	3 replicates x 5 cycles x 2 conditions = 30	Destructive Definition of Damage Zone Characteristics	30
9.	A. Baseline Tension and B. Compression	2 Laminates, no damage = 2	4 replicates x 2 strain rates x 2 tests x 2 conditions	Undamaged Material Static Strength	32
					426

residual strength study, based on the observed damage growth characteristics.

Items 6, 7, and 8 constituted the residual strength portion of this task. Twenty-three specimens of each laminate were initially inspected using the Holscan ultrasonic unit and then fatigue cycled to one of the five pre-selected cyclic N values, removed and again inspected using the Holscan. Three of the replicates were destructively analyzed to determine the damage zone characteristics by both metallographic sectioning and matrix dissolution (deplying) followed by examination by optical microscopy. Ten of the replicates were statically tested to failure in tension and ten in compression. This sequence was repeated for each of the five selected cyclic N values. Item 9 tests were designed to provide baseline material property data for undamaged laminates.

2.5 TASK III EXPERIMENTAL PROGRAM

The Task III test matrix is presented in Table III. Baseline static properties were determined in Items 1 through 3. Since Task III Specimens were fabricated at the same time as those of Task II the tests of 1, 2A, and 3A were intended to identify any change in static strength which may have occurred in the specimens during shelf storage. Tests of 2B, 3B, and 3C were to provide baseline data for new environmental and constraint conditions to which specimens were to be subjected during fatigue loading.

Three replicate specimens for each laminate were fatigue tested to failure to obtain a typical fatigue life for each of the three variations in fatigue test parameters as indicated in item 4 of Table III. A Holscan ultrasonic unit was used to monitor the damage growth of each specimen for a minimum of ten times during the life. From these results, typical fatigue life and damage growth rate characteristics were obtained for each of the new fatigue test conditions.

TABLE III: TASK III TEST MATRIX

Item	Test Type	Test Condition	Replications	Data Required	Total Specimens
1.	Q.A. Tension	2 laminates, no damage = 2	2 conditions x 2 each x 3 panels = 18	Basic Tension	12
2.	Static Tension	2 laminates x 1 damage = 2 A. RT Lab Air B. New Environment	2 cond. x 3 each = 6 2 cond. x 5 ea. x 2 strain rates = 20	Initial Strength for 2 Environments	26
3.	Static Compression	2 laminates x 1 damage = 2 A. Constraint # 1 B. Constraint # 2 C. New Env. Constr. #1	2 cond. x 3 each = 6 2 cond. x 3 each = 6 2 cond. x 5 ea. x 2 strain rates = 20	Initial Strength for 2 constraint conditions and environments	32
4.	Fatigue to Failure	2 laminates x 1 damage = 2 A. Task II R and Stress level, constr. cond. #2 B. New R and stress level, constr. cond. #1 C. Task II R, stress level, new environ.. constraint # 1	2 cond. x 3 each = 6 2 cond. x 3 each = 6 2 cond. x 3 each = 6	Basic Fatigue life and damage growth character- istics	18
5.	Tension Residual Strength	2 laminates x 1 damage = 2 - Fatigue Condition A - Fatigue Condition B - Fatigue Condition C	2 cond. x 3N x 3 ea. = 18 2 cond. x 3N x 3 ea. = 18 2 cond. x 3N x 3 ea.	Residual Tension Strength vs N added damage growth data	54
6.	Compression Residual Strength	2 laminates x 1 damage = 2 - Fatigue Condition A - Fatigue Condition B - Fatigue Condition C	2 cond. x 3N x 3 ea. = 18 2 cond. x 3N x 3 ea. = 18 2 cond. x 3N x 3 ea.	Residual Compre- ssion Strengths vs N, added damage growth data	54
					196

* Constraint Condition # 1 = Task II Fatigue Guide Support
2 = 4-bar Column Buckling Support

Three cycle levels were selected for the residual strength study based upon the observed damage growth characteristics. Specimens were initially inspected with the Holskan then fatigue cycled to one of the three preselected cyclic N values, removed and scanned again. Half of each set of specimens were statically tested to failure in tension (Item 5) and half in compression (Item 6). This sequence was repeated for each of the selected cyclic N values.

SECTION 3
MATERIAL AND SPECIMEN CHARACTERIZATION -- TASKS II AND III

All material procurement, panel fabrication and specimen fabrication were controlled to conform to the program Quality Control Plan requirements as presented in Volume III, Appendix A. Characteristics of the graphite/epoxy material used in this program are presented in this section.

3.1 PREPREG QUALITY CONTROL RESULTS

The graphite/epoxy material for the Task II and Task III studies was procured from Narmco Materials, Inc., as a single batch consisting of 18 rolls of 12 inch (305mm) T300/5208 tape designated as batch #1295. Narmco batch #1295 further identified by the Lockheed code WI had a resin content of 40% to 44% comparable to the 40% - 43% range for batch #1079 (TY) used in Task I. However, the average fiber strength of WI was 7.5% higher than that of TY as shown in Table IV. A slight (approximately 3%) increase in modulus is also apparent.

Batch acceptance testing was conducted according to the above mentioned Quality Control Plan by the Lockheed-California Company Quality Control Division and found to conform to all requirements. Results of these tests and those of the Narmco Materials, Inc. certification tests are presented in Tables V and VI.

TABLE IV
PROPERTIES OF T300 FIBERS USED IN TASKS I, II, & III

Narmco Batch No.	Lockheed Batch ID	Fiber Lot No.	Fiber Density lbs/in ³	Fiber Density g/cc	Fiber Tensile, Strength ksi	Fiber Strength MPa	Fiber Modulus psi x 10 ⁶	Fiber Modulus GPa
1079 (Task I)	TY	425-2	0.0625	1.73	440	3034	33.4	230
		433-2	0.0632	1.75	436	3006	33.6	232
		434-2	0.0628	1.74	448	3089	33.0	228
		Average	0.628	1.74	441	3043	33.3	230
1295 (Tasks II & III)	WI	571-2	0.0628	1.74	489	3372	34.0	234
		574-2	0.0636	1.76	485	3344	34.6	239
		575-2	0.0632	1.75	471	3247	34.6	239
		607-2	0.0632	1.75	469	3234	34.0	234
		620-2	0.0636	1.76	454	3130	34.1	235
		Average	0.0632	1.75	474	3268	34.3	236

TABLE V. SUMMARY OF THE NARMCO QUALITY CONTROL TESTS FOR RIGIDITE
5208-T300 CERTIFIED TEST REPORT NO. 35953

MATERIAL: Rigidite 5208-T300-12"
Batch # 1295

Roll	Amount	Resin Content	Areal Fiber Weight	Mfg. Date	Test Date
1	25.0 lbs.	42%	142 grams/sq. meter	11-14-78	11-16-78
2	25.1	42	142		
3	25.0	41	142		
4	24.9	42	141		
5	25.4	43	141		
6	26.6	44	141		
7	25.4	42	141		
8	25.7	42	142		
9	25.5	43	142		
10	25.4	43	142		
11	26.3	42	141		
12	25.3	41	142		
13	26.0	42	141		
14	26.6	42	142		
15	25.9	40	142		
16	25.8	42	142		
17	26.7	43	142		
18	28.2	44	142		

Volatiles: 0.4%
Flow: 24%
Gel Time: 24'43" min. @ 350°F.
Tack: Acceptable

Specific Gravity: 1.57/1.57/1.57: 1.57 g/cc average (8 plies)
1.56/1.57/1.57: 1.57 g/cc average (16 plies)
Fiber Volume: 65/64/65: 65% average (8 plies)
64/65/64: 64% average (16 plies)
Cured Ply Thickness: 0.0052" (8 plies, Tensile panel)
0.0049" (16 plies, Flex and Shear panel)
RT, 0° Flex: 261,100/282,820/290,420: 278,110 psi average
RT, 0° Flex Modulus: 19.86/19.57/20.21: 19.88 x 10⁶ psi average
RT, 0° Tensile: 225,960/219,170/206,540: 217,220 psi average
RT, 0° Tensile Modulus: 19.84/20.12/20.08: 20.01 x 10⁶ psi average
180°F., 0° Flex: 226,990/264,010/265,670: 252,230 psi average
180°F., 0° Flex Modulus: 18.77/19.10/19.44: 19.10 x 10⁶ psi average
RT Short Beam Shear: 19,440/18,010/18,780: 18,740 psi average
180°F. Short Beam Shear: 16,810/17,520/16,850: 17,060 psi average

RAW FIBER DATA

Lot #	Tensile Modulus	Tensile Strength	Yarn Density
620-2	34.1 psi x 10 ⁶	454 psi x 10 ³	1.76 g/cc
575-2	34.6	471	1.75
574-2	34.6	485	1.76
571-2	34.0	489	1.74
607-2	34.0	469	1.75

TABLE VI. SUMMARY OF LOCKHEED QUALITY CONTROL TESTS FOR MANMCO RIGIDITE 8208-T300 MATERIAL BATCH #1295

Material Property	Specification Requirements C-22-1379A/111 (9/13/77)	Measured Property	Accepted
1. Areal Fiber Weight (4 req)	139 - 149 g/m ²	140 g/m ² 142 " 141 " 141 " Avg. 141 "	X X X X X
2. Infrared Spectrophotometric Anal. (1 req)	Conformance to file spectrum	-	X
3. Volatiles (2 req) 60± 5 min at 350° F	3% Maximum	0.09% edge 0.16% center	X X
4. Dry resin content (4 req)(Soxhlet)	38 - 44%	42.5% left 41.9% left center 43.3% right center 43.2% right Avg. 42.7%	X X X X X
5. Resin Flow at 350° F and 85 psi (2 req)	15 - 29%	20.4 21.0	X X
6. Gel Time at 350° F (2 req)	For information only	21.5 minutes 21.9 minutes	- -
7. Fiber Orientation	0°	-	X
1. Cured Fiber Volume, 16 ply panel (3 req)	CURED LAMINATES 60 - 68%	65.6 66.0 65.3 Avg. 65.6%	X X X X
2. Cured Fiber Volume, 8 ply panel (3 req)	60 - 68%	62.9 63.2 63.4 Avg. 63.2%	X X X X
3. Specific Gravity, 16 ply panel (3 req)	1.55 - 1.62	1.585 1.584 1.586 Avg. 1.585	X X X X

TABLE VI. SUMMARY OF LOCKHEED QUALITY CONTROL TESTS FOR NAMCO RIGIDITE 5208-T300 MATERIAL BATCH # 1295 (Continued)

Material Property	Specification Requirements C-22-1379/111 (9/13/78)	Measured Property	Accepted
4. Specific Gravity, 8 ply panel (3 req)	1.55 - 1.62	1.569 1.568 <u>1.568</u> Avg. 1.568	x x x
5. Tensile Strength, longitudinal at 75°F (3 req)	170 ksi min.	220 222 <u>219</u> Avg. 220 ksi	x x x
6. Elastic Modulus, longitudinal at 75°F (3 req)	20·10 ⁶ psi min.	21.1·10 ⁶ 21.1·10 ⁶ <u>21.4·10⁶</u> Avg. 21.2·10 ⁶	x x x
7. Flexural Strength at 75°F (3 req)	210 ksi min.	263 270 <u>269</u> Avg. 268 ksi	x x x
8. Flexural Modulus at 75°F (3 req)	18·10 ⁶ psi min.	20.2 18.6 <u>19.3</u> Avg. 19.4·10 ⁶ psi	x x x
9. Flexural Strength at +180°F (3 req)	200 ksi min.	231 241 <u>227</u> Avg. 233 ksi	x x x
10. Flexural Modulus at +180°F (3 req)	16·10 ⁶ psi min.	19.3·10 ⁶ 19.9·10 ⁶ <u>18.7·10⁶</u> Avg. 19.3·10 ⁶ psi	x x x
11. Short Beam Shear Strength at 75°F (3 req)	13 ksi min.	18.5 17.8 <u>17.9</u> Avg. 18.1 ksi	x x x

TABLE VI. SUMMARY OF LOCKHEED QUALITY CONTROL TESTS FOR MAPCO RIGIDITE 5208-T300 MATERIAL BATCH #1295 (Continued)

Material Property	Specification Requirements C-22-1379/111 (9/17/78)	Measured Property	Accepted
12. Short Beam Shear Strength at +180° (3 req)	12 ksi min.	15.0 16.1 15.0 Avg. 15.4 ksi	x x x x
13. Thickness per ply, 16 ply panel (5 req)	0.0046 - 0.0056 inch	0.0048 0.0047 0.0047 0.0047 0.0048 Avg. 0.0047 inch	x x x x x x
14. Thickness per ply, 8 ply panel (5 req)	0.0046 - 0.0056 inch	0.0051 0.0051 0.0052 0.0052 0.0051 Avg. 0.0051 inch	x x x x x x
15. Digestion: Acid, Temperature, Time Resin Content	Information Only	H ₂ SO ₄ /350°F/2 hrs. 8 Ply = 30.0 wt. % 16 ply = 28.0 wt. %	

3.2 PANEL AND SPECIMEN FABRICATION

Subsequent to material acceptance panels were fabricated for both Tasks II and III according to the Quality Control Plan. Twenty-four 36 in. x 46 in. (914mm x 1168mm) panels were fabricated, nine of each laminate type (24-ply 67%, 0°, 32-ply quasi-isotropic) for Task II and three of each laminate for Task III. Panel numbers with the material code letter assigned to each panel are presented in Table VII. All panels received a standard production ultrasonic C-scan inspection using 1/4 and 1/2 inch diameter teflon disc standards, the results of which are also summarized in Table VII.

Each panel was then sectioned into three subpanels A, B, and C, 36 in. wide by 14 in. long (914mm x 356mm) from each of which ten specimens of the configuration previously shown in Figure 17 were then machined.

A 1 inch by 10.5 inch (25mm x 267mm) Q. C. tensile specimen was also removed from subpanels A & B. Panel layout was displayed in Figure 18.

For both laminate types, a center hole was drilled in the 3 inch (76mm) wide specimen blanks using a standard 3/8 inch (9.6mm) high speed drill with a drill speed of 600 rpm and feed rate of 0.004 in./rev (0.102mm/rev). To control damage size an Aluminum back-up plate with a central 0.625 in. (15.9mm) diameter hole opposite the drill bit was employed.

Tabs were bonded to the specimen blanks and specimens were inspected to drawing TL-1038 (Figure 17). Specimens not meeting drawing requirements were not used for this investigation. Adequate numbers of specimens were fabricated to allow for the exclusion of out-of-tolerance coupons. Specimens were weighed after fabrication and prior to each test to monitor possible moisture sorption during storage. These data are available in Volume III, Appendix B. All specimens were examined using the Holskan 400

TABLE VII
PANEL IDENTIFICATION CODES

Laminate Type	Panel No.	Assigned Panel Code	C-Scan Inspection Results
TASK II			
24-Ply 67% - 0°	2WI 1436	A	No Indications
	2WI 1408	B	
	1WI 1438	C	
	1WI 1406	D	
	1WI 1408	E	
	2WI 1438	F	
	1WI 1440	G	
	2WI 1440	H	
	1WI 1441	I	
32-Ply Quasi-Isotropic	1WI 1411	J	No Indications
	2WI 1411	K	
	1WI 1429	L	
	2WI 1429	M	
	1WI 1431	N	
	2WI 1431	P	
	1WI 1435	Q	
	2WI 1435	R	
	1WI 1436	S	
TASK III			
24-Ply 67% - 0°	2WI 1441	A	No Indications
	1WI 1443	B	
	2WI 1477	C	
32-Ply Quasi-Isotropic	1WI 1466	D	No Indications
	2WI 1466	E	
	1WI 1478	F	

system and the location, size and characteristics of the damage zone were photographically recorded. Specimens were identified using the following numbering system: AB-10 -- Panel I.D. = A, subpanel I.D. = B, specimen location within the panel = 10.

Samples for resin content analysis were removed from either subpanel A or B and were adjacent to the QC tensile specimens. Triplicate specimens were then cut from each sample and the density, specific gravity, fiber content and resin contents determined⁽⁶⁾.

The procedures used to determine the reported values were as follows:

The fiber volume testing was conducted in accordance with ANSI/ASTM D3171-73, Procedure A: "Fiber Content of Reinforced Resin Composites," except as noted below.

- a. Determinations for each strip were carried out in triplicate
- b. Specimen size was approximately 1 gram rather than 0.3 grams
- c. The column of Nitric Acid used for digestion was increased from 30 milliliters to 100 milliliters because of the larger specimen mass used.

The specific gravity testing was conducted in accordance with ANSI/ASTM D792-66, Procedure A-1: "Specific Gravity and Density of Plastics by Displacement."

Void content was calculated per ANSI/ASTM D2734, method B: "Void Content of Reinforced Plastics". The following values were used for the fiber and resin densities:

$$D_f = 1.75 \text{ gm/ml}$$

$$D_r = 1.265 \text{ gm/ml}$$

Resin, fiber and void analysis results are reported in Table VIII. All

TABLE VIII
RESIN, FIBER, AND VOID ANALYSIS RESULTS

	Panel Production No.	Resin Content wt. %	Fiber Content Vol %	Void ^a Content Vol %	Density gm/cc
24-Ply Task II	1WI 1406	27.5	65.5	0.12	1.581
	1WI 1408	26.8	66.2	0.20	1.584
	2WI 1408	27.7	65.1	0.41	1.576
	2WI 1436	27.1	65.7	0.45	1.578
	1WI 1438	28.6	64.3	0.10	1.576
	2WI 1438	27.7	65.1	0.28	1.577
	1WI 1440	27.9	65.1	0.02	1.581
	2WI 1440	27.8	65.2	0.07	1.580
	1WI 1441	28.1	64.8	0.15	1.577
24-Ply Task III	2WI 1441	27.9	65.1	-0.19 ^b	1.580
	1WI 1443	28.5	64.4	-0.14 ^b	1.576
	2WI 1477	27.6	65.3	-0.04 ^b	1.579
32-Ply Task II	1WI 1411	27.9	64.9	0.31	1.576
	2WI 1411	28.4	64.3	0.33	1.573
	1WI 1429	27.9	64.8	0.39	1.575
	2WI 1429	27.7	65.2	0.31	1.577
	1WI 1431	28.3	64.5	0.28	1.574
	2WI 1431	27.9	65.1	0.16	1.579
	1WI 1435	28.3	64.6	0.18	1.576
	2WI 1435	27.8	65.2	0.22	1.578
	1WI 1436	27.9	65.0	0.19	1.578
32-Ply Task III	1WI 1466	28.9	63.9	-0.05 ^b	1.573
	2WI 1466	28.5	64.3	-0.09 ^b	1.575
	1WI 1478	27.7	65.2	0.03	1.578
Average		27.9	65.0		1.577
Standard Dev.		0.47	0.51		0.0027
Coeff. of Var. %		1.68	0.78		0.17

^a Void content determined by standard chemical analysis procedures, accuracy is $\pm 1.6\%$

^b Artifact of chemical analysis procedure

results show little variation and are well within the range specified in the Quality Control Plan of $65 \pm 2\%$ for the fiber volume fraction, 1.58 ± 0.02 for specific gravity and void content $\ll 1\%$.

Calculated values of less than 1% for void content are an indication of the laminate density quality but do not yield a true void content because of the uncertainty in fiber and matrix densities and amount of absorbed moisture present in the test sample. The inherent error in this method of void determination can result in physically impossible negative void values. However, low void contents obtained in conjunction with the lack of C-scan indications imply that the void content of all the panels is extremely low.

SECTION 4

EXPERIMENTAL PROCEDURES

4.1 STATIC TENSION AND COMPRESSION TEST PROCEDURES

All tests were conducted in a 100 kip (440 kn) MTS closed loop universal test machine equipped with four-inch hydraulic self-aligning grips. Coupon alignment was assured by using a special exterior fixture attached to the grip assembly.

The 180°F (82°C) tests of Task III were conducted with a metal enclosure surrounding the test equipment, the internal space of which was supplied with heated air. This arrangement provided specimen temperatures which were uniform throughout the gage length and controlled to $\pm 2^{\circ}\text{F}$ ($\pm 1^{\circ}\text{C}$). A thermo-couple was attached to each specimen to monitor temperature. All other tests were performed at room temperature in laboratory air. High strain rate tests were conducted at $0.5\text{--}5\text{ min}^{-1}$ while those designated as standard (or low) strain rate progressed at 0.005 min^{-1} . Either a one-inch (25mm) or two-inch (51mm) extensometer was employed in testing of the one-inch (25mm) wide Quality Control tensile specimens. For three-inch (76mm) wide specimens, a continuous record of applied load vs stroke was obtained for each specimen. The decision not to use an extensometer was based on Task I experience wherein the extensometer was found to slip as a result of the occurrence of out of plane displacements in the region surrounding the hole. Modulus values determined from crosshead displacement data compared favorably with Task I results where displacements were obtained from extensometer measurements. A discussion of the interpretation and use of crosshead displacement data and comparison with extensometer and strain gage results are presented in Section 5.

Compression specimens tested in Task II and those in Task III with the exception of item 3b (see test matrix) were supported with the same buckling guides utilized for fatigue testing, shown installed in Figure 19. One set of compression tests in Task III (item 3b) was conducted employing four-bar buckling supports for specimen restraint. Both types of supports are described in more detail in Section 4.2.

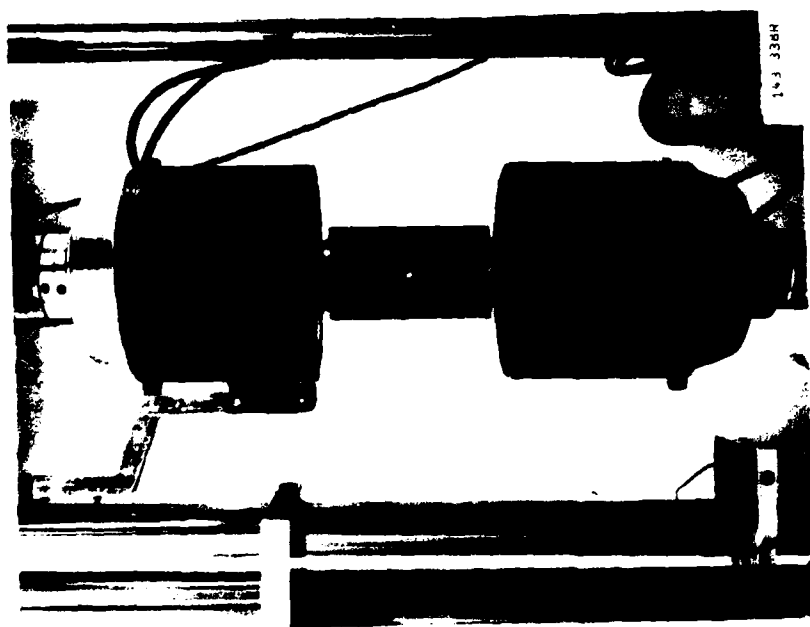
4.2 FATIGUE TEST PROCEDURES

Fatigue tests were conducted in vertical closed-loop electro-hydraulic test machines at a frequency of 5 Hz until failure or 2×10^6 cycles was achieved. Fatigue grips were primarily of the friction bolt type with integral alignment fixtures, although hydraulic grips were also employed. Each of the closed-loop electro-hydraulic fatigue machines is equipped with a peak and valley load monitoring system which allows the monitoring of the load signal maximum peak, maximum valley, and minimum peak and minimum valley with an accuracy of $\pm 1.0\%$ of full scale readings. Maximum peak and valley loads are monitored continuously and can be preset to sound an alarm or stop the test in the event of any loading deviation. Since previous work ⁽⁷⁾ has shown that early failures may result due to initial loading at normal fatigue loading rates, the following test start up procedure was adopted. Loading for the first ten cycles of the life of a specimen was conducted at a frequency of 0.05Hz then the frequency was increased to 5 Hz and the test continued to failure at 5 Hz. Damage zone size measurements and damage characterization examinations were made periodically during each test using the modified Holskan 400 Ultrasonic NDI system described in Section 4.3.

Due to the large compressive component experienced during the fully reversed fatigue tests, the method of test specimen support was of major



143 3392



143 3384

Figure 19: Specimen Supported by Restraining Fixture Used in Static Compression and Fatigue Tests Installed in Universal Testing Machine

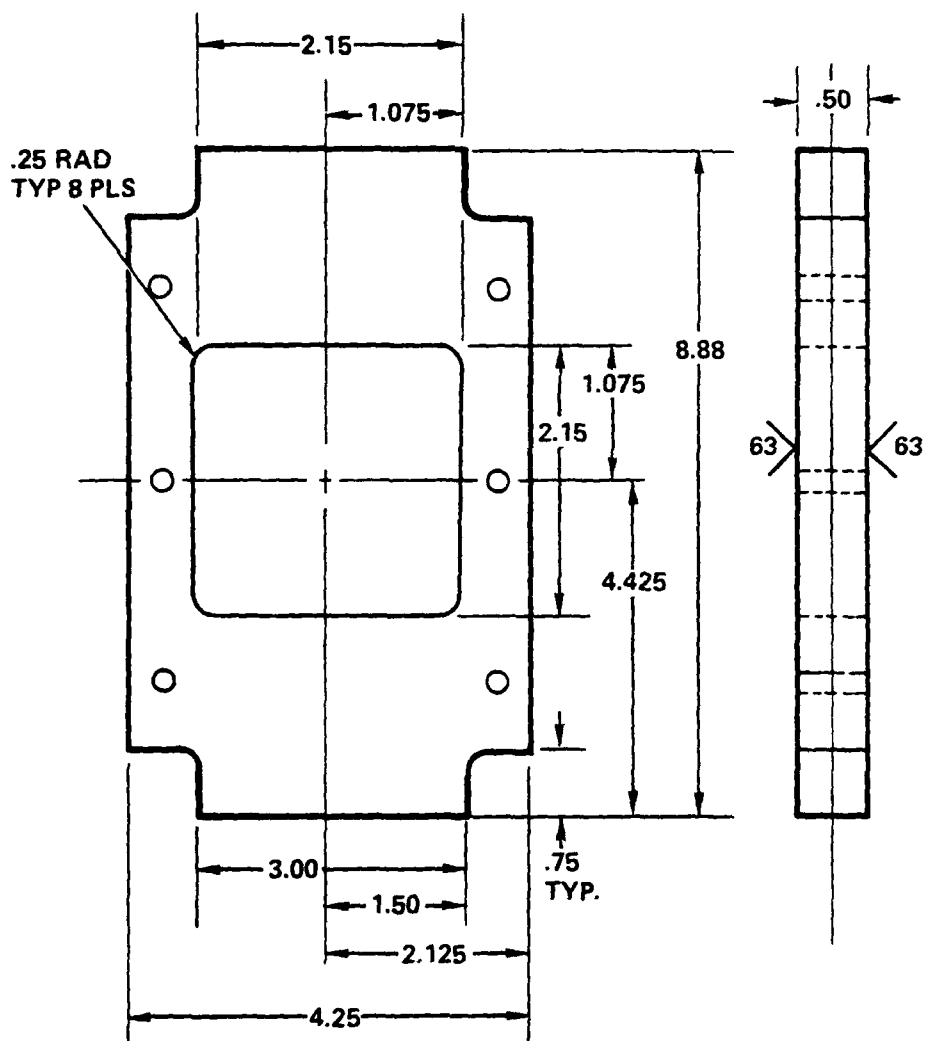
concern. Unrealistic supporting conditions such as full face plate buckling guides are not representative of aircraft structure loading and would interfere with both damage development and tracking. Thus the specimen support becomes an integral part of the test and must be considered in the evaluation of results.

The fatigue support design used for Task II and majority of Task III is shown in Figure 20. This configuration was designed to allow localized deflection normal to the plane of the specimen while still providing adequate constraint to prevent extensive gross buckling. In Task III, a different constraint configuration was evaluated under items 4B, 5B and 6B of the test matrix where tests were conducted with the four-bar buckling support (constraint condition #2) illustrated in Figure 21.

4.3 DAMAGE MONITORING METHOD

Based on the Task I investigation a pitch-catch type of ultrasonic scanning system was selected for further use on this program. This was a specially modified Holscan System 400 produced by Holosonics, Inc. Use of this system minimized the two main limitations of traditional ultrasonic C-scan methods: 1) the lack of detailed information from "go, no-go" C-scan methods; and 2) potentially adverse effects of sample immersion in a water bath. The basic Holosonics System Holscan 400 used on this program incorporated the following modifications:

- a. The "flex arm" transducer mount was replaced with a digital mechanical scanner control interfaced with the System 400 electronics. This overcame the basic system limitation of requiring a manual hand scanning of the specimen and enabled the addition of a recall memory capability. In addition, this mounting system permitted a large selection of transducers with the needed characteristics for use in the current program.



NOTE: All Dimensions in Inches (1 in. = 25.4 mm).

Figure 20: Fatigue Buckling Guide Design

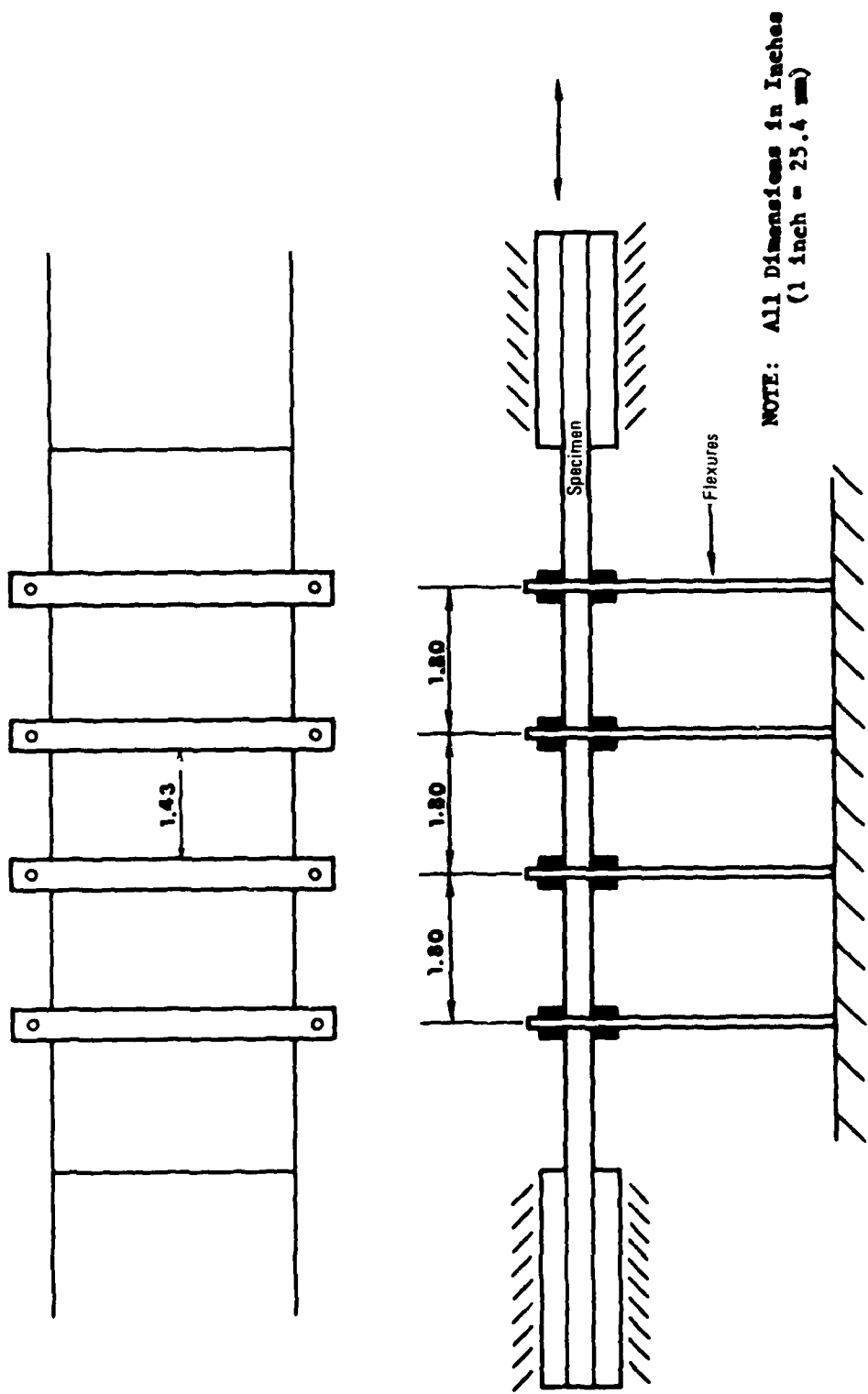


Figure 21: Four-Bar Buckling Support (Constraint Condition #2) Design

AD-A115 184

LOCKHEED-CALIFORNIA CO BURBANK

F/G 11/4

ADVANCED RESIDUAL STRENGTH DEGRADATION RATE MODELING FOR ADVANC--ETC(U)

JUL 81 K N LAURAITIS, J T RYDER, D E PETTIT

F33615-77-C-3084

UNCLASSIFIED

LR-28360-19

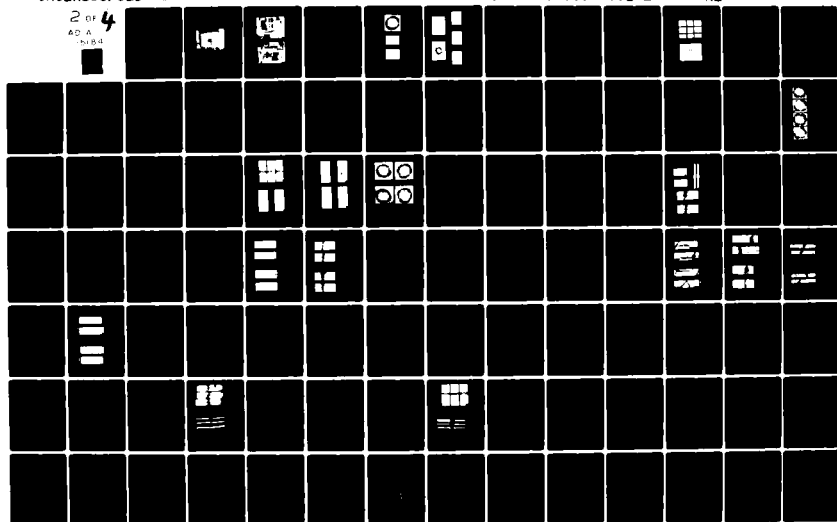
AFWAL-TR-79-3095-VOL-2

NL

2 OF 4

AD-A

115 184



5184



U.S. GOVERNMENT PRINTING OFFICE: 1963 O - 348-100

- b. A digital memory, real time image display electronic processor and dual mode scope were interfaced with the System 400 electronics to provide a digital memory storage unit for retention and subsequent display of data in C-scan and associated B-scan format as well as in 3-D isometric format. This provided a major tool to assess composite damage characteristics since the ply level at which damage occurred could be determined as well as the extent of damage at each level.

- c. A vertical mounting and coupling system was attached to the transducer/digital scanner (see Figure 22). Inclusion of this system provided a scanner which could be used on test specimens mounted in the test frame, thus eliminating the necessity to remove and reinstall specimens each time they were to be examined. This provided a major improvement also in that the specimen was not immersed in water for extended periods as would occur during normal C-scan, the water contact being limited to the 1/2 inch diameter water column directly in front of the scanning transducer. In addition, only a single scan was required, since data were available in the memory for further analysis.

The modified system 400 equipment, including digital mechanical scanner, vertical mounting system and digital memory is shown in Figure 23.

A more detailed discussion of this system is presented in Reference 8.



Figure 22: Digital Mechanical Scanner with Vertical Mounting in Place for Panel Examination.

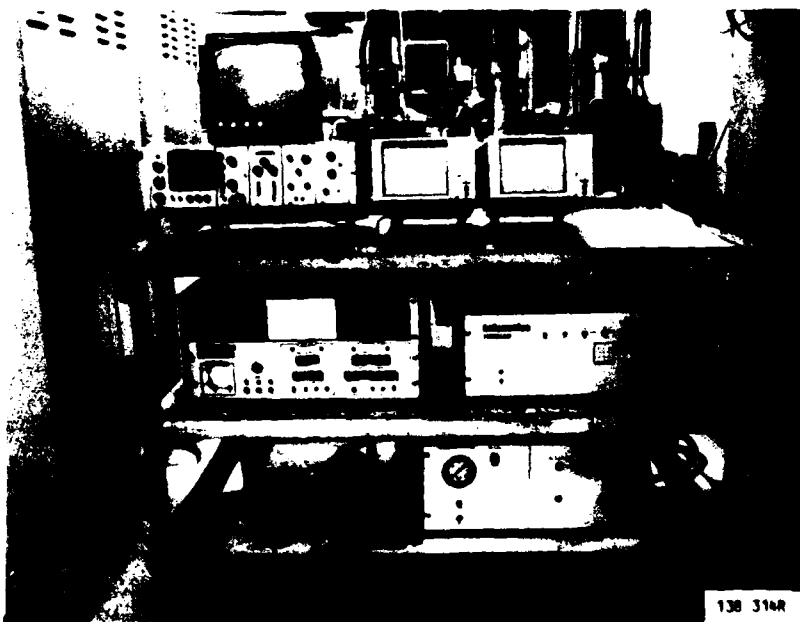
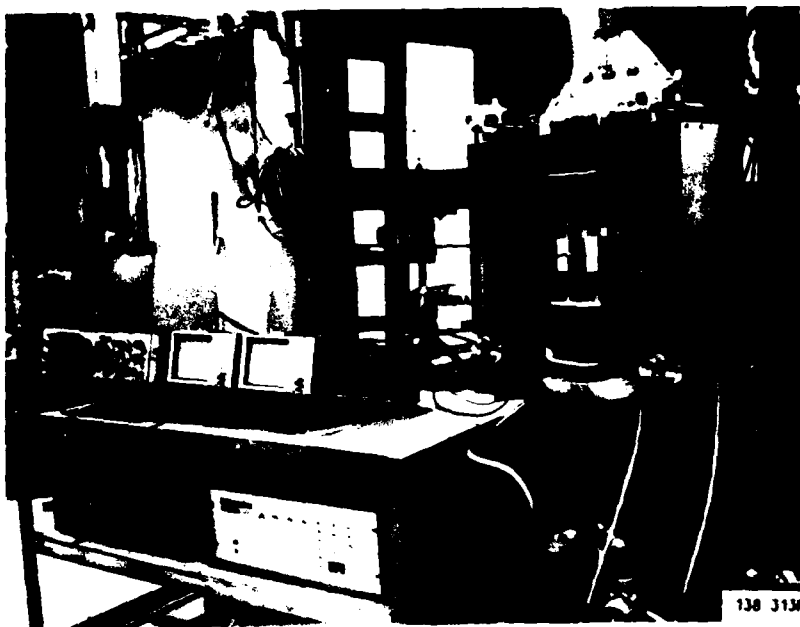


Figure 23: Modified Holosonic System 400 with Digital Mechanical Scanner, Vertical Mounting System and Digital Memory.

4.4 DAMAGE MEASUREMENT PROCEDURES

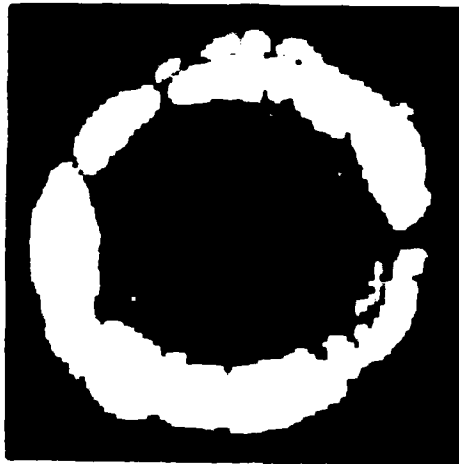
4.4.1 Recorded Data Available for Analysis

A typical set of Holscan data such as shown in Figure 24 consisted of the following basic information:

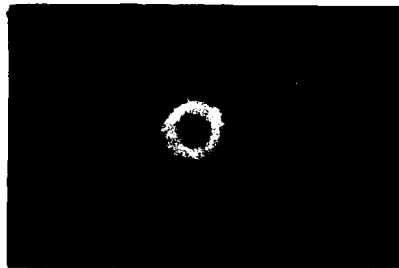
- a. A C-scan photo taken from the TV monitor. These data were recorded since the TV-monitor records nine levels of intensity proportional to the acoustic attenuation of the signal. As a result, it provided the maximum amount of C-scan information.
- b. A C-scan photo from the memory scope. These data are more typical of standard C-scan results and are based on the attenuation exceeding a specific level, i.e., as a go-no-go record.
- c. A cumulative B-scan which showed the levels at which damage was occurring.

In addition to this basic information recorded for each inspection interval, a second set of data was taken each time a significant change was observed in the basic damage characteristics. This second data set typically consisted of the following:

- d. A photo of the TV C-scan results with marker lines indicating the locations of single pass B-scans through the damage area.
- e. Photos of the individual B-scans taken through selected regions of the damage. A typical set of these data is shown in Figure 25.



a. T.V. Monitor C-Scan Results

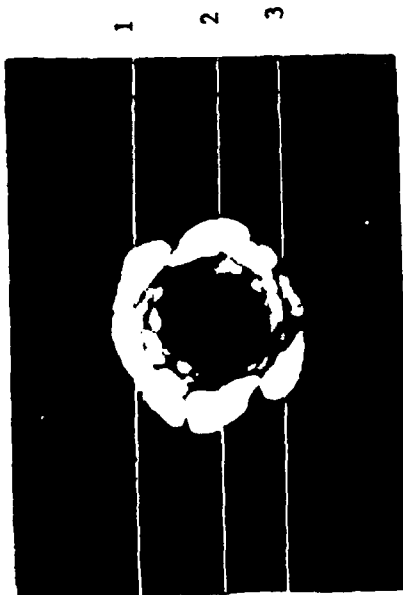


b. Memory Scope C-scan Results

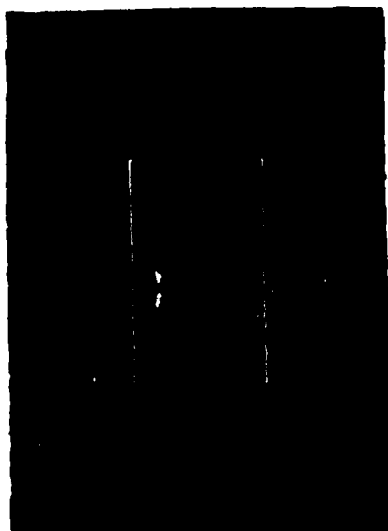


c. Cumulative B-scan Results

Figure 24 : Typical Holscan Data Available for Each Damage Growth Interval



T.V. Monitor C-Scan, IX



Cumulative B-Scan



Section 1 B-Scan



Section 2 B-Scan



Section 3 B-Scan

Figure 25: Typical Data Set Illustrating Single Pass B-Scan Results at Selected Locations Through the Damage

Ultrasonic inspection methods such as the Holskan normally present a projection of the total damage area parallel to the specimen surface, regardless of the level at which the damage may be occurring. Although B-scan data provide the location of the damage through the thickness, its extent on any particular level cannot be determined. However, in any realistic field situation these are the type of data that would be available and hold the greatest potential for practical use if a relationship can be established. While many possible ways exist to present this volume of data, three damage measurements illustrated in Figure 26 were selected for comparison and evaluation as possibly significant parameters for damage characterization.

- a. The damage area, A, determined from the C-scan photos as measured using a K & E model 4242 Planimeter by tracing around the outer periphery of the damage
- b. The maximum damage extension in the specimen width direction, X, as measured from the C-scan photo.
- c. The maximum damage extension in the 0° fiber direction, Y, as measured from the C-scan photos.

4.4.2 System Calibration and Area Measurement Procedures

In order to assure accurate scale factors for the photos, a calibration block of the 32-ply quasi-isotropic T300/5208 material was machined with two parallel milled cuts running vertically and two parallel machined cuts running horizontally across the block. The width and spacing of the slots were then measured with a tool makers microscope. The block was then scanned with the Holskan unit and photos taken of the TV monitor C-scan and the memory scope

↑ 0° FIBER, LOADING DIRECTION

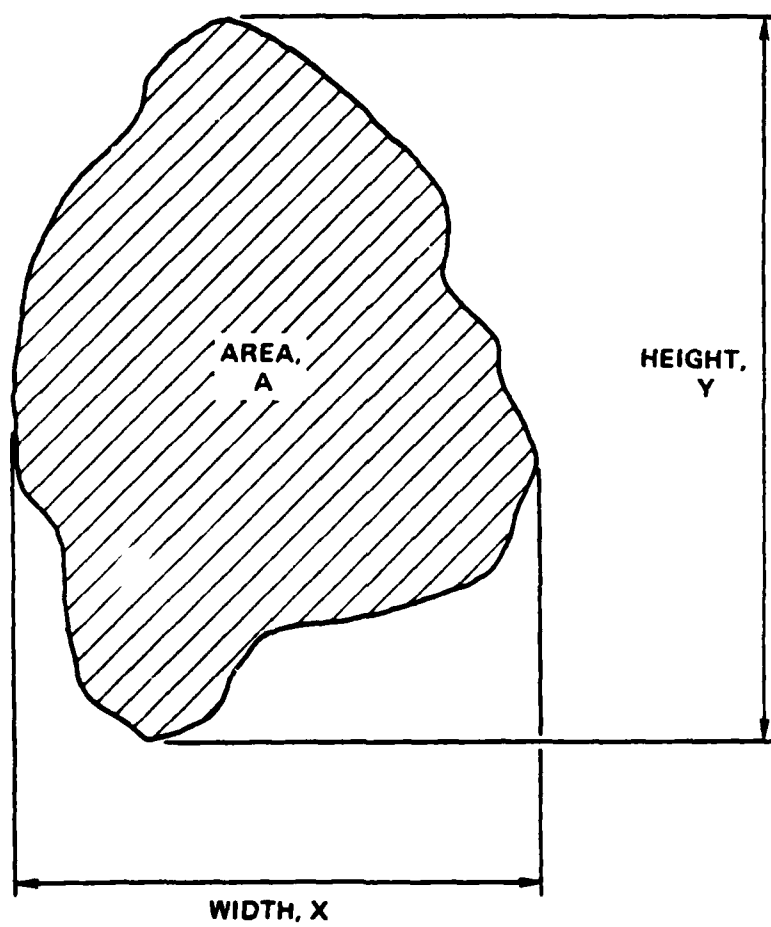


Figure 26: Illustration of the Damage Zone Size Parameters Evaluated

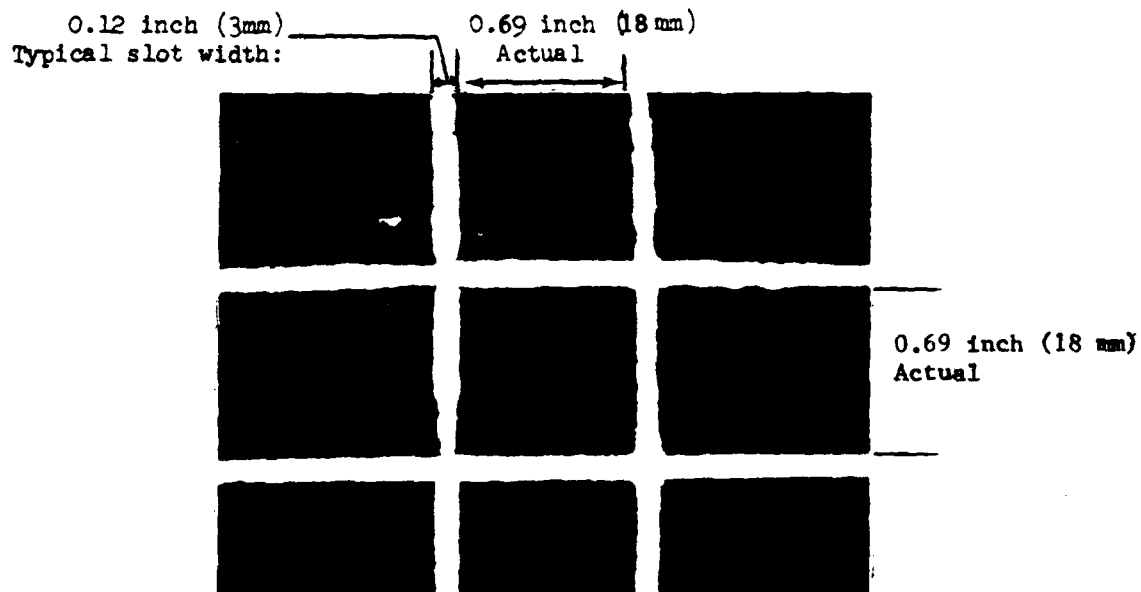
C-scan, as shown in Figure 27, and the spacings measured from the photos to obtain the scaling factors. These scans were repeated periodically to check for variations and were found to be stable over the course of the program.

Once the scale factors were obtained, the C-scan photos were measured using a K & E model 4242 Planimeter by tracing around the outer periphery of the damage indication to determine the area of the damage. A transparent scale marked to 0.01 in. (0.25 mm) was used to measure X and Y dimensions. TV monitor photos were used for all damage measurements. Comparison of repeated measurements by one reader with those of a second reader indicated area measurements were reproducible to approximately $\pm 5\%$.

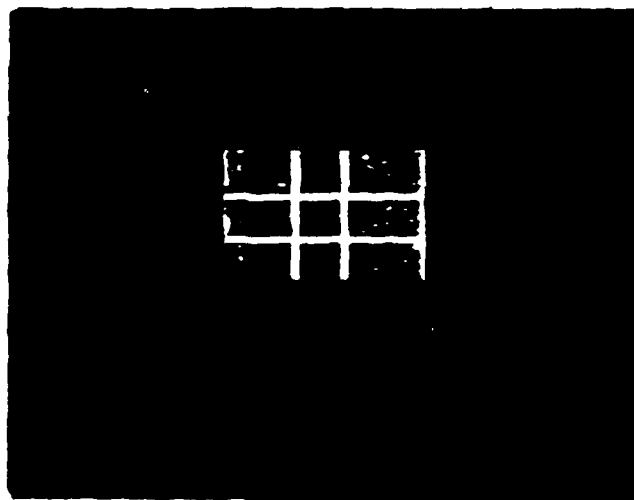
4.5 DESTRUCTIVE INSPECTION PROCEDURES

4.5.1 Resin Burn-out (Deply) Procedure

A high temperature furnace with inert gas purge was used to remove the resin matrix from the specimens leaving the intraply fibers essentially intact and bonded together. Specimens were cut to size (determined from Holskan data) then soaked in a solution of gold compound for various time intervals. Two hours for small (1.5 x 1.5 in. (38 x 38 mm)) 24-ply samples were determined as adequate for dye penetration, but longer times were required for thicker and larger samples. Specimens were removed from the dye, air dried and placed inside a small stainless steel cylinder (2 in. I.D. x 10 in. in length (51 mm x 254 mm)) with inlet and outlet lines provided for purge. Threaded end caps were installed, purge lines connected, and gas flow started (150-300cc/min). The cylinder was placed in a furnace and temperature applied. After reaching the desired temperature of 1050°F (566°C) specimens were held at temperature for four hours. The samples were removed from the cylinder after cool down and carefully deplied. Each lamina was mounted on a folder using tape to hold plies in proper orientation then photographed for permanent record.



A. TV Monitor Photo, 1X
 Scale Factor: 1-inch = 0.70 inch actual
 25mm = 18 mm actual



B. Memory Scope Photo
 Scale Factor: 1-inch = 3.08 inch actual
 25mm = 75mm actual

Figure 27: C-Scan Photos of Calibration Block

4.5.2 Metallographic Specimen Preparation

The areas to be examined were removed using a water cooled coarse alumina abrasive blade. Sections were then mounted in Buehler epoxide cold mounting medium. Fast removal of material was accomplished on a wet belt grinder using 80 grit silicon carbide belt, followed by 120 grit. Final removal (approximately 0.030 in.(0.76 mm)) of material was done very slowly on a lapmaster with John Crane 1900 Lapping Compound (9 micron size alumina) and 3M lapping vehicle. The two intermediate steps in the sample preparation were performed on a rotating bronze wheel covered with acetate cloth impregnated with 6 micron diamond lapping compound and Buehler Automet Oil, followed by 1 micron diamond. Final step in the sample preparation included a short polish on a Buehler Microcloth (polishing cloth) and LECO Finish-pol (cerium oxide fine abrasive).

SECTION 5
STATIC TENSION AND COMPRESSION RESULTS

Static testing included the determination of both damaged and undamaged properties of 3"-wide (76mm) specimens for two laminates, 24-ply, 67%-0° and 32-ply, quasi-isotropic. Static tension and compression tests were conducted under each task to provide the initial baseline distribution and indicate any change which may have occurred during shelf storage of specimens. Since specimens which are fatigue tested at 5 Hz experience much higher strain rates than those at which most static data are obtained, tension and compression data were developed for two strain rates: 1) a standard or low strain rate at which most static tests are conducted and 2) a high rate comparable to that experienced in a fatigue test.

In any high rate test, the accuracy of the maximum load determination deserves examination. For these tests the Lockheed Rye Canyon data central computer was used to monitor both stroke and load at a sampling rate of 1500 per second. A typical test failure occurred in approximately 0.35 to 0.40 seconds as shown in Figure 28. For the test shown in Figure 28, 546 scans were taken during the 0.364 seconds of the test as shown in Figure 29. The estimated error is thus less than 0.2% of the maximum load.

All Task II tests were conducted in a room temperature, laboratory air environment. Task III included the evaluation of 180°F (82°C) temperature on static properties and a second constraint condition on compression behavior. In addition, one inch (25mm) wide duplicate quality control tension specimens were removed from each panel and tested in the undamaged condition to provide a static strength reference and indicate any

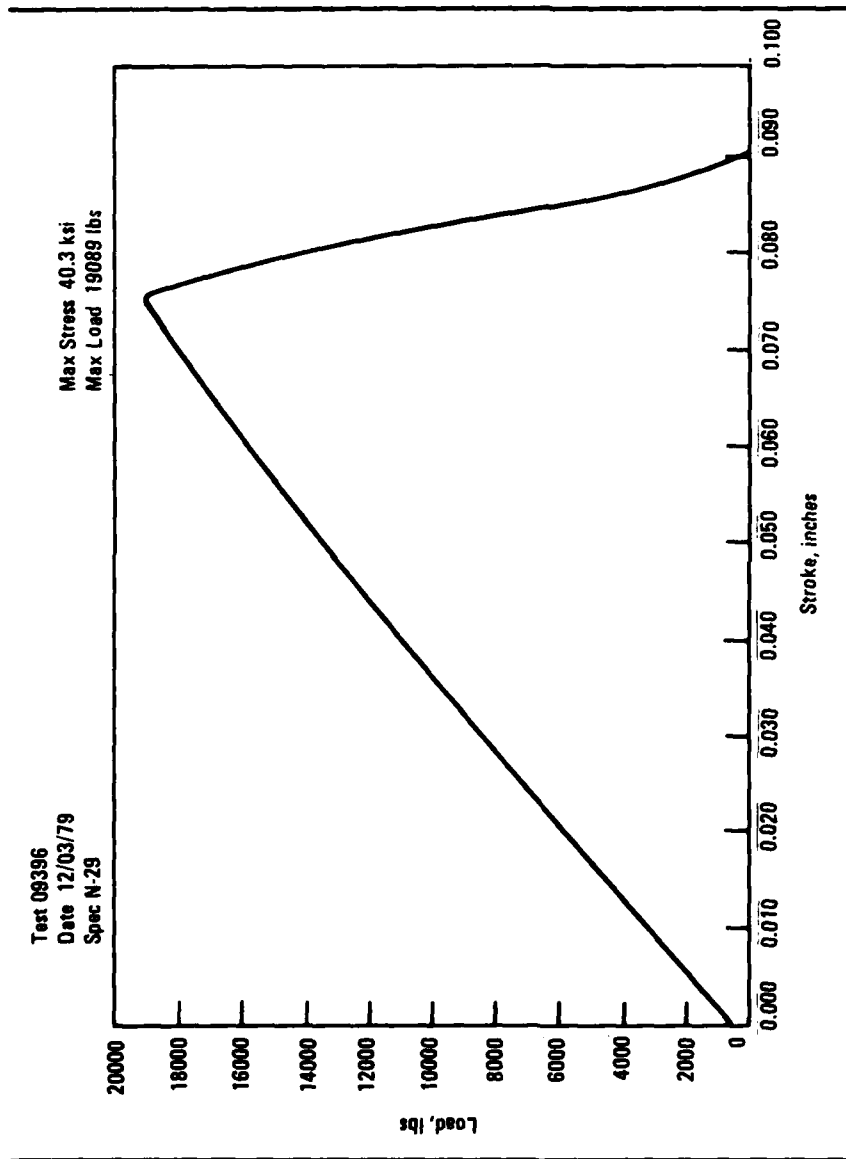


Figure 28: Typical Load vs. Deflection Curve for High Strain Rate Tests of 32-Ply Laminate (Spec. NC-29)

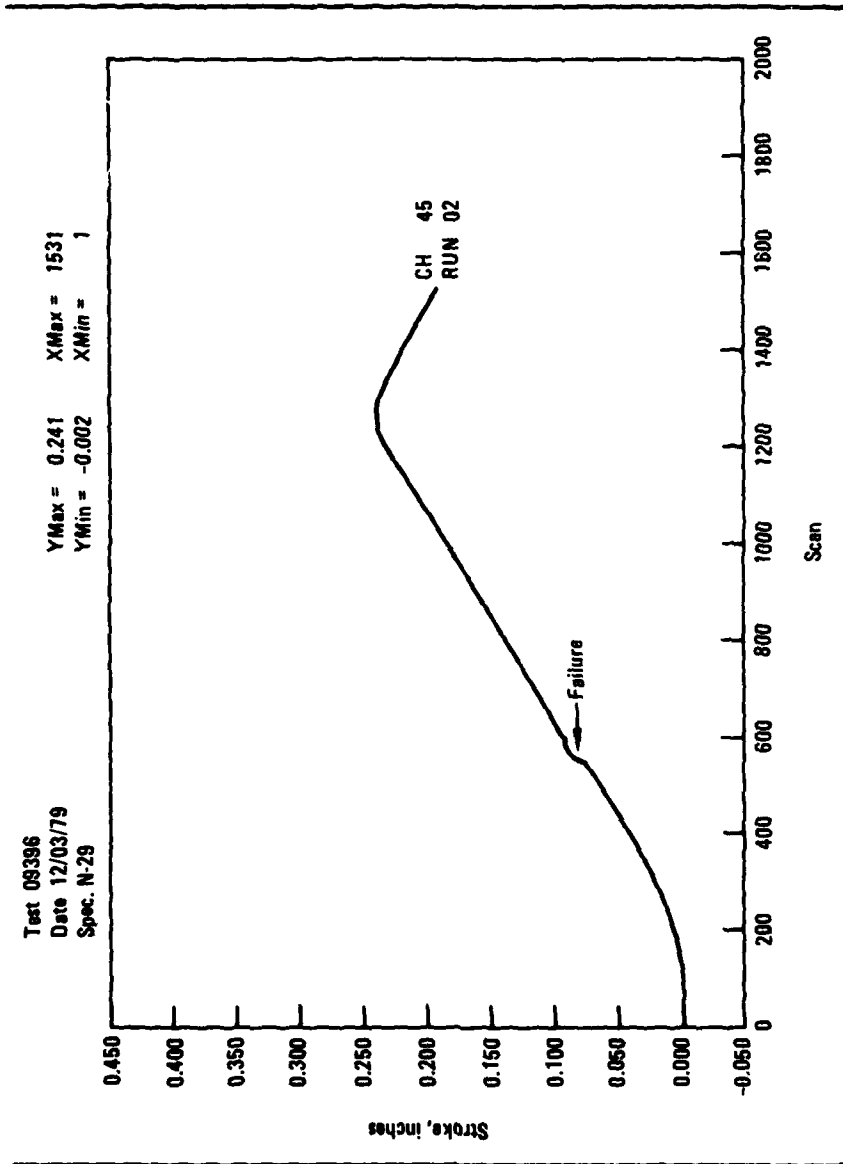


Figure 29: Typical Deflection vs. Number of Scans Curve for High Strain Rate Tests of 32-Ply Laminate (Spec. NC-29)

significant panel to panel variation in the base panel strength level. Testing was conducted according to the procedures outlined in Section 4. Test conditions are summarized in Table IX. Complete test data are available in Volume III, Appendix C of this report.

As indicated in the procedures of Section 4, extensometer data were obtained for the one-inch (25mm) wide QC specimens. However, values for both tension and compression moduli and failure strains for the three-inch (76mm) wide specimens were obtained from load vs. cross-head deflection plots due to the difficulties experienced in the first task in recording displacements with an extensometer. Measurements with an extensometer attached across the hole could be made only in the early loading portion of the tests, since higher loads produced out-of-plane displacements in the region surrounding the hole causing the extensometer to slip. Modulus data were required for the various test conditions under both tension and compression loading. Accordingly, some consistency in the method of measurement was desirable to permit comparison of any observed changes. However the anti-buckling guides prohibited measurement outside of the damage region. Furthermore no change in modulus would be expected over a short gage length away from the damage site. Available options, then, were to measure a local displacement across the hole or a global change over the entire specimen gage length. Besides the technical difficulties of obtaining measurements across the hole, little further change beyond the initially observed drop in modulus would be expected since much of subsequent damage growth would be outside the extensometer gage length. Also the meaningfulness of such local changes would be questionable whereas a global stiffness change can have significant design impact.

In Task I cross-head displacement measurements were obtained concurrently with the extensometer data. A comparison of the resulting modulus data is presented in Table X. Although generally the values compare well this agreement appears to be fortuitous. Stiffnesses obtained from measurements

TABLE IX
STATIC TEST MATRIX SUMMARY

Test Type ^a	Strain ^b Rate	Task	Test Plan Item No.	No. of Replicates
QA Tension	low	II	1	18
Undamaged		III	1	6
Undamaged Tension	low high	II	9A	4 4
Undamaged Compression	low high	II	9B	4 4
Damaged Tension	low	II	2A	15
		III	2	3
	high	II	3	5
Damaged Compression	low	II	4	15
		III	3A	3
	high	II	3	5
Damaged Comp. Constraint # 2 ^c	low	III	3B	3
Damaged Tension 180°F (82°C)	low high	III	2B	5 5
Damaged Comp. 180°F (82°C)	low high	III	3B	5 5
Damage Growth Tension	low	II	2B	3
Damage Growth Compression	low	II	4B	3
TOTAL NUMBER OF STATIC TESTS PER LAMINATE TYPE				115

a = All tests conducted on both laminates, 24-ply & 32-ply. Compression tests employed fatigue support, constraint #1, where not indicated otherwise.

b = Low: 0.005 min.⁻¹ high: 0.5 -5 min.⁻¹

c = 4-bar buckling support

TABLE X
COMPARISON OF MODULUS AND FAILURE STRAIN VALUES
DERIVED FROM EXTENSOMETER AND CROSS-HEAD DISPLACEMENT MEASUREMENTS

Specimen No.	1" (25 mm) Extensometer Across Hole		LVDT (Stroke)	
	Apparent Modulus E_i	Apparent Failure Strain E_f^a	Apparent Modulus E_i	Apparent Failure Strain E_f
AB-20	5.59	.0076	5.11	0.0081
BA-5	5.48	-	5.48	0.0083
BA-10	5.23	-	5.12	0.0078
CC-23	5.40	-	5.14	0.0079
CC-29	5.68	-	5.02	0.0088
DC-21	5.45	.0095	5.31	0.0081
EC-21	5.18	-	4.98	0.0089
HA-9	8.20	-	8.72	0.0091
HC-29	8.85	-	8.43	0.0093
JC-26	8.00	-	8.69	0.0085
JC-28	8.22	-	8.53	0.0084
KB-19	8.85	-	8.61	0.0086
KC-23	7.83	-	8.24	0.0086
LA-5	8.20	-	8.61	0.0087
LC-27	7.97	-	8.69	0.0083
MA-3	7.94	-	9.02	0.0089
MA-6	8.19	-	8.54	0.0085

^a Where no entries listed, extensometer slipped due to out-of-plane deflections

over the entire nine-inch (229mm) gage length would not be expected to be similar to those from localized readings across a hole. Hence an undamaged 32-ply coupon was strain gaged and the stress vs. strain curves derived from gage and cross-head displacement readings compared (Figures 30 & 31). Note that the modulus calculated from the displacement data for this unnotched coupon is nearly identical to the values obtained for the notched while that derived from the strain gage results is approximately 40% higher and comparable to the values obtained for the undamaged Q.C. specimens. Similarly modulus values for the undamaged baseline tests (Task II, Item 9) where stroke was measured for consistency, did not differ from those for the damaged coupons but they were considerably lower than expected for those laminates based upon extensometer data. As anticipated, additional deflection in the gripping system contributed to the measured specimen displacement, but this error appeared to be constant. Hence all modulus and failure strain data for 3 inch (76mm) coupons presented in this report are to be used for comparison only.

5.1 QUALITY CONTROL TENSION TEST RESULTS - TASKS II AND III

Unnotched Quality Control tension tests were conducted on duplicate 1-inch (25mm) wide by 10.5-inch (267mm) long specimens selected from subpanels A & B for each of the nine panels of each laminate (24 and 32-ply) for Task II and each of the 3 panels per laminate type of Task III. A comparison of the average values for Tasks I, II and III is presented in Table XI.

Unlike the 24-ply Task I laminates those in Tasks II and III, with the exception of one specimen, did not display a totally linear to failure curve. Stress-strain curves were generally linear to approximately 50% - 75% of the failure stress with steadily increasing slope from this point to failure as illustrated in Figure 32. Behavior of this type is typical of all 0° laminates and could be expected in a laminate containing a high percentage of 0° fibers. Again, in Task II as in Task I, most of the

TEST 11896 RUN 3

Y-AXIS CH 46

X-AXIS CH 47

YMAX = .3811E 02 YMIN = .5078E-01

XMAX = .5128E 04 XMIN = .1652E 02

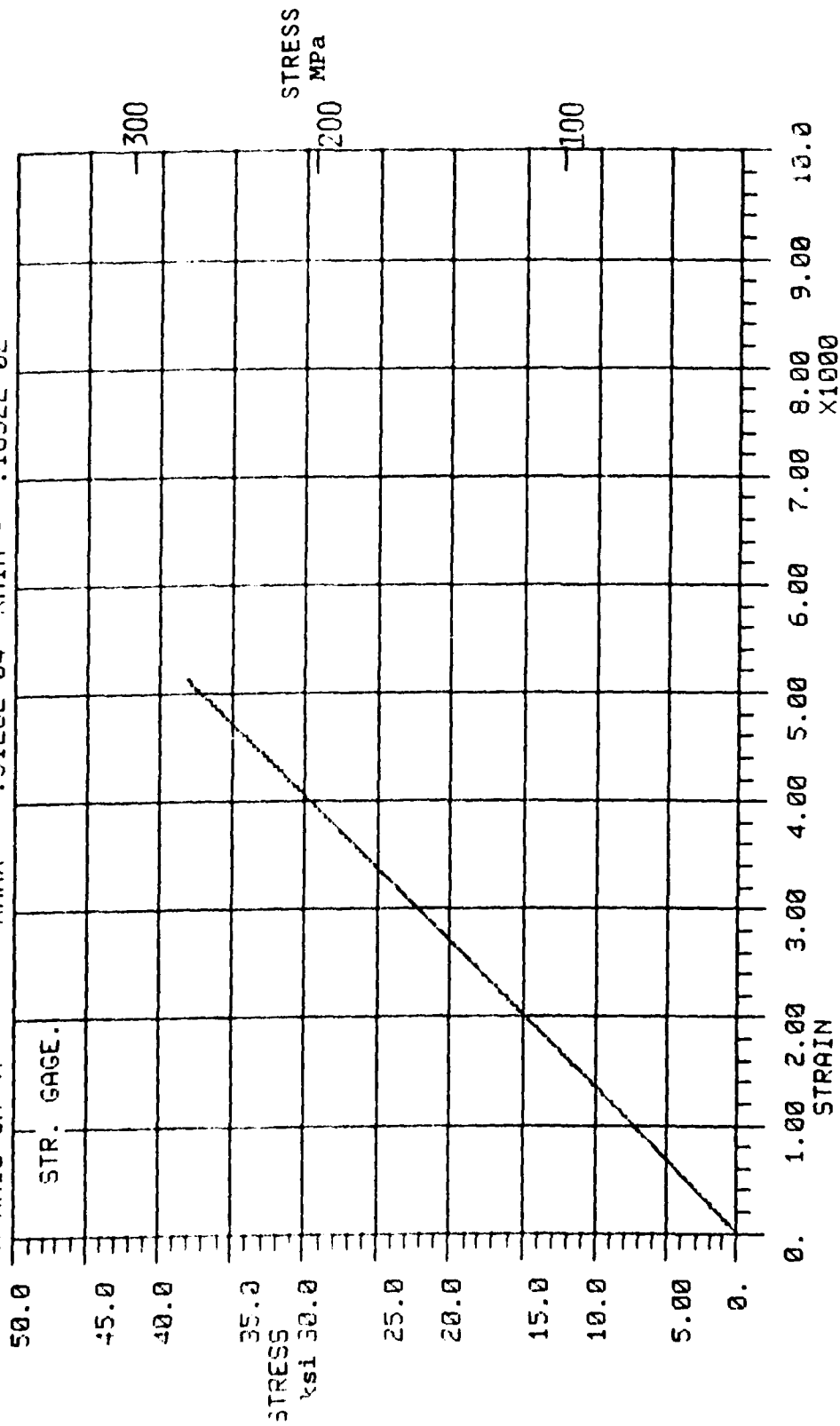


Figure 30: Stress-Strain Curve for Quasi-Isotropic Specimen NA-5 Derived From Strain Gage Measurements Yielding $E = 7.5 \times 10^6$ psi (52 GPa).

TEST 11896 RUN 3

Y-AXIS CH 46

YMAX = .3811E 02 YMIN = .5078E-01

X-AXIS CH 48

XMAX = .7490E 04 XMIN = -.6944E 02

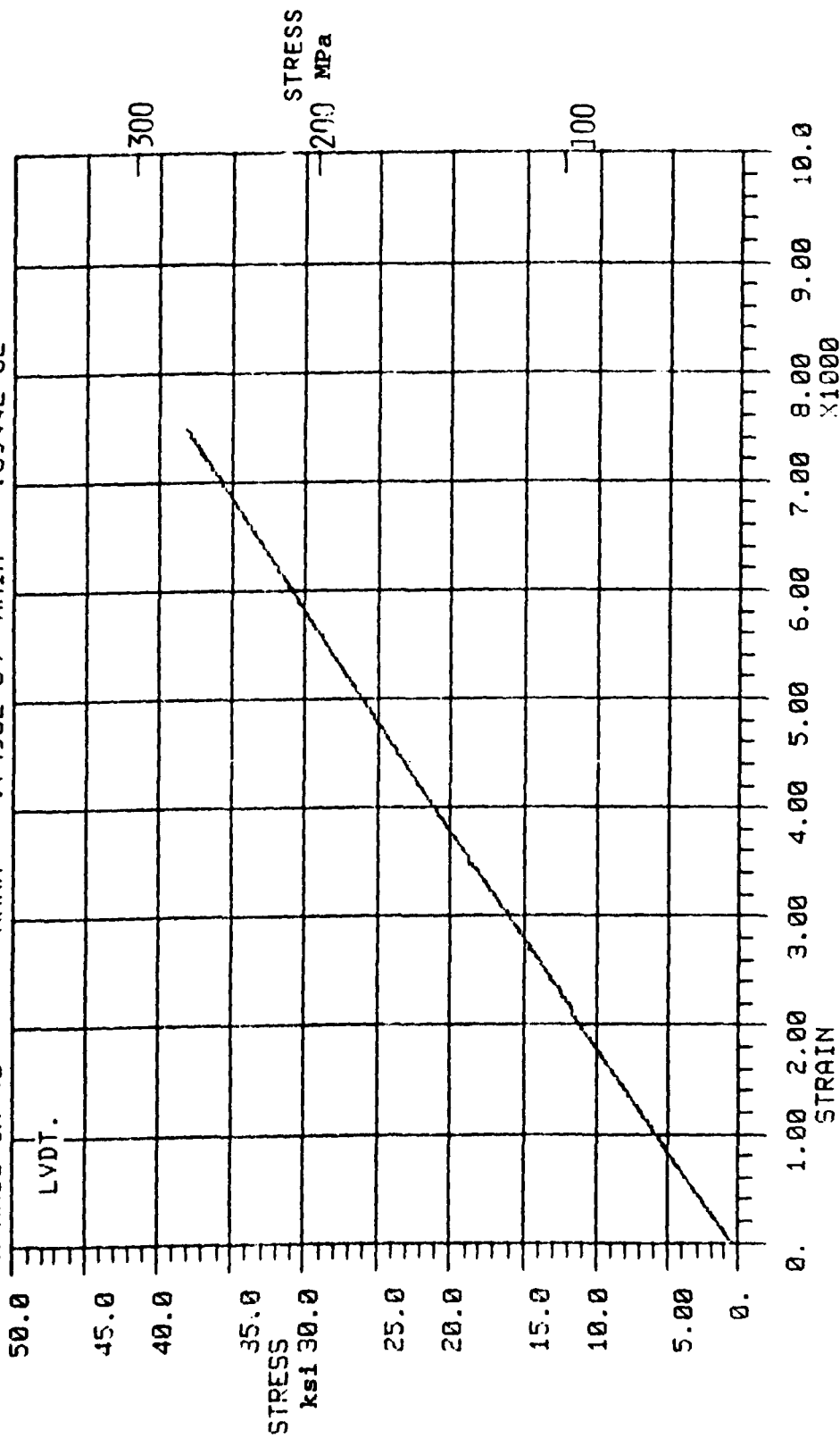


Figure 31: Stress-Strain Curve for Quasi-Isotropic Specimen NA-5 Derived from Stroke Measurements yielding $E = 5.2 \times 10^6$ psi (36 GPa)

TABLE XI
COMPARISON OF AVERAGE Q.C. TENSION
DATA FOR TASKS I, II AND III

		Ultimate Stress		Ultimate Strain ^a	Apparent Modulus		No. of Spec.
		ksi	MPa	in./in. mm/mm	psi · 10 ⁶	GPa	
24-Ply Laminate	Task I	\bar{x}	147.4	1096	0.0095	15.3	106
		S	6.3	43	0.0002	0.3	2
		V%	4.3	4	2.0	2.0	13
	Task II	\bar{x}	163.2	1125	0.0105	15.2	105
		S	7.5	52	0.0005	0.4	3
		V%	4.6	32	4.8	2.4	17
	Task III	\bar{x}	157.9	1089	0.0109	14.6	101
		S	3.6	25	0.0003	0.3	2
		V%	2.3	2	2.5	1.8	2
32-Ply Laminate	Task I	\bar{x}	77.4	534	0.0100	8.1	56
		S	5.0	34	0.0006	0.2	1
		V%	5.4	6	5.7	2.6	18
	Task II	\bar{x}	77.5	534	0.0101	8.1	56
		S	3.3	23	0.0005	0.3	2
		V%	4.3	30	4.8	3.5	24
	Task III	\bar{x}	72.3	498	0.0097	8.2	57
		S	5.6	39	0.0012	0.7	4
		V%	7.8	8	11.9	8.5	9

^a One inch (25mm) extensometer used in Tasks I & II, two inch (51mm) extensometer used in Task III

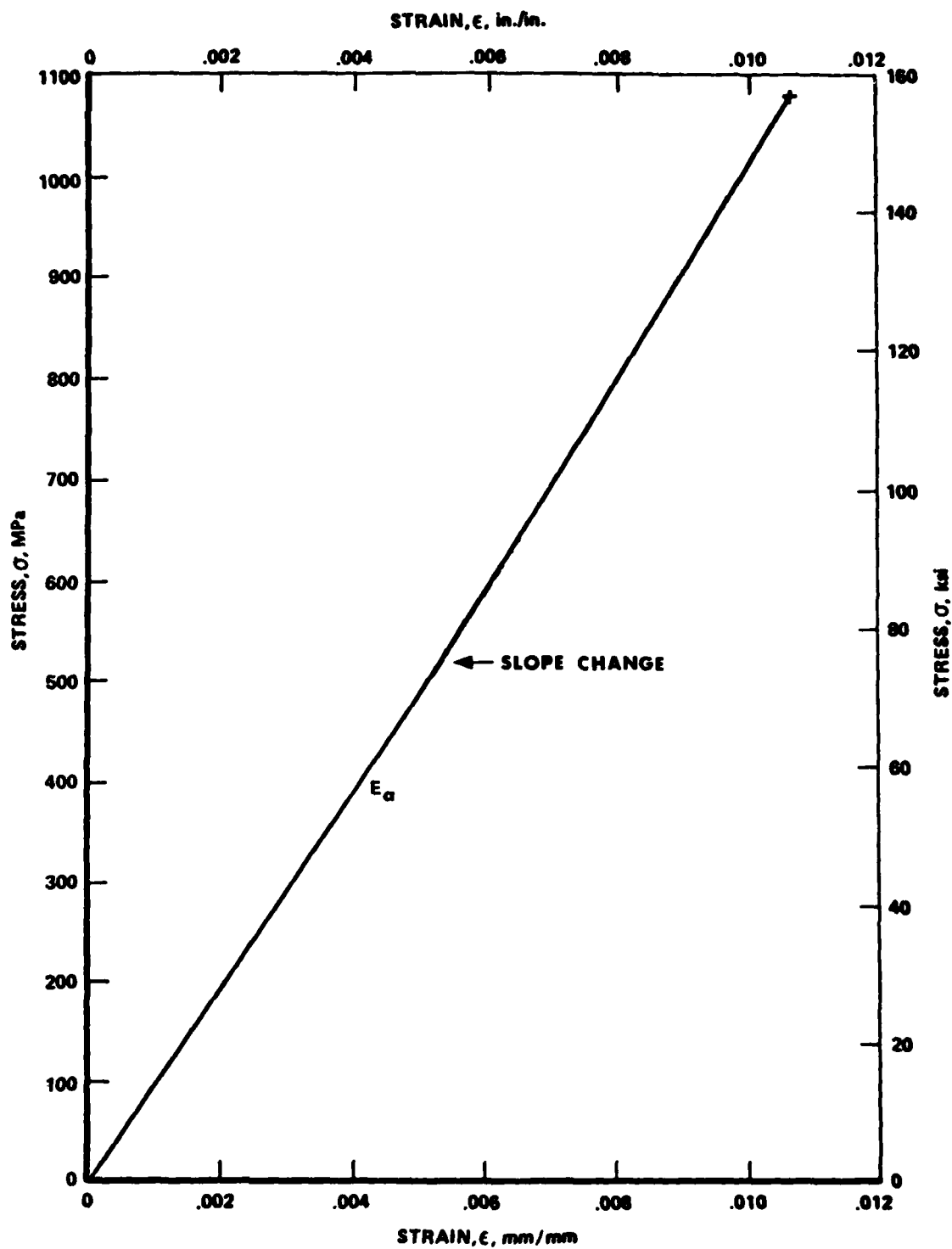


Figure 32: Typical Stress Strain Curve Measured for the 24-Ply 67% 0° Laminate

failures extended to the tab region but only one failure at the tab occurred in Task III. However, as indicated previously, ⁽¹⁾ these near tab failures did not appear to constitute a different population. Of the five highest strength values in Task II, only one corresponded to a specimen which failed away from the tab region and the near tab failure of Task III was one of the two highest strength values obtained. Variability of the data within each task for this laminate was not large as indicated in Table XI. However it is also apparent from this table that the 24-ply Task II and III laminates have a higher average strength and failure strain than those of Task I. The Task II and III average fiber volumes of 65.23% and 64.93%, respectively are not significantly greater than the Task I average of 64.56% and would not account for the observed strength increase for this material batch. The total range in fiber volume was 1.8%, 1.9% and 0.90% for Tasks I, II and III, respectively. Increase in the 24-ply laminate failure strength appears to be due primarily to the higher fiber strength of the second batch of materials used for both Tasks II and III. This is evident upon examining the ratios of average laminate strength to average fiber strength of the prepreg batches which were 0.33 for Tasks I and III and 0.34 for Task II. Fiber properties are reported in Section 3, Table II.

The 32-ply laminates exhibited stress-strain curves having a double slope as shown in Figure 33 which was also observed for the Task I material and is typical of this quasi-isotropic lay-up. Stress and strain corresponding to the intersection of the two slopes were determined and are reported in Appendix C of Volume III as slope deviation stress and strain. Results for all three tasks were within a range of approximately $\pm 10\%$ which is typical for data sets involving several processing runs. Very little difference existed between the average fiber volumes for the 32-ply panels of Tasks I, II and III which were 64.96%, 64.84% and 64.47% respectively. Slightly less scatter in fiber volume was apparent in the 32-ply Task II panels which exhibited 0.83% range compared to the 1.9% range for the Task

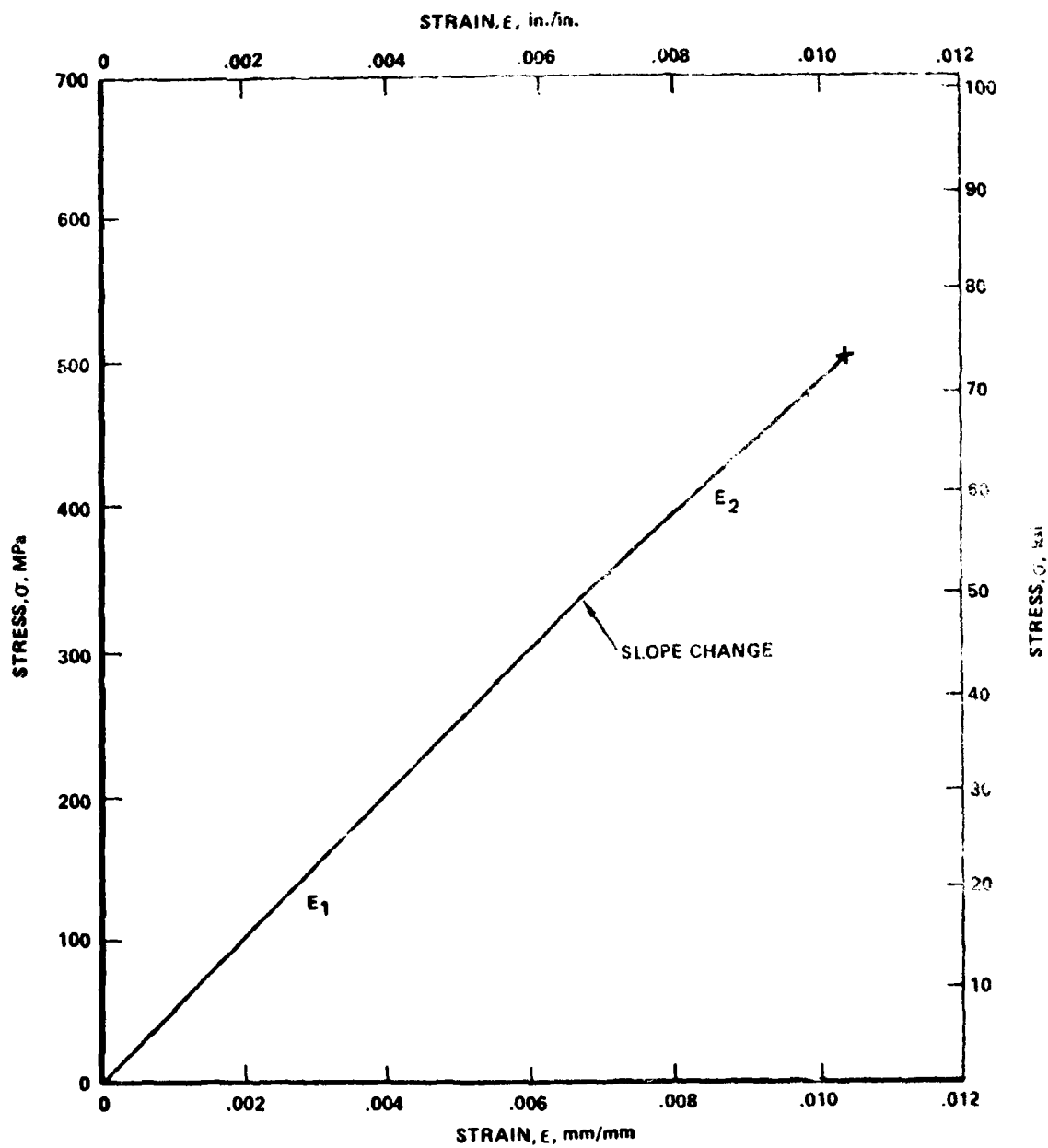


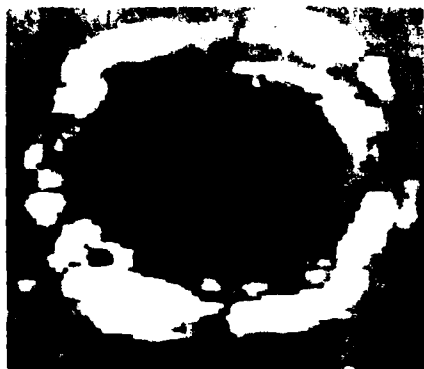
Figure 33: Typical Stress Strain Curve Measured for the 32 Ply Quasi-Isotropic Laminate

I panels and 1.3% for Task III panels. Not unexpectedly, the higher fiber strength of the material batch used for Tasks II and III was not evident in the 32-ply quasi-isotropic laminate strength where only 25% of the fibers were at 0° , as it was for the fiber dominated 24-ply laminate. As generally observed for this laminate, none of the failures occurred at the tab edge and were usually well within the gage length.

5.2 STATIC TENSION AND COMPRESSION RESULTS FOR DAMAGED 24-PLY LAMINATE SPECIMENS

Tension and compression tests of damaged laminates were conducted on 3-inch (76mm) wide x 14-inch (356 mm) long specimens containing a center hole drilled with a 3/8-inch (9.5 mm) diameter drill resulting in typical damage areas as shown in the Holscan C-scans of Figure 34, which are similar to those obtained for Task I specimens. Damage size was very consistent extending approximately 0.15 in. (4 mm) around the hole. No correlation of damage size with failure load was evident. Tests were conducted at strain rates of 0.005 min^{-1} and 5 min^{-1} which provided a comparison between a standard static rate and a rate equivalent to that of a fatigue test. Compression tests were conducted with the two different constraint conditions which were employed during the fatigue testing, a platen support with window (Figure 20) and 4-bar buckling guides (Figure 21). Results for the static tension and compression tests are summarized in Table XII. Detailed test results are available in Volume III, Appendix C.

Tension stress-strain records for the damaged laminate differed from those obtained for the undamaged QC specimens. Initial portion of the curve was linear to approximately 30% of the failure stress with steadily decreasing slope thereafter to failure. Compression stress vs. strain curves were totally non-linear with continuously decreasing slope. Therefore, secant modulus data were reported. As in Task I, the damaged tension data



AB-17
Compression
 $\sigma_{uc} = 40 \text{ ksi (276 MPa)}$



HB-16
Compression
 $\sigma_{uc} = 40 \text{ ksi (276 MPa)}$



BB-18
Tension
 $\sigma_{ut} = 73 \text{ ksi (505 MPa)}$



DA-7
Tension
 $\sigma_{ut} = 69 \text{ ksi (476 MPa)}$

Figure 34: Typical Initial C-Scans of Damaged Poles in Compression and Tension Test Specimens of 24-Ply 67% 0° Laminate

revealed a drop of over 50% in strength in comparison to the undamaged tension results. An additional reduction from the damaged tension data of over 40% was observed for the damaged compression specimens of Task II which is slightly greater than the approximately 34% decrease observed for the Task I and III specimens. Compression buckling strength with the 4-bar support was comparable to that obtained with the fatigue guide. The effect of the increased fiber strength apparent in the undamaged coupons as discussed in Section 5.1 appears to have completely disappeared in compression tests of damaged coupons. Tension and compression moduli and failure strains were obtained from load vs. cross-head deflection plots as discussed in the introduction to this section. Some of the differences between Task I, II, and III results may be due to inaccuracies in stroke measurements although the average tensile strain measured in Task II and III was more than 30% greater than for Task I while the modulus was only 9% higher. This higher failure strain is likely due to the higher strength and strain at failure of the fiber used in the batch from which the Task II and III panels were fabricated (See table IV). Comparison of damaged compression failure strain and moduli indicates a decrease of approximately 10% in strain for Task II over Task I with essentially no change in modulus. The higher compression failure strain for Task III is probably an artifact of the small sample size. Although provided for comparison, statistics for Task III data are not meaningful due to the inadequate sample size.

To determine the effect of high strain rates on the behavior of damaged laminates, five specimens were tested in tension and 5 in compression at a rate of 5 min^{-1} . These results are also summarized in Table XII and displayed in graphical form in Figure 35. Comparison of the Task II results for the two strain rates reveals no change in modulus or shape of the stress-strain curve for either tension or compression but a decrease in strength and failure strain in both cases, with decreases on the order of 10 to 15%.

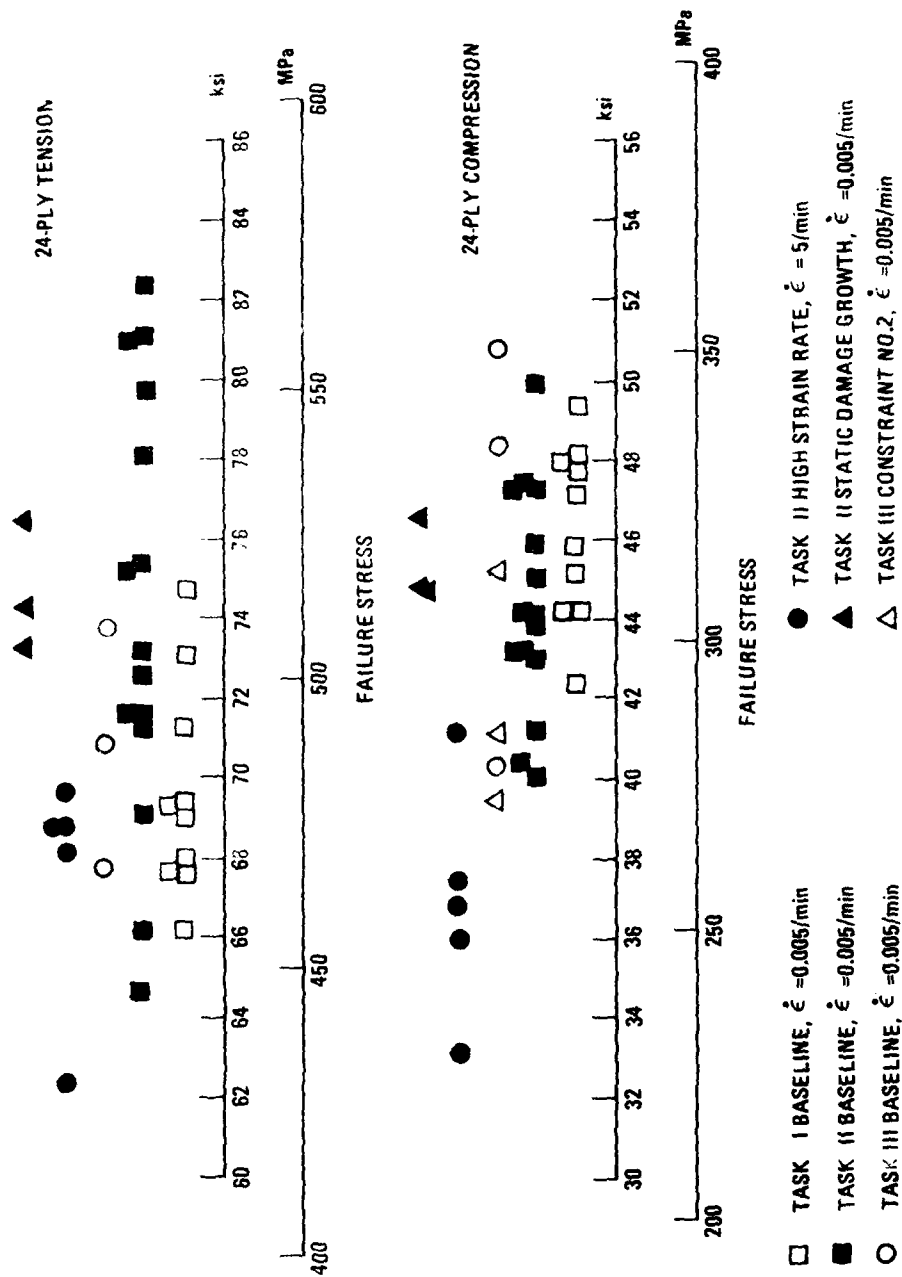


Figure 35: Effect of Loading Rate and Pre-Loading on the Static Strength of 24-ply Laminate Specimens Containing a Damaged Hole

Typical fracture characteristics of 24-ply damaged hole specimens tested in tension and compression are presented in Figures 36 - 38. No differences between tension fractures at the two strain rates were discernible. The fracture surface was roughly normal to the loading direction for a short distance on either side of the hole then extended at a 45° angle to the specimen edges often resulting in complete breaking out of triangular pieces on one or both sides of the specimen as evident in Figure 36. Little delamination accompanied the failure. Specimens tested in compression with the 4-bar support (constraint # 2) failed by buckling of the entire section containing the hole. However those tested with the fatigue support buckled in the unsupported section with outer plies "bulging" out the window while the restrained edges failed in a compression crushing mode or fractured on a 45° plane to the specimen surface. More surface cracking and delamination was evident in specimens tested with the 4-bar support than fatigue guides but overall amount of ply separation was not large for either case. High strain rate specimens differed from those tested at low strain rate only by the degree of surface ply buckling as evident in Figure 38.

5.3 STATIC TENSION AND COMPRESSION RESULTS FOR DAMAGED 32-PLY LAMINATE SPECIMENS

Tension and compression tests of damaged 32-ply laminates were also conducted on 3-inch (76 mm) wide specimens containing a center hole drilled with a 3/8-inch (9.52 mm) diameter drill resulting in typical damage areas of approximately 0.55 in. (14 mm) in diameter centered about the hole and similar to those obtained for Task I specimens (Figure 39). Since damage size was fairly uniform and data scatter minimal no correlation of strength with damage size was evident. As for the 24-ply laminate, tests were conducted at high and low strain rates and with two constraint conditions in compression. Summary of results for the static tension and

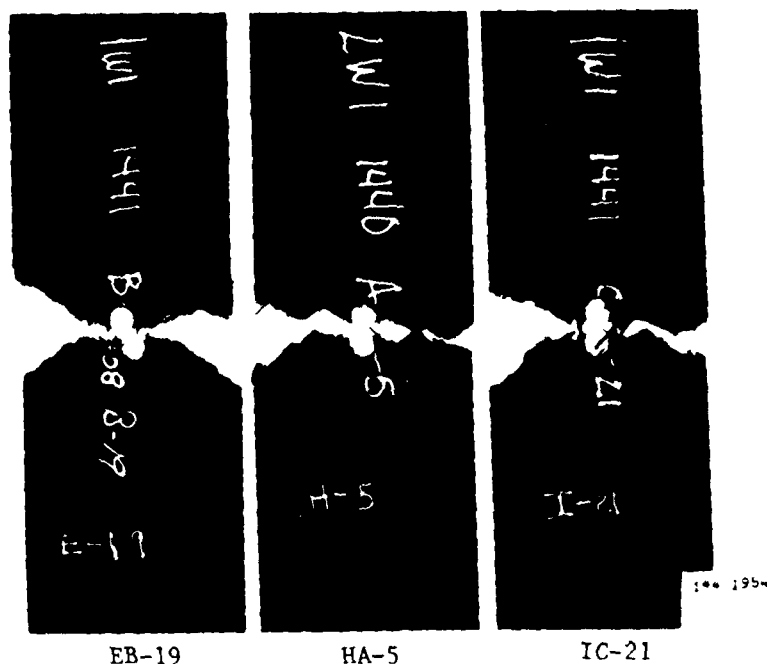


Figure 36: Fracture Features Typical of both Strain Rates For Damaged 24-Ply Specimens Tested in Tension.

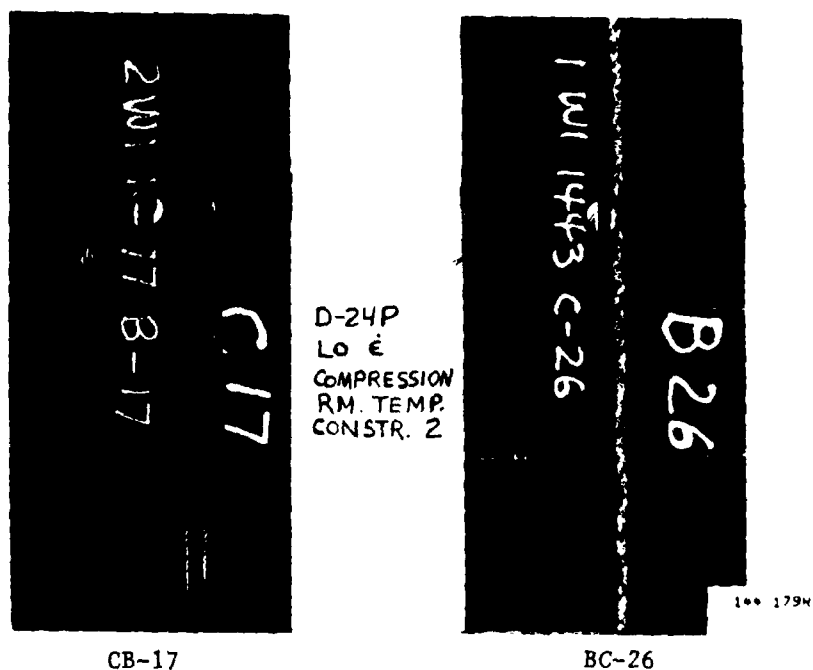
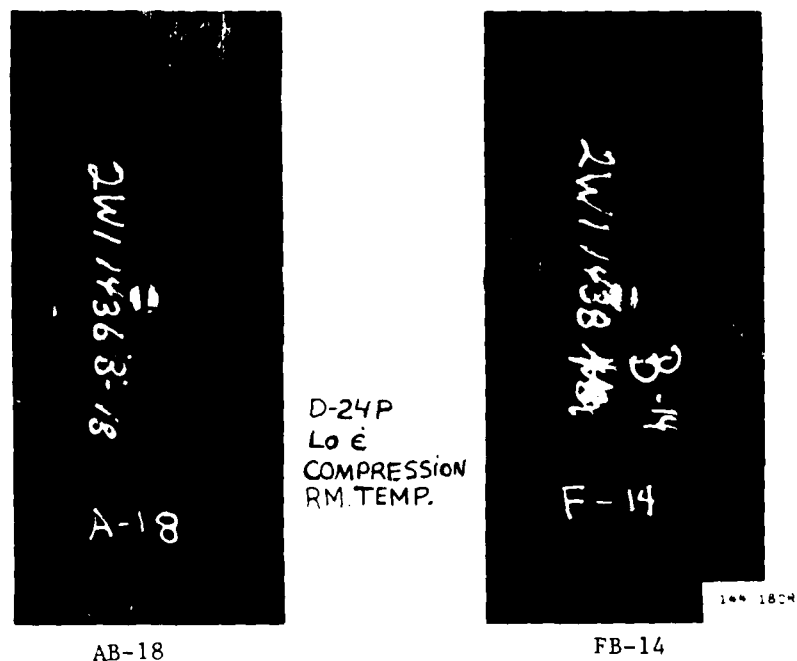
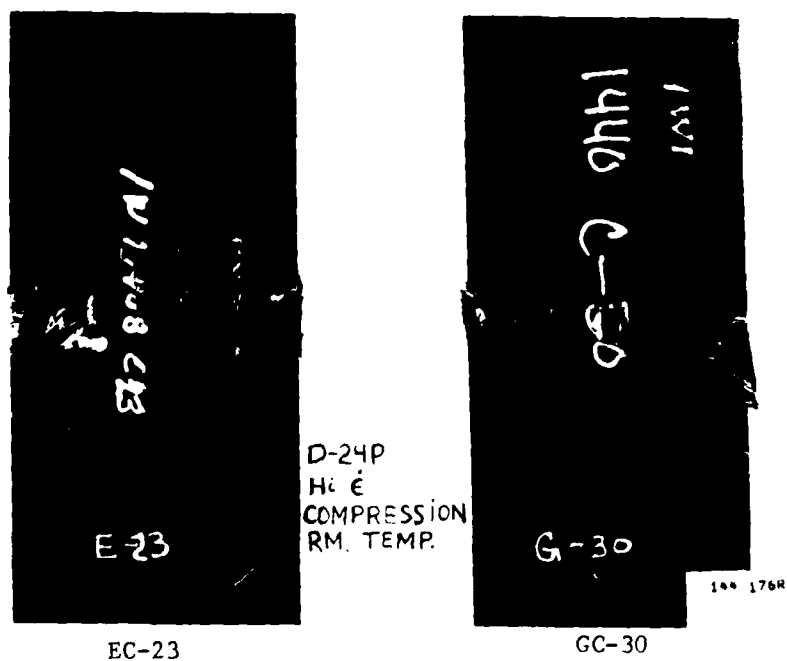


Figure 37: Typical Fractures of Damaged 24-Ply Specimens Tested in Compression with 4-Bar Buckling Supports at Standard Strain Rate



a. Standard Strain Rate



b. High Strain Rate

Figure 38: Typical Fractures of Damaged 24-Ply Specimens Tested in Compression with Fatigue Guides



RB-16
Compression
 $\sigma_{uc} = 35 \text{ ksi (241 MPa)}$



RB-18
Compression
 $\sigma_{uc} = 34 \text{ ksi (234 MPa)}$



KC-25
Tension
 $\sigma_{ut} = 41 \text{ ksi (281 MPa)}$



PB-11
Tension
 $\sigma_{ut} = 42 \text{ ksi (290 MPa)}$

Figure 10. Tension and Compression of Damaged Holes in Compression and Tension of K_2 -Ply and I_1 -Isotropic Laminate

compression tests is presented in Table XIII. The two stage essentially linear behavior observed in the tension stress-strain record of the undamaged QC specimens was also evident for the damaged specimens but, as in Task I, the strength decreased by approximately 50%. An additional reduction from the damaged tension data of 15% was observed for the damaged compression specimens which was essentially the same as the decrease observed for the Task I specimens. Compression stress-strain curves were totally non-linear with a continuously decreasing slope, hence secant modulus values were determined. Results of Tasks I, II and III for the 32-ply laminate were very similar with the slight disparity primarily in the larger data dispersion of Task I damaged compression strengths and failure strains. The average failure strains for the Task III static tests were slightly higher, but also the sample size was small. Compression data obtained with the 4-bar support (constraint #2) were more widely scattered than with the buckling guide but were in the same range as the latter results.

High strain rate tests were conducted at rates of $0.5 - 2 \text{ min}^{-1}$ in tension and compression with five specimens per condition. These results also appear in Table XIII and are presented in Figure 40. No change in modulus or shape of the stress-strain curves was observed for either tension or compression but a significant (approximately 14%) decrease in compression strength and failure strain was apparent. While tension strength was unaffected, data dispersion increased. Typical fracture features are shown in Figure 41. No significant differences in failure appearances between high and low strain rate tests were observed for either the tension or compression loading. Tension failures were primarily normal to the loading direction with limited 45° fiber pull out. Delamination was minimal with none observed for some specimens. Compression fractures were similar to

TABLE XIII
SUMMARY OF TENSION AND COMPRESSION RESULTS
FOR DAMAGED 32-PLY LAMINATES

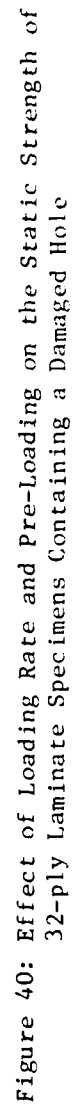
Data Set	Strength ksi (MPa)		Apparent Failure Strain in. 9 in. (23 mm)		Apparent Modulus psi x 10 ⁶ (GPa)	
	\bar{x}	s	\bar{x}	s	\bar{x}	s
32-PLY DAMAGED TENSION						
- Task I (Std. Rate) ^b	40.2 (277)	1.5 (10)	0.0078	0.0002	5.4 (37)	0.2 (1.4)
- Task II (Std. Rate)	40.4 (279)	1.6 (11)	0.0082	0.0003	5.1 (35)	0.1 (0.7)
- Task II (High Rate) ^c	40.0 (275)	3.4 (23)	0.0085	0.0012	5.3 (37)	0.2 (1.4)
- Task III (Std. Rate)	40.0 (275)	1.9 (13)	0.0083	0.0005	5.1 (35)	0.2 (1.3)
32-PLY DAMAGED COMPRESSION						
- Task I (Std. Rate)	35.4 (244)	3.9 (27)	0.0078	0.0009	4.9 (33)	0.1 (0.7)
- Task II (Std. Rate)	34.2 (236)	1.5 (10)	0.0072	0.0004	5.1 (35)	0.1 (0.7)
- Task II (High Rate)	29.3 (202)	4.5 (31)	0.0063	0.0011	5.1 (35)	0.2 (1.4)
- Task III (Std. Rate)	35.7 (246)	0.4 (3)	0.0093	0.0003	4.6 (32)	0.1 (0.4)
- Task III (Std. Rate) Constraint # 2 ^d	35.0 (241)	5.4 (37)	0.0076	0.0014	4.9 (34)	0.1 (0.5)

a. \bar{x} = mean, s = standard deviation, V% = coefficient of variation

b. Tested at standard strain rate of 0.005/min; Task I - 10 point data set, Task II- 15 point data set, Task III - 3 point data set.

c. Tested at high strain rate of 2/min Tension, 0.05/min compression; 5 point data set.

d. Constraint #2 - 4-bar support (Figure 21); other tests with constraint #1 - Fatigue Guide (Figure 20).



those observed for the damaged 24-ply laminate. Buckling failures occurred in the unsupported regions which for constraint #2 was the entire specimen width. The effect of the edge constraint offered by the fatigue guide is evident in the edge views of Figure 41 where specimen JC-26 exhibits a compression failure mode while EA-2 a buckling mode. Delaminations and 0° surface ply cracking were present in the region of the hole for both constraint conditions but were slightly more extensive for constraint #2, although not severe for either condition.

5.4 DAMAGE GROWTH UNDER STATIC LOADING

To evaluate the early stages of damage growth under static loading, a series of tests were conducted by initially loading a set of specimens to predetermined levels, unloading and characterizing the damage growth, if any. Results of these tests are shown in Table XIV. For the 24-ply specimens the results indicate some damage growth at stress levels above 56 ksi (386 MPa) in tension and above 34 ksi (234 MPa) in compression. For the 32-ply specimens damage growth occurred at stress levels above 34 ksi (234 MPa) in tension and 25 ksi (172 MPa) in compression.

Specimens were then loaded to failure, and the failure properties recorded as shown in Table XV. No significant difference was observed in the final failure properties as compared to those of baseline specimens. Thus, the load/unload cycle was assumed to have no significant effect on the static fracture behavior.

5.5 STATIC TEST RESULTS FOR DAMAGED LAMINATES AT ELEVATED TEMPERATURE

One of the variables evaluated under fatigue loading in Task III (Items 5C and 6C of Test Matrix) was the effect of elevated temperature. To provide a static baseline for this condition five specimens with damaged holes were tested in tension and five in compression at 180°F (82°C) for each

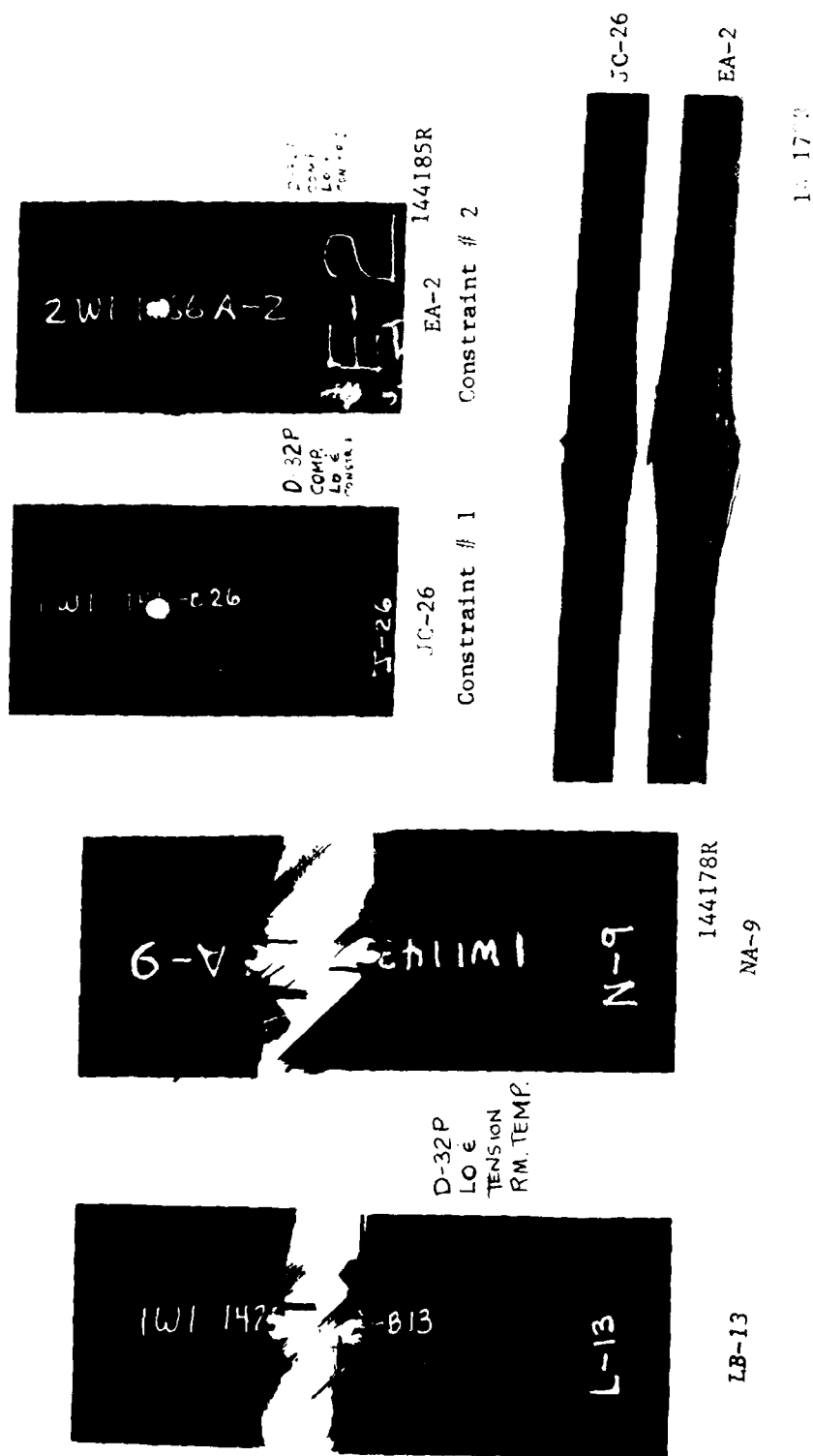


Figure 41: Fracture Features Typical of High and Low Strain Rate Tests for Damaged 32-ply Specimens

TABLE XIVa
DAMAGE GROWTH UNDER
STATIC TENSION AND COMPRESSION LOADING

		INITIAL MEASUREMENTS			PRE-LOAD STRESS (ksi)	MEASUREMENT AFTER PRE-LOAD			FAILURE STRESS σ_{ult} (ksi)	BASELINE FAILURE STRESS σ_{ult} (ksi)
		A^2 (in ²)	X (in)	Y (in)		A^2 (in ²)	X (in)	Y (in)		
24-PLY TENSION	EB-18	0.40	0.65	0.74	56.0	0.47	0.66	0.91	74.3	Average = 74.2
	FB-12	0.41	0.63	0.81	63.0	0.43	0.65	0.85	76.5	+ 8.2
	BA-7	0.39	0.64	0.76	67.0	0.42	0.63	0.83	73.3	- 9.5
COMPRESSION	BA-27	0.39	0.63	0.74	-34.0	0.40	0.65	0.79	46.6	Average = 44.4
	CA-7	0.40	0.63	0.75	-38.0	0.39	0.66	0.76	44.9	+ 5.6
	GA-7	0.39	0.66	0.75	-40.0	0.40	0.68	0.74	44.8	- 4.4
	NC-24	0.48	0.78	0.81	30.3	0.47	0.77	0.81	*	Average = 40.4
32-PLY TENSION	PC-29	0.53	0.79	0.88	34.3	0.55	0.79	0.91	*	+ 3.1
	SC-25	0.55	0.81	0.91	36.4	0.54	0.77	0.92	*	- 2.7
	MB-19	0.51	0.79	0.86	25.7	0.61	1.09	.79	30.0	34.2
COMPRESSION	LC-28	0.51	0.82	0.79	29.1	0.68	1.23	0.80	32.7	+ 2.1
	KB-15	0.47	0.73	0.83	30.8	0.59	0.79	0.84	39.8	- 2.3

* Final tests run in compression rather than tension, compressive ultimate strengths 32.0, 32.3 and 33.6 ksi respectively.

TABLE XIVb
DAMAGE GROWTH UNDER
STATIC TENSION AND COMPRESSION LOADING

		INITIAL MEASUREMENTS			PRE-LOAD STRESS (MPa)	MEASUREMENT AFTER PRE-LOAD			FAILURE STRESS σ_{ult} (MPa)	BASELINE FAILURE STRESS σ_{ult} (MPa)
		K (mm ²)	X (mm)	Y (mm)		K_0 (mm ²)	X (mm)	Y (mm)		
24-PLY TENSION	EB-18	258	17	19	385	303	17	23	512	Average = 512
	FB-12	265	16	21	434	277	17	22	527	+57
	BA-7	252	16	19	462	271	16	21	505	-66
COMPRESSION	BA-27	252	16	19	234	258	17	21	321	Average = 306
	CA-7	258	16	19	262	252	17	19	310	+39
	CA-7	252	17	19	276	258	17	19	309	-30
32-PLY TENSION	NC-24	310	20	21	209	303	20	21	*	Average = 279
	PC-29	342	20	22	236	355	20	23	*	+21
	SC-25	355	21	23	251	348	20	23	*	-19
COMPRESSION	MB-19	329	20	22	177	394	28	20	207	Average = 236
	LC-28	329	21	20	201	439	31	20	225	+14
	KB-15	303	19	21	212	381	20	21	274	-16

* Final tests run in compression rather than tension, compressive ultimate strengths were 221, 223, and 232 MPa respectively.

TABLE XVa

STATIC TENSION AND COMPRESSION TEST RESULTS
AFTER PRELOAD FOR 24-PLY AND 32-PLY DAMAGED
HOLE SPECIMENS

Specimen ID	Average Gross Area, A (in. ²)	Failure Load, P _{ult} , kip	Gross Failure Stress, σ_{ult} , ksi	Apparent Strain, At Failure ϵ_f , in./in.	Secant Modulus At Failure E_{sf} , psi x 10 ⁶	Initial Tangent Modulus E_i , psi x 10 ⁶
24-Ply Tension						
BA-7	0.362	26.5	73.3	0.0089	8.2	8.7
EB-18	0.363	27.0	74.3	0.0092	8.1	8.7
FB-12	0.363	27.8	76.5	0.0094	8.1	8.8
24-Ply Compression						
BC-27	0.362	16.9	46.6	0.0060	7.8	8.9
CA-7	0.362	16.2	45.0	0.0061	7.4	9.4
GA-7	0.362	16.2	44.8	0.0058	7.7	8.9
32-Ply Compression						
KB-15	0.486	19.4	39.8	0.0086	4.6	5.0
LC-28	0.481	15.8	32.7	0.0069	4.7	5.0
MB-19	0.483	14.5	30.0	0.0065	4.6	5.1

TABLE XVb
 STATIC TENSION AND COMPRESSION TEST RESULTS
 AFTER PRELOAD FOR 24-PLY AND 32-PLY DAMAGED
 HOLE SPECIMENS

Specimen ID	Average Gross Area, A (mm ²)	Failure Load, P _{ult.} (kN)	Gross Failure Stress, $\sigma_{ult.}$ (MPa)	Apparent Fracture Strain, ϵ_f , mm/mm in 225 mm	Secant Modulus At Failure E _{sf.} (GPa)	Initial Tangent Modulus E _{i.} (GPa)
24-Ply Tension						
BA-7	234	118	505	0.0089	57	60
EB-18	234	120	512	0.0092	56	60
FB-12	234	124	527	0.0094	56	61
24-Ply Compression						
BC-27	234	75	321	0.0060	54	61
CA-7	234	72	310	0.0061	51	65
GA-7	234	72	309	0.0058	53	61
32-Ply Compression						
KB-15	314	86	274	0.0086	32	34
LC-28	310	70	225	0.0069	32	34
MB-19	312	64	207	0.0065	32	35

TABLE XVI
COMPARISON OF ELEVATED AND ROOM TEMPERATURE
STRENGTH DATA AT TWO STRAIN RATES
FOR DAMAGED LAMINATES

			TENSION		COMPRESSION	
			ksi	σ_{ut} MPa	ksi	σ_{uc} MPa
24-Ply 180°F (82°C)	Standard Strain Rate ^a	Mean	80.9	558	36.6	252
		Std. Dev.	5.2	36	3.9	27
		Coef. of Var. %	6.5	6.5	10.7	10.7
	High Strain Rate ^b	Mean	74.9	516	36.0	248
		Std. Dev.	2.1	14	1.3	9
		Coef. of Var. %	2.8	2.8	3.5	3.5
24-Ply Room Temperature	Standard Strain Rate	Mean	74.2	512	44.4	306
		Std. Dev.	5.5	38	2.8	19
		Coef. of Var. %	7.3	7.3	6.3	6.3
	High Strain Rate ^c	Mean	67.5	465	36.9	254
		Std. Dev.	3.0	21	2.9	20
		Coef. of Var. %	4.4	4.4	7.8	7.8
32-Ply 180°F (82°C)	Standard Strain Rate	Mean	44.5	307	27.6	190
		Std. Dev.	2.5	17	0.6	4
		Coef. of Var. %	5.7	5.7	2.2	2.2
	High Strain Rate ^b	Mean	40.8	281	26.2	181
		Std. Dev.	1.6	11	1.4	10
		Coef. of Var. %	3.9	3.9	5.4	5.4
32-Ply Room Temperature	Standard Strain Rate	Mean	40.4	279	34.2	236
		Std. Dev.	1.6	11	1.5	10
		Coef. of Var. %	4.0	4.0	4.5	4.5
	High Strain Rate ^d	Mean	40.0	275	29.3	202
		Std. Dev.	3.4	23	4.5	31
		Coef. of Var. %	9.2	9.2	15.5	15.5

a = 0.005 min⁻¹

b = 4 min⁻¹

c = 5 min⁻¹

d = 2 min⁻¹ tension, 0.5 min⁻¹ compression

laminate type at two strain rates. Results are summarized in Table XVI along with Task II room temperature data which are included for comparison. The overall effect of high strain rate for all conditions evaluated and both laminates types was a reduction in the strength of laminates containing damaged holes. Compression strength decreases due to the higher strain rate were insignificant at elevated temperatures for both laminates while at room temperature the reduction was on the order of 15%. Tension strength dropped approximately 8% as a result of high strain rate for all cases except the 32-ply laminate room temperature condition where no change was evident. Elevated temperature produced an increase in tensile strength in all cases, most likely due to a reduction in notch acuity. As expected, compressive strength decreased as a consequence of the increased propensity towards buckling which is evident in the photographs of Figure 42. Tension fractures at elevated temperatures did not differ measurably in appearance from room temperature tests. Typical examples are displayed in Figure 43.

5.6 TENSION AND COMPRESSION DATA FOR UNDAMAGED LAMINATES

Included in the Task II test matrix (Item 9) was a set of baseline material tests to be conducted on 3-inch (76 mm) wide specimens identical to the damaged hole specimens of Figure 17 except that they contained no hole or intentional damage. Four replicates of each laminate per a condition were tested.

The 24-ply and 32-ply laminate undamaged tension and compression test results, at strain rates of 0.005 min^{-1} and 2.3 min^{-1} are presented in Tables XVII and XVIII and comparison with the QC data is shown in Figures 44 and 45. A number of 24-ply specimens tested in tension were machined to a 2.5-inch (64 mm) width since the load required to fail the wider specimens exceeded the 55,000 lb. (245 kn) load capacity of the hydraulic grips.

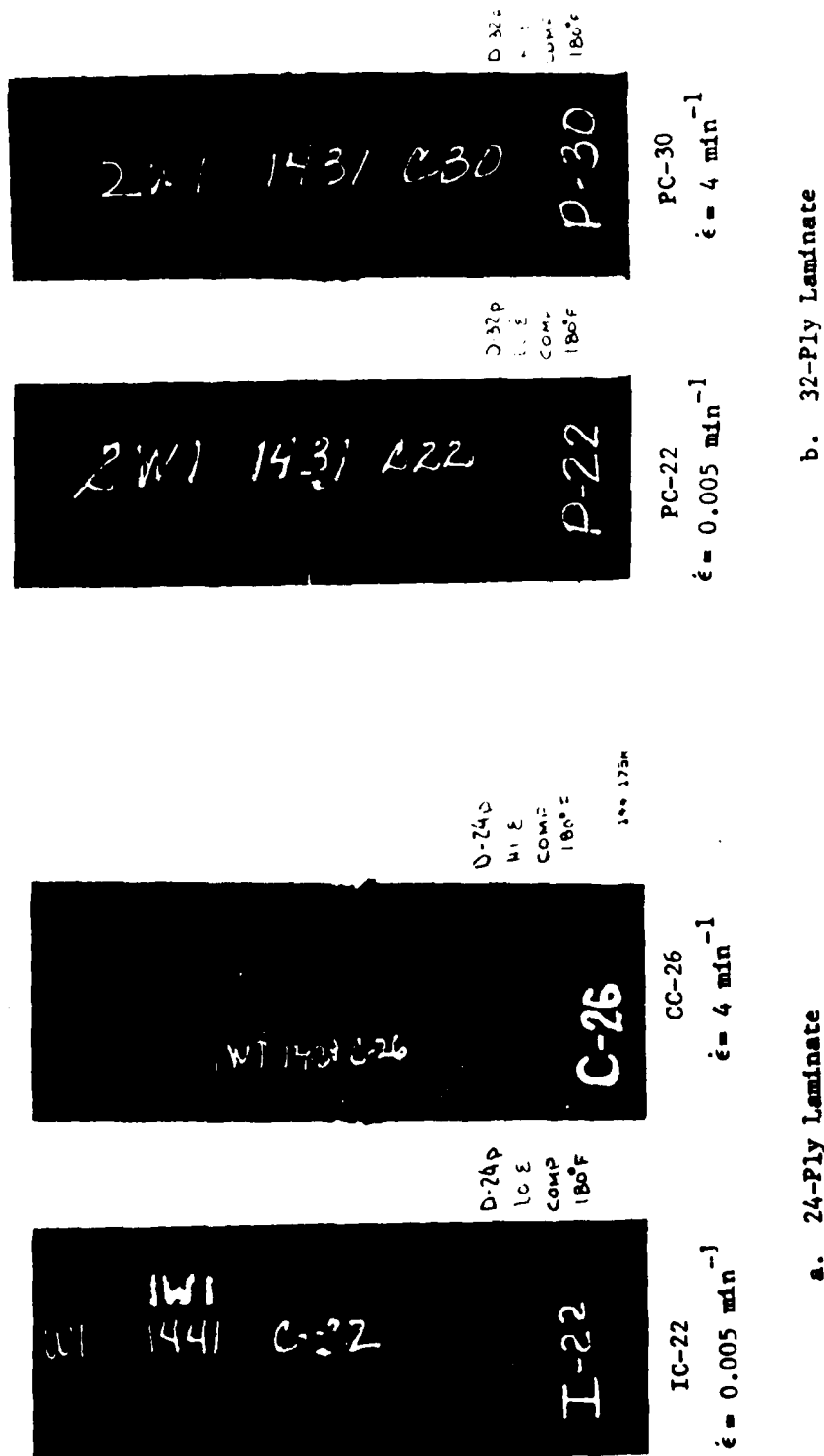


Figure 42: Typical Fractures of Damaged Laminates Tested in Compression at 180°F (82°C)

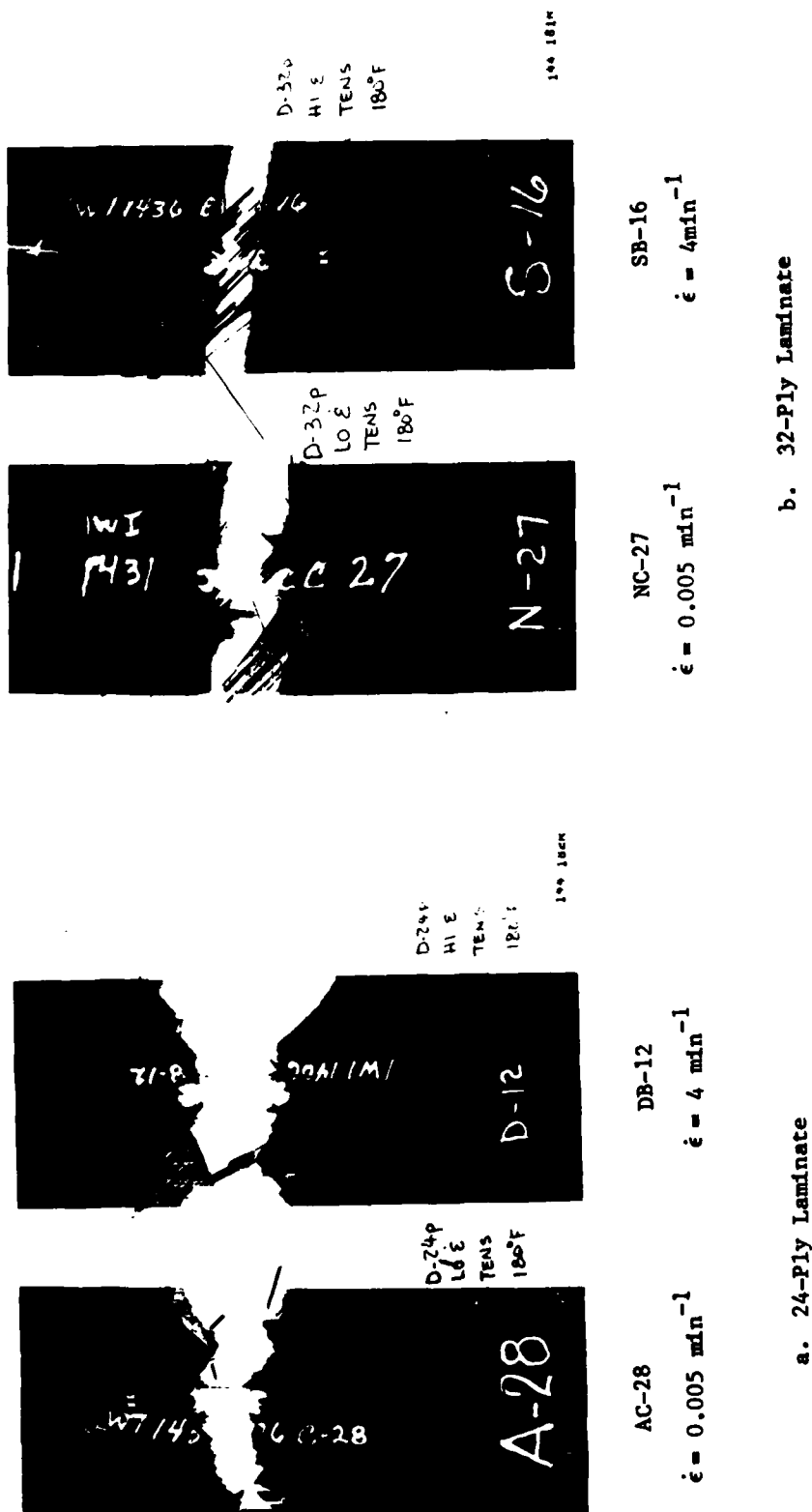


Figure 43: Typical Fractures of Damaged Laminates Tested in Tension at 180°F (82°C)

TABLE XVII
TENSION STRENGTH DATA
FOR UNNOTCHED SPECIMENS

Laminate Type	STANDARD STRAIN RATE			HIGH STRAIN RATE		
	Specimen ID	ksi	σ_{ult} MPa	Specimen ID	ksi	σ_{ult} MPa
Unnotched 24-Ply 67% - 0° Laminate	BB-11	161.2	1111	AC-22	118.5	817
	BC-24	a,b	-	DA-9	166.7	1149
	EB-13	a,b	-	FC-22	152.4	1051
	EC-28	157.8	1088	GB-13	145.2	1001
	HB-14	a	-			
	IB-18	149.4 ^b	1030			
	Mean	156.1	1076		145.7	1005
	Std. Dev.	6.1	42		20.2	139
	Coef. of Var. %	3.9	3.9		13.9	13.9
Unnotched 32-Ply Quasi- Isotropic Laminate	JB-13	77.6	535	KA-1	76.0	524
	LC-22	78.3	540	PC-28	82.5	569
	QB-15	82.7	577	SC-28	78.4	541
	RA-9	72.2	498			
	Mean	77.7	536		79.0	545
	Std. Dev.	4.3	30		3.3	23
	Coef. of Var. %	5.5	5.5		4.2	4.2

a = Loaded to grip capacity without failure

b = 3 inches wide

NOTE: Specimens Machined to 2.5-inch (64 mm) Width Except Where Noted Otherwise

TABLE XVIII
COMPRESSION STRENGTH DATA
FOR UNNOTCHED SPECIMENS

Laminate Type	STANDARD STRAIN RATE			HIGH STRAIN RATE		
	Specimen ID	ksi σ_{ult}	MPa	Specimen ID	ksi σ_{ult}	MPa
Unnotched 24-Ply 67° - 0° Laminate	CB-13	85.8	592	AC-23	93.7	646
	CC-29	85.5	590	BA-3	93.5	645
	EA-2	88.3	609	GA-8	86.9	599
	FC-28	93.9	647	GC-28	97.1	669
				IC-26	85.6	590
	Mean	88.4	609		92.5	638
	Std. Dev.	3.9	27		4.9	34
	Coef. of Var. %	4.4	4.4		5.3	5.3
Unnotched 32-Ply Quasi- Isotropic Laminate	NB-12	54.7	377	JA-2	60.3	416
	NC-23	51.3	354	KC-29	63.7	439
	PA-2	58.1	401	MA-9	57.1	394
	QB-18	59.4	410	QA-10	75.9	523
				RB-16	68.2	470
	Mean	55.9	385		65.0	448
	Std. Dev.	3.6	25		7.3	50
	Coef. of Var. %	6.5	6.5		11.3	11.3

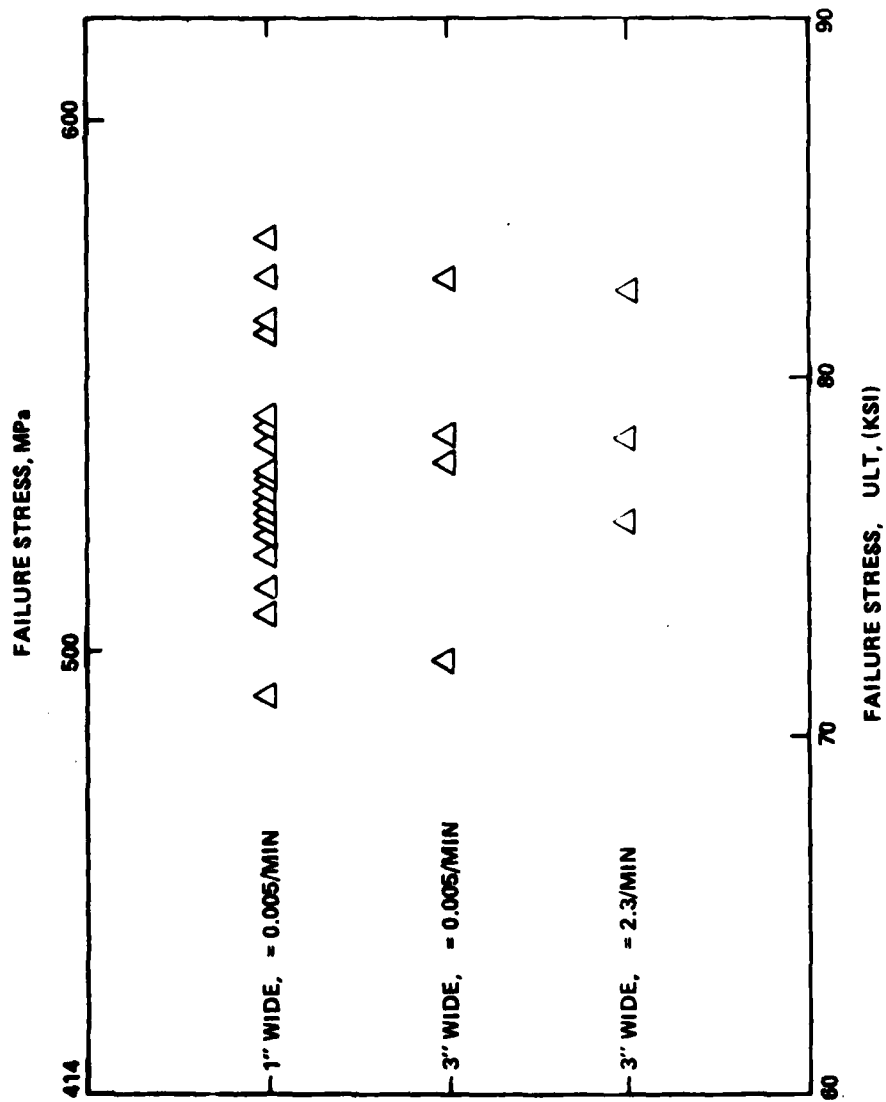


Figure 44: Effect of Specimen Width and Loading Rate on the Tensile Strength of Undamaged, 32-ply Laminate Specimens

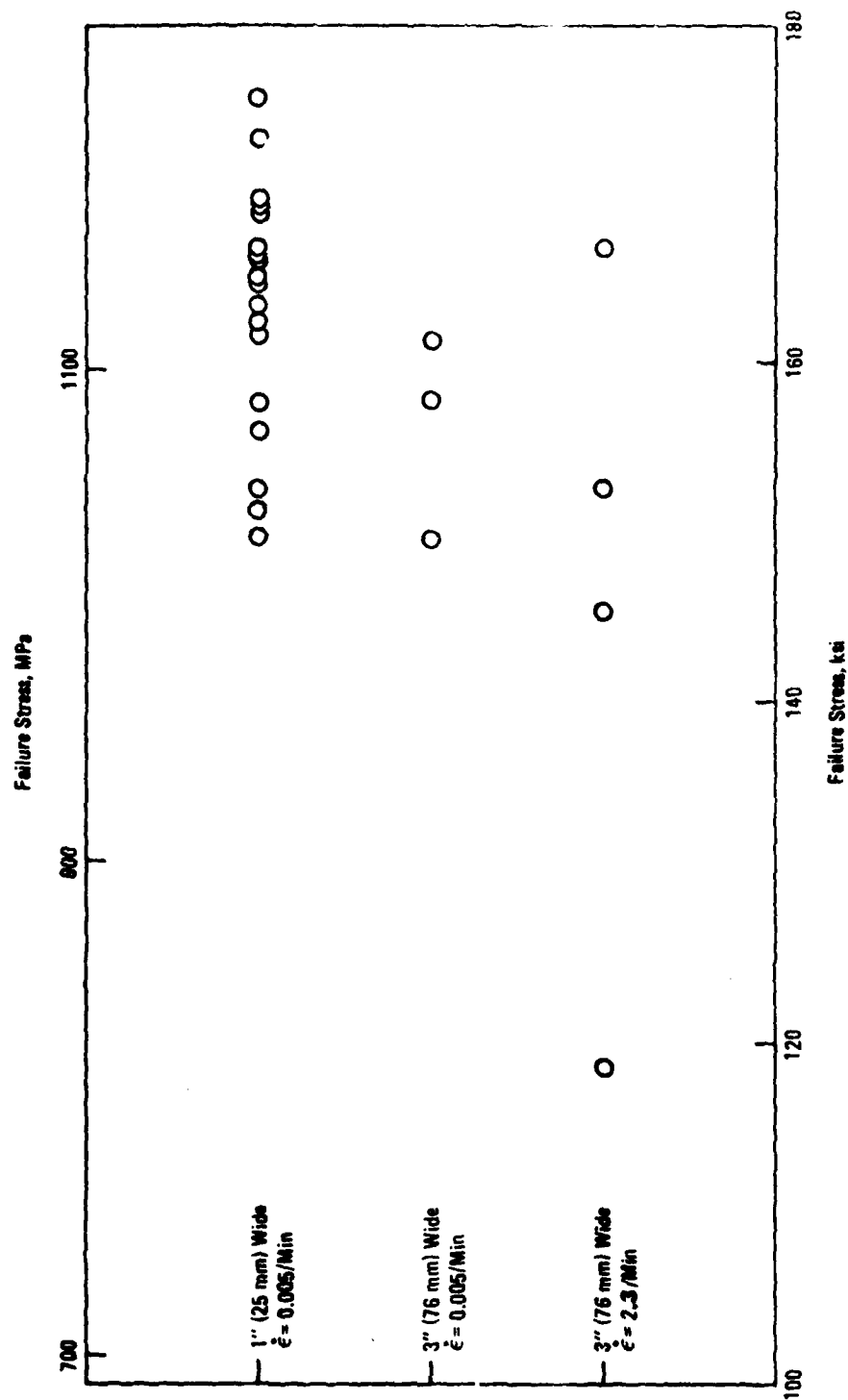


Figure 45: Effect of Specimen Width & Loading Rate on the Tensile Strength of Undamaged, 24-Ply Laminate Specimens

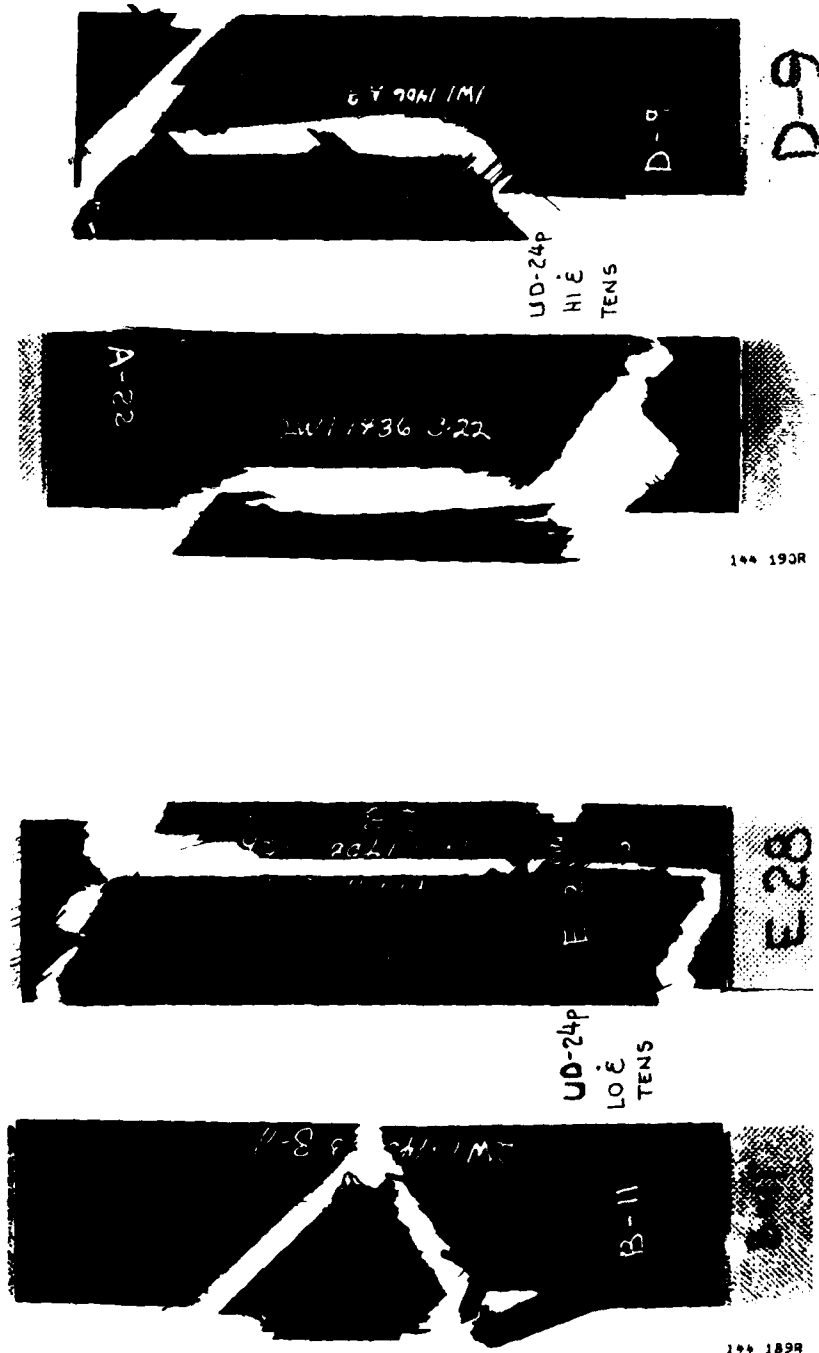
The sample size was too small to determine whether an effect existed.

There seemed to be an increase in compression strength for both laminates at the higher strain rate while the tension strength appeared to be unaffected for the 32-ply laminate and reduced for the 24-ply laminate.

The linear two stage slope exhibited by the unnotched one-inch (25 mm) wide and the notched three inch (76 mm) 32-ply specimens was also evident in the tension stress-strain record obtained for the 3-inch (76 mm) wide unnotched coupons. However, these wide unnotched 24-ply specimens displayed a tension stress-strain curve more comparable to that of the notched specimens and unlike the fairly linear record of the narrow unnotched coupons. The tensile curve was linear to only approximately 20% of the strength then progressed at a continuously decreasing slope to failure. Compression stress vs. strain records were totally non-linear for both laminates and similar to previously observed behavior.

Low strain rate tension specimens of the 24-ply laminate exhibited the two types of fractures shown in Figure 46a. Either a 45° triangle was split from the center of the specimen or a longitudinal piece was separated from the specimen at a 45° angle at either end. Final fracture was always at a 45° angle and accompanied by almost no delamination. These failures were very similar to those observed for the higher strength impact damaged specimens of Task I. The high strain rate tension failures were very similar to the second mode of failure exhibited by the low strain rate specimens differing by perhaps some slight delamination near the fracture.

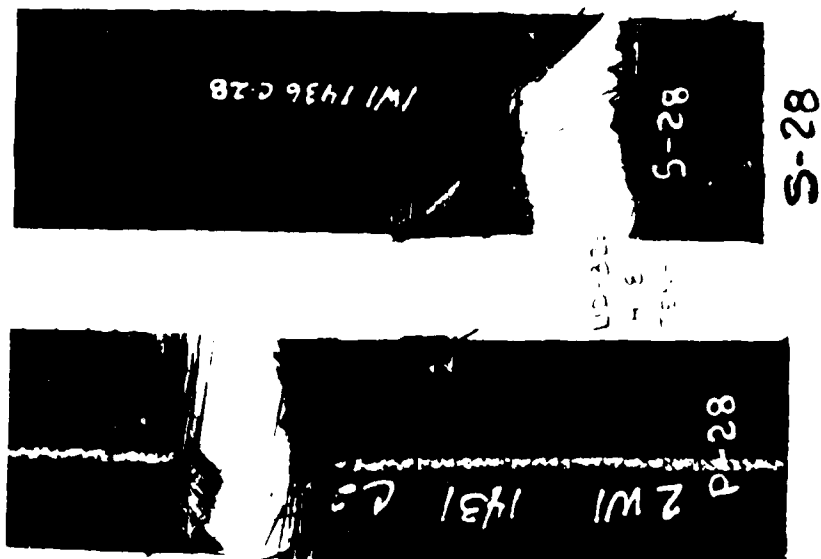
Low and high strain rate tension failures of the 32-ply laminates were indistinguishable. Failures occurred away from the tab usually normal to the load direction accompanied by a secondary crack at a 45° angle (Figure 47). Some delamination was present but was not extensive as was the case for the impact failures in Task I. Tension fractures of both the 24-ply and 32-ply



BB-11 EC-28 AC-22 DA-9

a. Strain rate = 0.005 min^{-1} b. Strain rate = 2 min^{-1}

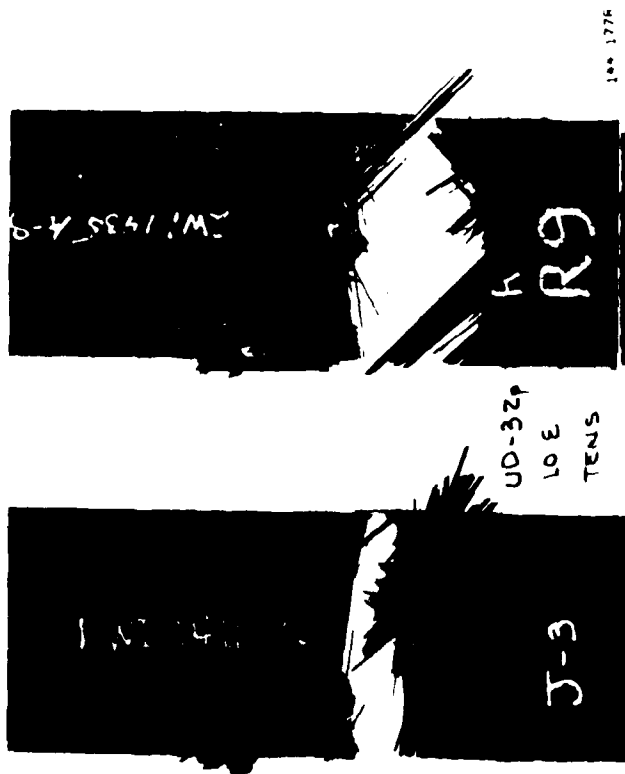
Figure 46: Typical Fractures of Undamaged 24-Ply Laminate Specimens Tested in Tension at Room Temperature



100 172M

PC-28 SC-28

b. Strain rate = 2 min⁻¹

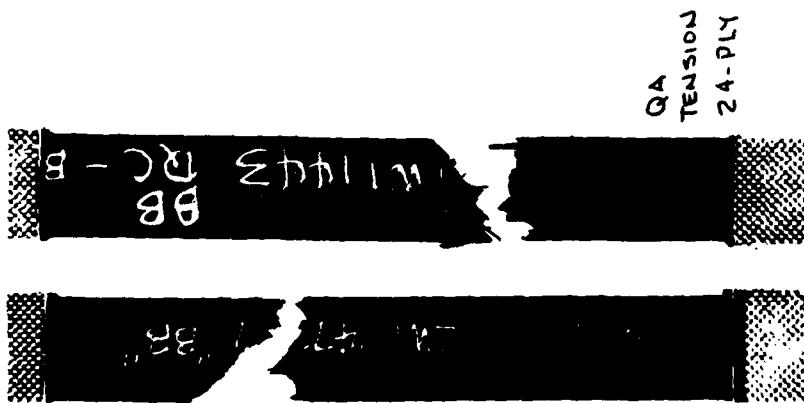


100 177M

JA-3 RA-9

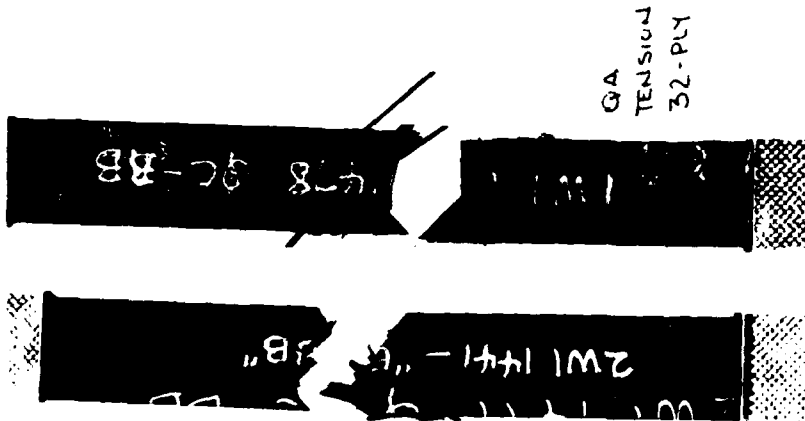
a. Strain rate = 0.005 min⁻¹

Figure 47: Typical Fractures of Undamaged 32-Ply Laminate Specimens Tested in Tension at Room Temperature



144 186R

a. 24-Ply Laminate



144 173H

b. 32-Ply Laminate

Figure 48: Typical Fractures of Undamaged One-Inch (25 mm) Wide Q.C. Specimens Tested in Tension at Standard Strain Rate

wide specimen had some similarity to the fractures of the narrow QC specimens as shown in Figure 48. Longitudinal splitting was not observed in the narrow 24-ply coupons while this failure type dominated in the wide specimens.

Since undamaged compression specimens were tested with the fatigue guide support the obvious failure location was the unsupported length near the tab which occurred for all conditions as shown in Figure 49.

5.7 COMPARISON OF TASK I AND TASK II DATA

The results of the Task I and Task II tension and compression data were represented by two-parameter Weibull statistical distributions (see Figures 50 through 55 and Table XIX) of the type described in Appendix K. The commonly used Weibull distribution is a specific form of the third asymptotic function of the statistical theory of extreme values ⁽²⁷⁾ and can be thought of as a generalization of the exponential probability distribution function.

Interpretation of a comparison of the experimental results by using the Weibull parameters shown in Table XIX often leads to conflicting inferences. This problem results because simple contrast of shape and characteristic value parameters does not always allow easy inference of whether distribution functions are different. For example, the population pairs represented by the first, second and sixth entries of Table XIX are probably different and that of entry five the same, but whether those of entries three and four are truly different is less clear.

Non-parametric statistical procedures were used to solve such problems in discrimination. In essence, differences in the Weibull parameters of two populations is a necessary condition for their distribution to be

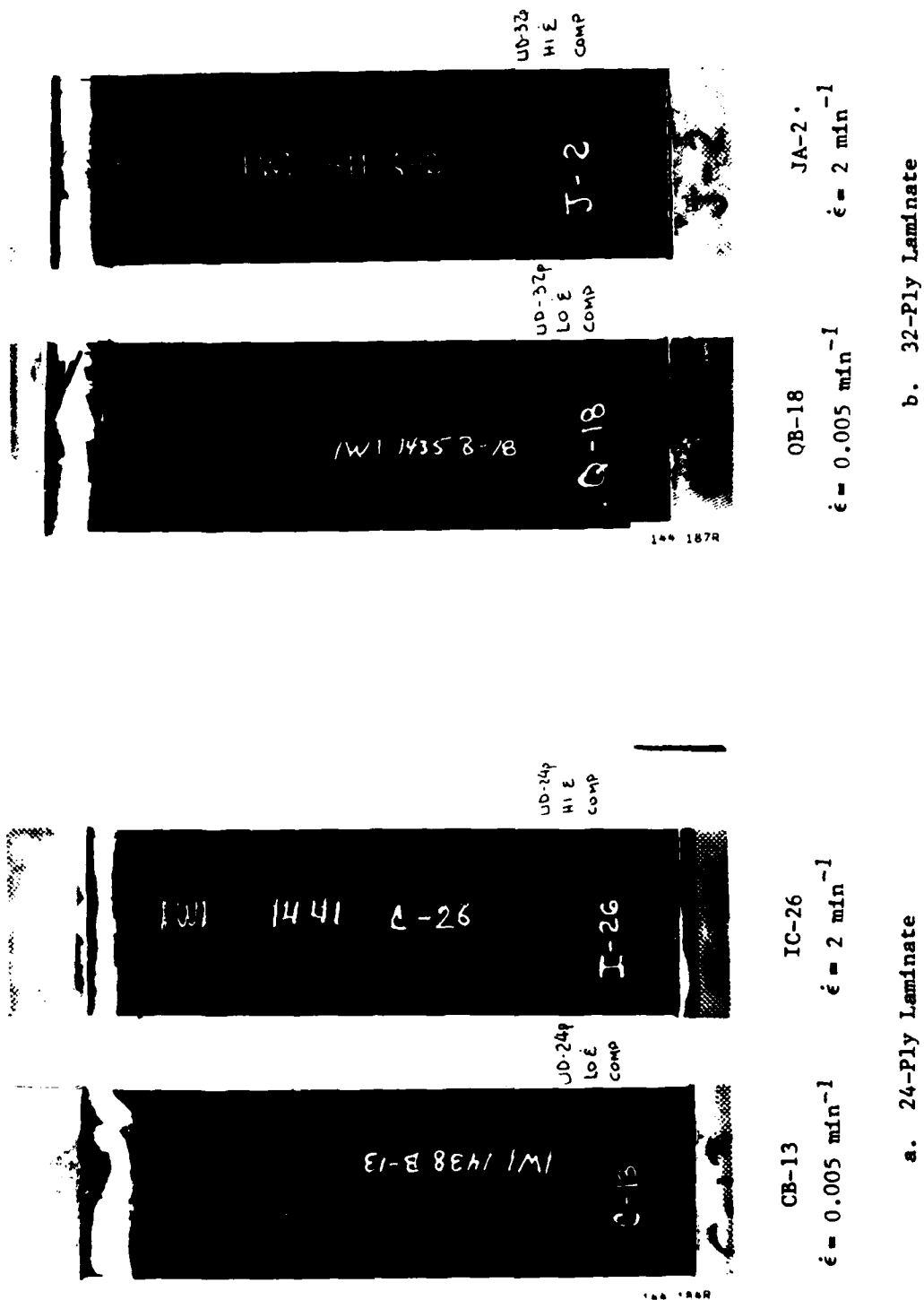


Figure 49: Typical Fractures of Undamaged Specimens Tested in Compression at Room Temperature

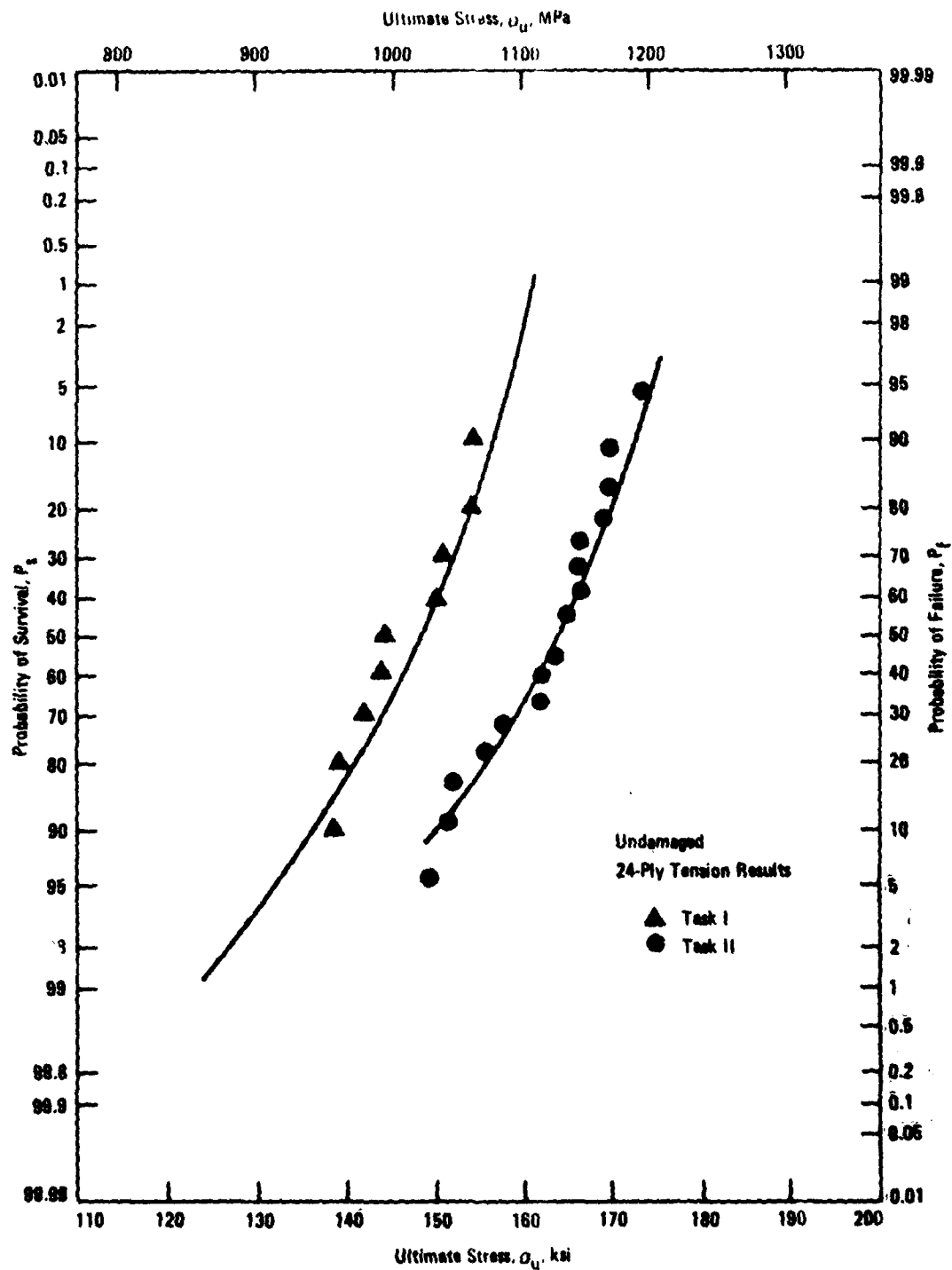


Figure 50 : Comparison of Two Parameter Weibull Curve Fit for Undamaged Task I and II 24-Ply Tension Data

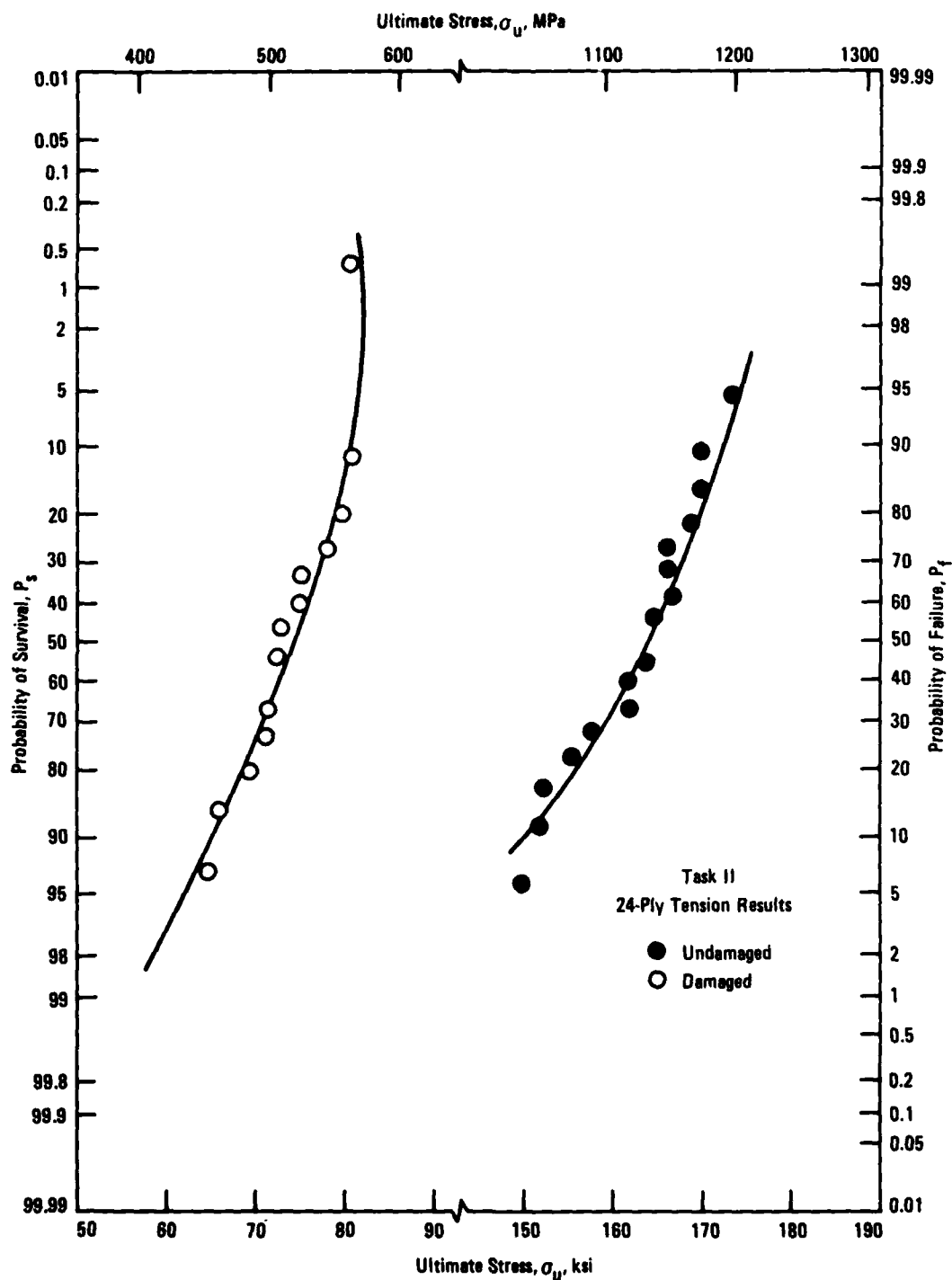


Figure 51: Comparison of Two Parameter Weibull Curve Fit for Undamaged and Damaged Task II 24-Ply Tension Data

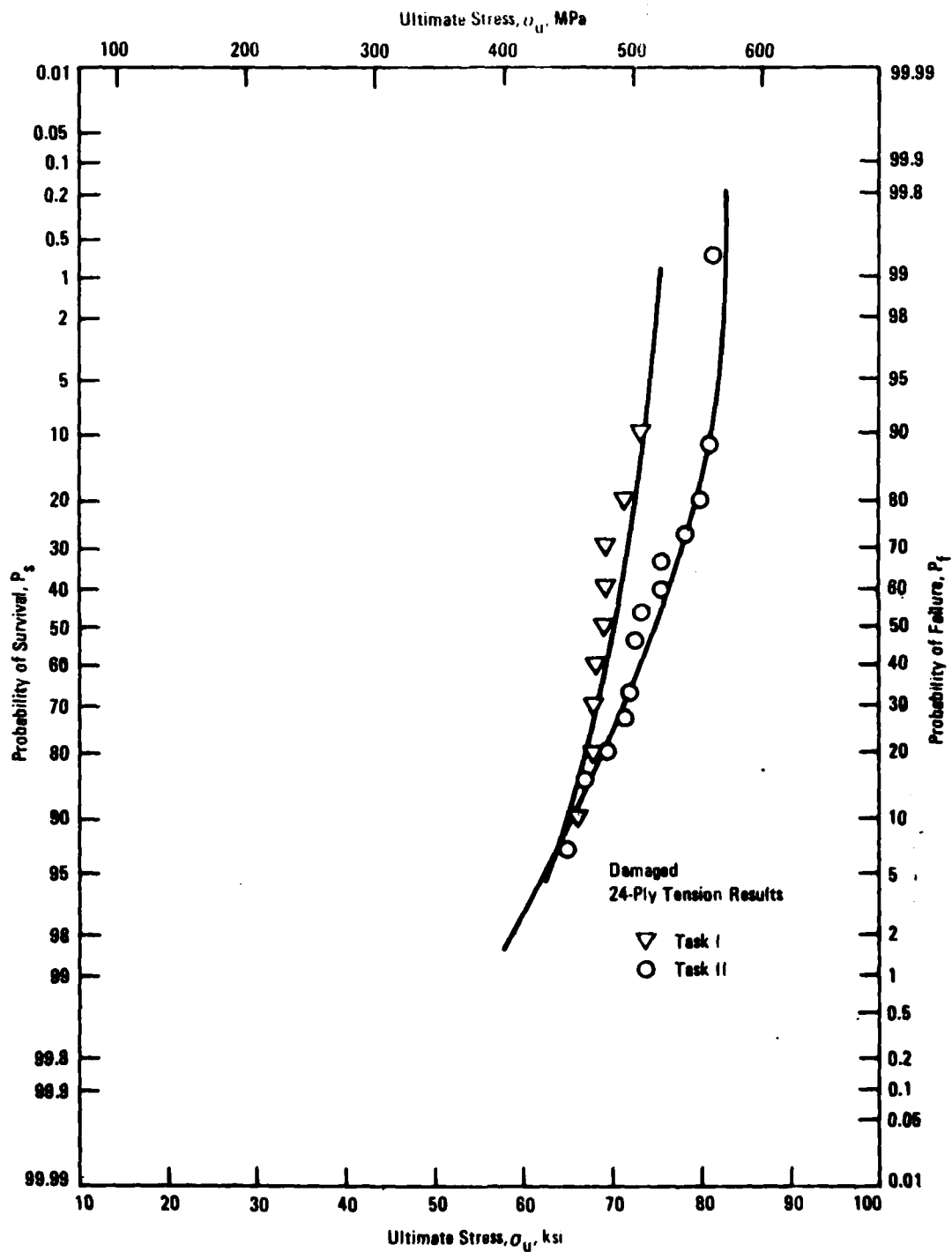


Figure 52: Comparison of Two Parameter Weibull Curve Fit for Damaged Task I and II 24-Ply Tension Data

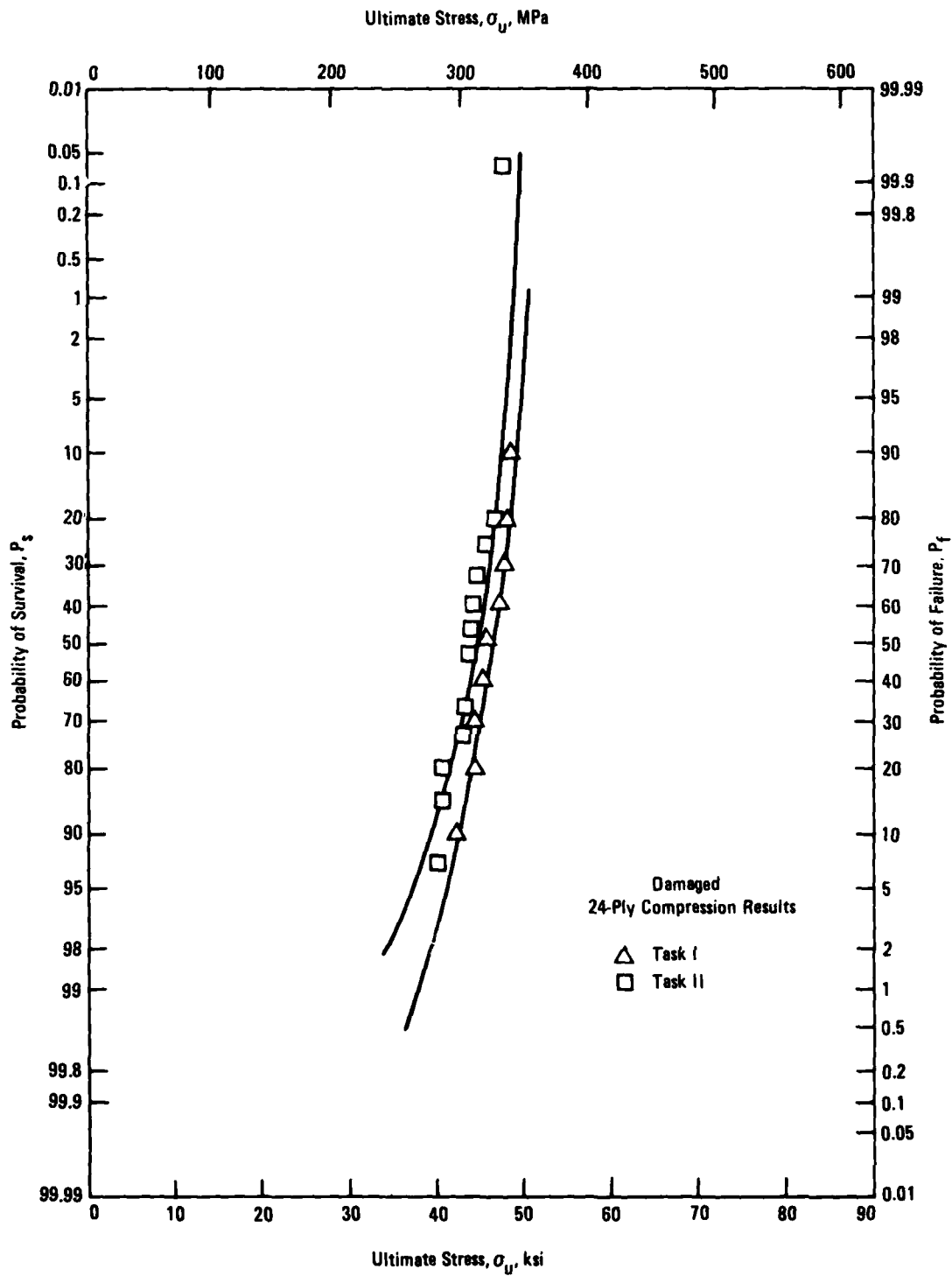


Figure 53: Comparison of Two Parameter Weibull Curve Fit for Damaged Task I and II 24-Ply Compression Data

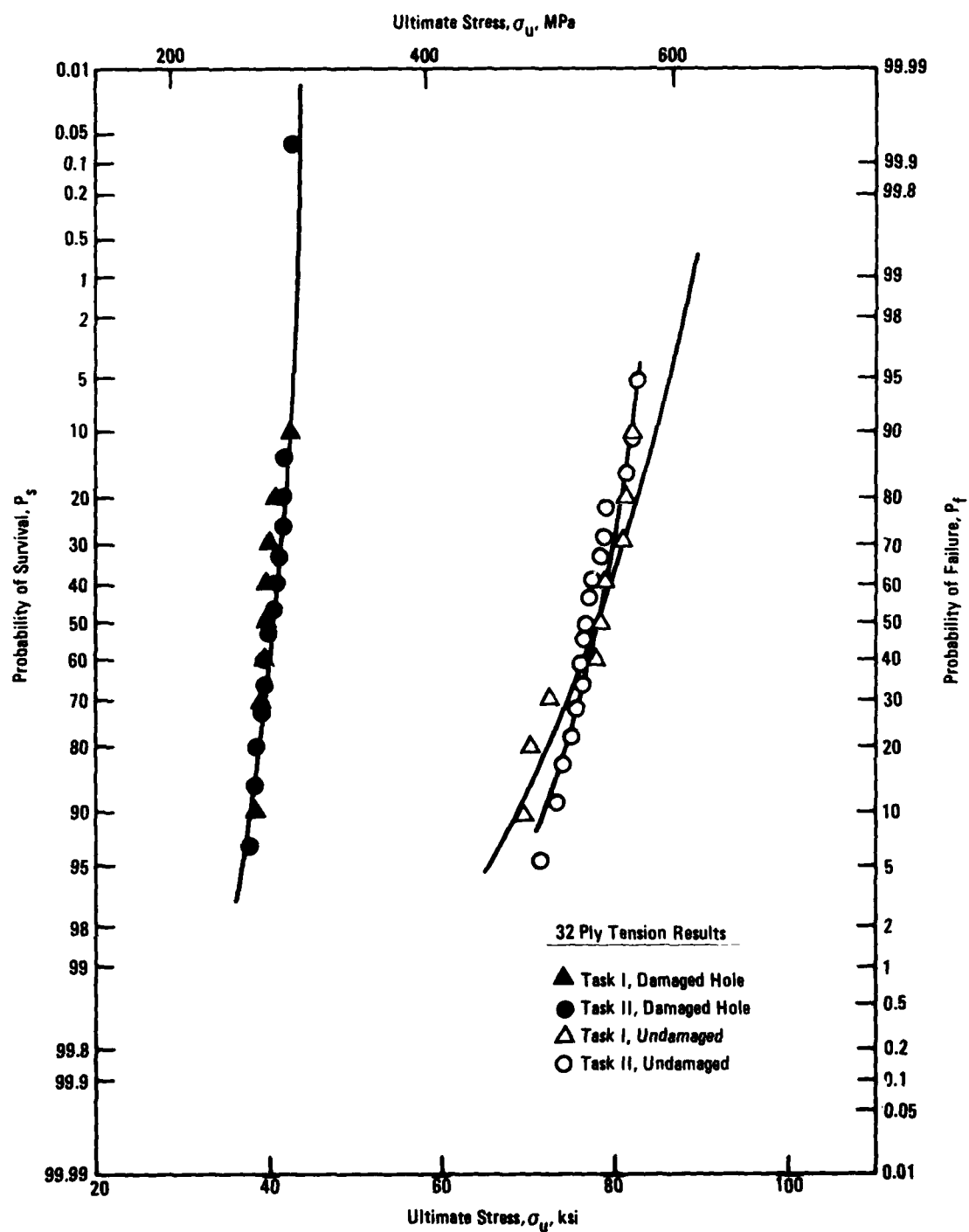


Figure 54: Comparison of Two Parameter Weibull Curve Fit for Task I and Task II 32-Ply Tension Data

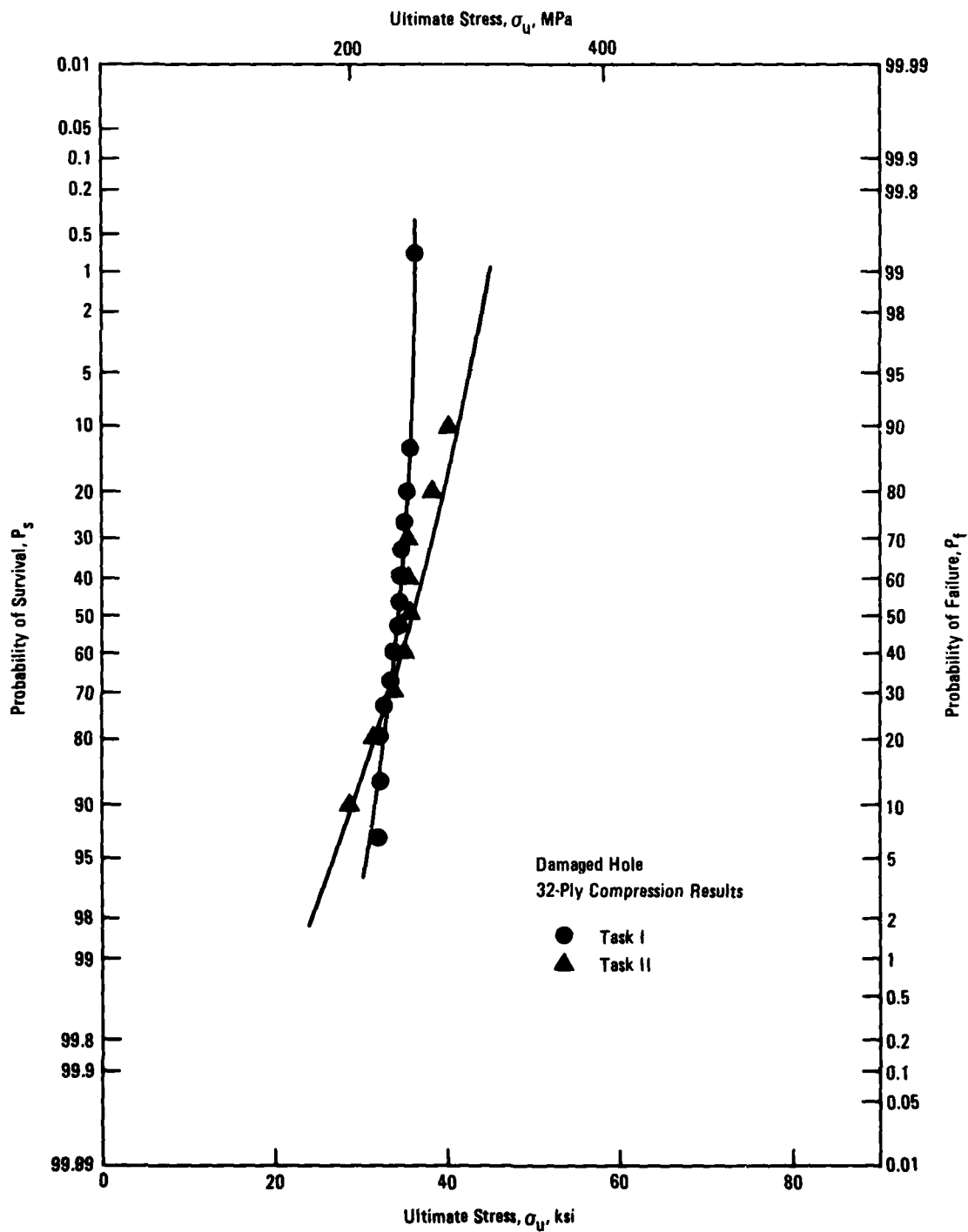


Figure 55: Comparison of Two Parameter Weibull Curve Fit for Task I and Task II 32-Ply Compression Data

TABLE XIX
COMPARISON OF TWO PARAMETER WEIBULL DATA FIT PARAMETERS
FOR TASK I AND TASK II

Data Set	Shape Parameter, k	Characteristic Value, v	Fit Parameter, r
24-Ply Unnotched Tension			
- Task I	22.61	150.51	0.9619
- Task II	23.05	166.80	0.9862
24-Ply Damaged Tension			
- Task I	24.70	71.09	0.9228
- Task II	14.05	76.81	0.9826
24-Ply Damaged Compression			
- Task I	20.60	47.32	0.9871
- Task II	16.23	45.77	0.9698
32-Ply Unnotched Tension			
- Task I	14.70	79.93	0.9625
- Task II	24.20	79.12	0.9635
32-Ply Damaged Tension			
- Task I	24.96	40.97	0.9082
- Task II	26.16	41.15	0.9807
32-Ply Damaged Compression			
- Task I	8.77	37.30	0.9777
- Task II	22.85	34.94	0.9756

different, but is not sufficient. This fact was born out by the results of the comparisons made using the non-parametric statistical procedures.

The non-parametric statistical test procedures selected for comparing data were the Mann-Whitney ⁽²⁸⁾ and Wald-Wolfowitz ⁽²⁸⁾ tests for determining whether the distribution functions of two different populations are the same. Both procedures were used because the sample size of the Task I data is not quite adequate to achieve an acceptable level of confidence for the Wald-Wolfowitz procedure. Because of the inadequacy of the population sample sizes for the Wald-Wolfowitz procedure, greater confidence was placed in the inferences based on the Mann-Whitney procedure. None of the Task III data were compared to the data of Tasks I and II using non-parametric statistical procedures because sample sizes must be at least greater than or equal to eight. This criterion was clearly not met for the Task III data where population sample sizes totaled three for damaged conditions and six for the undamaged.

Non-parametric statistical procedures were applied in such a manner as to evaluate whether the distributions of two populations were the same or different to a five percent risk of error confidence level. Each pair of the six Task I and Task II data groups shown in Table XIX were compared. The results of the comparison are summarized as follows:

Data Set	Mann-Whitney Statistic	Distribution Functions Are:
24-Ply Unnotched Tension	3.37	Probably Different
24-Ply Damaged Tension	2.77	Probably Different
24-Ply Damaged Compression	1.83	May Be Different

Data Set	Mann-Whitney Statistic	Distribution Functions Are:
32-Ply Unnotched Tension	0.14	Probably Same
32-Ply Damaged Tension	0.33	Probably Same
32-Ply Damaged Compression	1.23	May Be Different

The comparison table shows that the Task I and Task II 24-ply unnotched tension data are probably different thus reflecting the difference in fiber properties for the material batches discussed in Section 3. The table also shows that the significance of the difference in fiber properties was much less for the 24-ply damaged tension experiments and even less for the 24-ply damaged compression. The effect of fiber difference can be seen to be negligible for the 32-ply laminate. These conclusions as to the sensitivity, or insensitivity, of the laminates to fiber strength support the conclusion made in Section 5.2 based on the quality assurance data.

With regards to relating the non-parametric statistical procedure results to the Weibull parameter comparison of Table XIX, several comments are warranted. First, large differences in shape parameters do not mean that distribution functions are different as shown by the 32-ply unnotched tension data comparison. Second, the 24-ply damaged tension and compression results show that differences in shape or characteristic value parameters may mean that the distribution functions are different. These two inferences are supportive of the hypothesis that differences in Weibull parameters appear to be necessary for inferring distribution function differences, but are not sufficient. Third, the possible difference between the Task I and Task II 32-ply compression results is believed to be due to the fact that the population sample sizes are too small to accurately represent the actual distribution functions.

SECTION 6

TASK II FATIGUE RESULTS

Cyclic tests were conducted in this task primarily to establish the fatigue life and residual strength distributions by generating statistically significant data sets for the 24-ply and 32-ply laminates and to document in detail the fatigue induced damage growth characteristics. To this end, twenty replicate specimens for each laminate were subjected to fully reversed cyclic loading at a single stress level with damage growth for each specimen monitored a minimum of ten times during its life using a Holosonics Series 400 Holscan unit. Based on these results, five cycle levels were selected for the residual strength study. Twenty-three specimens of each laminate were inspected, cycled to one of the five preselected N values and Holscanned again. Three of the replicates were destructively analyzed while the other surviving specimens were tested in static tension or compression. This sequence was repeated for each of the five N values.

Due to the high compressive load component, specimens were supported with the fatigue guides of Figure 20 which consisted of full platen restraints with a 2.15 in. (55mm) square window. All tests were conducted in room temperature laboratory air. Testing details are presented in Section 4.2. Detailed test results are available in Volume III, Appendix E & F of this report.

6.1 FATIGUE LIFE RESULTS

6.1.1 Fatigue Life Distribution for the 24-Ply Laminate

Since the average damaged and undamaged tension strength of the 24-ply laminate for the Task II material batch appeared to be higher than that of

the Task I batch but the damaged compression strength showed no change as reported in Section 5.2, preliminary fatigue tests were conducted to determine whether the ± 35 ksi (241 MPa) stress level selected as a result of the Task I testing could still be expected to yield cyclic lives in the range of 10^5 to 10^6 cycles. Extra specimens which did not strictly meet the dimensional tolerance requirements were used for this evaluation. Three specimens were cycled at each of two stress levels, ± 34 ksi (234 MPa) and ± 38 ksi (262 MPa) and compared to the Task I results.

Results were as follows:	<u>± 34 ksi (234 MPa)</u>	<u>± 38 ksi (262 MPa)</u>
N =	1,142,500 ^b	92,784
	9,530	58,507
	18,430	10,211

For these specimens there was no correlation between life and the amount by which the specimens did not meet dimensional tolerances. Although there appeared to be an increase in the data dispersion, which was not unexpected, most of the lives were anticipated to be in the desired range for the selected stress level of ± 35 ksi (241 MPa). A series of twenty specimens was then fatigue cycled to failure at a stress level of ± 35 ksi (241 MPa) ($R = -1$) to determine the scatter at a given stress level. The Holskan ultrasonic unit was used to periodically measure the damage during the specimen life. Results of these tests are presented in Figure 56 along with the preliminary Task II and Task I test data. Task I and II results were consistent with data dispersion extending over just less than two orders of magnitude. Figures 57 and 58 respectively show the fatigue scatter results with the two parameter and three parameter Weibull curve fits for the Task II data.

b = Specimen failed due to accidental overload

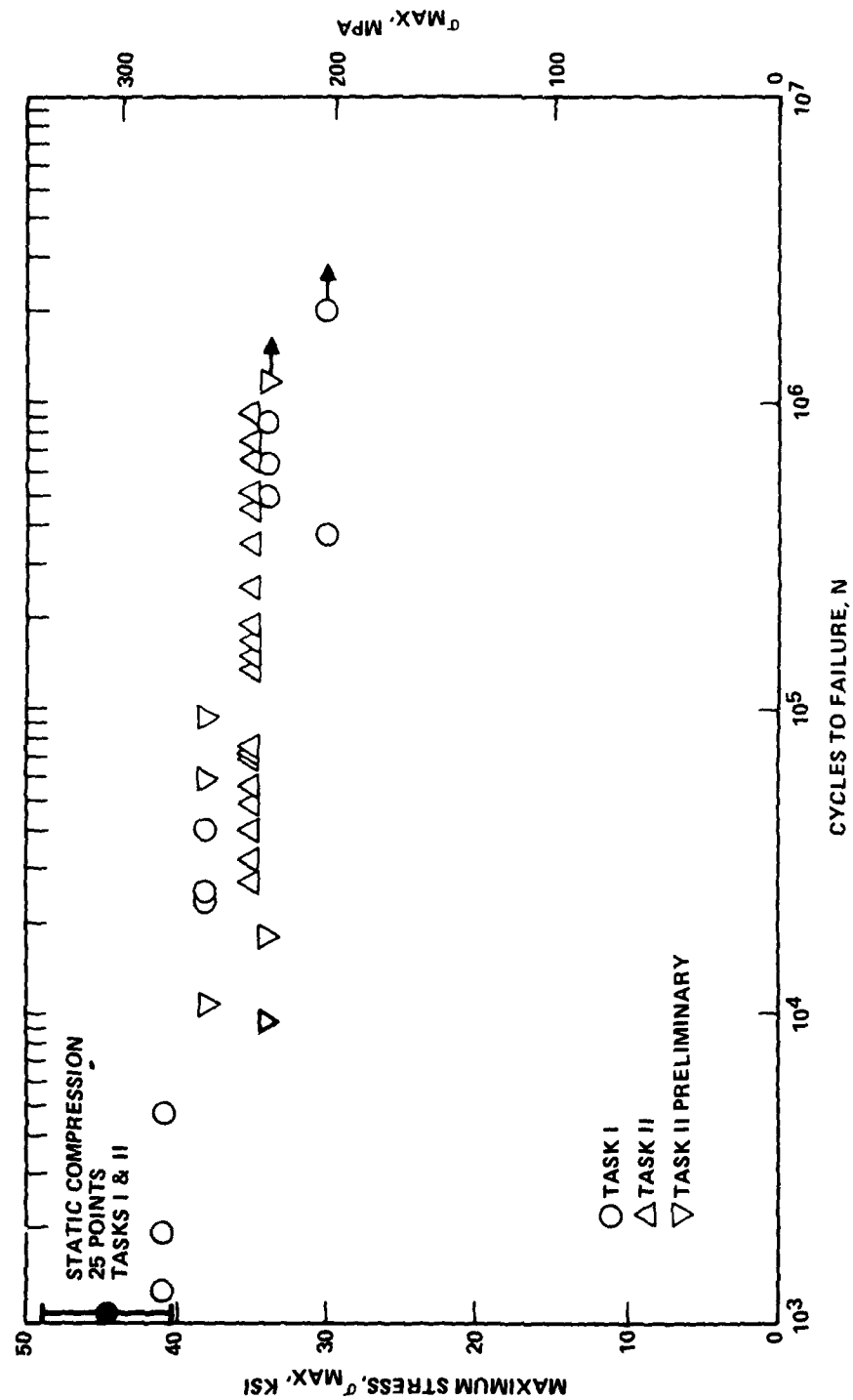


Figure 56 : Fatigue Scatter Results For 24-Ply Damaged Hole Specimens

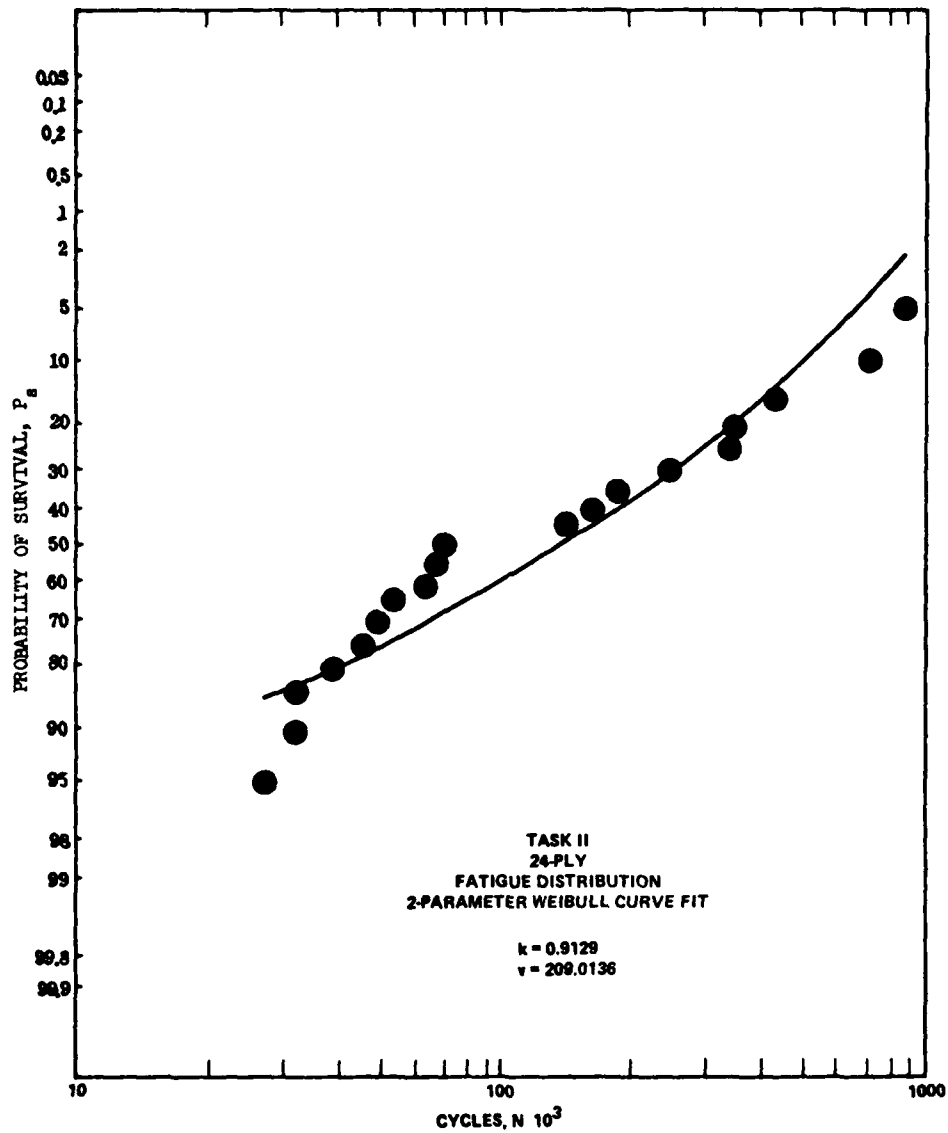


Figure 57: Two Parameter Weibull Curve Fit for Task II 24-Ply Fatigue Data, $\sigma_{Max} = 35$ ksi (241 MPa), $R = -1$

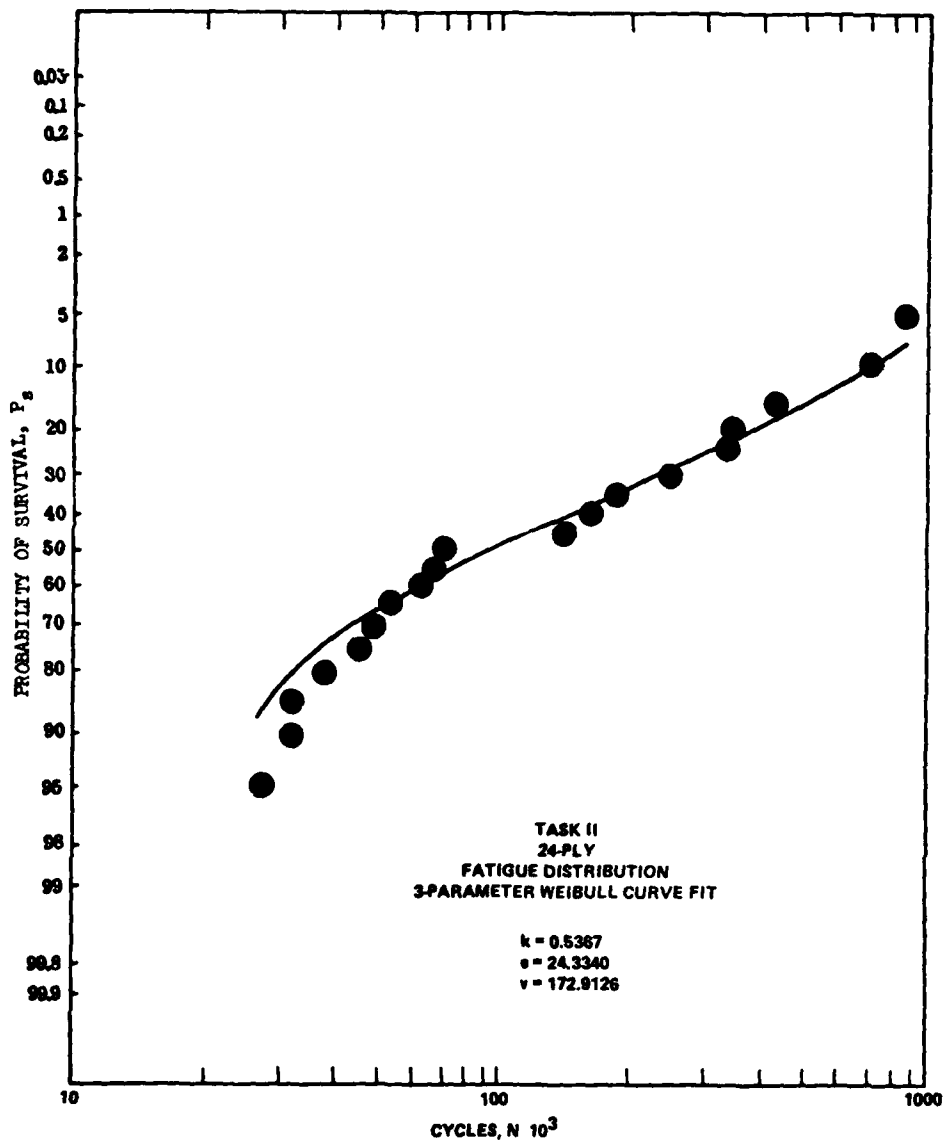
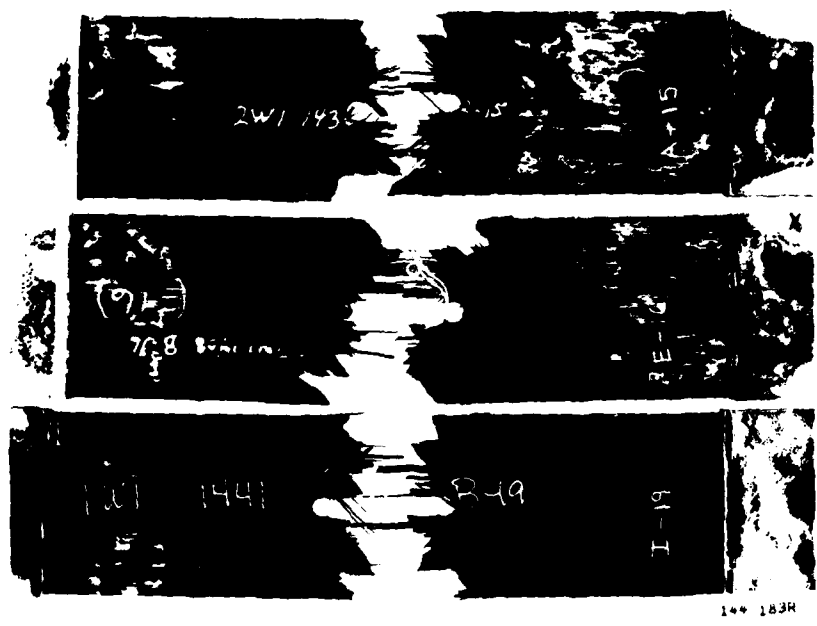


Figure 58: Three Parameter Weibull Curve Fit for Task II 24-Ply Fatigue Data, $\sigma_{Max} = 35$ ksi (241 MPa), $R = -1$

Typical fractures representative of the range of lives are shown in Figure 59. Considerably more delamination is evident for these specimens than for those tested under static loading.

6.1.2 Fatigue Life Distribution For The 32-ply Laminate

A preliminary set of three fatigue tests was conducted on slightly out of tolerance specimens of the 32-ply quasi-isotropic laminate at a maximum stress level of 20 ksi (138 MPa), $R = -1$. Fatigue lives of 214,421 cycles to failure, 1,378,770 cycles with no failure, and 1.8×10^6 cycles with no failure were observed. Since this indicated fatigue lives longer than the target mean life of 4×10^5 cycles, a second set of these specimens was tested at a maximum stress level of 24 ksi (165 MPa) and yielded lives between 68,000 and 100,000 cycles to failure. As a result, a stress level of 22 ksi (152 MPa) was selected for use in Task II. Subsequently a series of twenty specimens was fatigue cycled to failure at the selected stress level ($R = -1$) to determine the scatter at a given stress. The Holskan ultrasonic unit was used to periodically measure damage during the specimen life. Results of these tests are presented in Figure 60 along with the preliminary Task II and Task I test results. Data dispersion was much smaller for the 32-ply laminate coupons by comparison to the 24-ply with scatter extending over slightly more than one order of magnitude. Figures 61 and 62 display the fatigue scatter results for the two and three parameter Weibull curve fits to the Task II data. Typical fracture features are shown in Figure 63. Failures occurred on the compression cycle evident in the compression crushing fractures of the supported width which can be noted in both the face and edge views of Figure 63. Delamination and surface ply splitting was more extensive than observed for static loading.



AB-15
352,330 Cycles

EB-16
901,762 Cycles

IB-19
50,662 Cycles



AB-15

EB-16

IB-19

Figure 59: Fatigue Fracture Appearance of Damaged 24-Ply 67% - 0° Fiber Specimens Tested at 35 ksi (241 MPa), R = -1

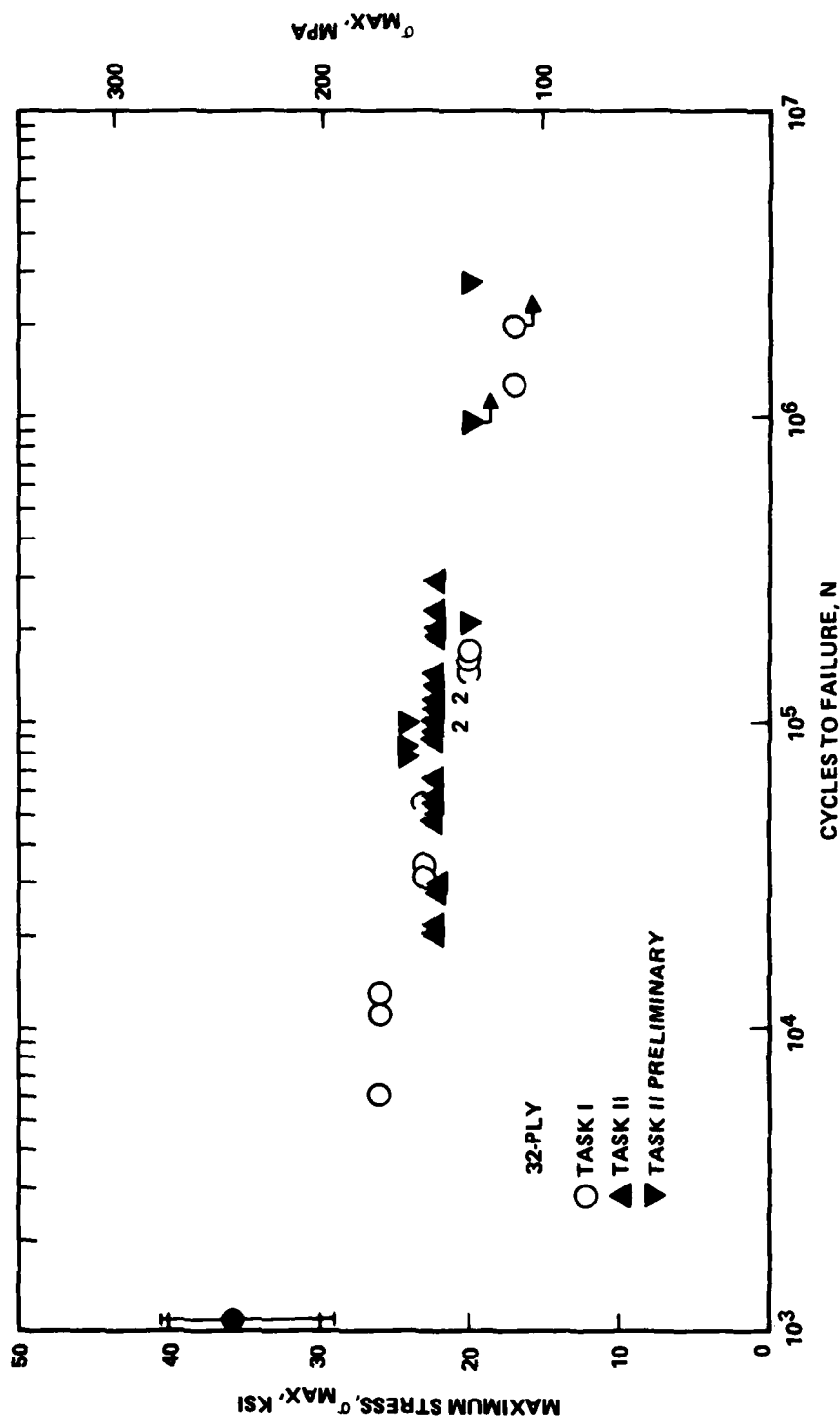


Figure 60: Fatigue Scatter Results for 32-Ply Damaged Hole Specimens

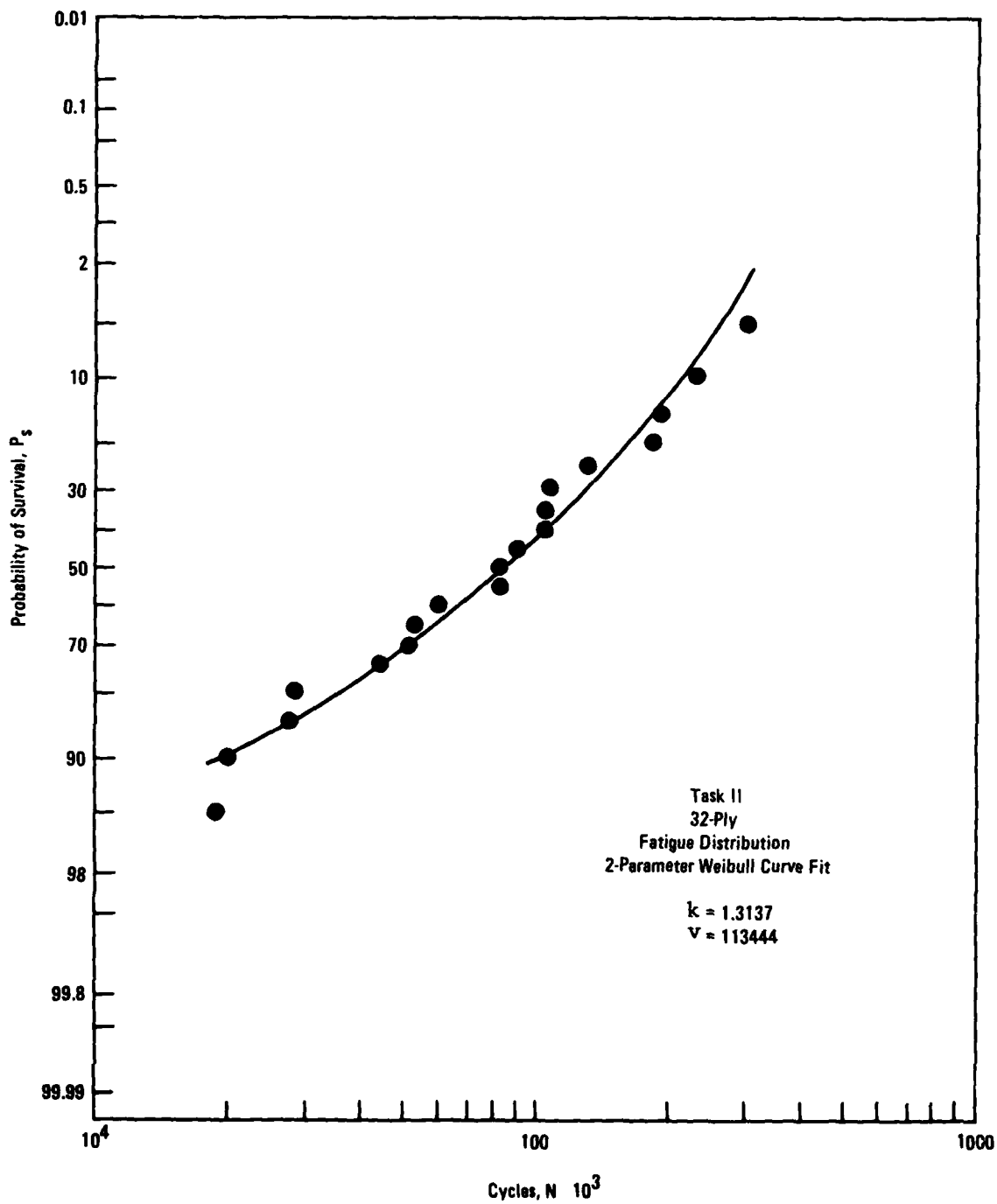


Figure 61: Two Parameter Weibull Curve Fit for Task II, - 32-Ply Fatigue Data, $\sigma_{Max} = 22$ ksi (152 MPa), $R = -1$

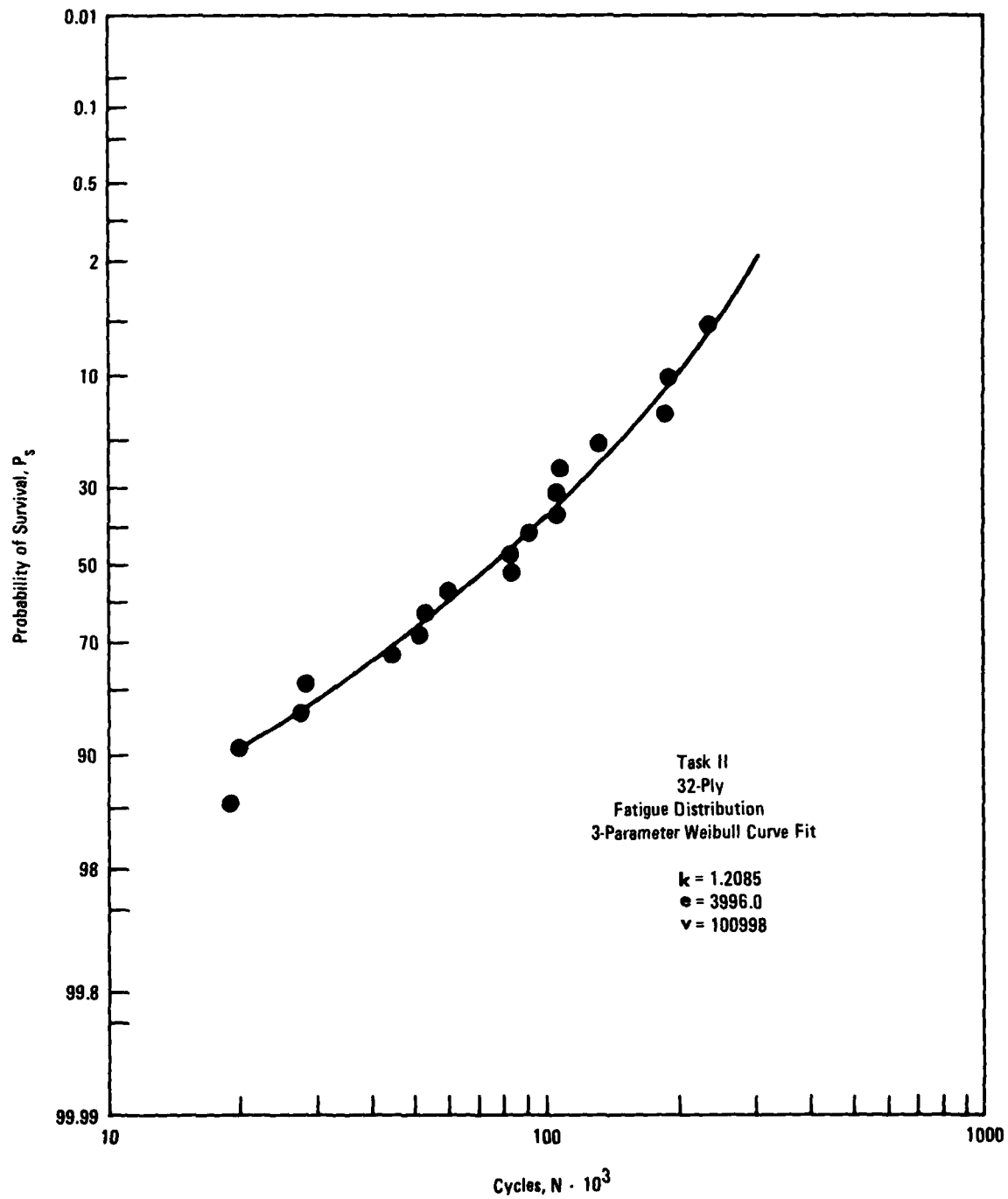
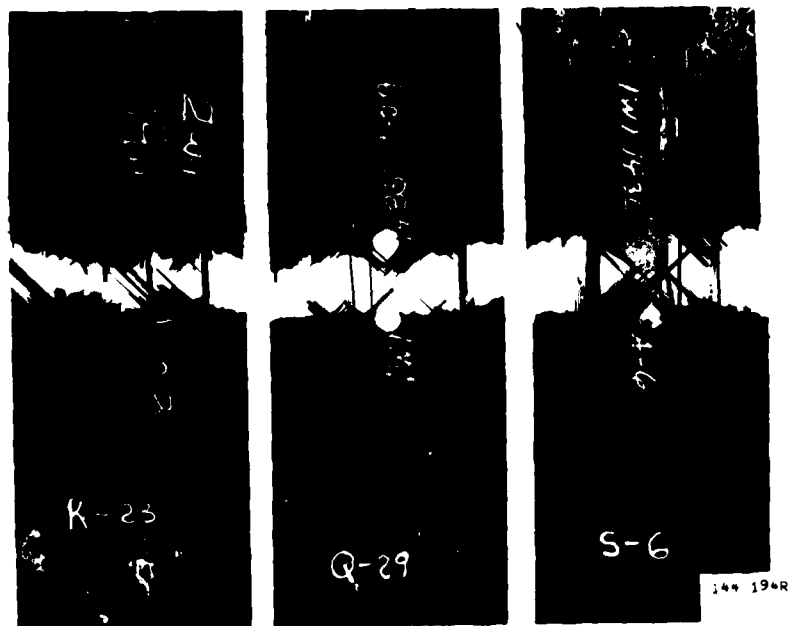


Figure 62: Three Parameter Weibull Curve Fit for Task II, - 32-Ply Fatigue Data, $\sigma_{\text{Max}} = 22 \text{ ksi (152 MPa)}$, $R = -1$



KC-23 QC-29 SA-6
 19,242 Cycles 105,780 Cycles 303,911 Cycles

144 205R



Figure 63: Fatigue Fracture Appearances of Damaged 32-Ply Quasi-Isotropic Specimens Tested at 22 ksi (152 MPa), $R = -1$

6.2 DAMAGE GROWTH UNDER FATIGUE LOADING

Definition of damage growth characteristics in composite materials is considerably more difficult than in metals where a single crack length parameter can be used to characterize damage. In composite materials the wide variety of potential damage modes, many of which may occur in a single damage region, and their sensitivity to the NDI method employed for detection make the selection of a meaningful damage parameter or parameters difficult.

In Task I various types of damage possible in composite materials were considered prior to the selection of the impact and damaged hole conditions for investigation in that Task, which in turn led to the selection of the single damaged hole condition for study in Tasks II and III. The primary manifesting change in the material as a result of the tool drop impact loading or drilling methods employed was delamination. Because delamination was most evident, is often observed in composite materials, necessarily present in fatigue failures, widely considered to be detrimental to structural integrity, and assumed by many to grow in a crack-like manner it was identified as the "damage" of interest for this investigation. Thus, the NDI method selected for the damage tracking was primarily sensitive to delamination. However, the range of validity of the recorded growth information could be restricted by the clamping effect of the fatigue buckling guides. As noted in the Task I Summary, delamination growth appeared to slow or stop at the boundaries of the 2.15-inch (55 mm) square window. Consequently, X and Y measurements beyond the window size had to be evaluated with this consideration in mind. Damage measurement procedures are detailed in Section 4.4.

6.2.1 Damage Growth Results for the 24-Ply Laminate

Since, as discussed above, damage size was expected to be limited by the fatigue specimen restraints resulting in very little damage growth at ± 35 ksi (241 MPa) beyond 300,000 cycles with most of the growth occurring early in the cyclic life, the following Holscan inspection intervals were selected (in thousands of cycles): 0, 1, 5, 10, 20, 30, 45, 60, 90, 125, 225, 500, 1000, 2000. Damage growth data obtained from the twenty fatigue replicates are tabulated in Tables XX - XXII for the damage area (A), width (X) and height (Y) parameters, respectively.

At this stress level none of the damage growth measurements attained the dimensions of the window size until just prior to fracture. Even then only two specimens (HC-27, IB-18) reached the window size in the X-direction and two (AC-30, CC-25) in the Y-direction. Discarding these points would decrease the scatter slightly but would also bias the data, since if the fatigue supports are slowing the growth (i.e. the damage size would otherwise be larger) the scatter would be greater and average damage size larger. The means of the damage measurements are already significantly biased by the occurrence of fatigue failures, for clearly, when specimens fail the larger damage sizes drop out of the population. For this reason plots which include all data for individual specimens are presented in Figures 64 - 66 rather than average values.

Representative data for several specimens were plotted with a linear life scale to illustrate the early growth characteristics. For most specimens initial growth was rapid then slowed, progressing at a much lower rate to failure as shown in Figure 67. The shorter lived specimens exhibited the behavior shown in Figure 68 where the growth rate never slowed. Since for the few specimens tested in Task I the X or Y dimension at which the growth rate reduction occurred seemed to correspond to the size of the

TABLE XXa
 AREA DAMAGE GROWTH (inches²) FOR DAMAGED HOLE
 24-PLY LAMINATES FATIGUE CYCLED AT +35 ksi
 (Includes all available data points)

Specimen ID	Cycles X 10 ³												Cycles To Failure X 10 ³
	0	1	5	10	20	30	45	60	90	125	225	500	
AA-2	0.36	0.40	0.47	0.48	0.67	0.92	1.06	1.30	1.13	2.68			143.7
AB-15	0.38	0.39	0.42	-	-	-	0.79	0.67	-	0.93	1.32		352.3
AC-30	0.38	0.38	0.48	0.57	0.67	-	0.95	0.88	0.94	1.25	-	1.92	747.0
BB-17	0.38	0.54	0.56	0.50	0.86	1.07							32.6
BC-29	0.36	0.48	1.02	1.22	1.37	1.46	1.79	1.85					70.6
CA-1	0.38	0.39	0.54	0.83	1.43	2.34							39.0
CC-25	-	0.51	0.68	0.75	0.83	-	1.23	1.95	1.59	1.92	2.48		252.2
DA-6	0.42	0.44	0.54	0.55	0.64	0.89	1.40	2.16	0.67	0.83	1.20		73.6
DC-28	0.38	0.39	0.38	0.48	0.51	0.58	0.55	0.64	0.60	0.68	0.81	1.12	345.7
DE-30	0.24	0.41	0.42	0.46	0.47	0.51	0.55	0.70	0.60	0.68			500.0+
EA-6	0.38	0.50	0.61	0.84	1.25	1.54	1.61	1.67	1.88	2.34			166.6
EB-16	0.34	0.43	0.39	0.49	0.61	0.69	0.80	0.83	0.89	0.78	1.68	1.81	901.8
FA-3	0.41	0.50	0.62	0.80	1.10	1.14	1.71						47.8
FC-23	0.41	0.44	0.80	0.96	0.95	1.45	1.22						56.3
GC-27	0.36	0.31	0.40	0.57	0.64	0.87	0.90	1.04	1.11	1.23			189.7
HC-26	0.38	0.32	0.39	-	0.51	0.61	0.67	0.72	0.94	0.85	-		448.6
HC-27	0.41	0.44	2.10	2.42	2.42								27.8
IB-13	0.42	0.45	0.95	1.20	1.55	2.34							32.8
IB-19	0.40	0.47	0.44	0.64	0.99	1.34	1.82						50.7
IC-25	0.33	0.41	0.58	0.54	0.61	0.70	1.33	1.13					67.2
Mean	0.33	0.43	0.64	0.80	0.96	1.16	1.15	1.19	1.08	1.35	1.50	1.62	
Std. Dev.	0.04	0.06	0.39	0.47	0.49	0.57	0.43	0.54	0.41	0.71	0.63	0.43	
Coeff. Var. %	10	14	61	59	51	49	37	45	38	53	42	27	

TABLE XXb
AREA DAMAGE GROWTH (mm) FOR DAMAGED HOLE
24-PLY LAMINATES FATIGUE CYCLED AT + 241 MPa
(Includes all available data points)

Specimen ID	Cycles X 10 ³											Cycles To Failure X 10 ³
	0	1	5	10	20	30	45	60	90	125	225	500
AA-2	232	258	303	309	432	593	683	838	729	1729		143.7
AB-15	245	251	270	-	-	-	509	432	-	599	851	352.3
AC-30	245	245	309	367	432	-	612	567	606	806	-	747.0
BB-17	245	348	361	322	554	690						32.6
BC-29	232	309	658	787	883	941	1154	1193				70.6
CA-1	245	251	348	535	954	1509						39.0
CC-25	-	329	438	483	535	-	793	1258	1025	1238	1599	252.2
DA-6	270	283	348	354	412	574	903	1393				73.6
DC-28	245	251	245	309	329	374	354	412	432	535	774	345.7
DC-30	154	264	270	296	303	329	354	451	387	438	522	500.0+
EA-6	245	322	393	541	806	993	1038	1077	1212	1509		166.6
EB-16	219	277	251	316	393	445	516	535	574	503	1083	901.8
FA-3	264	322	399	516	709	735	1103					47.8
FC-23	264	283	516	619	612	935	787					56.3
GC-27	232	199	258	367	412	561	580	670	716	793	-	189.7
HC-26	245	206	251	-	329	393	432	464	606	548		448.6
HC-27	264	283	1354	1561	1561							27.8
IB-13	270	290	612	774	1006	1509						32.8
IC-19	258	303	283	412	638	864	1174					50.7
IC-25	245	264	374	348	393	451	858	729				67.2
Mean	245	277	412	516	619	748	741	767	696	870	967	1045
Std. Dev.	25	38	251	303	316	367	277	348	264	458	406	277
Coef. of Var. %	10	14	61	59	51	49	37	45	38	53	42	27

TABLE XXIIa
DAMAGE GROWTH IN X (WIDTH) DIRECTION (inches)
FOR DAMAGED HOLE 24-PLY LAMINATES FATIGUE CYCLED AT \pm 35 ksi
(Includes all available data points)

Specimen ID	Cycles $\times 10^3$												Cycles To Failure $\times 10^3$
	0	1	5	10	20	30	45	60	90	125	225	500	
AA-2	0.77	0.72	0.85	0.87	0.89	1.12	1.18	1.27	1.10	1.91			143.7
AB-15	0.61	0.66	0.73	-	-	-	1.01	1.02	-	1.21	1.26		352.3
AC-30	0.64	0.67	0.70	0.78	0.82	-	1.00	0.93	0.90	1.05	-	1.47	747.0
BB-17	0.61	0.81	0.83	0.78	1.07	1.24	1.70	1.70					32.6
BC-29	0.61	0.79	1.24	1.45	1.35	1.42							70.6
CA-1	0.61	0.72	1.00	1.17	1.52	1.84							39.0
CC-25	-	0.86	0.99	1.06	1.10	-	1.28	1.72	1.41	1.57	1.55		252.2
DA-6	0.67	0.74	0.84	0.90	0.94	1.11	1.37	1.83					73.6
DC-28	0.60	0.60	0.61	0.65	0.72	0.74	0.73	0.75	0.77	0.80	0.96		345.7
DC-30	0.47	0.68	0.63	0.61	0.65	0.62	0.72	0.95	0.68	0.67	0.72	0.75	500.0
EA-5	0.63	0.82	0.94	1.13	1.27	1.60	1.75	1.63	1.84	2.04			166.6
EB-16	0.60	0.67	0.65	0.69	0.93	0.91	0.95	0.94	1.09	0.99	1.58	1.70	901.9
FA-3	0.66	0.85	0.91	1.01	1.20	1.24	1.90						47.8
FC-23	0.66	0.80	1.24	1.30	1.14	1.56	1.52						56.3
GC-27	0.63	0.58	0.66	0.98	0.90	1.16	0.98	1.09	0.97	1.02			189.7
HC-26	0.64	0.61	0.68	-	0.65	0.68	0.70	0.72	1.02	0.72	-		448.6
HC-27	0.65	0.68	2.28	2.38	2.34								27.8
IB-13	0.67	0.68	1.35	1.53	1.63	2.17							32.8
IB-19	0.67	0.72	0.72	1.03	1.44	1.51	1.58						50.7
IC-25	0.67	0.74	0.86	0.88	0.84	0.93	1.43	1.37					67.2
Mean	0.64	0.72	0.94	1.07	1.13	1.24	1.23	1.23	1.09	1.20	1.22	1.30	
Std. Dev.	0.05	0.08	0.39	0.42	0.41	0.43	0.39	0.39	0.35	0.48	0.38	0.49	
Coef. of Var. %	08	11	41	39	36	35	31	31	32	40	31	38	

TABLE XX1b
DAMAGE GROWTH IN X (WIDTH) DIRECTION (mm)² + 241 MPa
FOR DAMAGED HOLE 24-PLY LAMINATES FATIGUE CYCLED AT ± 241 MPa
(Includes all available data points)

Specimen ID	Cycles X 10 ³												Cycles To Failure X 10 ³
	0	1	5	10	20	30	45	60	90	125	225	500	
AA-2	19.5	18.2	21.5	22.1	26.6	28.4	29.9	32.2	27.9	48.5			143.7
AB-15	15.4	16.7	18.5	-	-	-	25.6	25.9	-	30.7	32.0		352.3
AC-30	16.2	17.0	17.7	19.8	20.8	-	25.4	23.6	22.8	26.6	-	37.3	747.0
BB-17	15.4	20.5	21.0	19.8	27.1	31.4	43.1	43.1					32.6
BC-29	15.4	20.0	31.4	36.8	34.2	36.0							70.6
CA-1	15.4	18.2	25.4	29.7	38.6	46.7							39.0
CC-25	-	21.8	25.1	26.9	27.9	-	32.5	43.6	35.8	39.8	39.3		252.2
DA-6	17.0	18.7	21.3	22.8	23.8	28.1	34.7	46.4					73.6
DC-28	15.2	15.2	15.4	16.5	18.2	18.7	18.5	19.0	19.5	20.3	24.3		345.7
DE-30	11.9	17.2	16.0	15.4	16.5	15.7	18.2	24.1	17.2	17.0	18.2	19.0	500.0*
EA-6	16.0	20.8	23.8	29.9	32.2	40.6	44.4	41.4	46.7	51.8			166.6
EB-16	15.2	17.0	16.5	17.5	23.6	23.1	24.1	23.8	27.7	25.1	40.1	43.1	901.8
FA-3	16.7	21.5	23.1	25.6	30.4	31.4	48.2						47.8
FC-23	16.7	20.3	31.4	33.0	28.9	39.6	38.6						56.3
GC-27	16.0	14.7	16.7	24.8	22.8	29.4	24.8	27.6	24.6	25.9			189.7
HC-26	16.2	15.4	17.2	-	16.5	17.2	17.7	18.2	25.9	18.2	-		448.6
HC-27	16.5	17.2	57.9	60.4	60.4								27.8
ID-13	17.0	17.2	34.2	38.8	41.4	55.1							32.8
IB-19	17.0	18.2	18.2	26.1	36.5	38.3	40.1						50.7
IC-25	17.0	18.7	21.8	22.3	21.3	23.6	36.3	34.7					67.2
Mean	16.2	18.2	23.8	27.1	28.7	31.4	31.2	31.2	27.6	30.4	30.9	33.0	
Std. Dev.	1.3	2.0	9.9	10.6	10.4	10.9	9.9	9.9	8.9	12.1	9.7	12.4	
Coef. of Var.	08	11	41	39	36	35	31	31	32	40	31	38	

TABLE XXIIa
DAMAGE GROWTH IN Y (HEIGHT) DIRECTION (inches) +
FOR DAMAGED HOLE 24-PLY LAMINATES FATIGUE CYCLED AT - 35 ksi
(Includes all available data points)

Specimen ID	Cycles X 10 ³											Cycles To Failure X 10 ³
	0	1	5	10	20	30	45	60	90	125	225	500
AA-2	0.72	0.70	0.66	0.66	1.17	1.34	1.44	1.59	1.77	1.87		143.7
AB-15	0.74	0.79	0.89	-	-	-	1.14	0.93	-	1.30	1.57	352.3
AC-30	0.74	0.80	0.99	1.04	1.23	-	1.49	1.59	1.83	2.06	-	747.0
AD-17	0.74	0.88	0.99	0.96	1.16	1.22	1.69	1.52				32.6
AE-29	0.74	0.83	1.13	1.23	1.45	1.37	1.69	1.52				73.6
AF-1	0.74	0.81	0.89	1.03	1.43	1.66						39.0
AG-25	-	0.78	0.89	1.05	1.11	-	1.41	1.65	1.72	1.82	2.19	252.2
AH-6	0.82	0.82	0.85	0.99	1.03	1.22	1.44	1.66				73.6
AI-28	0.82	0.87	0.89	0.98	1.03	1.13	1.16	1.21	1.33	1.44	1.75	345.7
AJ-30	0.68	0.83	0.92	1.00	0.88	1.03	1.13	1.17	1.17	1.30	1.56	500.0*
AK-5	0.76	0.85	1.00	1.09	1.28	1.39	1.36	1.42	1.50	1.65		166.6
AL-16	0.72	0.83	0.93	1.03	1.07	1.17	1.24	1.28	1.30	1.21	1.72	901.8
AM-3	0.79	0.89	0.96	1.07	1.22	1.43	1.64					47.8
AN-23	0.77	0.76	0.84	0.92	1.03	1.24	1.22	1.51	1.69	1.91		56.3
AO-27	0.72	0.75	0.82	0.81	0.99	1.06	1.08	1.37	1.63	1.70	-	189.7
AP-26	0.74	0.69	0.85	-	1.07	1.12	1.31					443.6
AQ-27	0.79	0.88	1.56	1.66	1.64			1.16				27.8
AR-13	0.92	0.84	1.07	1.23	1.47	1.67						32.8
AS-19	0.80	0.88	0.93	0.93	1.12	1.35	1.54					50.7
AT-25	0.74	0.81	0.96	0.93	1.06	1.10	1.46	1.16				67.2
Mean	0.74	0.81	0.96	1.04	1.18	1.29	1.36	1.39	1.55	1.63	1.76	2.07
Std. Dev.	0.04	0.06	0.16	0.18	0.19	0.19	0.18	0.23	0.24	0.30	0.25	0.26
Coeff. of Var.	0.06	0.07	0.16	0.18	0.16	0.15	0.14	0.16	0.15	0.18	0.15	0.13

TABLE XXIIb

DAMAGE GROWTH IN Y (HEIGHT) DIRECTION (mm)
 FOR DAMAGED HOLE 24-PLY LAMINATES FATIGUE CYCLED AT ± 241 MPa
 (Includes all available data points)

Specimen ID	Cycles $\times 10^3$											Cycles To Failure $\times 10^3$
	0	1	5	10	20	30	45	60	90	125	225	500
AA-2	18.2	17.7	21.8	21.8	29.7	34.0	36.5	40.3	44.9	47.4		143.7
AB-15	18.7	20.0	22.3	-	-	-	28.9	23.6	-	33.0	39.8	352.3
AC-30	18.7	20.3	25.1	26.4	31.2	-	37.8	40.3	46.4	52.3	-	747.0
BB-17	18.7	22.3	25.1	24.3	29.4	30.9	42.9	38.6				32.6
BC-29	18.7	21.0	28.7	31.2	36.8	34.7						70.6
CA-1	18.7	20.5	22.6	26.1	36.3	42.1						39.0
CC-25	-	19.8	22.6	26.6	28.1	-	35.8	41.9	43.6	46.2	55.6	252.2
DA-6	20.8	20.8	24.1	25.1	26.1	30.9	36.5	42.1				73.6
DC-28	20.8	22.0	22.6	24.8	26.1	28.7	29.4	30.7	33.7	36.5	44.4	345.7
DC-30	17.2	21.0	23.3	25.4	22.3	26.1	28.7	29.7	29.7	33.0	39.6	500.0+
EA-6	19.3	21.8	25.4	27.6	32.5	35.3	34.5	36.0	39.1	41.9		166.6
EB-16	16.0	21.0	23.6	26.1	27.1	29.7	31.4	32.5	33.0	30.7	43.6	901.8
FA-3	20.0	22.6	24.3	27.1	30.9	37.6	41.6					47.8
FC-23	19.5	19.3	21.3	23.3	26.1	31.4	30.9					56.3
GC-27	18.2	19.0	20.8	20.5	25.1	26.9	27.4	38.3	42.9	48.5		189.7
HC-26	18.7	17.5	21.5	-	27.1	28.4	33.2	34.7	41.4	43.1		448.6
HC-27	20.0	22.3	39.6	42.1	41.6							27.8
IB-13	20.8	21.3	27.1	31.2	37.3	42.4						32.8
IB-19	20.3	22.3	23.6	23.6	28.4	34.2	39.1					50.7
IC-25	18.7	20.5	24.3	23.6	26.9	27.9	37.0	29.4				67.2
Mean	18.7	20.5	24.3	26.4	29.9	32.7	34.5	35.3	39.	41.4	44.7	52.5
Std. Dev.	1.01	1.5	4.16	4.6	4.8	4.8	4.6	5.8	6.1	7.6	6.4	6.6
Coeff. of Var. %	06	07	16	18	16	15	14	16	15	18	15	13

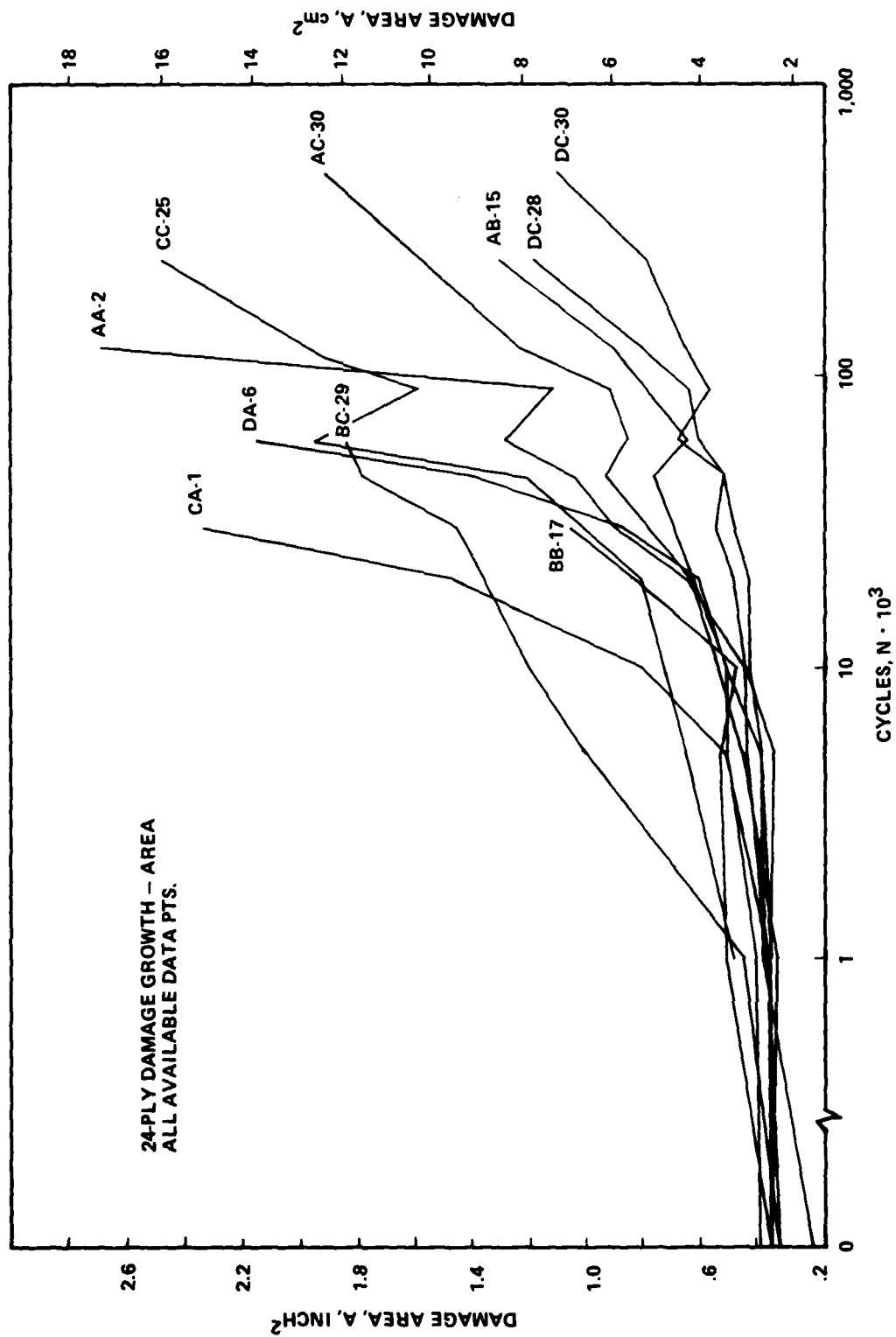


Figure 64a: Area Damage Growth for the 24-Ply Fatigue Distribution Specimens (Specimens 1 thru 10).

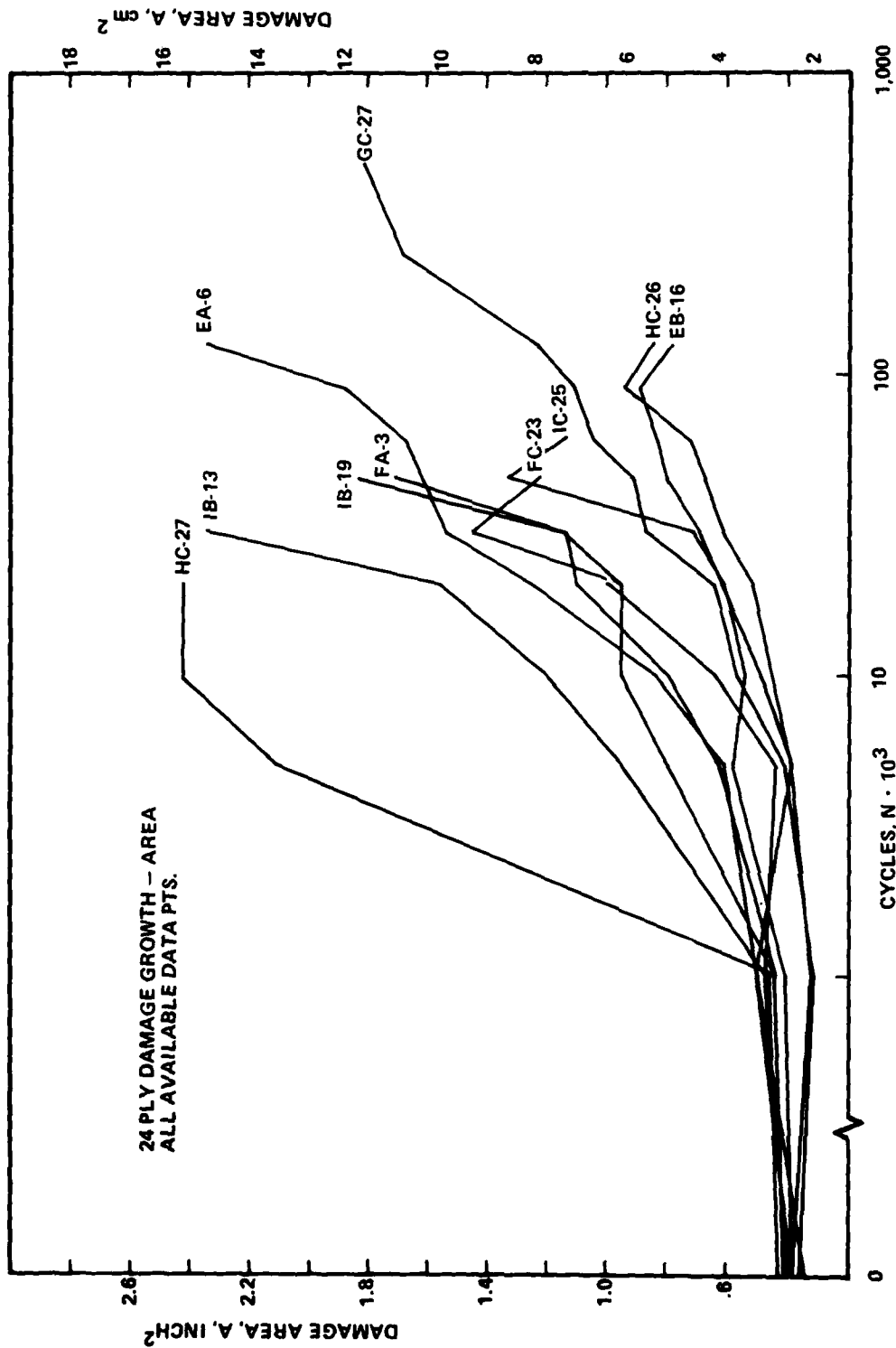


Figure 64b: Area Damage Growth for the 24-Ply Fatigue Distribution Specimens (Specimens 11 thru 20).

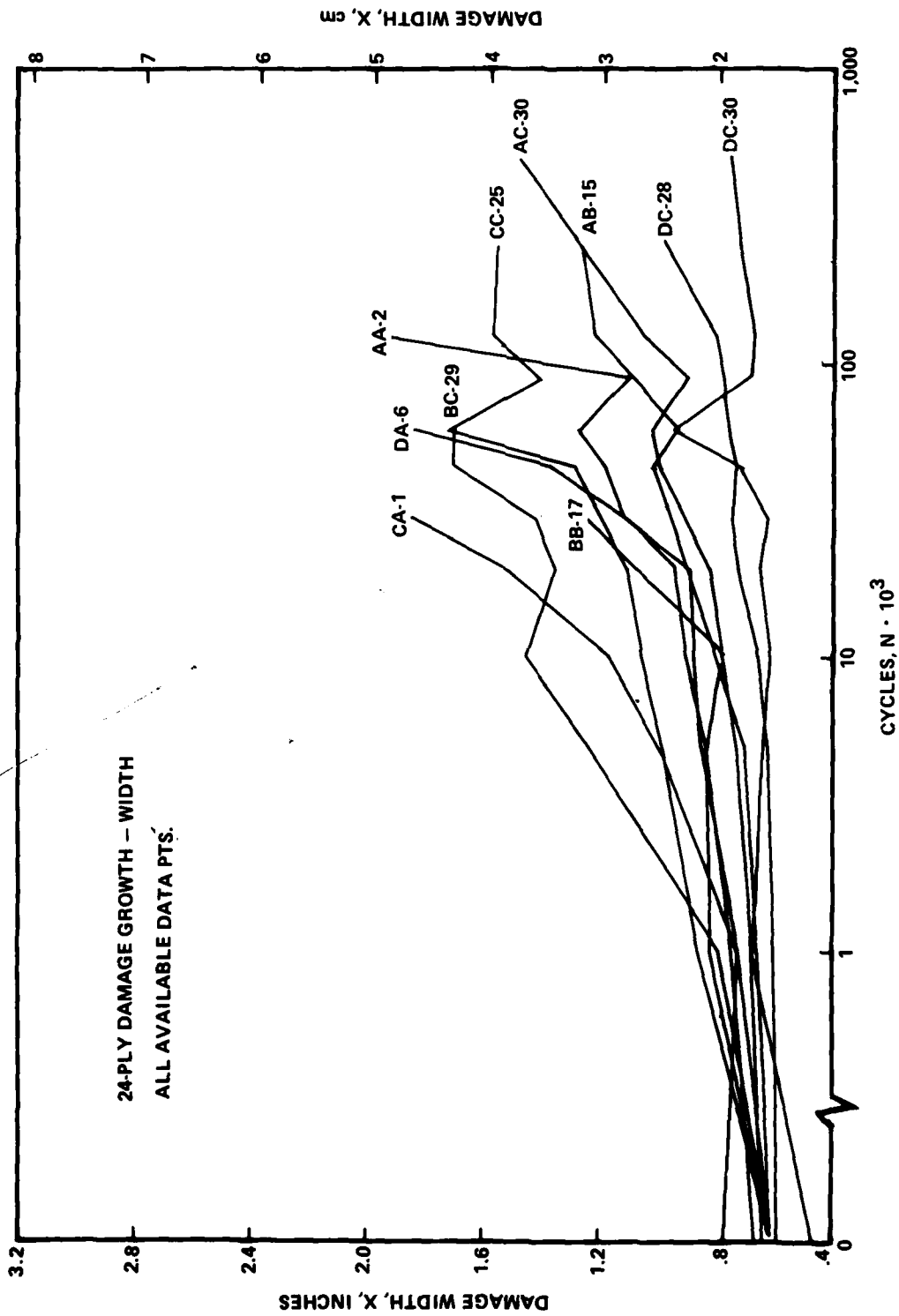


Figure 65a: Damage Growth in Width Dimension for the 24-Ply Fatigue Distribution Specimens (Specimens 1 thru 10).

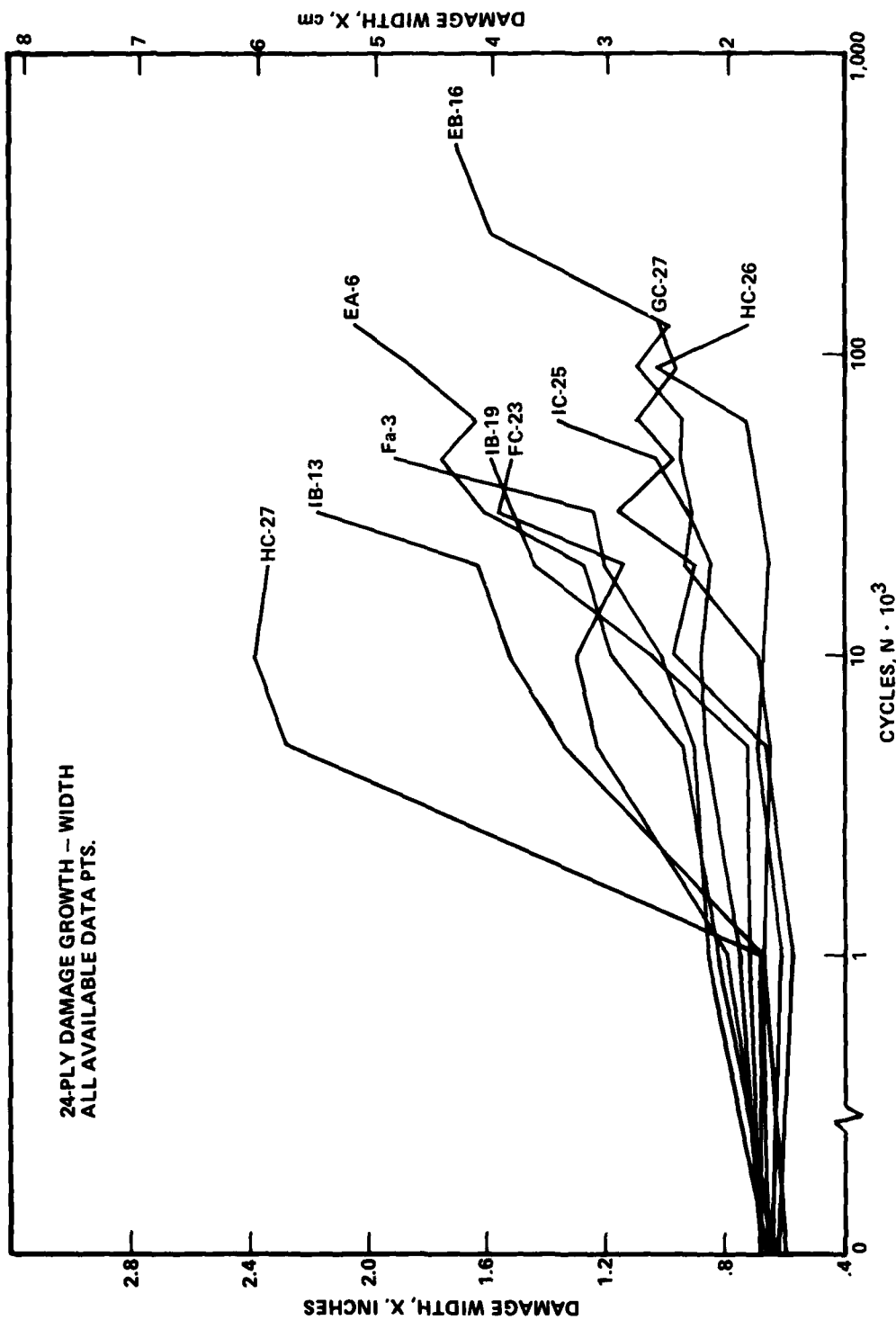


Figure 65b: Damage Growth in Width Dimension for the 24-Ply Fatigue Distribution Specimens (Specimens 11 thru 20).

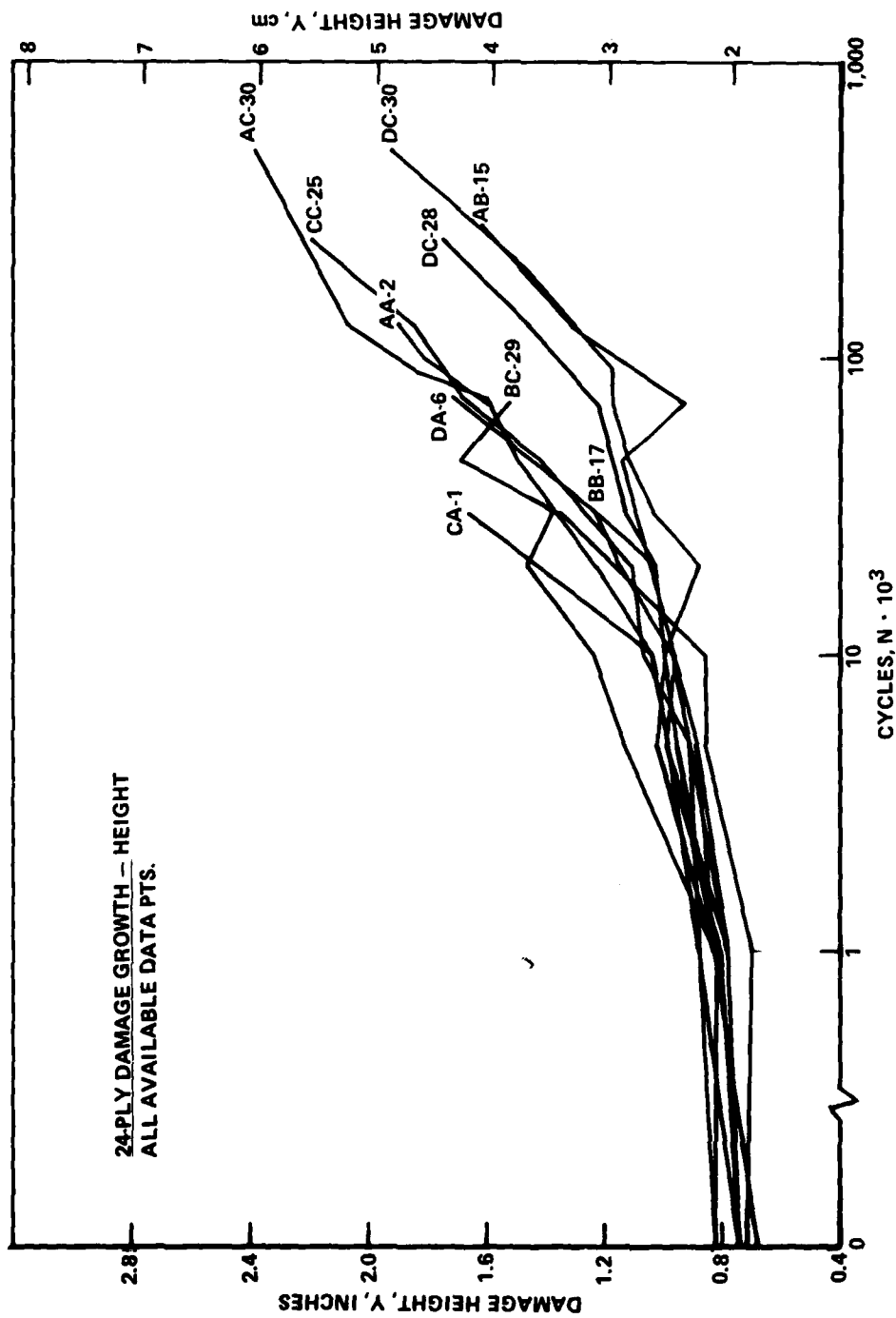


Figure 66a: Damage Growth in Height Dimension for the 24-Ply Fatigue Distribution Specimens (Specimens 1 thru 10).

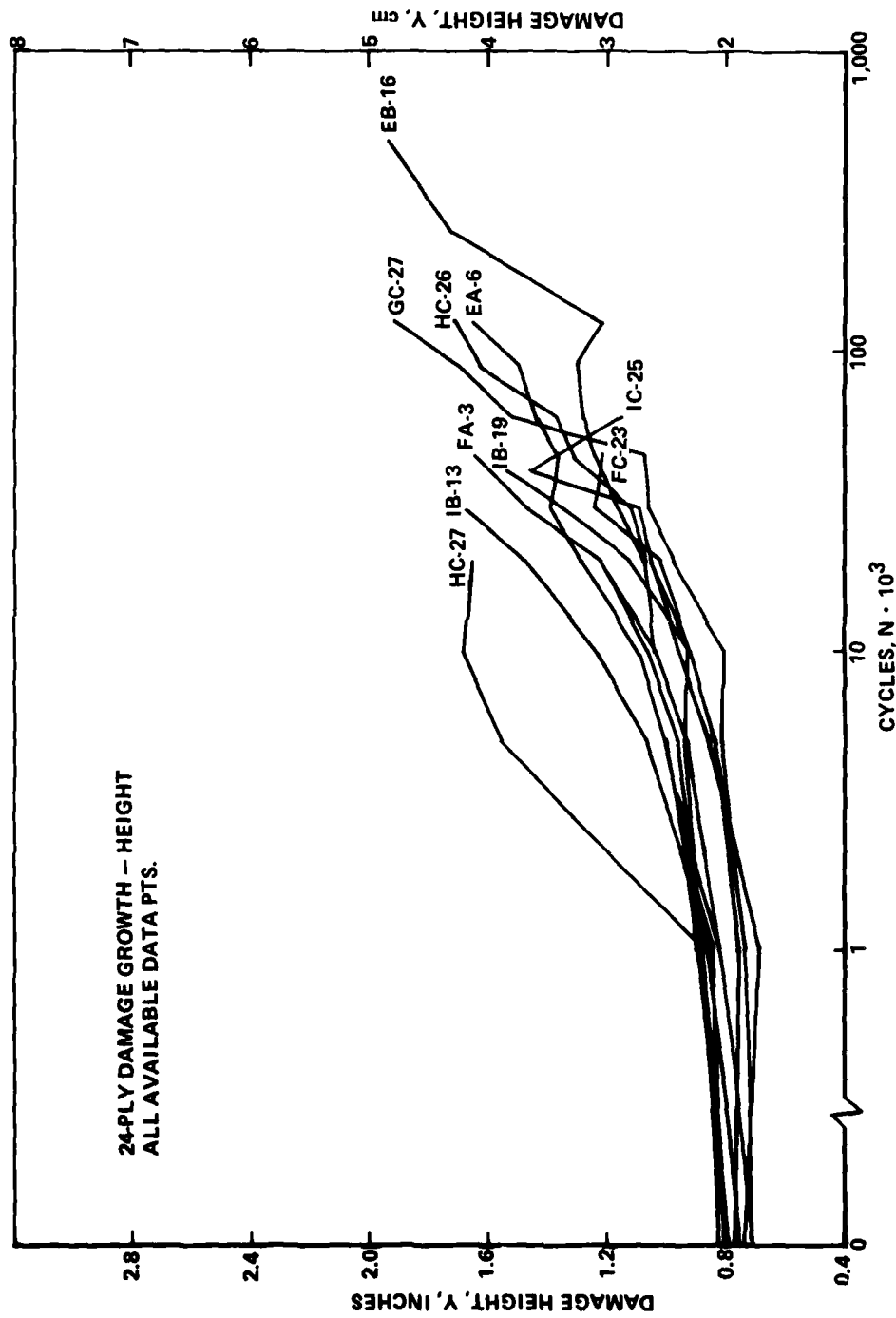


Figure 66b: Damage Growth in Height Dimension for the 24-Ply Fatigue Distribution Specimens (Specimens 11 thru 20).

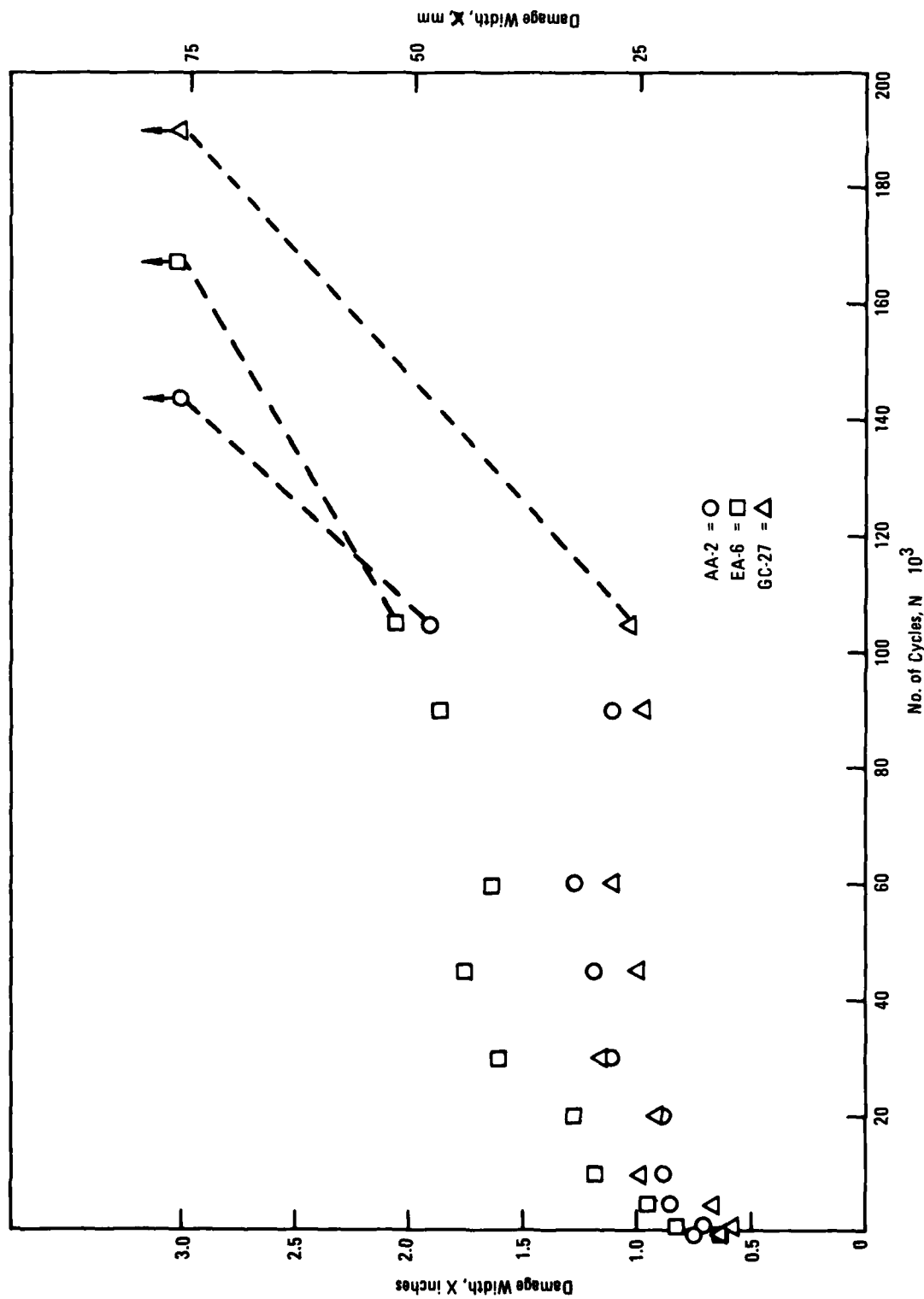


Figure 67: Damage Growth Behavior of Typical Longer Lived 24-Ply Laminate Specimens

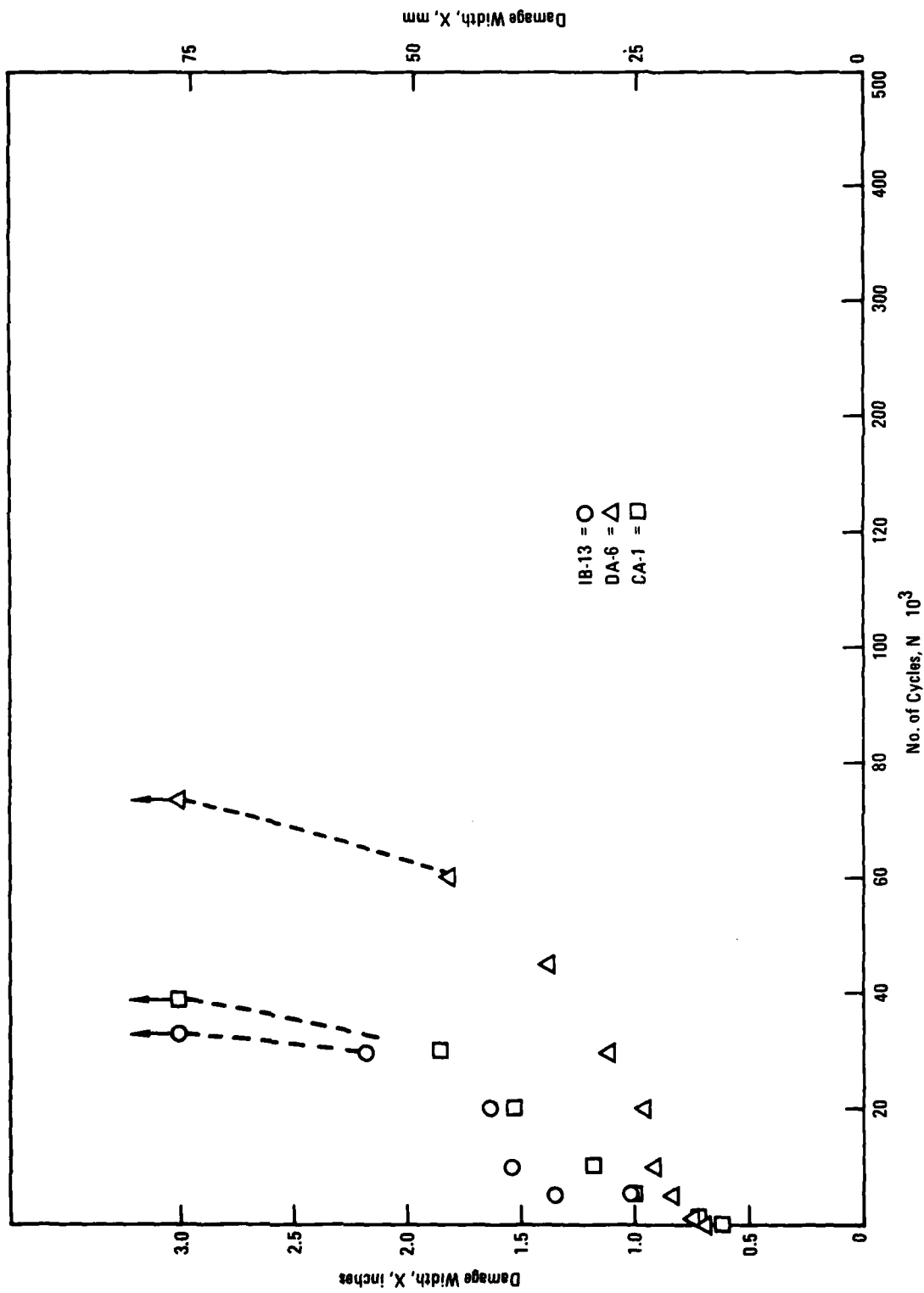


Figure 68: Damage Growth Behavior of Typical Shorter Lived 24-Ply Laminates
Specimens

fatigue guide "window", it was postulated that this rate reduction may be due to the clamping effect of the supports. This supposition does not appear to be strongly supported by the larger data set of Task II at one stress level. A number of specimens exhibited no rate reduction while for those that did the slowed growth appeared to be a characteristic behavior of the laminate occurring at approximately the same N value but having a corresponding damage dimension (X or Y) ranging from less than one inch (25 mm) to over 2 inches (51 mm).

The general shapes of the damage vs N curves of Figures 64 - 66 are very similar to a vs N curves obtained for metals but the scatter is considerably larger. Area and width data exhibit coefficients of variation on the order of twice those for the growth in the Y direction. However, because Y-direction growth is the most uniform and orderly it is least likely to correlate to life. If a relationship between damage size and life existed, the larger dispersion in life data would require a large variation in damage size at any given number of cycles. This would also be true if the residual strength were expected to degrade to the fatigue stress. Examination of the Holscans indicates that the major growth occurs in the X not Y direction. Moreover, failures occurred during the compressive load excursion due to instability. Damage growth strictly in the specimen length (Y) direction for a specimen supported as in this study would not be expected to significantly affect the specimen stability and thus the life. Accordingly, if the failure problem is one of stability, neither damage width nor area may be expected to relate to life directly, except for a generally higher probability of failure as damage grows. That this is, in fact, the case is evident from Figures 69 and 70 which present in two different forms the lack of correspondence between damage size and fatigue life. This lack of relationship is also immediately apparent upon examining the initial flaw sizes which do not vary greatly and noting the factor of 30 difference in life. Clearly inspection for initial flaw sizes can offer no better than a prediction within 2 orders of magnitude.

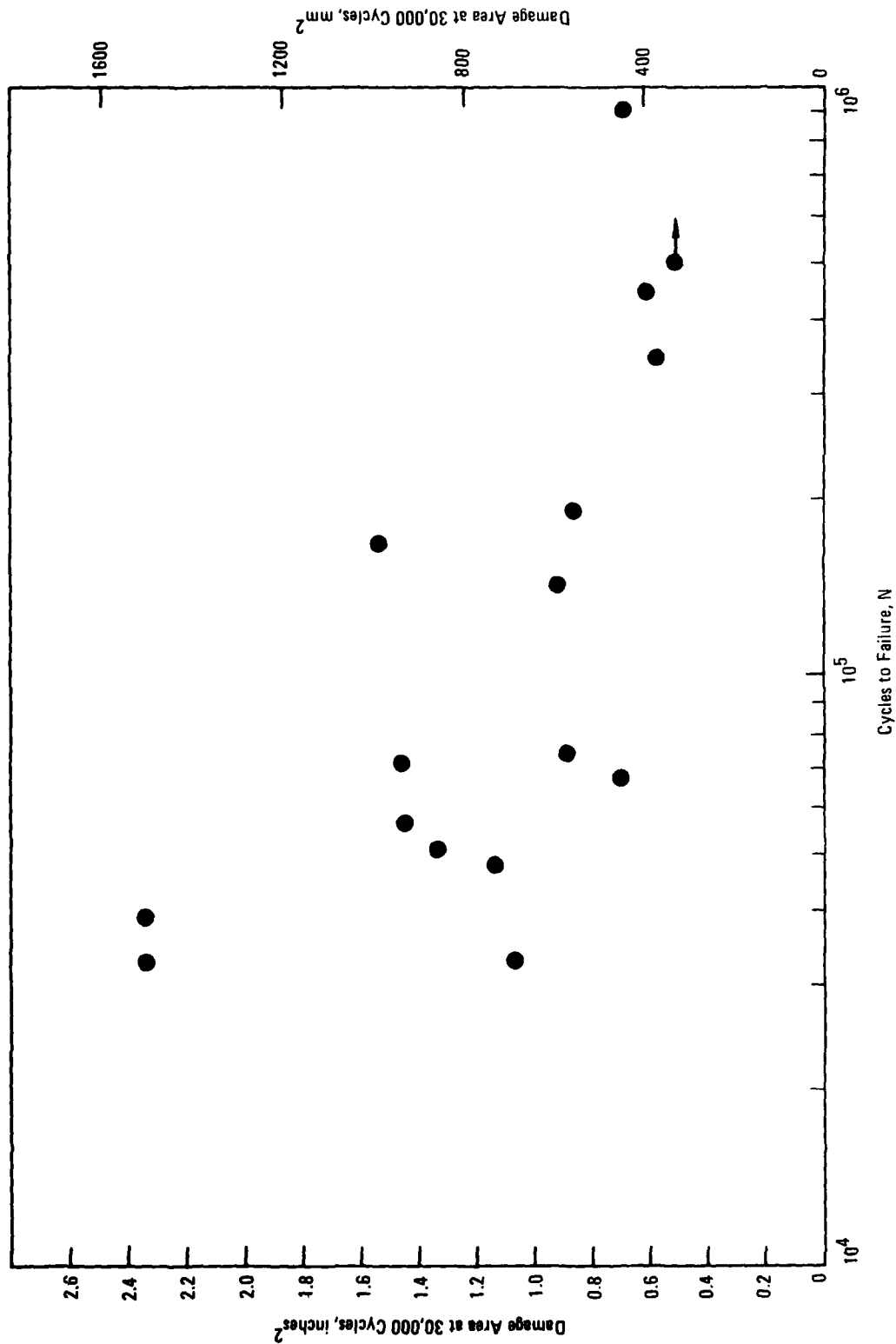


Figure 69: Damage Size at 30,000 Cycles vs Life for the 24-Ply Laminate

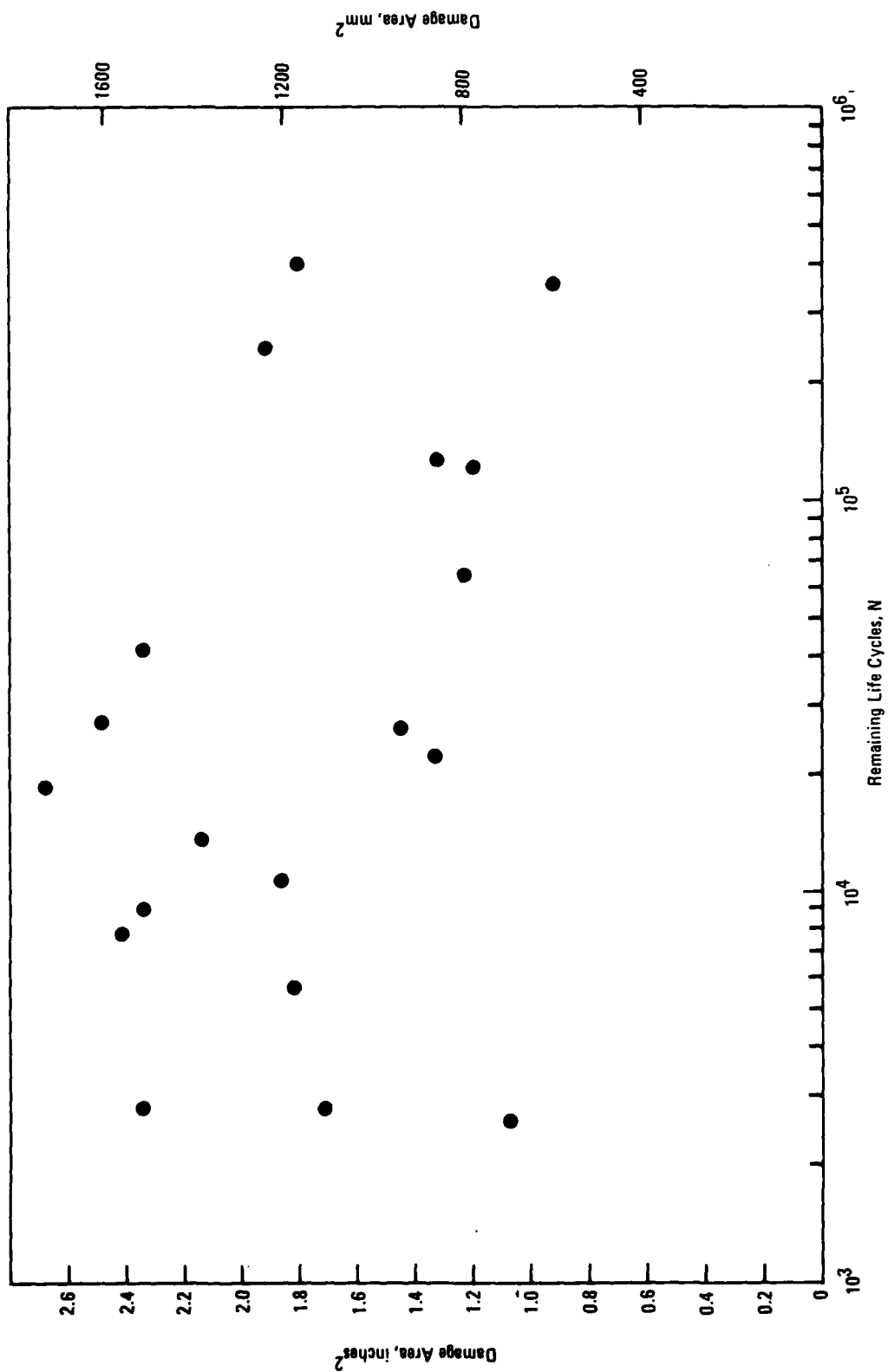


Figure 70: Last Recorded Damage Size Prior to Failure vs. Remaining Life For
The 24-ply Laminate

Typical Holscans illustrating damage growth behavior from which measurements were obtained are presented in Figures 71 and 72. Additional growth data are available in Volume III, Appendix D. Note that the major growth is in the width (X) direction. Figure 71b provides a good example as to why area serves as a better damage growth parameter since it reflects both X and Y extension. There is little difference between the X (vertical in photo) measurements at 45,000 and 60,000 cycles since the maximum X dimension does not change, yet clearly there is additional X growth which tends to fill out the damage contour. This growth is reflected in the area measurement.

6.2.2 Damage Growth Results for the 32-Ply Laminate

This quasi-isotropic laminate had been selected because it is prone to delamination early in life. Therefore, the cycles selected for Holscan inspection concentrated on an earlier portion of the life than for the 24-ply laminates. These were (in thousands of cycles) 0, 0.1, 0.5, 1, 2.5, 5, 10, 20, 50, 100, 250, 500, 1000. Damage growth data obtained from the twenty replicates are presented in Tables XXIII through XXV for area (A), width (X) and height (Y) parameters, respectively. Delamination growth in the width direction did attain the dimensions of the window size for most of the specimens but these were always the last one or two recorded measurements prior to failure. When two such measurements were recorded, in half of these the second reading was equal to or smaller than the first. This is not necessarily indicative of the slowing of the growth, but usually due to the loss of C-scan indications as a result of surface ply cracking and delamination. Measurements approximating the window size were not discarded from the data set to avoid data bias which would then result as discussed for the 24-ply laminate. Damage growth behavior is displayed in graphical form for individual specimens in Figures 73 - 75. To illustrate the early growth characteristics, data for typical specimens are plotted using a linear life scale in Figure 76. Major delamination growth

AD-A115 184

LOCKHEED-CALIFORNIA CO BURBANK

F/G 11/4

ADVANCED RESIDUAL STRENGTH DEGRADATION RATE MODELING FOR ADVANC--ETC(U)

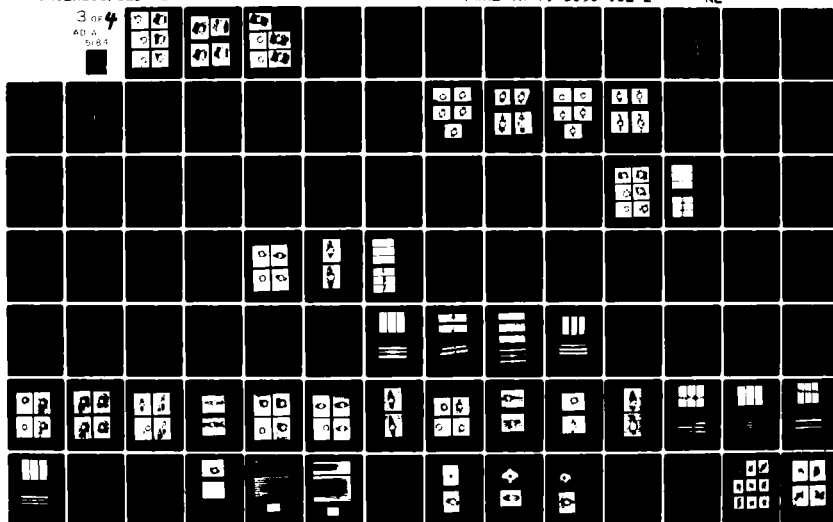
JUL 81 K N LAURAITIS, J T RYDER, D E PETTIT

F33615-77-C-3084

UNCLASSIFIED LR-28360-19

AFWAL-TR-79-3095-VOL-2

NL

3 of 4
AD A
5184

A

5184

1.0

2.8

2.5

3.2

2.2

3.6

2.0

4.0

1.8

1.1

1.25

1.4

1.6

U.S. GOVERNMENT PRINTING OFFICE: 1963

→ 0°



N = 0



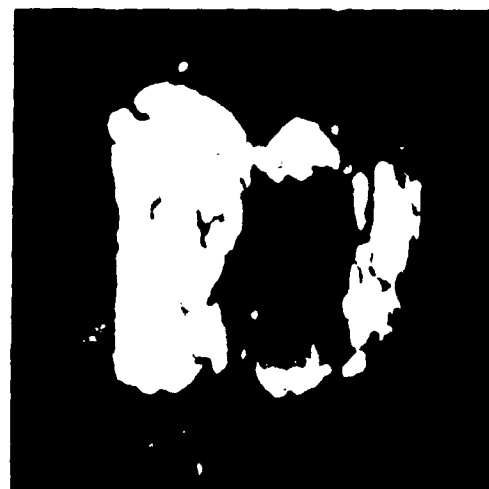
N = 1,000



N = 5,000



N = 10,000



N = 20,000



N = 30,000

Figure 7la: Typical Damage Growth Characteristics of Initially Damaged 24-Ply, 67% 0 Fiber Specimens (Specimen EA-6, $N_f = 166,600$)

↑ 0°



N = 45,000



N = 60,000



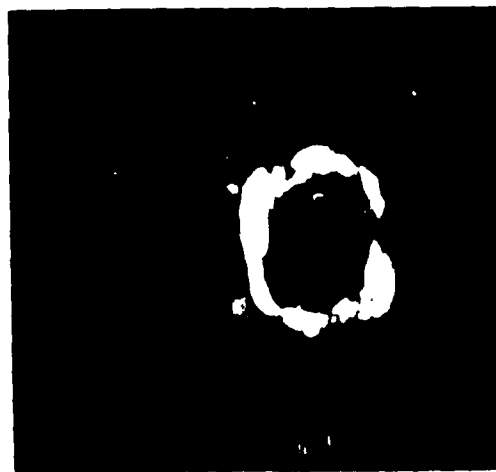
N = 90,000



N = 125,000

Figure 71b: Typical Damage Growth Characteristics of Initially Damaged 24-Ply, 67% 0° Fiber Specimens (Specimen EA-6, $N_f = 166,600$)

→ 0°



N = 0



N = 1,000



N = 10,000



N = 20,000



N = 5,000

Figure 72: Damage Growth Characteristics of Initially Damaged 24-Ply Specimen HC-27 Which Exhibited Parity Growth ($N_f = 27,800$)

TABLE XXIIIa
AREA DAMAGE GROWTH (inches²) FOR DAMAGED HOLE
32-PLY LAMINATES FATIGUE CYCLED AT ± 22 ksi
(Includes all available data points)

Specimen ID	Cycles $\times 10^3$											Cycles To Failure $\times 10^3$
	0	0.1	0.5	1.0	2.5	5	10	20	50	100	250	
JA-1	0.54	0.50	0.60	0.64	0.63	0.58	0.72	1.24	-			60.0
JA-6	0.53	0.54	0.54	0.57	0.59	0.70	1.02	1.23	1.69			83.4
JC-24	0.51	0.55	0.59	0.60	0.69	0.71	0.81	0.86	1.01	1.28		191.1
KC-23	0.54	0.54	0.53	0.71	0.59	0.89	1.16					19.2
LA-6	0.54	0.50	0.52	0.56	0.62	0.74	0.92	1.02	1.54			53.1
LC-24	0.50	0.47	0.54	0.51	-	0.62	0.50	0.70	-	1.08		105.1
LC-30	0.49	0.51	0.51	0.53	0.60	0.60	0.68	0.91	1.19	1.29		188.9
MB-17	0.66	0.62	0.57	0.59	0.64	0.75	0.82	1.27				27.7
MC-27	0.53	0.59	0.60	0.57	0.56	0.73	0.85	1.03	1.33	1.74		108.9
NA-3	-	0.65	0.60	0.79	0.84	1.04	1.28	1.43				44.6
PA-5	0.42	0.42	0.50	0.57	0.60	0.64	0.84	0.82	1.04	-		234.2
PB-19	0.46	0.51	0.60	0.71	0.69	0.78	1.02	1.60	-			82.4+
PC-23	0.45	0.42	-	0.52	0.53	0.54	0.55	0.69	1.09			91.5
QA-8	0.35	0.38	-	-	0.40	0.59	0.86	1.05	1.19	1.36		131.9
QC-29	0.51	0.54	0.58	0.63	0.79	0.69	0.76	0.93	1.60	1.56		105.8
RA-8	0.69	0.69	0.71	0.74	0.90	0.95	1.26	1.97				20.1
RB-14	0.50	0.59	0.64	0.68	0.71	0.80	0.86	1.36	1.68			51.4
SA-6	0.46	-	0.44	0.44	0.48	0.47	0.46	0.63	0.72	0.79	1.14	303.9
SC-24	0.55	0.61	0.68	0.70	0.67	0.77	0.90	0.95	1.53			83.3
SC-30	0.52	0.60	0.56	0.59	0.79	1.03	1.05	1.43				28.5
Mean	0.51	0.54	0.57	0.61	0.65	0.73	0.87	1.11	1.30	1.30	1.14	
Std. Dev.	0.08	0.08	0.07	0.09	0.12	0.15	0.23	0.34	0.31	0.31		
Coef. of Var.	15	15	11	15	19	21	26	31	24	24		

TABLE XXIIIb
AREA DAMAGE GROWTH (mm^2) FOR DAMAGED HOLE
32-PLY LAMINATES FATIGUE CYCLED AT ± 152 MPa
(Includes all available data points)

Specimen ID	Cycles $\times 10^3$											Cycles To Failure $\times 10^3$
	0	0.1	0.5	1.0	2.5	5	10	20	50	100	250	
JA-1	348	323	387	413	406	374	465	800	-			60.0
JA-6	342	348	348	368	381	452	658	794	1090			83.4
JC-24	329	355	381	387	445	458	523	555	652	826		191.1
KC-23	348	348	342	458	381	574	748					19.2
LA-6	348	323	335	361	400	477	594	658	994			53.1
LC-24	323	303	348	329	-	400	323	452	-	697		105.1
LC-30	316	329	329	342	387	387	439	587	768	832		188.9
MB-17	426	400	368	381	413	484	529	819				27.7
MC-27	342	381	387	368	361	471	548	665	858	1123		108.9
NA-3	-	419	387	510	542	671	826	923				44.6
PA-5	271	271	323	368	387	413	542	529	671	-		234.2
PB-19	297	329	387	458	445	503	658	1032	-			82.4+
PC-23	290	271	-	335	342	348	355	445	703			91.5
QA-8	226	245	-	-	258	381	555	677	768	877		131.9
QC-29	329	348	374	406	510	445	490	600	1032	1006		105.8
RA-8	445	445	458	477	581	613	813	1271				20.1
RB-14	323	381	413	439	458	516	555	877	1084			51.4
SA-6	297	-	284	284	310	303	297	406	465	510	735	303.9
SC-24	355	394	439	452	432	497	581	613	987			83.3
SC-30	335	387	361	381	510	665	677	923				28.5
Mean	329	348	368	394	419	471	561	716	839	839	735	
Std.Dev.	52	52	45	58	77	97	148	219	200	200		
Coeff. of Var. %	15	15	11	15	19	21	26	31	24	24		

TABLE XXIVa
DAMAGE GROWTH IN X (WIDTH) DIRECTION (inches)
FOR DAMAGED HOLE 32-PLY LAMINATES FATIGUE CYCLED AT ± 22 ksi
(Includes all available data points)

Specimen ID	Cycles $\times 10^3$											Cycles To Failure $\times 10^3$
	0	0.1	0.5	1.0	2.5	5	10	20	50	100	250	
JA-1	0.87	0.81	0.96	0.97	1.10	1.12	1.55	2.01	-			60.0
JA-6	0.81	0.88	0.88	0.99	1.04	1.28	1.81	2.19	2.37			83.8
JC-24	0.83	0.88	0.91	0.97	1.18	1.28	1.36	1.44	1.82	2.15		191.1
KC-23	0.80	0.86	0.88	1.19	1.00	1.84	2.14					19.2
LA-6	0.83	0.86	0.97	1.08	1.15	1.32	1.77	2.28	2.19			53.1
LC-24	0.81	0.83	0.90	0.88	-	1.08	0.94	1.30	-	1.77		105.1
LC-30	0.83	0.87	0.92	0.98	1.06	1.14	1.35	1.49	1.84	1.97		188.9
MB-17	0.93	0.89	0.86	0.96	1.04	1.39	1.65	2.21				27.7
MC-27	0.82	0.88	0.95	0.94	0.96	1.21	1.54	1.85	2.39	2.37		108.9
NA-3	-	1.04	1.08	1.34	1.53	1.81	2.11	2.44				44.6
PA-5	0.76	0.90	1.15	1.30	1.46	1.47	1.74	2.04	2.25	-		234.2
PB-19	0.76	0.83	1.02	1.28	1.24	1.46	1.76	2.51	-			82.4+
PC-23	0.79	0.77	-	0.95	0.97	0.97	1.04	1.28	1.89			91.5
QA-8	0.68	0.75	-	-	0.77	1.39	1.10	2.03	2.22	2.17		131.9
QC-29	0.79	0.82	0.97	1.08	1.40	1.19	1.41	1.84	2.46	2.32		105.8
RA-8	0.92	0.94	0.91	1.04	1.50	1.52	2.13	2.48				20.1
RB-14	0.76	0.99	1.11	1.16	1.13	1.37	1.48	2.29	2.48			51.4
SA-6	0.79	-	0.77	0.76	0.81	0.81	0.82	1.24	1.22	1.24	1.81	303.9
SC-24	0.83	0.90	1.10	1.08	1.01	1.23	1.63	1.81	2.29			83.3
SC-30	0.75	1.07	1.04	1.09	1.38	1.84	1.96	1.53				28.5
Mean	0.81	0.88	0.97	1.05	1.14	1.34	1.56	1.91	2.12	2.00	1.81	
Std. Dev.	0.06	0.08	0.10	0.15	0.22	0.27	0.39	0.42	0.37	0.39		
Coeff. of Var. %	7	9	10	14	20	20	25	22	17	20		

TABLE XXIVb
DAMAGE GROWTH IN X (WIDTH) DIRECTION (mm)
FOR DAMAGED HOLE 32-PLY LAMINATES FATIGUE CYCLED AT ± 152 MPa
(includes all available data points)

Specimen ID	Cycles $\times 10^3$											Cycles To Failure $\times 10^3$
	0	0.1	0.5	1.0	2.5	5	10	20	50	100	250	
JA-1	22.1	20.6	24.4	24.6	27.9	28.4	39.4	51.1	-			60.0
JA-6	20.6	22.4	22.4	25.1	26.4	32.5	46.0	55.6	60.2			83.8
JC-24	21.1	22.4	23.1	24.6	30.0	32.5	34.5	36.6	46.2	54.6		191.1
KC-23	20.3	21.8	22.4	30.2	25.4	46.7	54.4					19.2
LA-6	21.1	21.8	24.6	27.4	29.2	33.5	45.0	57.9	55.6			53.1
LC-24	20.6	21.1	22.9	22.4	-	27.4	23.9	33.0	-	45.0		105.1
LC-30	21.1	22.1	23.4	24.9	26.9	29.0	34.3	37.8	46.7	50.0		188.9
MB-17	23.6	22.6	21.8	24.4	26.4	35.3	41.9	56.1				27.7
MC-27	20.8	22.4	24.1	23.9	24.4	30.7	39.1	47.0	60.7	60.2		108.9
NA-3	-	26.4	27.4	34.0	38.9	46.0	53.6	62.0				44.6
PA-5	19.3	22.9	29.2	33.0	37.1	37.3	44.2	51.8	57.2	-		234.2
PB-19	19.3	21.1	25.9	32.5	31.5	37.1	44.7	63.8	-			82.4+
PC-23	20.1	19.6	-	24.1	24.6	24.6	26.4	32.5	48.0			91.5
QA-8	17.3	19.1	-	-	19.6	35.3	27.9	51.6	56.4	55.1		131.9
QC-29	20.1	20.8	24.6	27.4	35.6	30.2	35.8	46.7	62.5	58.9		105.8
RA-8	23.4	23.9	23.1	26.4	38.1	38.6	54.1	63.0				20.1
RB-14	19.3	25.1	28.2	29.5	28.7	34.8	37.6	58.2	63.0			51.4
SA-6	20.1	-	19.6	19.3	20.6	20.6	20.8	31.5	31.0	31.5	46.0	303.9
SC-24	21.1	22.9	27.9	27.4	25.7	31.2	41.4	46.0	58.2			83.3
SC-30	19.1	27.2	26.4	27.7	35.1	46.7	49.8	38.9				28.5
Mean	20.6	22.4	24.6	26.7	29.0	34.0	39.6	48.5	53.8	50.8	46.0	
Std. Dev.	1.5	2.0	2.5	3.8	5.6	6.9	9.9	10.7	9.4	9.9		
Coeff. of Var. %	7	9	10	14	20	20	25	22	17	20		

TABLE XXVa
DAMAGE GROWTH IN Y (HEIGHT) DIRECTION (inches)
FOR DAMAGED HOLE 32-PLY LAMINATES FATIGUE CYCLED AT ± 22 ksi
(Includes all available data points)

Specimen ID	Cycles $\times 10^3$											Cycles To Failure $\times 10^3$
	0	0.1	0.5	1.0	2.5	5	10	20	50	100	250	
JA-1	0.86	0.81	0.82	0.86	0.85	0.77	0.80	0.93	-			60.0
JA-6	0.80	0.79	0.77	0.79	0.78	0.78	0.83	0.87	1.04			83.8
JC-24	0.78	0.81	0.81	0.81	0.83	0.81	0.86	0.90	1.00	1.01		191.1
KC-23	0.91	0.90	0.83	0.87	0.82	0.86	0.87					19.2
LA-6	0.86	0.86	0.81	0.81	0.81	0.80	0.83	0.91	1.04			53.1
LC-24	0.83	0.83	0.79	0.72	-	0.77	0.78	0.81	-	1.12		105.1
LC-30	0.75	0.76	0.74	0.76	0.76	0.77	0.82	0.91	0.97	1.03		188.9
MB-17	0.95	0.91	0.90	0.88	0.92	0.90	0.91	0.98				27.7
MC-27	0.86	0.90	0.90	0.81	0.81	0.92	0.93	1.03	1.09	1.07		108.9
NA-3	-	0.90	0.82	0.87	0.88	0.81	0.85	0.85				44.6
PA-5	0.74	0.72	0.71	0.75	0.75	0.69	0.73	0.78	0.86	-		234.2
PB-19	0.75	0.79	0.80	0.79	0.80	0.79	0.86	0.93	-			82.4+
PC-23	0.75	0.72	-	0.77	0.75	0.76	0.79	0.86	0.90			91.5
QA-8	0.65	0.69	-	-	0.70	0.70	0.75	0.77	0.87	0.90		131.9
QC-29	0.83	0.82	0.83	0.83	0.83	0.83	0.83	0.88	1.01	1.10		105.8
RA-8	0.97	0.97	0.99	0.98	0.97	0.99	1.00	1.10				20.1
RB-14	0.85	0.83	0.83	0.83	0.86	0.83	0.83	0.91	0.99			51.4
SA-6	0.75	-	0.73	0.75	0.78	0.77	0.79	0.83	0.86	0.92	1.01	303.9
SC-24	0.87	0.88	0.91	0.93	0.93	0.93	0.90	0.90	1.01			83.3
SC-30	0.86	0.85	0.81	0.78	0.85	0.88	0.83	0.99				28.5
Mean	0.82	0.83	0.82	0.82	0.83	0.82	0.84	0.90	0.97	1.02	1.01	
Std. Dev.	0.08	0.07	0.07	0.07	0.07	0.08	0.06	0.08	0.08	0.09		
Coeff. of Var. \bar{x}	10	9	8	8	8	9	7	9	8	8		

TABLE XXVb
DAMAGE GROWTH IN Y (HEIGHT) DIRECTION (mm)
FOR DAMAGED HOLE 32-PLY LAMINATES FATIGUE CYCLED AT ± 152 MPa
(Includes all available data points)

Specimen ID	Cycles $\times 10^3$											Cycles To Failure $\times 10^3$
	0	0.1	0.5	1.0	2.5	5	10	20	50	100	250	
JA-1	21.8	20.6	20.8	21.8	21.6	19.6	20.3	23.6	-			60.0
JA-6	20.3	20.1	19.6	20.1	19.8	19.8	21.1	22.1	26.4			83.8
JC-24	19.8	20.6	20.6	20.6	21.1	20.6	21.8	22.9	25.4	25.7		191.1
KC-23	23.1	22.9	21.1	22.1	20.8	21.8	22.1					19.2
LA-6	21.8	21.8	20.6	20.6	20.6	20.3	21.1	23.1	26.4			53.1
LC-24	21.1	21.1	20.1	18.3	-	19.6	19.8	20.6	-	28.4		105.1
LC-30	19.1	19.3	18.8	19.3	19.3	19.6	20.8	23.1	24.6	26.2		188.9
MB-17	24.1	23.1	22.9	22.4	23.4	22.9	23.1	24.9				27.7
MC-27	21.8	22.9	22.9	20.6	20.6	23.4	23.6	26.2	27.7	27.2		108.9
NA-3	-	22.9	20.8	22.1	22.4	20.6	21.6	21.6				44.6
PA-5	18.8	18.3	18.0	19.1	19.1	17.5	18.5	19.8	21.8	-		234.2
PB-19	19.1	20.1	20.3	20.1	20.3	20.1	21.8	23.6	-			82.4+
PC-23	19.1	18.3	-	19.6	19.1	19.3	20.1	21.8	22.9			91.5
QA-8	16.5	17.5	-	-	17.8	17.8	19.1	19.6	22.1	22.9		131.9
QC-29	21.1	20.8	21.1	21.1	21.1	21.1	21.1	22.4	25.7	27.9		105.8
RA-8	24.6	24.6	25.1	24.9	24.6	25.1	25.4	27.9				20.1
RB-14	21.6	21.1	21.1	21.1	21.8	21.1	21.1	23.1	25.1			51.4
SA-6	19.1	-	18.5	19.1	19.8	19.6	20.1	21.1	21.8	23.4	25.7	303.9
SC-24	22.1	22.4	23.1	23.6	23.6	23.6	22.9	22.9	25.7			83.3
SC-30	21.8	21.6	20.6	19.8	21.6	22.4	21.1	25.1				28.5
Mean	20.8	21.1	20.8	20.8	21.1	20.8	21.3	22.9	24.6	25.9	25.7	
Std. Dev.	2.0	1.8	1.8	1.8	1.8	2.0	1.5	2.0	2.0	2.3		
Coeff. of Var. %	10	9	8	8	8	9	7	9	8	8		

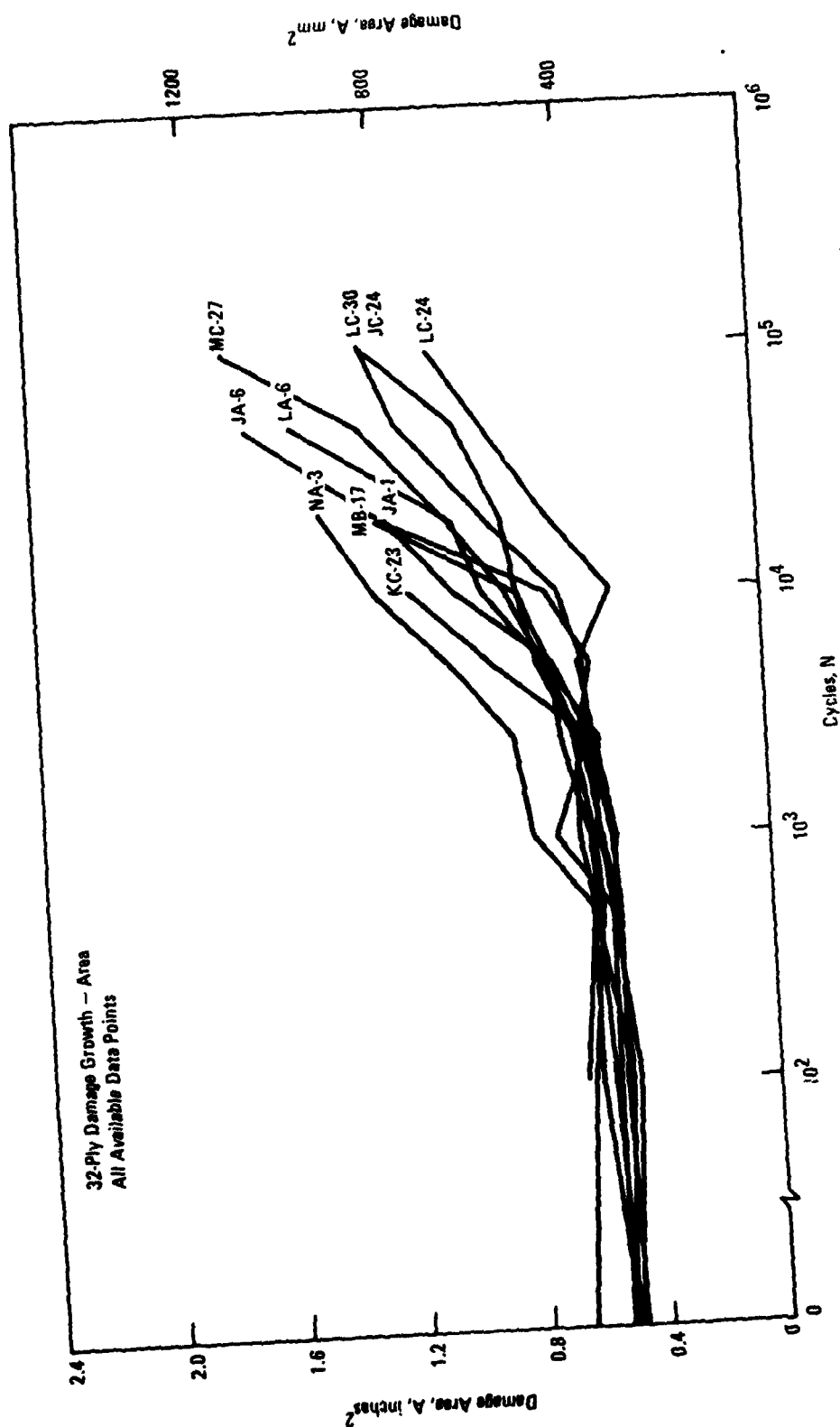


Figure 73a: Area Damage Growth for the 32-Ply Fatigue Distribution Specimens (Specimens 1 thru 10)

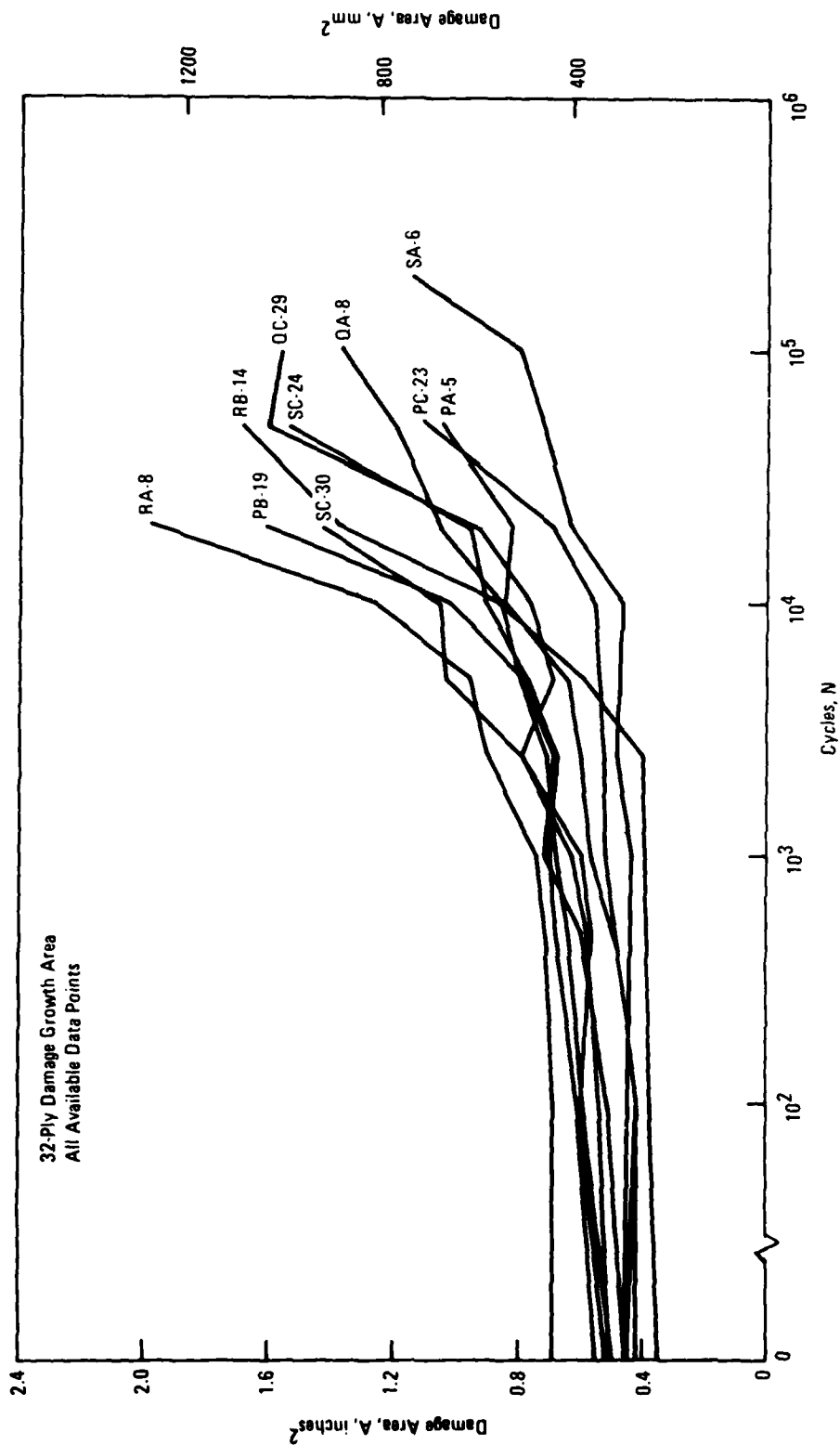


Figure 73b. Area Damage Growth for the 32-Ply Fatigue Distribution Specimens (Specimens 11 thru 20)

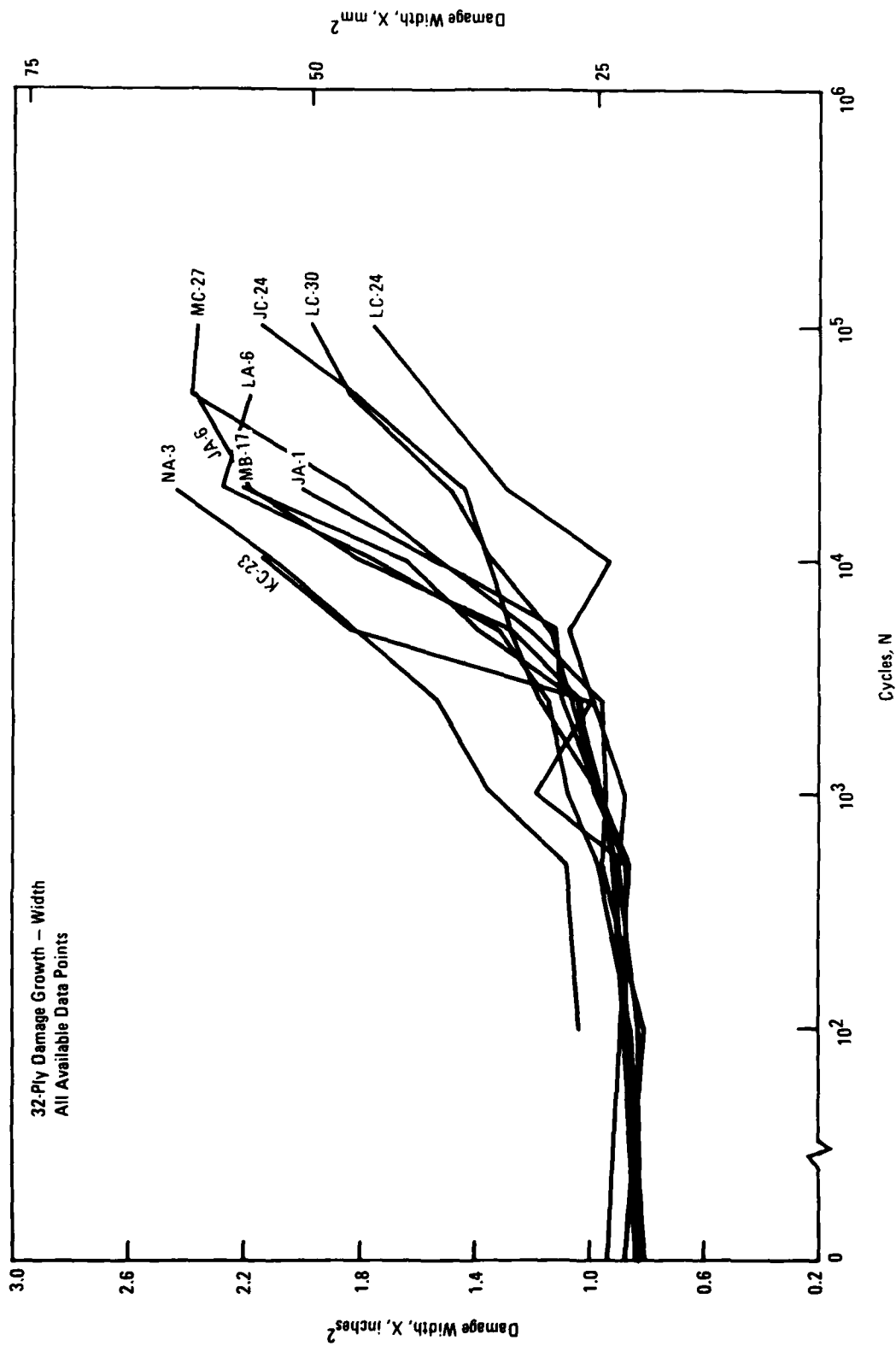


Figure 74a: Damage Growth in the Width Direction for the 32-ply Fatigue Distribution Specimens (Specimens 1 thru 10)

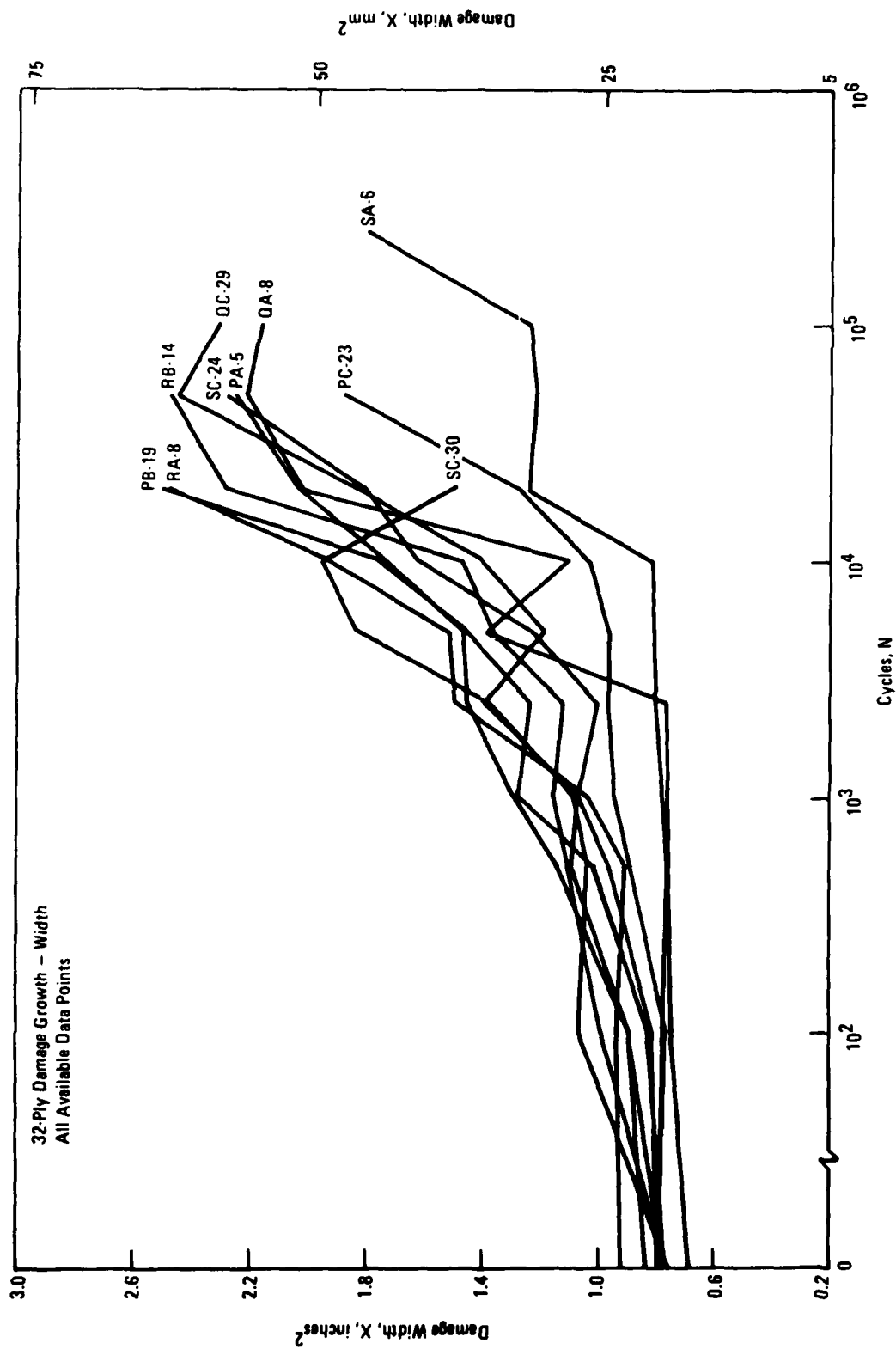


Figure 74b: Damage Growth in the Width Direction for the 32-Ply Fatigue Distribution Specimens (Specimens 11 thru 20)

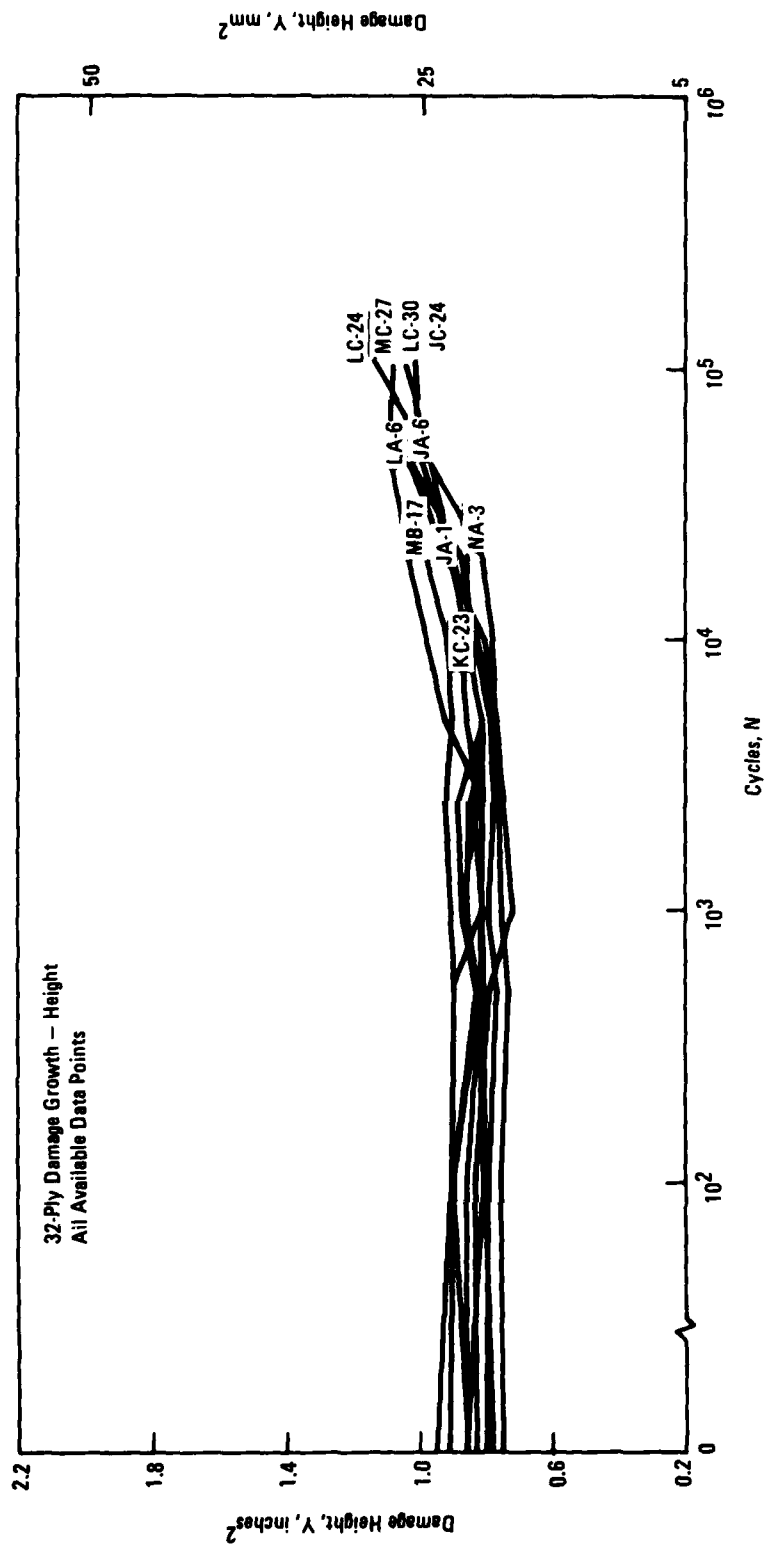


Figure 75a: Damage Growth in the Height Direction for the 32-Ply Fatigue Distribution Specimens (Specimens 1 thru 10)

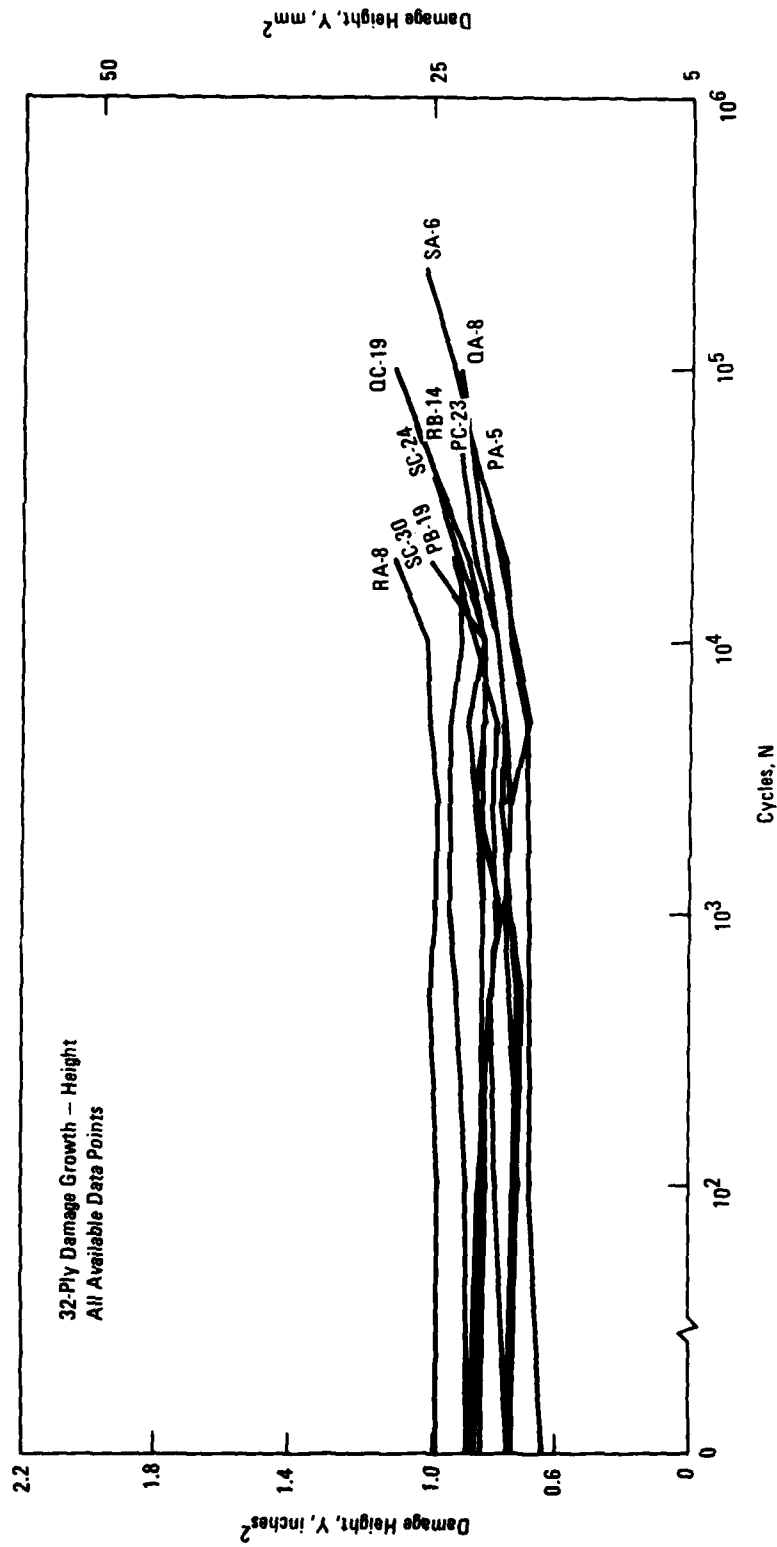


Figure 75b: Damage Growth in the Height Direction for the 32-Ply Fatigue Distribution Specimens (Specimens 11 thru 20)

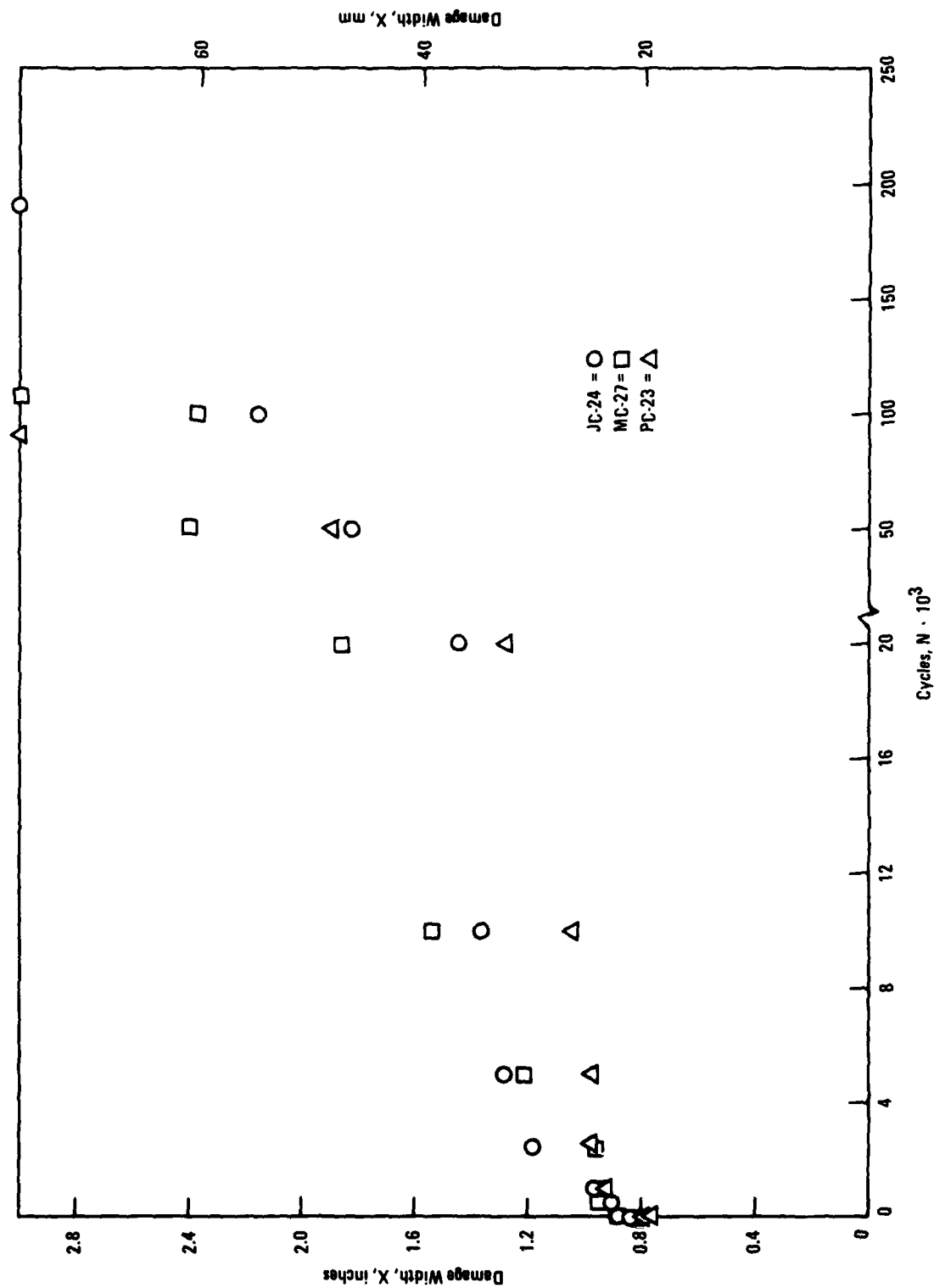


Figure 76: Typical Damage Growth of 32-ply Laminate Specimens

for this laminate was also across the width (X), but unlike the 24-ply laminate case, Y growth was minimal resulting in area measurements which primarily reflected the X extension. Thus, area could be used to quantify delamination development in both laminates.

Scatter in the damage size data was not as large for this laminate, but then neither was the dispersion in the life data. Thus, a slightly better correspondence between damage size at 20,000 cycles (at which point one failure had occurred) and life is apparent in Figure 77 than was observed for the 24-ply laminate. But, as the damage size increased nearer to failure even this tenuous relationship disappeared as evident from Figure 78. Also, as for the 24-ply laminate variation in initial damage size was not large but the life data were spread over an order of magnitude. Hence, prediction of life based upon inspection for initial flaws size could be no better than within one order of magnitude.

Typical Holscans illustrating the damage growth behavior of the 32-ply laminate are displayed in Figures 79 and 80. Additional data are available in Volume II. Note in Figure 80 that area measurements would reflect the growth of this type of delamination much more accurately than width or height, although the measured maximum X or Y dimension may at times remain unchanged, X and Y growth will occur filling out the contour.

6.3 RESIDUAL STRENGTH RESULTS

One hundred and fifteen specimens in five groups of twenty-three each were fatigue cycled at one stress level with $R = -1$ for each laminate type. Each of the groups of specimens was Holscanned prior to testing, cycled to one of five selected life values for each laminate and Holscanned again. Then, one to three specimens (depending upon the number surviving) per group were removed for destructive inspection and half of the remaining

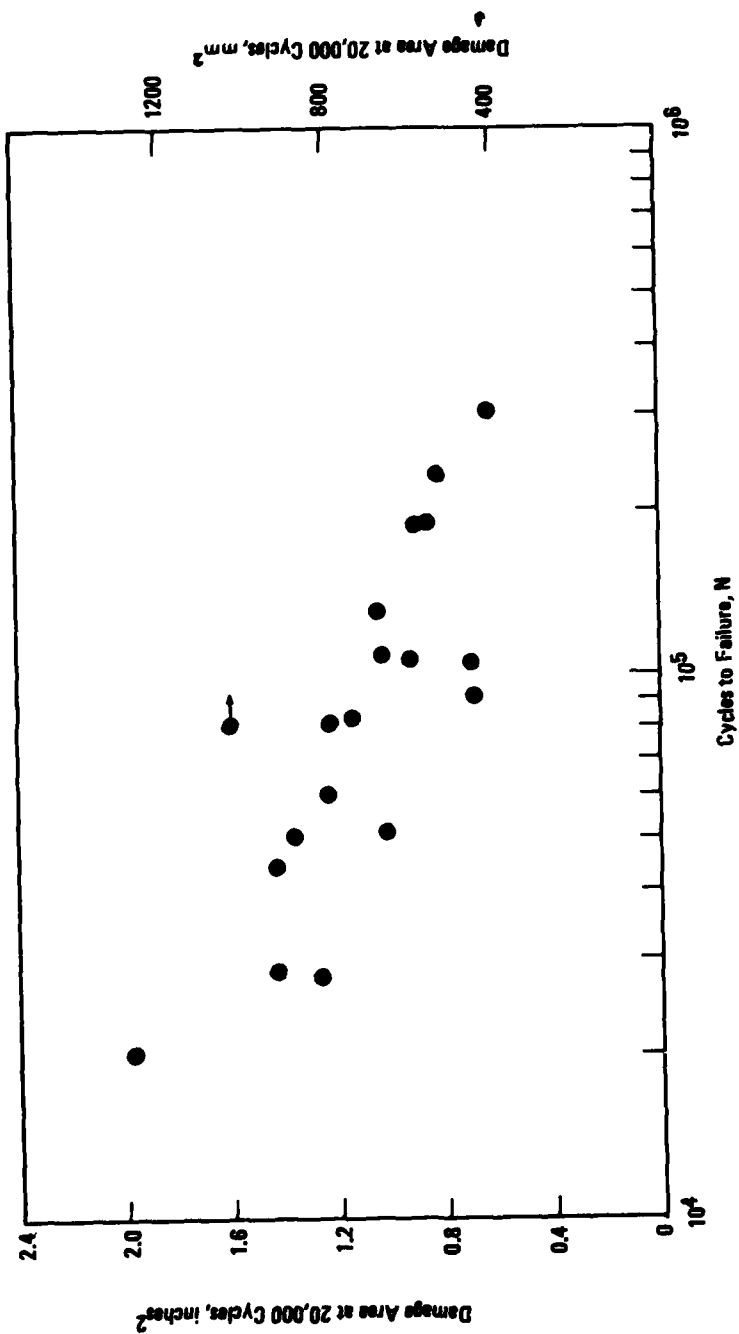


Figure 77: Damage Size at 20,000 Cycles vs. Life for the 32-ply Laminate

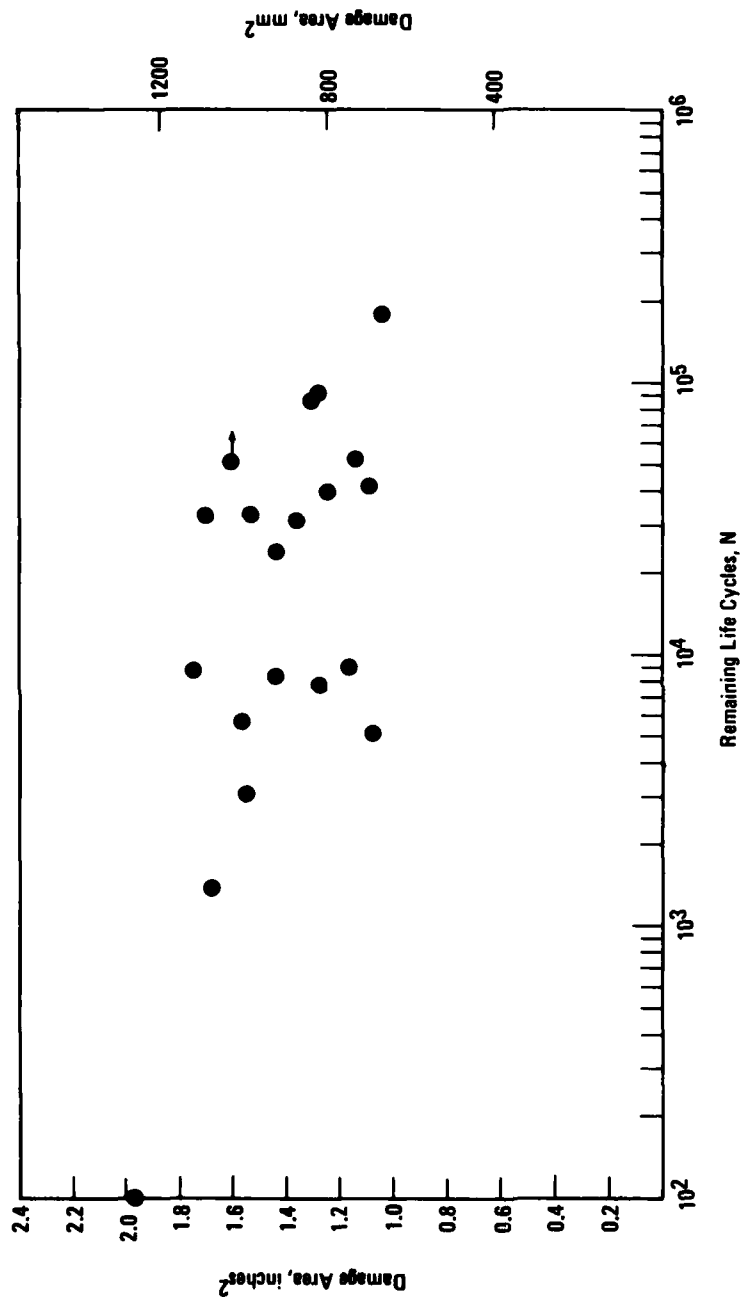


Figure 78: Last Recorded Damage Size Prior to Failure vs. Remaining Life for the 32-ply Laminate

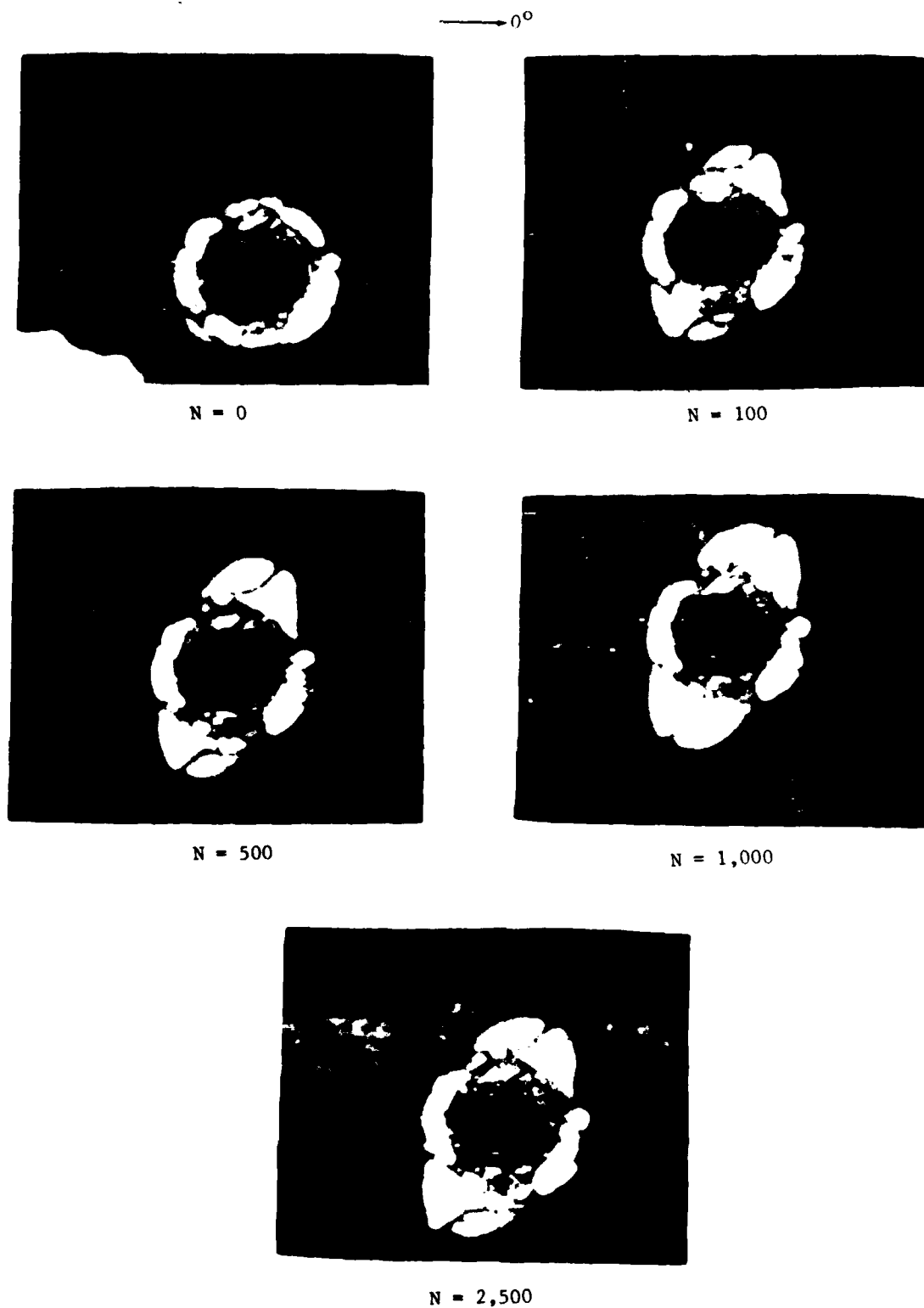


Figure 79a: Typical Damage Growth Characteristics of Initially Damaged 32-Ply Quasi-Isotropic Specimens (Specimen RB-14, $N_f = 51,400$)

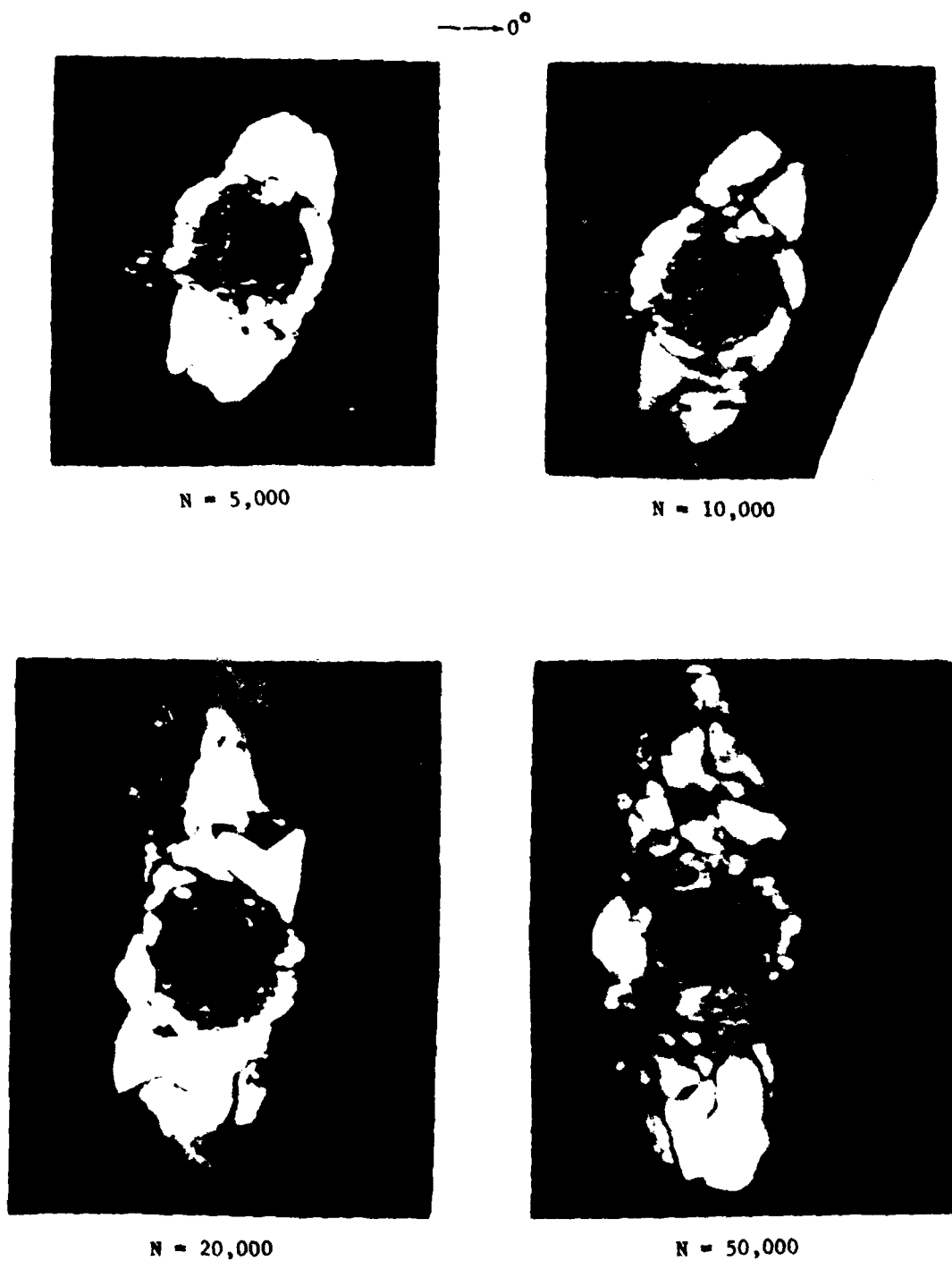


Figure 79b: Typical Damage Growth Characteristics of Initially Damaged 32-Ply Quasi-Isotropic Specimens (Specimen RB-14, $N_f = 51,400$)

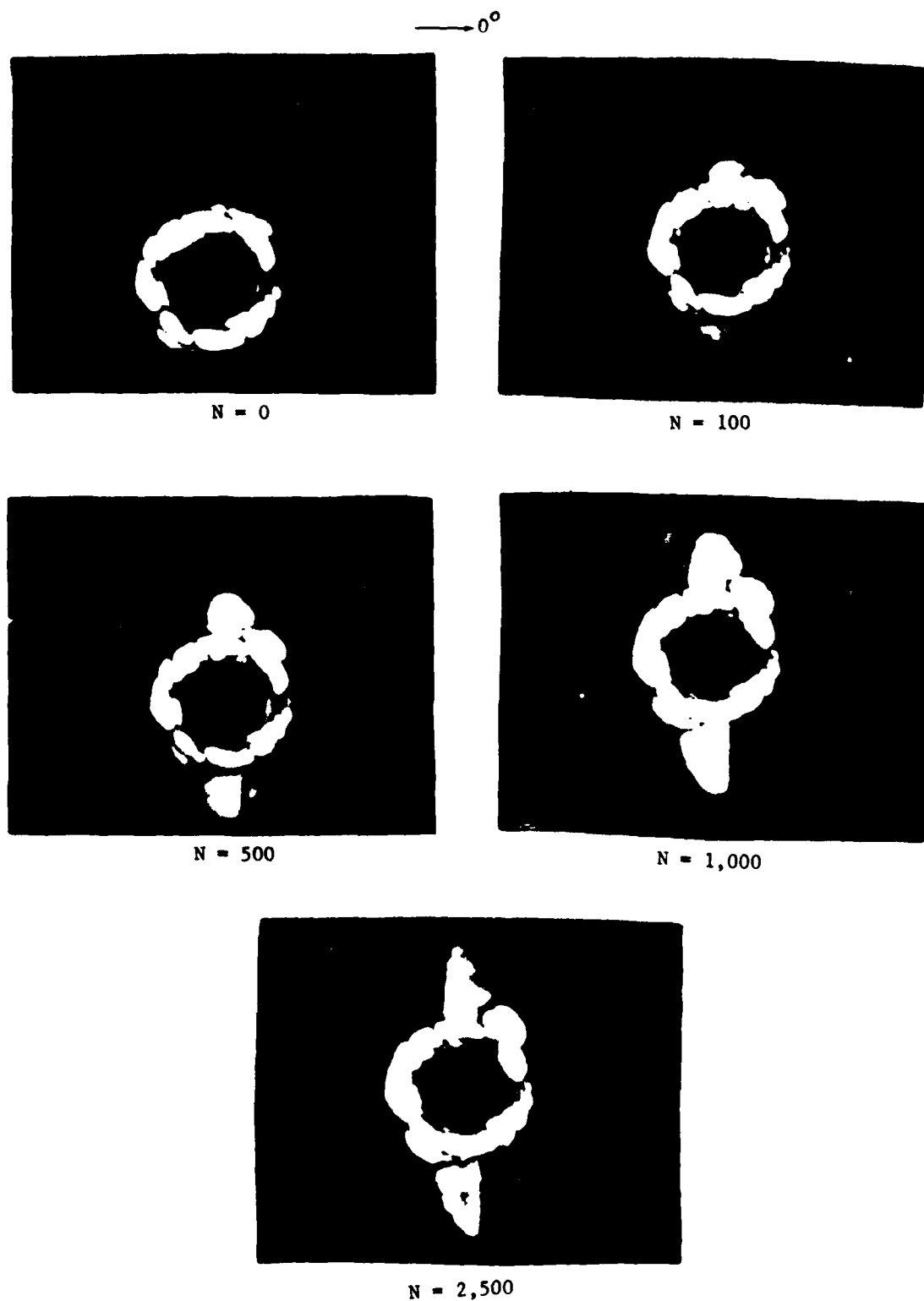


Figure 80a: Typical Damage Growth Characteristics of Initially Damaged 32-Ply Quasi-Isotropic Specimens (Specimen OA-5, $N_f = 234,200$)

→ θ^0



N = 5,000



N = 10,000



N = 20,000



N = 50,000

Figure 80b: Typical Damage Growth Characteristics of Initially Damaged 32-Ply Quasi-Isotropic Specimens (Specimen QA-5, $N_f = 234,200$)

specimens of each group were tested for residual tensile strength and half for compressive strength.

Selection of the five fatigue cycle intervals was based upon the following considerations:

- 1) The intervals selected should provide an assessment of the relative static strength loss over the range from very early in the history through to the 80% probability of survival cycle level as determined from the fatigue distribution (Item 5) data. Selection of the 80% probability of survival point as the upper cyclic bound was made since: (1) longer target lives would increase the number of fatigue failures prior to achieving the desired cycle count; and (2) residual strength data at cycle intervals beyond the 80% survivability point were considered to be of questionable design significance.
- 2) The intervals should provide information for the correlation of damage size with the mechanical response of the material. Therefore, when damage growth has occurred uniformly during the entire life, a range of varying damage sizes should be evaluated. If, however, the damage growth occurred slowly during a significant portion of the life, it would be of value to examine two cycle levels which are widely separated numerically but show only minor changes in the damage size to determine if damage occurred during the cyclic intervals which was not revealed by C-scan.

The mechanics of implementing the above considerations were the following. First the 80% probability of survival cycle value was determined from the results of Item 5 tests, which defined the maximum cyclic life interval for study, hereafter referred to as N_p . The distributions of damage sizes for

the 20 replicates were evaluated as a function of cycles. A plot was made of the mean value damage sizes vs the number of fatigue cycles. The mean damage size corresponding to the N_p cycle level was determined along with the mean damage size at $N = 0$ cycles. The difference between mean damage sizes at $N = 0$ and $N = N_p$ was divided into five equal damage size intervals and the corresponding numbers of cycles N_1 , N_2 , N_3 , N_4 , and N_p were defined for the residual strength tests (Items 6, 7).

6.3.1 Residual Strength Results for the 24-Ply Laminate

The five groups of twenty-three specimens each were fatigue cycled to the selected life values under the same conditions as the specimens used to determine the baseline fatigue distribution with a maximum stress of 35 ksi (241 MPa), $R = -1$. The 80% probability of survival life based upon the baseline distribution of 20 specimens was 40,000 cycles, N_5 . However, once testing was in progress there appeared to be a shift in the distribution towards shorter lives from the baseline results with failures occurring after a few thousand cycles. The twenty specimen baseline data scattered over nearly two orders of magnitude with lives ranging from 27,000 cycles to slightly over 900,000 cycles. Since large numbers of failures were occurring the intervals $N_1 - N_4$ were shifted towards the shorter life end from the originally proposed equally spaced intervals as follows: $N_1 = 4,000$, $N_2 = 8,000$, $N_3 = 12,000$, $N_4 = 20,000$ with N_5 remaining at 40,000.

Testing was temporarily discontinued while all possible equipment, mechanical, electrical and human variables were checked out including: machine and specimen alignment, load cell calibration, possible electrical transients, input signals, uniformity of all fatigue support sets and bolt torques on supports and grips. No irregularities or problems were discovered. Several additional possibilities were then examined. There was slight evidence that a machine bias may exist, therefore, all testing was returned to the two original machines. However, no effect was noted

due to the change in machine. It was ascertained that the first ten cycles of the life of a specimen on all machines were run at the required 0.05 Hz with incrementally increasing stress reaching 90% σ_{max} on the tenth cycle, since in previous investigations it was discovered that immediate application of the alternating stress at 5 Hz resulted in shorter lives. There was also no measurable change in specimen weight eliminating the possibility that absorbed moisture may be affecting the results. The only remaining variable was the fact that the baseline tests were conducted with periodic stops to measure damage growth using the Holscan equipment while the specimens for residual strength testing were being cycled without interruption to a given number of cycles. Temperature build up in the latter group was suspected of possibly causing shorter lives.

To investigate the possibility that specimen life might be prolonged by periodic cooling, fatigue testing to 20,000 cycles (N_4) was interrupted with one hour holds at mean (zero) stress after 1,000, 5,000, and 10,000 cycles which corresponded to the scanning intervals of the baseline distribution. Concurrently, under an independent research program, several specimens were fatigue cycled to failure with periodic one hour holds corresponding to the scanning intervals. Specimens were air cooled during the hold periods. Specimen temperatures before and after the holds were recorded. Temperature built to a high of about 95°F (35°C) and then cooled to lab temperature during hold. The first specimen failed at slightly over 158,000 cycles, the second completed 500,000 without failure when it was stopped. However, the next two failed at short lives of 20,960 and 9,610, both shorter than the shortest life of the baseline distribution. Further testing was discontinued. Specimens being cycled to N_4 (20,000 cycles) also revealed no beneficial effect of the hold time with 11 out of 23 failing. Results of the fatigue testing to N_1 through N_5 are presented in Table XXVI. Examination of these data does not appear to indicate a machine bias nor a panel bias which were suggested by the baseline results (see Table XXVII). All the panels are represented among the early failures

TABLE XXVI
FATIGUE RESULTS FOR SPECIMENS TESTED
FOR TENSION AND COMPRESSION RESIDUAL STRENGTH
24-PLY LAMINATE

CYCLING TO $N_1 = 40,000$			CYCLING TO $N_4 = 20,000$			CYCLING TO $N_3 = 12,000$			CYCLING TO $N_2 = 8,000$		
Specimen ID	Number of Cycles	Machine Number	Specimen ID	Number of Cycles	Machine Number	Specimen ID	Number of Cycles	Machine Number	Specimen ID	Number of Cycles	Machine Number
HA-3	6,261	15	CA-4	5,140	15	DA-2	10,080	15	AA-9	3,370	15
EB-15	12,425		EB-17	10,160		DB-19	12,000	NF	BB-12	4,310	
DC-26	24,460		BB-14	20,000	NF				BB-1	6,440	
GC-26	34,460		DB-14	20,000	NF	CA-6	6,270		AA-7	8,000	NF
GA-3	38,754		FA-2	20,000	NF	EA-4	6,500		AC-24	8,000	
BC-25	40,000	NF ^a	FC-29	20,000	NF	HB-19	8,400		CB-16	8,000	
CB-19	40,000	NF	GC-23	20,000	NF	FB-18	9,450		DB-18	8,000	
FC-27	40,000	NF				AA-5	12,000	NF	DC-29	8,000	
GA-9	40,000	NF	CA-9	2,350	17	AC-27	12,000	NF	FA-6	8,000	
HC-30	40,000	NF	HC-29	8,844		BB-19	12,000		CA-6	8,000	
			HB-12	8,870		BC-21	12,000		1B-15	8,000	
			BA-8	15,360		CA-2	12,000				
CA-3	5,418	17	AA-3	20,000	NF	CB-14	12,000		BC-30	8,000	NF
AA-8	6,677		CB-17	20,000	NF	DB-15	12,000		CB-12	8,000	
1B-17	30,000	NF ^b	FB-15	20,000	NF	FA-1	12,000		DA-5	8,000	
FA-7	30,460					CB-18	12,000		EC-24	8,000	
GA-1	33,360		1B-14	3,331	18	CA-5	12,000		EC-29	8,000	
DB-13	34,080		AB-17	4,840		CB-18	12,000		FB-11	8,000	
BB-15	34,080	NF	BC-28	7,864		HC-21	12,000		FC-26	8,000	
EC-30	40,000	NF	BC-22	13,550		1A-6	12,000		GC-22	8,000	
			EC-26	18,080		1A-8	12,000		HB-16	8,000	
GB-15	12,270	18	AC-25	20,000	NF				1C-27	8,000	
AC-26	40,000	NF	GC-24	20,000	NF	HA-6	12,000	NF	HR-15	7,128	27
CC-24	40,000	NF	CC-25	20,000	NF	HA-8	12,000		EA-5	8,000	27
CC-27	40,000	NF	1B-12	20,000	NF	1A-2	12,000				
EA-9	40,000	NF									
1B-16	40,000	NF									

NOTES:

1. Cycling to $N_1 = 4000$ -- all 23 specimens completed 4000 cycles without failure. However, larger than expected damage growth was observed for some specimens.
 2. Baseline (damage growth) tests were conducted in machines 17 and 18.
- a - Completed cycles without failure
b - An additional specimen was tested to replace 1-17

TABLE XXVII
 BASELINE FATIGUE LIFE DISTRIBUTION
 BY MACHINE

	MACHINE 17	MACHINE 18
24-Ply Laminate		
Mean Life (Cycles)	102,300	310,500
Std. Dev.	113,600	287,700
Coef. of Var.	111%	93%
No. of Specimens	8	12
32-Ply Laminate		
Mean Life (Cycles)	114,100	100,300
Std. Dev.	100,300	69,900
Coef. of Var.	88%	70%
No. of Specimens	7	10

and percentages of short lives occurring in each machine are nearly the same when the complete data set is considered as indicated in Table XXVIII. The 32-ply specimens were tested in the same machines and no such difficulties were encountered, indicating that the scatter is a characteristic of the laminate. Because of the extremely large dispersion of life data for the 24-ply laminate (approximately 2.5 orders of magnitude) the twenty specimen data set used to determine the fatigue life distribution was inadequate for establishing the behavior and probably at least twice that number would be required.

Due to the high percentage of failures, the number of specimens available for residual strength testing was reduced by half for the last two intervals. However, the trend indicated in summary Tables XXIX and XXX is still fairly definitive in that the tensile residual strengths and failure strains increased as the number of cycles completed increased. There was only a slight indication of a similar trend in compression, but it was clear that no decrease in properties occurred with cycling to 40,000 cycles. Also, no change in tension or compression residual modulus after cycling was evident. Since a number of fatigue failures had occurred during cycling to the desired N_x value, some of the tension increase was likely due to a screening effect as shown by the reduction in strength data scatter. But, not entirely, since the average tensile strength after 40,000 cycles was greater than the maximum baseline value. The additional increase was due to the reduction in notch acuity associated with the expanding "damage" zone.

Prior to residual strength testing, each specimen was inspected (using the Holscan ultrasonic C-scan equipment) to determine damage area, width and length. These results are given in detail in Appendix, F of Volume III. Summaries of the measurements for the 24-ply laminate are presented in Tables XXXIa and b. Despite the fact that damage was found to increase in a systematic manner as the number of applied cycles increased (discussed in

Section 6.2) data scatter was so large that no trend was observed which could be represented by a simple mathematical expression. As shown in Table XXXIa, the average damage area did not increase systematically as cycles increased. The reason for this is indicated by the percent coefficient of variation values shown in Table XXXIa and delineated in Table XXXIb. In the latter table, one can see that the damage area reached at a particular number of cycles did not systematically depend on the initial damage area. Equally as important, no apparent trend in the relationship between damage size (as defined by C-scan) and residual strength was found (see Figures 81 and 82 and representative Holoscans in Figure 83). The conclusion was made that the relationship between damage size and remaining fatigue life or residual strength, for these coupons, is not of engineering significance.

The effect of delamination damage on strength for these laminates is not that of the dominant flaw. The damage appears to be significant only when it is of a size where it affects the stability of the structure (coupon/support configuration) resulting in failures. Further discussion appears in Section 9.

Typical fracture appearances of residual strength tested specimens are shown in Figure 84. Slightly more delamination was evident than in baseline specimens, however little difference over the range of 4,000 to 40,000 cycles was apparent.

6.3.2 Residual Strength Results for the 32-Ply Laminate

Each of five groups of 23 specimens was fatigue cycled at 22 ksi (152 MPa), $R = -1$ to one of the following N_x values: $N_1 = 1,000$, $N_2 = 5,000$, $N_3 = 10,000$, $n_4 = 20,000$ and $N_5 = 28,000$ where N_5 corresponded to the 80% probability of survival life based upon the baseline distribution of 20

TABLE XXVIII
 FAILURE DISTRIBUTION BY TEST MACHINE
 FOR 24-PLY LAMINATE SPECIMENS FATIGUE TESTED TO $N_1 - N_5$
 FOR RESIDUAL STRENGTH DETERMINATION

	<u>Machine 15</u>	<u>Machine 17</u>	<u>Machine 18</u>
Failures < 8,000 cycles	17%	15%	11%
Failures < 12,000 cycles	21%	27%	17%
Failures < 20,000 cycles	24%	40%	40%

TABLE XXIX
TENSION RESIDUAL STRENGTH DATA SUMMARY
24-PLY, 67% 0° FIBER LAMINATE

Property	Number of Fatigue Cycles Completed					
	Baseline ⁰	4,000	8,000	12,000	20,000	40,000
Average Strength ksi	74.2	79.2	81.0	83.8	83.0	87.2
Standard Dev.	5.5	3.0	4.6	3.9	3.6	2.4
Coefficient of Variation %	7.3	3.7	5.7	4.7	4.3	2.8
Average Failure Strain, in./in.	0.0099	0.0104	0.0106	0.0115	0.0113	0.0112
Standard Dev.	0.0009	0.0007	0.0008	0.0008	0.0006	0.0005
Coefficient of Variation %	9.1	7.0	7.7	7.1	4.9	4.5
Average Secant Modulus at Failure psi x 10 ⁶	7.5	7.6	7.6	7.4	7.4	7.8
Standard Dev.	0.19	0.42	0.28	0.38	0.08	0.21
Coefficient of Variation %	2.5	5.5	3.7	5.1	1.1	2.6
Average Initial Tangent Modulus psi x 10 ⁶	8.9	8.9	8.9	8.8	8.8	9.1
Standard Dev.	0.20	0.28	0.21	0.26	0.18	0.33
Coefficient of Variation %	2.3	3.1	2.4	2.9	2.1	3.7
No. of Spec. in Data Set	15	9	9	8	5	5
Percent Failures	-	0	17	22	40	48

TABLE XXX
COMPRESSION RESIDUAL STRENGTH DATA SUMMARY
24-PLY, 67% 0° FIBER LAMINATE

Property	Number of Fatigue Cycles Completed					
	0 Baseline	4,000	8,000	12,000	20,000	40,000
Average Strength, ksi	44.4	46.0	45.3	49.2	45.3	47.8
Standard Dev.	2.8	4.2	3.0	3.3	4.3	4.9
Coefficient of Variation %	6.3	9.2	6.6	6.8	9.4	10.2
Average Failure Strain, in./in.	0.0054	0.0060	0.0057	0.0064	0.0057	0.0060
Coefficient of Variation %	7.6	10.6	6.2	7.3	7.2	11.8
Average Secant Modulus at Failure psi x 10 ⁶	8.2	7.8	7.9	7.7	8.0	8.0
Standard Dev.	0.17	0.16	0.19	0.23	0.26	0.23
Coefficient of Variation %	2.0	2.1	2.4	3.0	3.2	2.8
Average Secant Modulus at 30 ksi psi x 10 ⁶	8.7	8.5	8.5	8.4	8.5	8.8
Standard Dev.	0.15	0.13	0.31	0.23	0.19	0.11
Coefficient of Variation %	1.7	1.6	3.6	2.7	2.3	1.3
No. of Spec. in Data Set	15	10	9	8	5	5
Percent Failures	-	0	17	22	48	48

TABLE XXXIa
SUMMARY OF DAMAGE MEASUREMENTS FOR 24-PLY LAMINATE SPECIMENS

Damage Dimension	Number of Fatigue Cycles Completed				
	4,000	8,000	12,000	20,000	40,000
Average Damage Area, A, in. ²	0.71	1.09	0.89	1.00	1.48
Standard Deviation	0.27	0.58	0.39	0.32	0.69
Coeff. of Variation %	38.10	53.40	44.30	31.60	46.70
Average Maximum Damage Width, X, in.	1.03	1.24	1.10	1.21	1.39
Standard Deviation	0.25	0.44	0.34	0.33	0.38
Coeff. of Variation %	24.20	35.70	31.00	27.10	27.50
Average Maximum Damage Length, Y, in.	0.96	1.22	1.11	1.18	1.23
Standard Deviation	0.12	0.32	0.16	0.15	0.48
Coeff. of Variation %	12.70	25.90	14.10	12.40	39.10
No. of Specimens in Data Set	23	19	18	12	12

TABLE XXXIb

Initial Damage Area A _i , inch ²	Number of Fatigue Cycles Completed Prior to Residual Strength Testing					
	12,000		20,000		40,000	
	Failed Total No.	Range of Final Damage Area A _f , inch ²	Failed Total No.	Range of Final Damage Area A _f , inch ²	Failed Total No.	Range of Final Damage Area A _f , inch ²
0.33 to 0.36	$\frac{0}{3}$	0.47 to 1.00	$\frac{0}{0}$	—	$\frac{1}{9}$	0.71 to 2.16
0.37 to 0.40	$\frac{2}{10}$	0.53 to 0.88	$\frac{5}{10}$	0.69 to 1.74	$\frac{6}{7}$	0.93
0.41 to 0.44	$\frac{3}{7}$	0.74 to 1.64	$\frac{2}{7}$	0.49 to 1.30	$\frac{2}{3}$	1.35
0.45 to 0.48	$\frac{0}{3}$	1.20 to 1.93	$\frac{2}{5}$	0.89 to 1.16	$\frac{0}{1}$	2.86
0.49 to 0.61	$\frac{0}{0}$	—	$\frac{1}{1}$	—	$\frac{1}{2}$	2.50

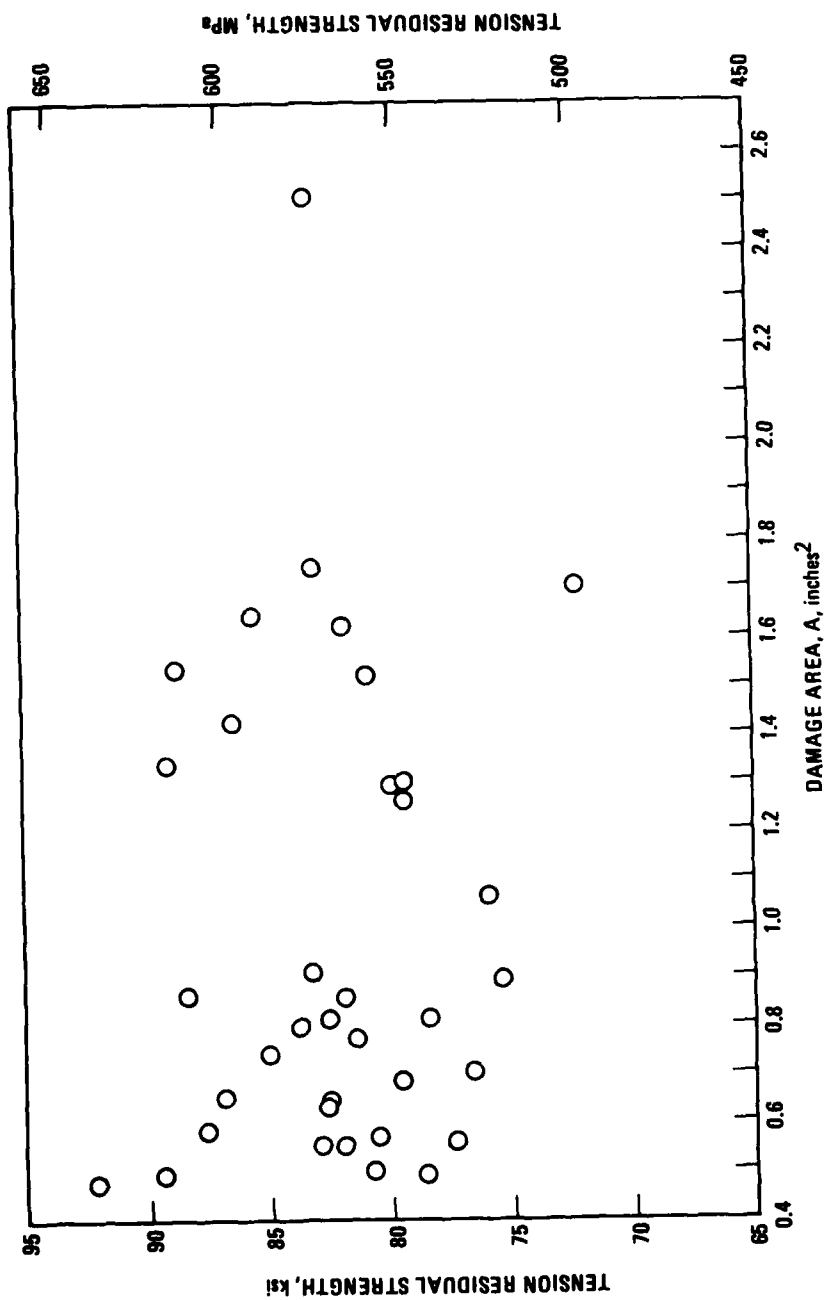


Figure 81: Relationship of Tension Residual Strength to Damage Area as Detected by the Holiscan Ultrasonic C-scan for 24-ply Laminated Specimens.

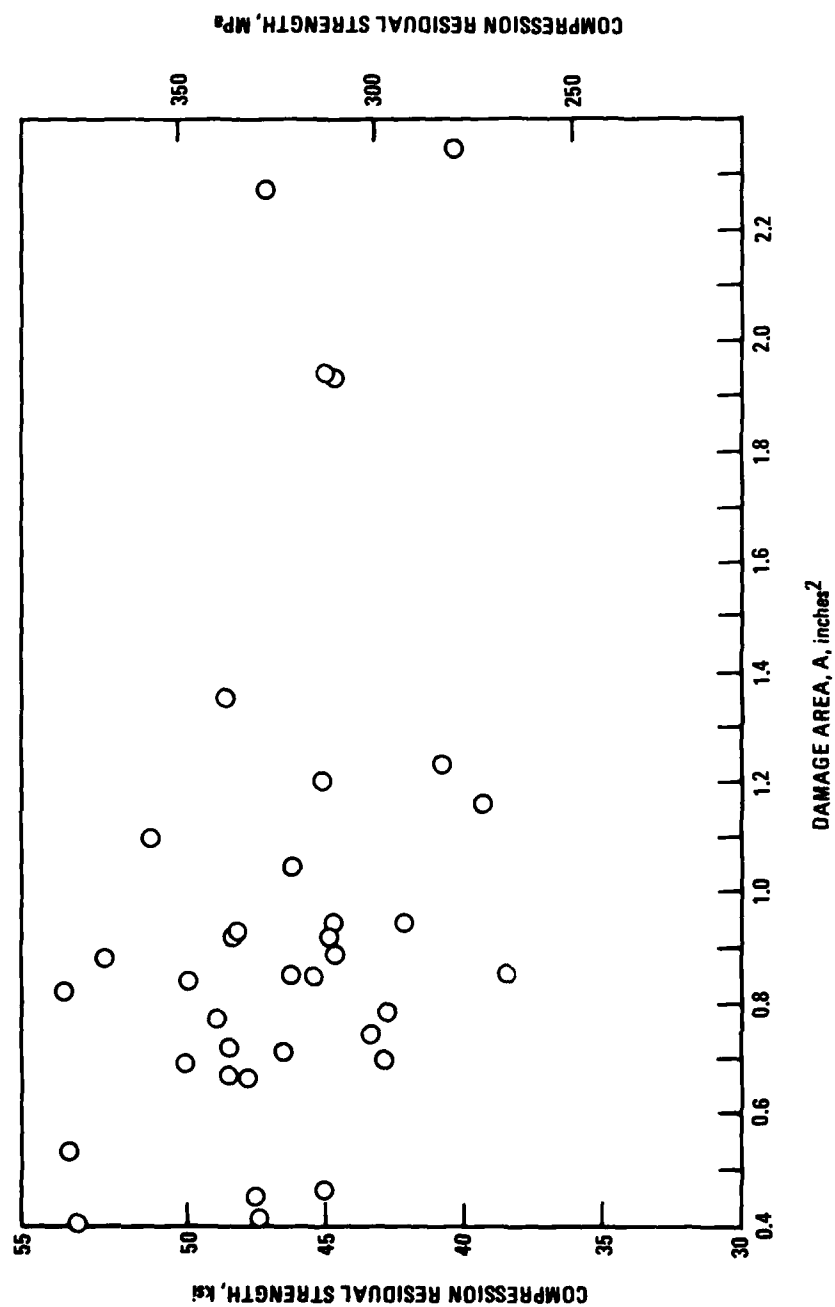


Figure 82: Relationship of Compression Residual Strength to Damage Area as Detected by the Holscan Ultrasonic C-scan for 24-ply Laminate Specimens

Note: Areas of Displayed Specimens are approximately equal to the average for each N_x value.

—→0°

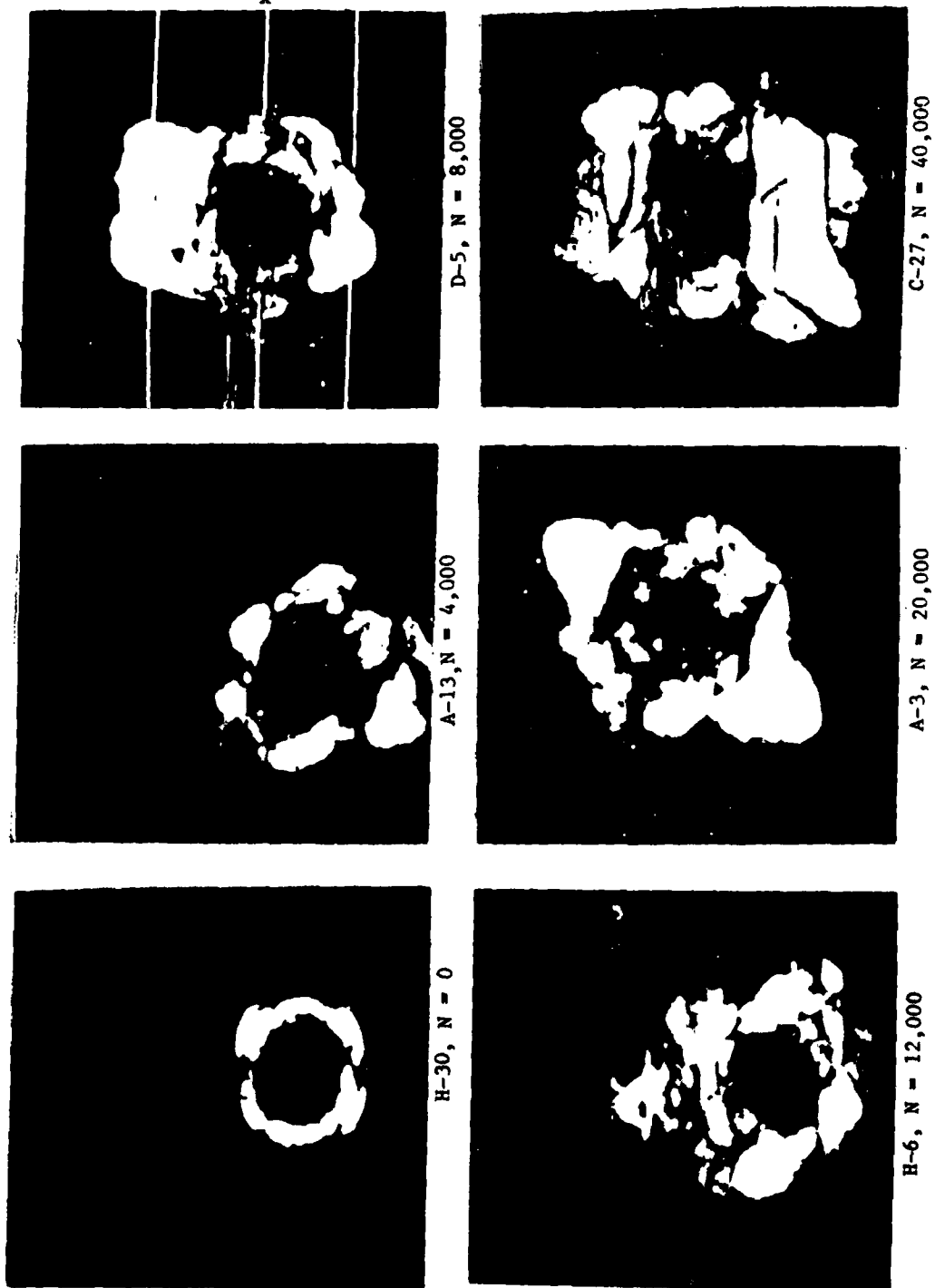
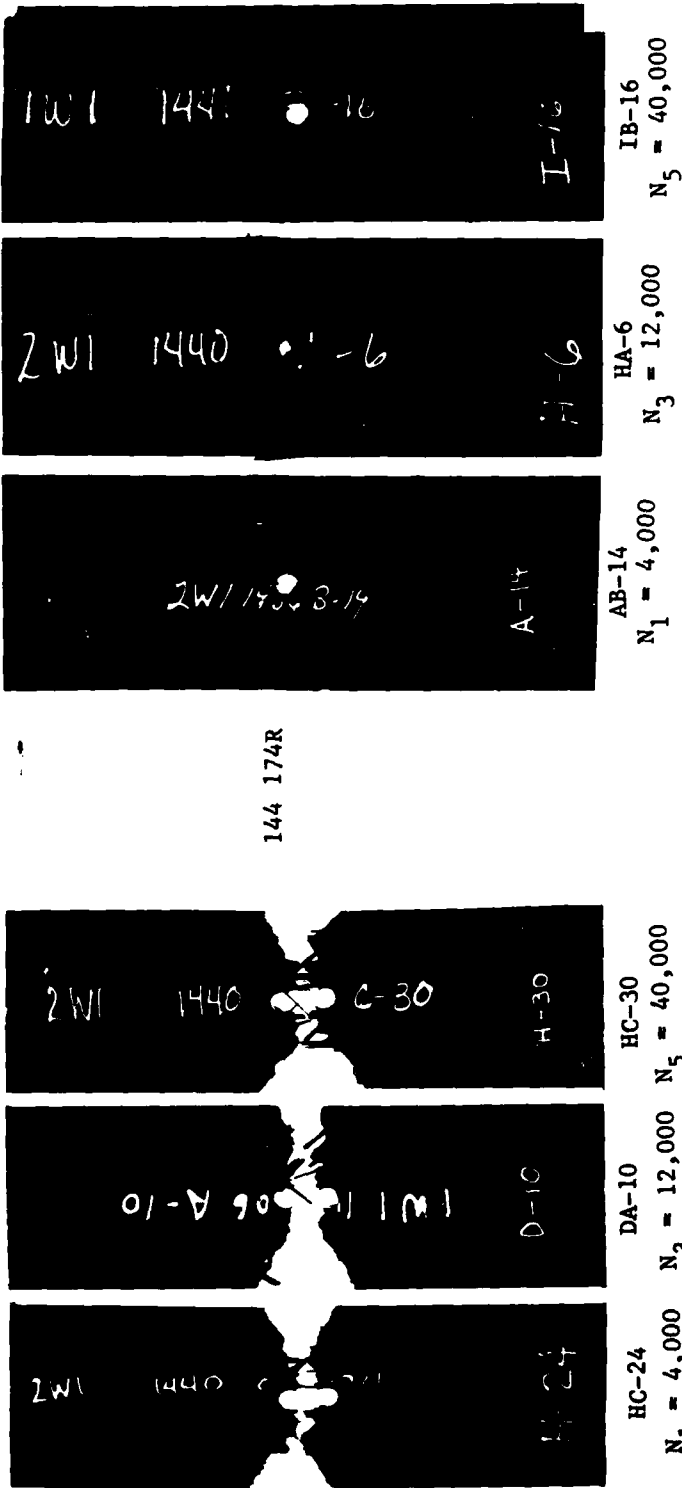


Figure 83: Typical Damage Characteristics of 24-Ply Specimens Fatigue Cycled at +35 ksi (+241 MPa) for Residual Strength Determination



a. Tension Residual Strength

b. Compression Residual Strength

Figure 84: Typical Fracture Appearances of 24-Ply Specimens Tested for Residual Strength After Fatigue Cycling

specimens. Unlike the 24-ply laminate, all but one of the 115 specimens survived the fatigue testing to the selected number of cycles. The single failure occurred in the N_u interval at 14,860 cycles. Tension and compression residual strength data are summarized in Tables XXXII and XXXIII. There appears to be a very slight but insignificant increase (6% - 11%) in tensile residual strength and a similar decrease in compressive residual strength. Residual static properties do not appear to be affected by fatigue cycling to 80% of the probability of survival life for this laminate.

More consistent damage growth was displayed by the 32-ply laminate than the 24-ply which is reflected in all of the damage parameters summarized in Table XXXIV. However as for the 24-ply case the data dispersion is large and no apparent relationship exists between damage size as detected by the Holscan unit and residual strength, which is evident from Figures 85 and 86. Representative holscans are presented in figures 87.

For this quasi-isotropic laminate, as for the 24-ply, damage is related to strength to the extent that it affects the stability of the structure which while it is stable shows no degrading effect, but once it becomes unstable, failure is catastrophic. This is discussed in greater detail in Section 9.

Typical fracture appearances of residual strength tested specimens are displayed in Figure 88. Very little difference in the static fractures was noticed due to the cycling from 1,000 to 25,000 cycles. However, more delamination than in the baseline specimens was observed.

TABLE XXXII
TENSION RESIDUAL STRENGTH DATA SUMMARY
32-PLY QUASI-ISOTROPIC LAMINATE

Property	Number of Fatigue Cycles Completed					
	0 Baseline	1,000	5,000	10,000	20,000	28,000
Average Strength ksi	40.4	42.9	44.0	44.4	43.8	45.0
Standard Dev.	1.6	1.1	2.5	2.1	1.0	1.8
Coeff. of Variation %	4.0	2.5	5.6	4.7	2.3	4.0
Average Failure Strain, in./in.	0.0082	0.0097	0.0094	0.0091	0.0091	0.0096
Standard Dev.	0.0003	0.0004	0.0006	0.0004	0.0002	0.0004
Coeff. of Variation %	4.2	4.3	5.9	4.6	2.3	4.2
Average Secant Modulus at Failure psi x 10 ⁶	4.93	4.43	4.70	4.87	4.81	4.68
Standard Dev.	0.10	0.12	0.17	0.10	0.10	0.14
Coeff. of Variation %	2.1	2.6	3.6	2.0	2.1	3.0
Average Initial Tangent Modulus psi x 10 ⁶	5.10	4.87	5.14	5.12	5.10	5.03
Standard Dev.	0.10	0.11	0.29	0.13	0.13	0.24
Coeff. of Variation %	2.0	2.2	5.6	2.5	2.6	4.8
No. of Spec. in Data Set	15	10	10	10	10	10

TABLE XXXIII
COMPRESSION RESIDUAL STRENGTH DATA SUMMARY
32-PLY QUASI-ISOTROPIC LAMINATE

Property	Number of Fatigue Cycles Completed					
	⁰ Baseline	1,000	5,000	10,000	20,000	28,000
Average Strength	34.2	32.8	33.2	32.1	31.2	32.0
Standard Dev.	1.5	2.0	2.4	2.6	2.7	2.3
Coeff. of Variation %	4.5	5.9	7.3	8.1	8.7	7.1
Average Failure Strain, in./in.	0.0072	0.0077	0.0075	0.0073	0.0067	0.0075
Standard Dev.	0.0004	0.0009	0.0006	0.0007	0.0004	0.0009
Coeff. of Variation %	5.3	12.2	8.4	9.2	6.2	12.5
Average Secant Modulus at Failure psi x 10 ⁶	4.76	4.27	4.45	4.43	4.61	4.39
Standard Dev.	0.07	0.28	0.11	0.11	0.17	0.19
Coeff. of Variation %	1.5	6.6	2.4	2.4	3.6	4.2
Average Secant Modulus at 20 ksi psi x 10 ⁶	5.05	4.80	4.80	4.78	4.94	4.77
Standard Dev.	0.07	0.12	0.12	0.12	0.12	0.11
Coeff. of Variation %	1.4	2.5	2.5	2.5	2.5	2.3
No. of Spec. in Data Set	15	9	10	9	10	10

TABLE XXXIV
SUMMARY OF DAMAGE MEASUREMENTS FOR 32-PLY LAMINATE SPECIMENS

Damage Dimension	Number of Fatigue Cycles Completed				
	1,000	5,000	10,000	20,000	28,000
Average Damage Area, A, in ²	0.66	0.81	0.91	1.04	1.44
Standard Deviation	0.12	0.16	0.37	0.22	0.53
Coeff. of Variation %	17.60	19.60	40.90	20.70	36.70
Average Maximum Damage Width, X, in.	1.02	1.43	1.50	1.75	2.22
Standard Deviation	0.17	0.33	0.42	0.45	0.53
Coeff. of Variation %	16.90	22.90	27.80	25.90	23.90
Average Maximum Damage Length, Y, in.	0.83	0.85	0.86	0.93	1.07
Standard Deviation	0.05	0.05	0.06	0.06	0.35
Coeff. of Variation %	5.90	5.70	7.50	6.10	33.50
No. of Specimens in Data Set	23	23	23	22	23

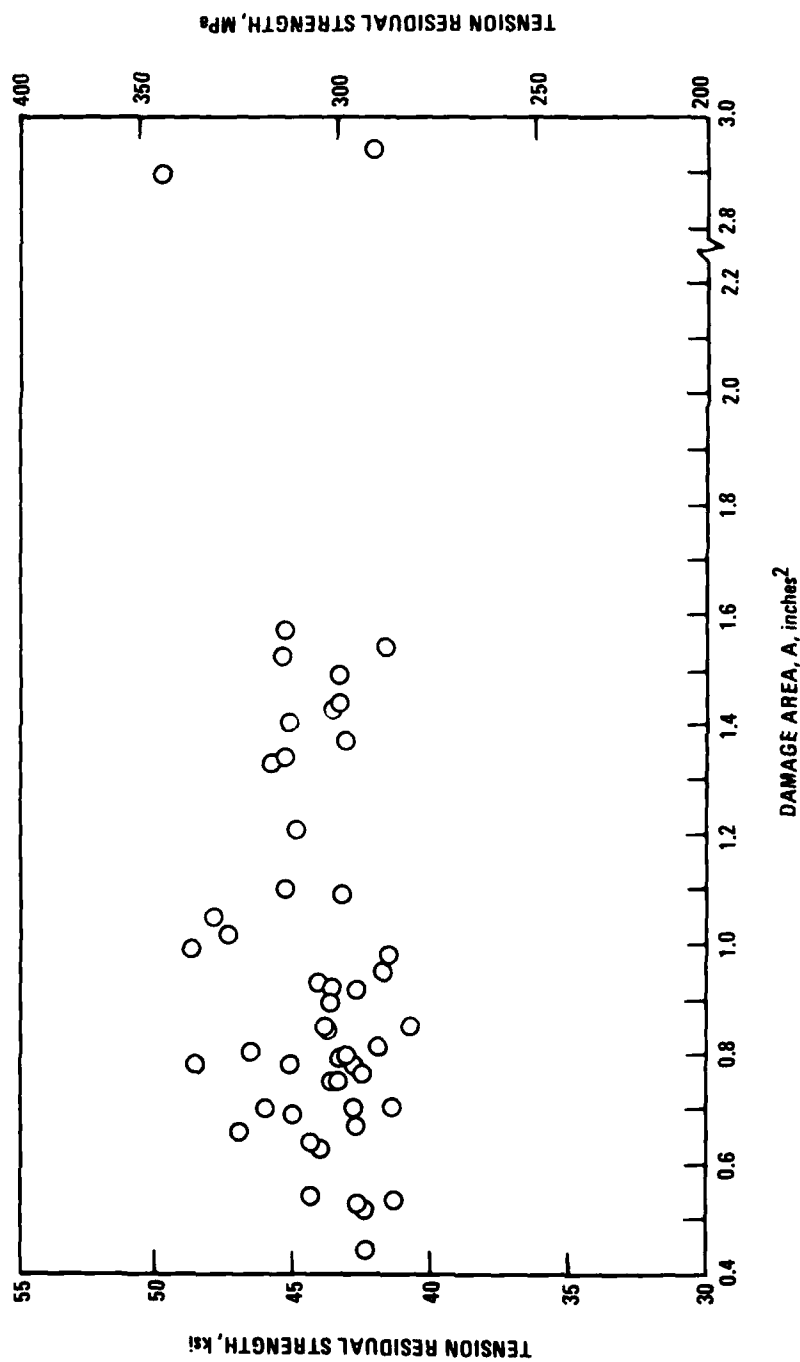


Figure 85: Relationship of Tension Residual Strength to Damage Area as Detected by the Holscan Ultrasonic C-scan for 32-ply Laminate Specimens.

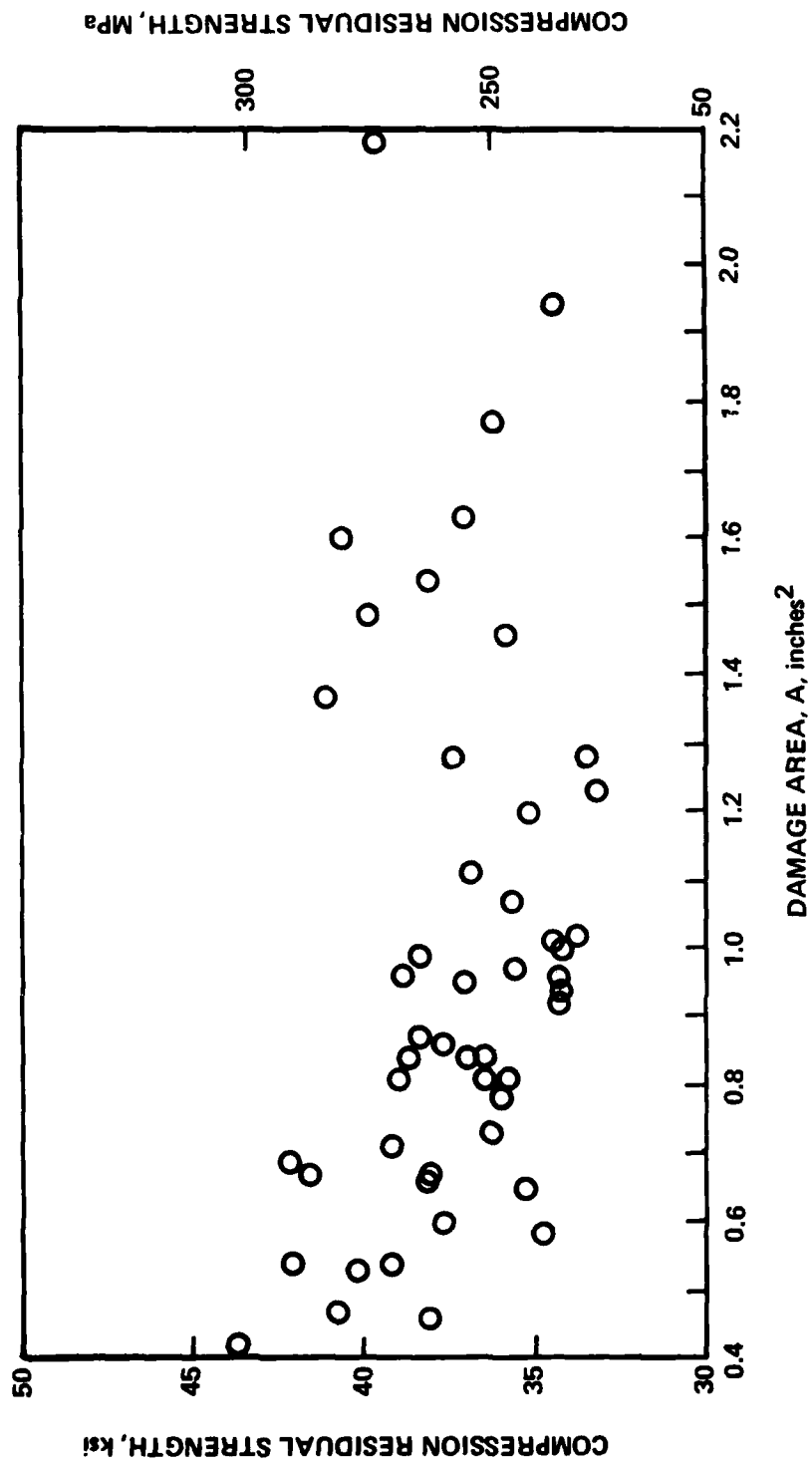
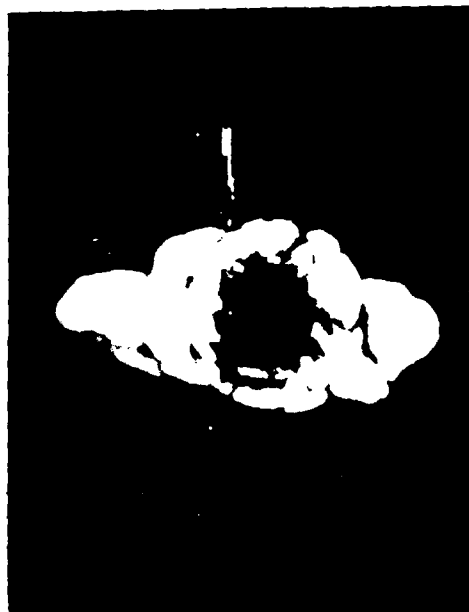


Figure 86: Relationship of Compression Residual Strength to Damage Area as detected by the Holscan Ultrasonic C-scan for 32-ply Laminate Specimens.

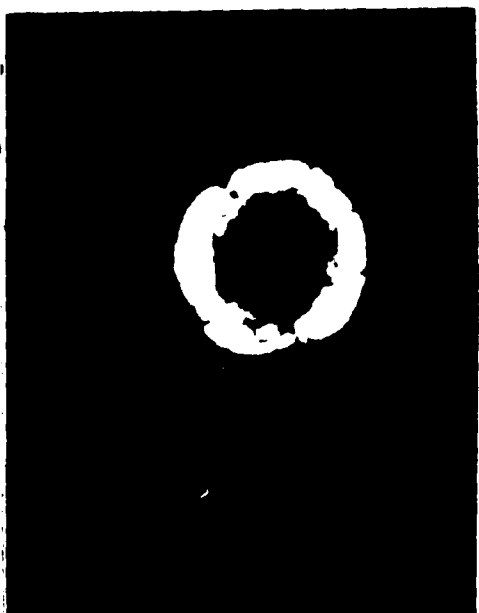
NOTE: Areas of Displayed Specimens are approximately equal to the average for each N_x value.



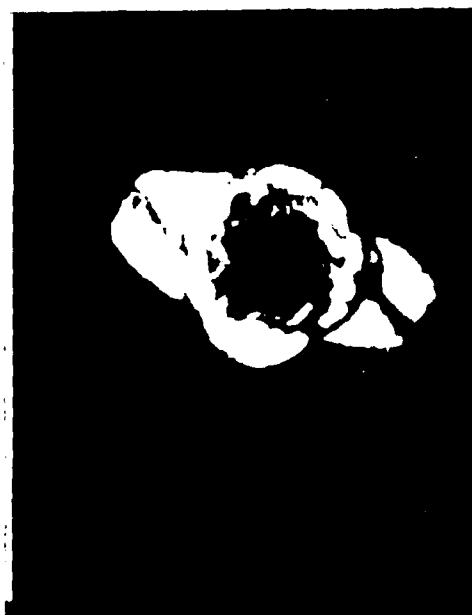
PA-9, $N = 1,000$



RB -17, $N = 10,000$



KB-14, $N = 0$



QC-28, $N = 5,000$

Figure 87a: Typical Damage Characteristics of 32-Ply Specimens Fatigue Cycled at ± 22 ksi (± 152 MPa) for Residual Strength Determination

NOTE: Areas of Displayed Specimens are approximately equal to the average for each N_x value.

→ 0°



MB-13, N = 20,000



RA-5, N = 28,000

Figure 87b: Typical Damage Characteristics of 32-Ply Specimens Fatigue Cycled at ± 22 ksi (± 152 MPa) for Residual Strength Determination

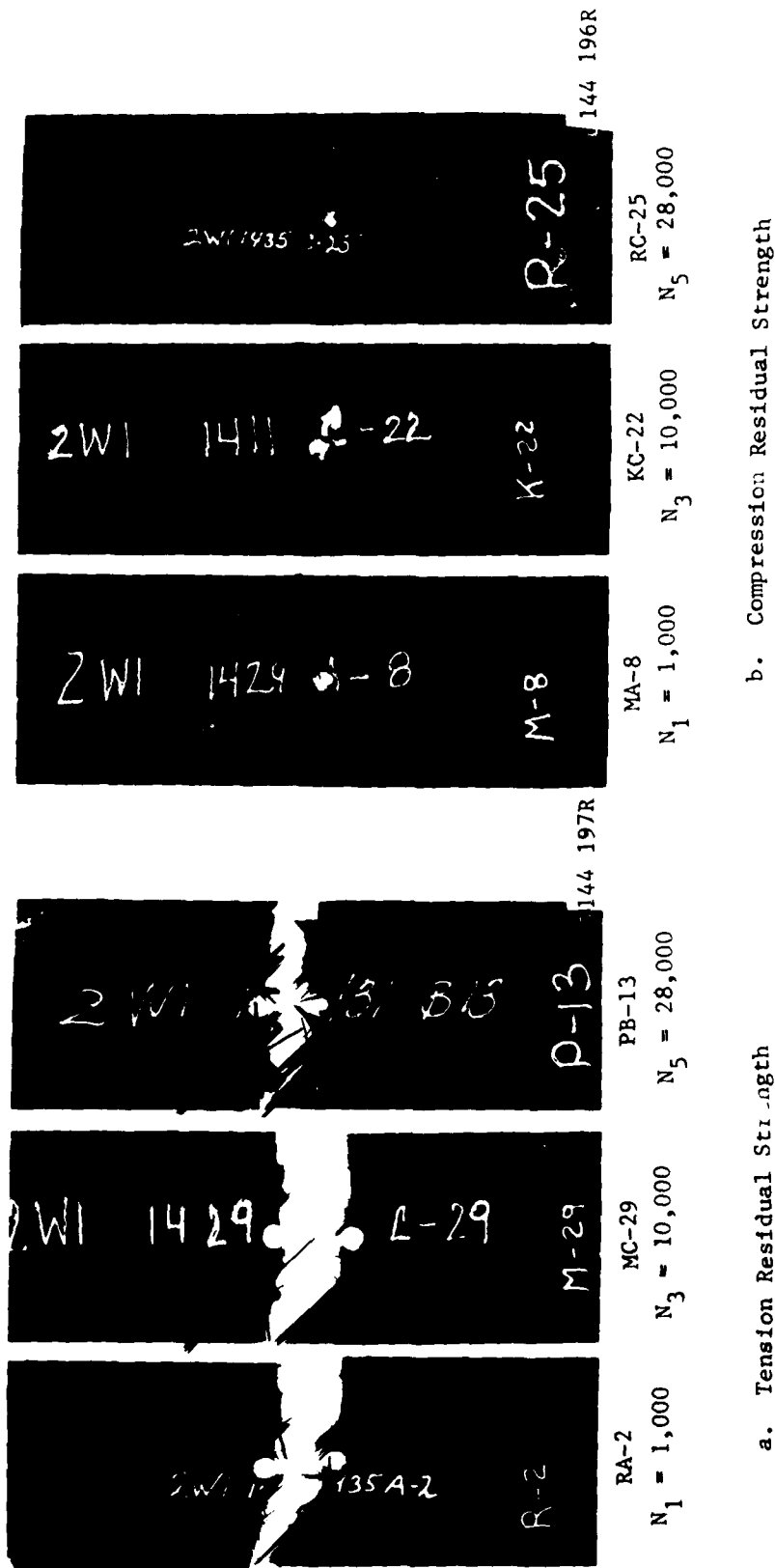


Figure 88: Typical Fracture Appearances of 32-ply Specimens Tested For Residual Strength After Fatigue Cycling

SECTION 7

TASK III FATIGUE RESULTS

Task III was intended to be a limited test program designed to assess the effect of different fatigue and environmental test conditions on the residual strength and damage growth process. As a considerably scaled down version of Task II it was to provide data which might establish the range of validity of the analytical methodology expected to emerge from Task II. The sample size was limited by the available funding and an interest in examining at least three variables.

Based upon the constraints of the above objectives and limitations, the variables selected for further examination were specimen restraint, stress level and temperature. The test conditions are summarized in Table XXXV. Some of the considerations leading to this selection are presented below.

7.1 FATIGUE TEST PARAMETER SELECTION

7.1.1 Case A

The effect of the method of restraining out-of-plane buckling of a specimen is of major concern in evaluating fatigue data for highly compression dominated cyclic loading. Since a primary damage propagation mode is that of delamination growth, the extent that the method of specimen buckling support limits or restrains local out-of-plane ply buckling would be expected to significantly affect resulting damage growth. Consequently, the extent of this variant component of the behavior must be defined to allow determination of the material invariant behavior.

TABLE XXXV
SUMMARY OF TEST CONDITIONS FOR VARIATIONS IN
FATIGUE LOADING/ENVIRONMENT

CASE A

- Task II stress ratio, $R = -1$
- Task II stress level, σ_{\max} , 24-ply: 35 ksi (241 MPa), 32-ply: 22 ksi (152 MPa)
- Task II environment, RT lab air
- New constraint condition, #2, 4 bar support (Figure 4.3)

CASE B

- New stress ratio, $R = -0.3$
- New stress level σ_{\max} , 24-ply: 54 ksi (372 MPa), 32-ply: 34 ksi (234 MPa)
- Task II environment, RT lab air
- Task II constraint condition, #1, platen supports with window (Figure 4.2)

CASE C

- Task II stress ratio, $R = -1$
- Task II stress level, σ_{\max}
- New environment, 180°F (82°C) dry
- Task II constraint condition, #2

The alternate support system selected for this study was a 4-bar (5-bay) column buckling fixture of the type shown schematically in Figure 21 in Section 4. The 5-bay column buckling support spacing was 1.8 inch (46mm) between center lines, which was similar to the 2.15 inch (55mm) vertical window of the Task II fatigue support while still providing an odd number of bays, i.e., no support over the specimen center (damage area). However, the actual spacing between the 3/8 inch (9.5 mm) bars was 1.43 inches (36 mm). This configuration of horizontal support only, freed the vertical edges thereby permitting unimpeded growth in the horizontal direction. As shown in Figure 89, the 4 bar (5-bay) support is stable to stresses of approximately 30 ksi for the 32-ply damaged hole specimens and 40 ksi for the 24-ply damaged hole specimens.

For this series of tests, the stress ratio ($R = -1$), stress levels and environment were retained from Task II.

7.1.2 Case B

Of the major loading variables the compressive stress component has been recognized as having a significant effect on both notched and unnotched fatigue behavior. Thus, the primary variable preferred for isolation in this case was the influence of the compressive load portion of the cycle. Tests were conducted at a stress ratio of $R = -0.3$ employing the same environment, stress range ($\sigma_{\max} - \sigma_{\min}$) and fatigue supports used in Task II. A stress ratio of -0.3 was selected since it represented a value: 1) typical of an important type of application, a lower wing skin; 2) that decreased the severe compression part of the cycle; yet 3) maintained some compression loading in the cycle since under tension-tension fatigue loading notched specimens can exhibit very flat S-N curves and only minor changes in residual strength. Stress levels associated with this stress ratio, $R = -0.3$, were selected to provide fatigue lives in the range of 10^5 - 10^6 cycles. Results of other programs ⁽⁹⁾ have indicated that in the

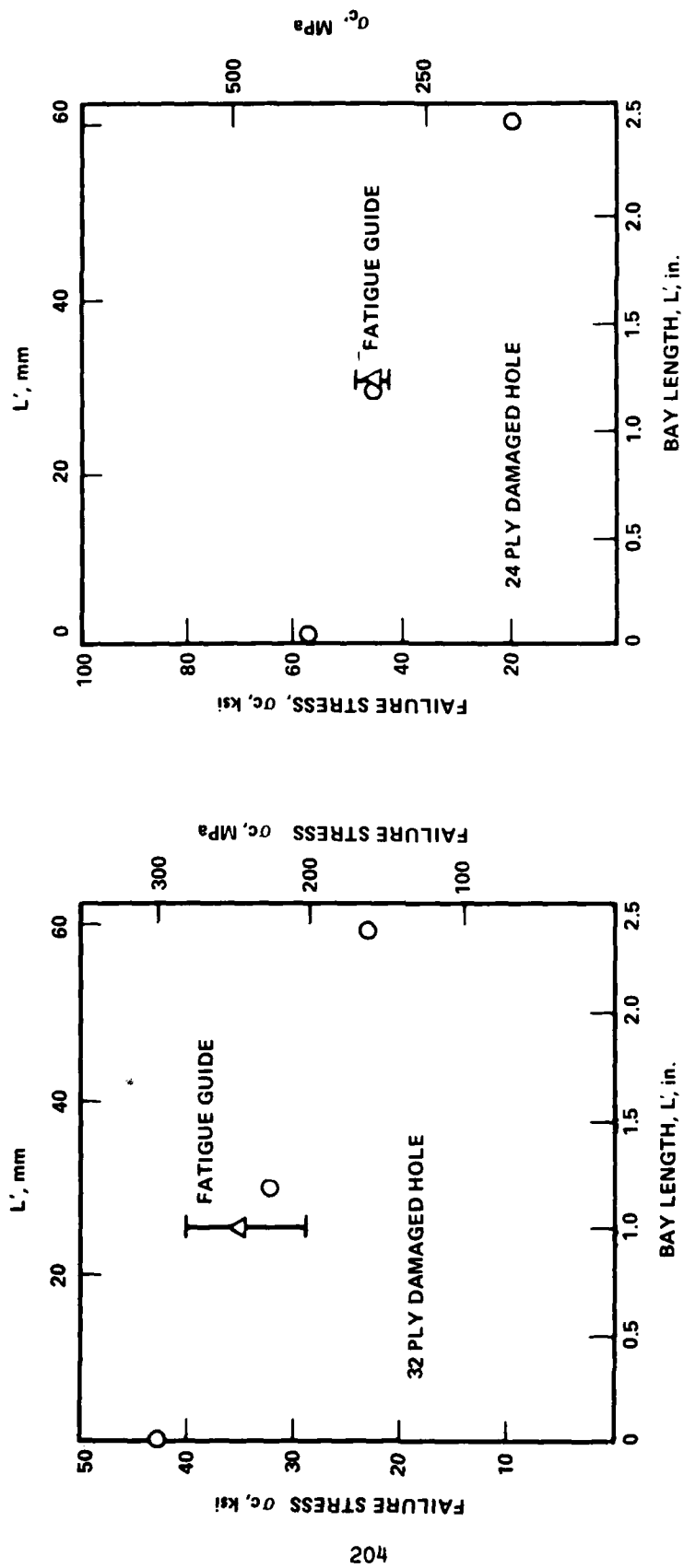


Figure 89: Column Buckling Results from Task 1 (1)

longer fatigue life region the life is dominated by stress range ($\sigma_{\max} - \sigma_{\min}$) rather than by maximum stress. As a result maximum stress levels were chosen to provide the same stress range used for the Task II tests. Maximum and minimum stresses for the 24-ply and 32-ply specimens were, respectively: $\sigma_{\max} = 54.0$ ksi (372 MPa), $\sigma_{\min} = -16.2$ ksi (-112 MPa); $\sigma_{\max} = 34.0$ ksi (234 MPa) $\sigma_{\min} = -10.2$ ksi (-70 MPa).

7.1.3 Case C

The role of environment, both external chemical and thermal operating environment and "internal" specimen moisture level, is a complex problem that has been under extensive study during the last 5 years. Recent test results have indicated that internal moisture level can have a significant effect on fatigue life of unnotched specimens tested at elevated temperature. The effect of these variables was in the range of an order of magnitude decrease in life. A problem encountered in evaluating the effect of moisture and temperature is that under normal elevated temperature conditions the moisture in the specimen will evaporate with testing time, making the assessment of the effect of moisture very difficult. Because this was a limited effort, intended primarily to ascertain the applicability of an analytical model, a simple change introducing only one additional variable was desirable which resulted in the selection of a 180°F (82°C) dry laboratory air condition, along with the stress ratio and stress levels used in Task II.

7.2 FATIGUE AND DAMAGE GROWTH BEHAVIOR

Three replicates per each laminate for each of the fatigue cases (A, B, or C) were tested to discern the basic fatigue life and damage growth characteristics as determined at selected intervals during the life with the Holscan unit. Fatigue life data for these conditions are presented in Figure 90 and area damage growth results appear in Figures 91-96.

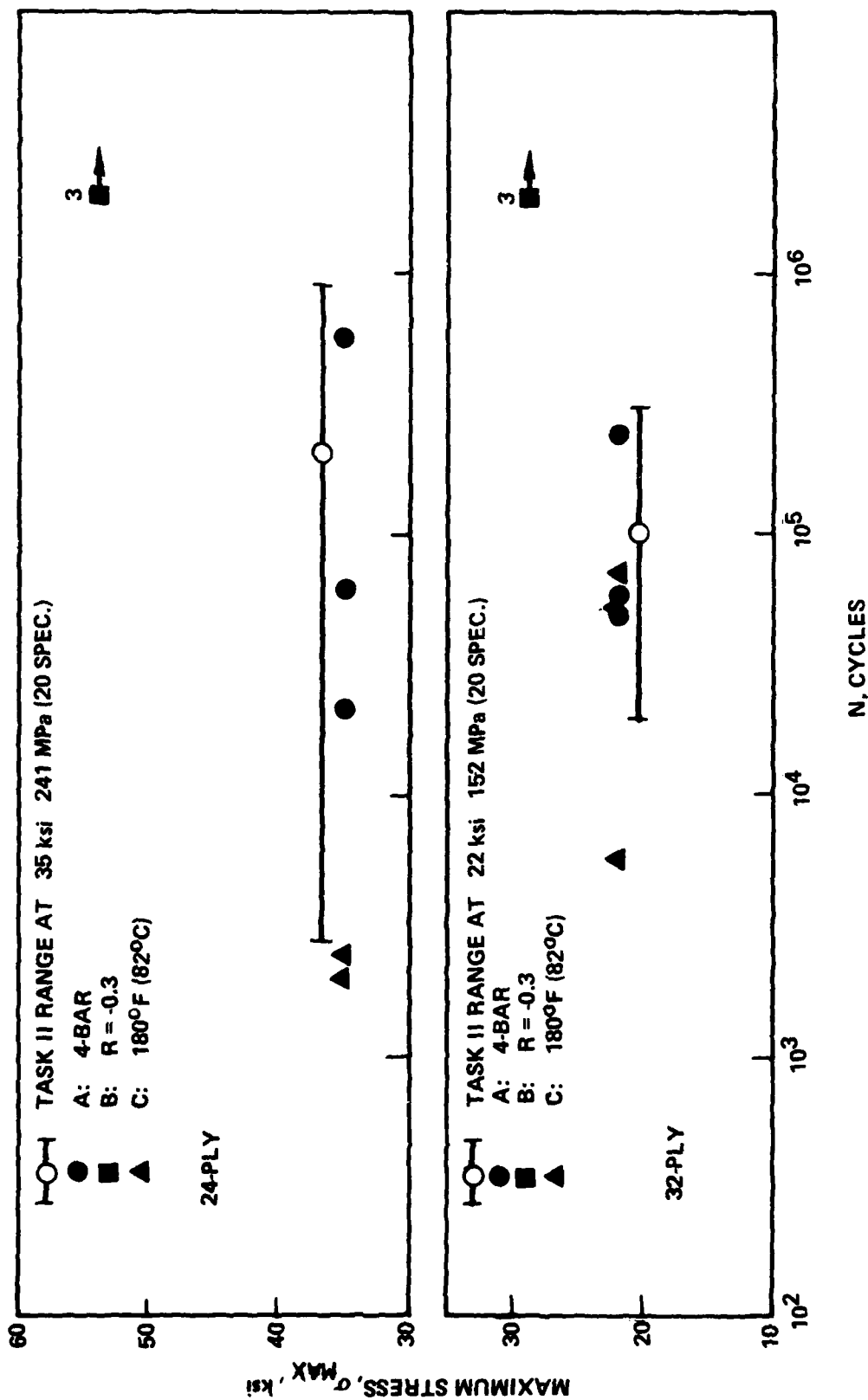


Figure 90: Fatigue Life Data for 24 and 32-Ply Laminates for Variations in Constraint Condition, Stress Ratio and Temperature Summarized in Table XXV.

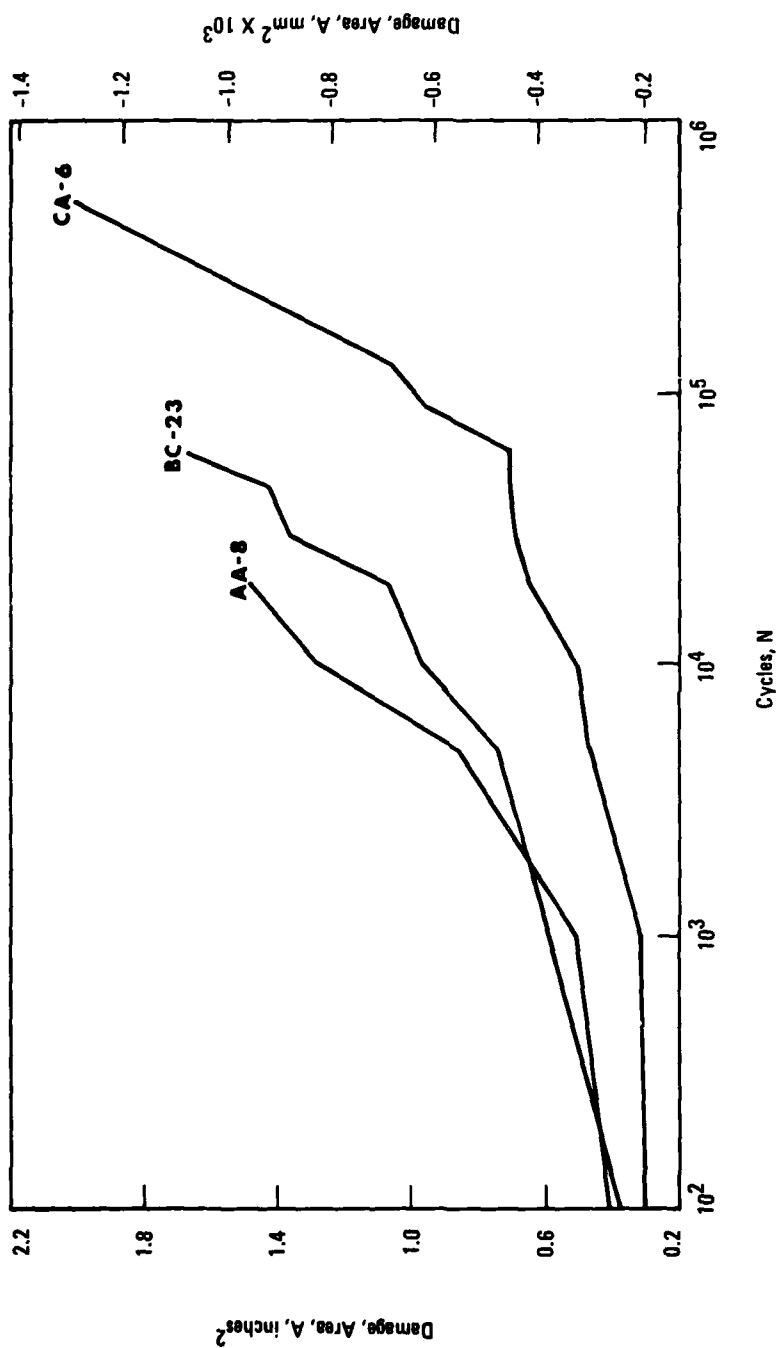


Figure 91: Area Damage Growth Behavior for 24-Ply Specimens, Case A (4-Bar).

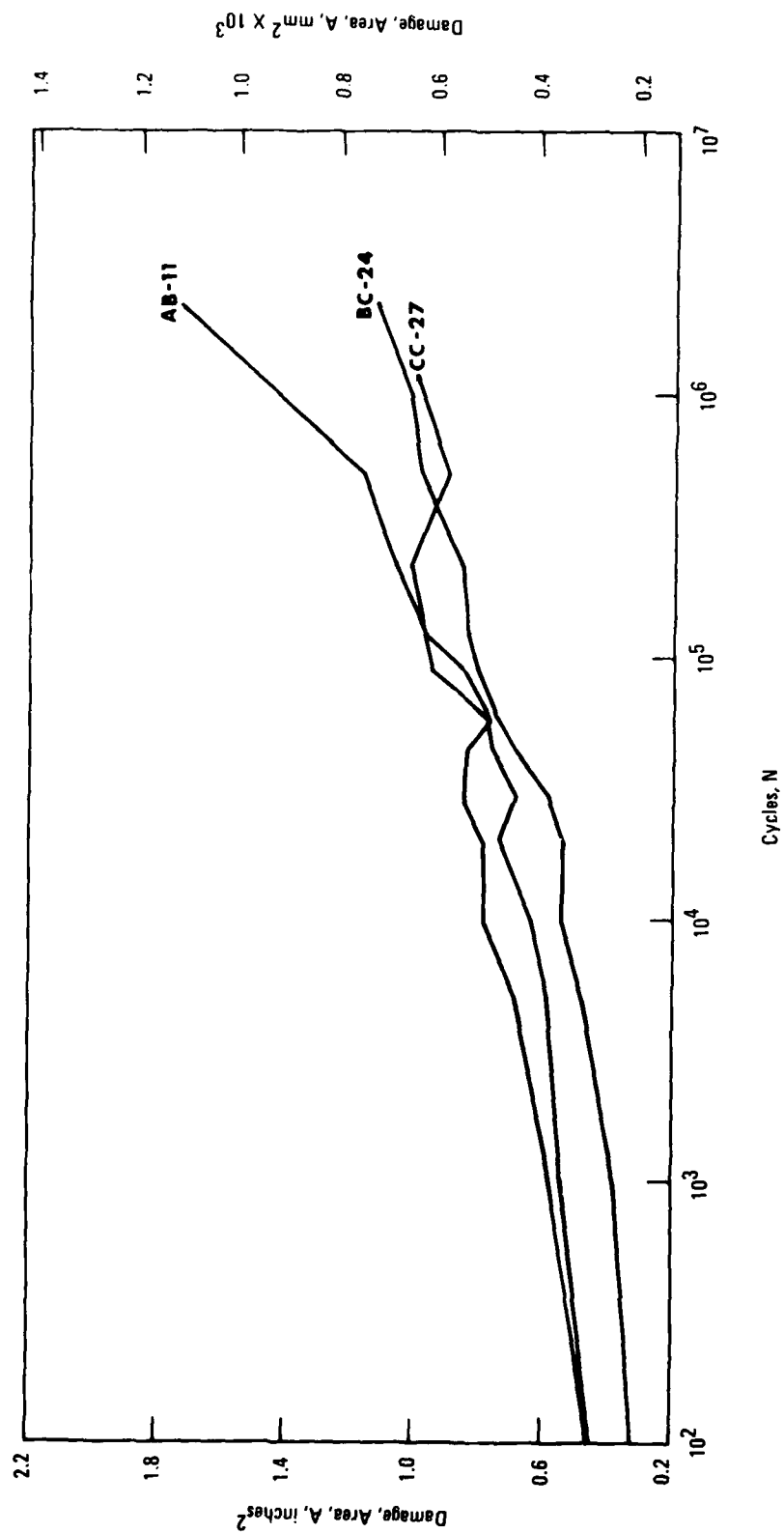
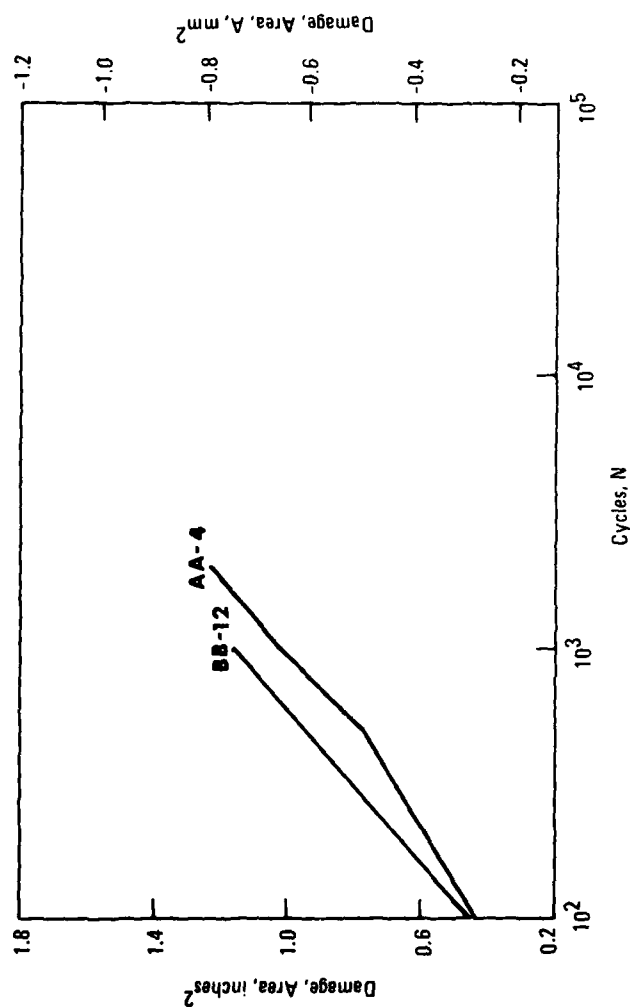


Figure 92: Area Damage Growth Behavior for 24-ply Specimens, Case B ($R = -0.3$).



Note: Specimen CA-4 failed at 100 cycles before first measurement

Figure 93: Area Damage Growth Behavior for 24-ply Specimens, Case C (180°F)

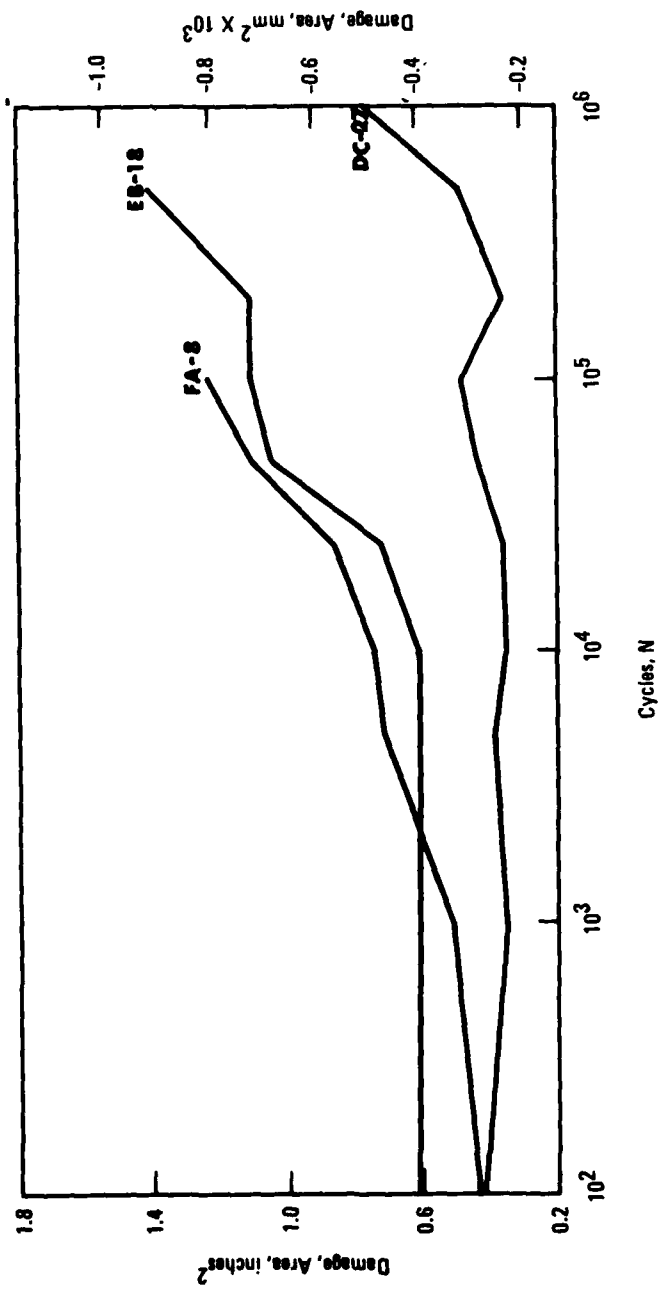


Figure 94: Area Damage Growth Behavior for 32-Ply Specimens, Case A (4-Bar).

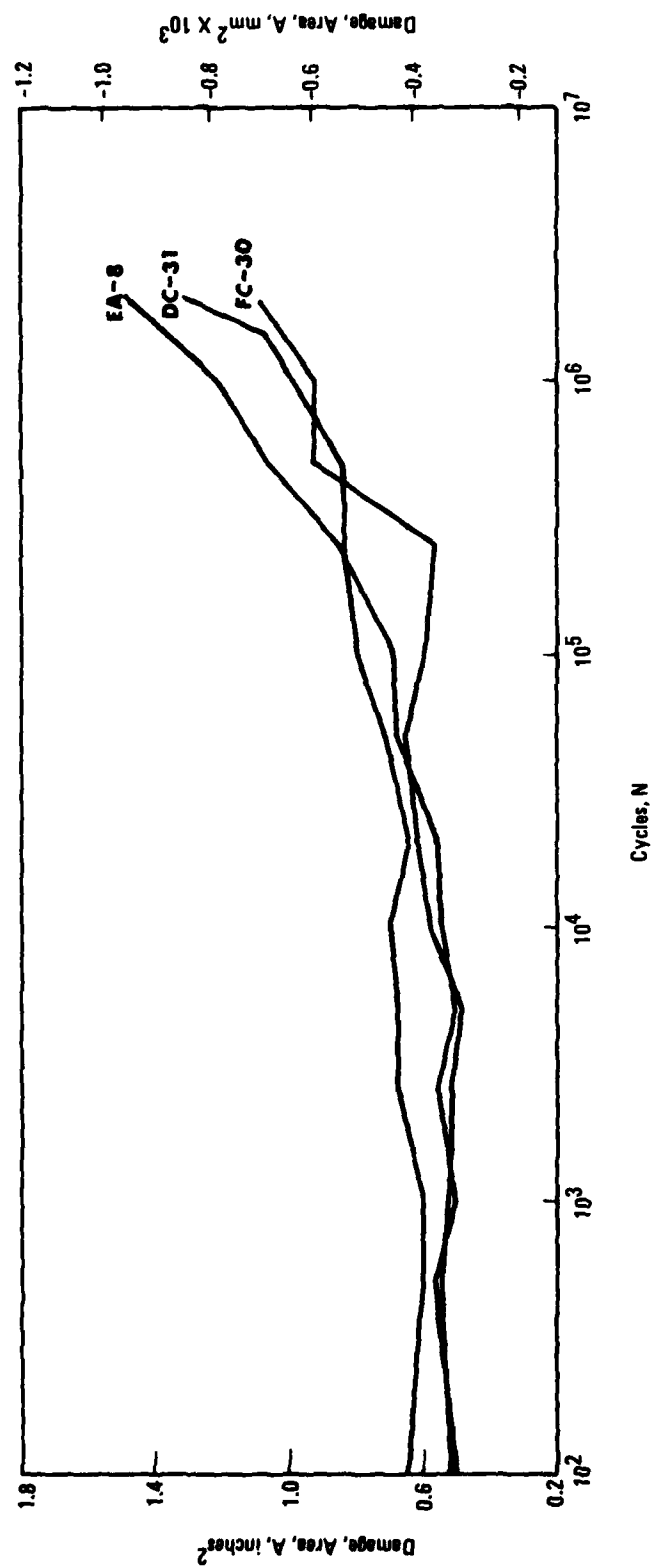


Figure 95: Area Damage Growth Behavior for 32-Ply Specimens, Case B ($R = -0.3$).

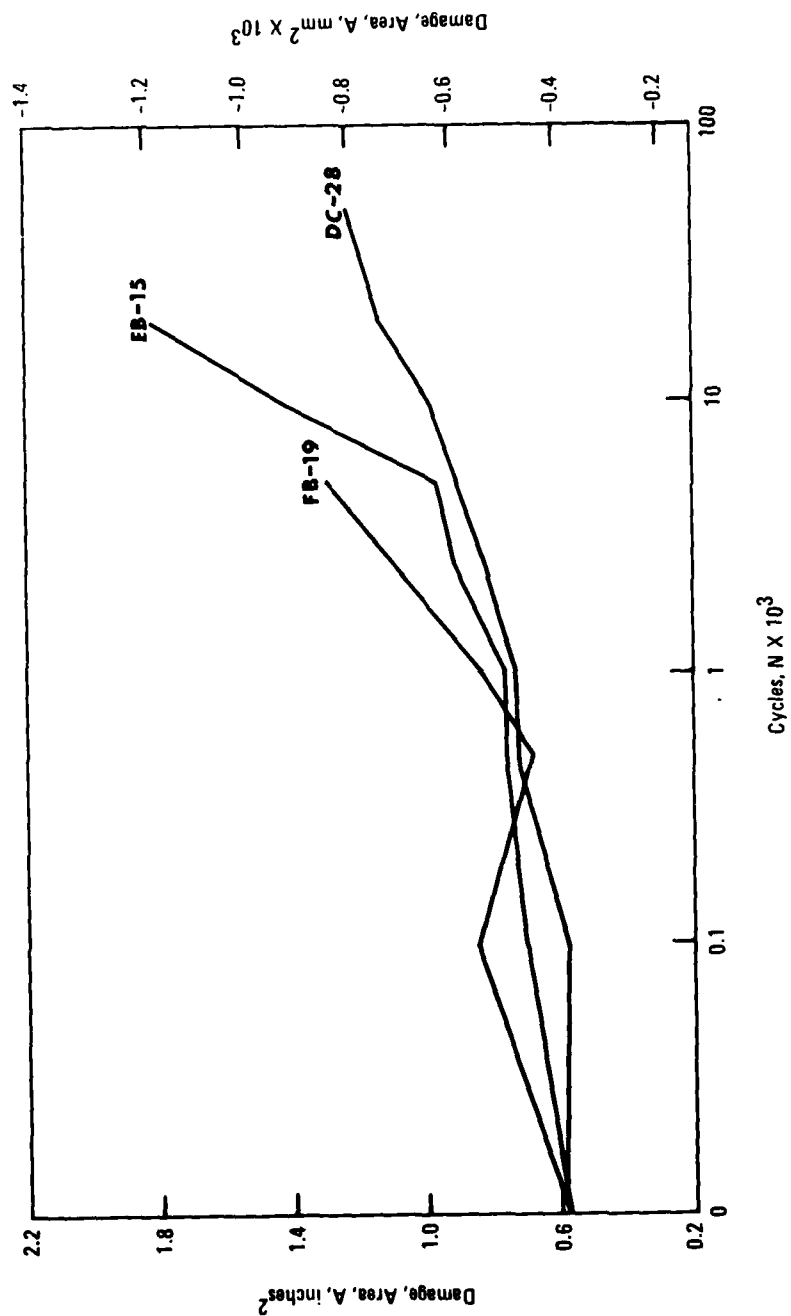
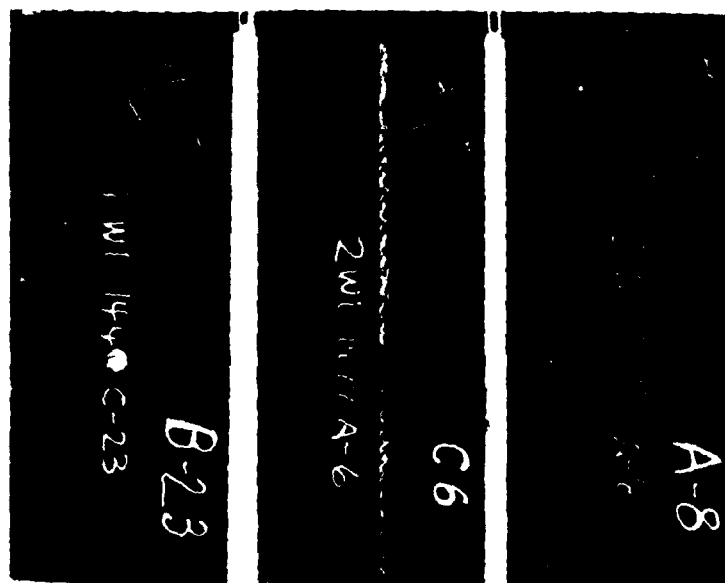


Figure 96: Area Damage Growth Behavior for 32-Ply Specimens, Case C (180°F).

The 4-bar constraint condition #2 employed in Case A which yielded the same average static compression strength as for constraint #1 for both laminates also produced fatigue lives within the scatter band of the Task II tests conducted with constraint #1, the platen fatigue supports with 2.15 inch window. Photographs of failed specimens appear in Figures 97 and 98. Specimens failed in a buckling mode across the width accompanied by significant delamination. The major difference between these and those tested with constraint #1 is in the delaminated buckling failure of the unrestrained edges.

Under the $R = -0.3$ Case B loading, all specimens of both laminates completed 2 million cycles without failure. Most notable was the change in damage development, especially for the 24-ply laminate for which no growth in the width direction was evident with extensive growth in the length direction. Damage growth for the 32-ply laminate for $R = -0.3$ was also primarily in the length direction with very slight growth in the width direction. This change in direction from that for the $R = -1$ case is due to the alteration of the stress state in the vicinity of the notch. The high axial compressive stress for $R = -1$ produced localized buckling of the unsupported region surrounding the hole which did not occur for the $R = -0.3$ condition and therefore, resulted in a change in the major growth direction.

Although the sample size was small for Case C conditions there appeared to be an order of magnitude decrease in life due to the 180°F (82°C) temperature exposure during cycling with more rapid initial damage growth for the 24-ply laminate. The elevated temperature also appeared to have shortened the life of the 32-ply laminate although not as severely as for the 24-ply case. The effect of the elevated temperature on specimen fracture appearances is evident in Figures 99 and 100 in the pronounced buckling of the delaminated plies. The restrained edges, once again exhibited the compression/crushing failure mode.



BC-23
 $N_f = 62,710$

CA-6
 $N_f = 569,499$

AA-8
 $N_f = 21,142$



BC-23

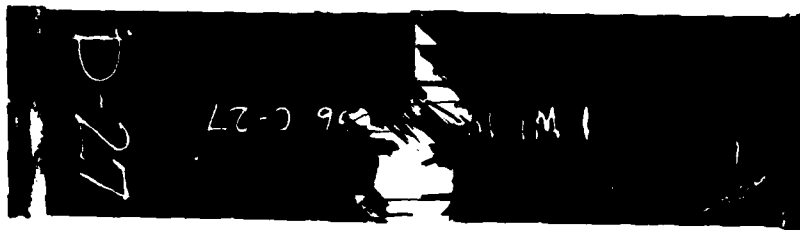
CA-6

AA-8

Figure 97: Fracture Appearances of 24-Ply Specimens Tested in Fatigue with Constraint #2, Case A



EB-18
 $N_f = 58,005$



DC-27
 $N_f = 238,138$

145082R



EB-18

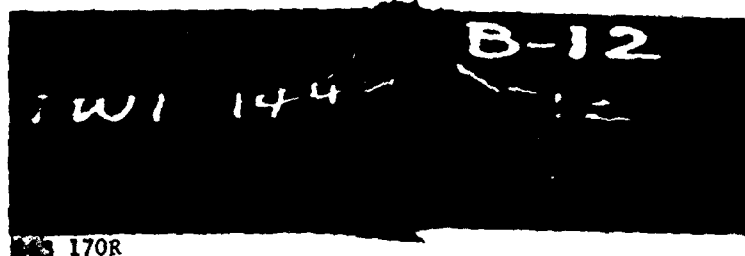
DC-27

145083R

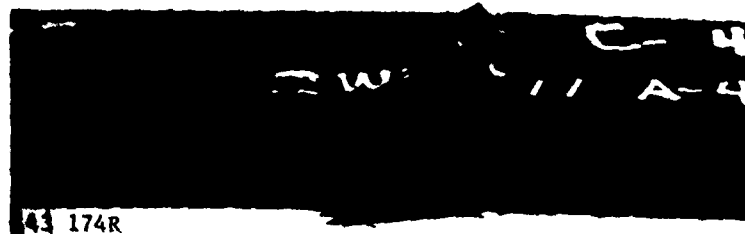
Figure 98: Fracture Appearances of 32-Ply Specimens Tested in Fatigue with Constraint #2, Case A



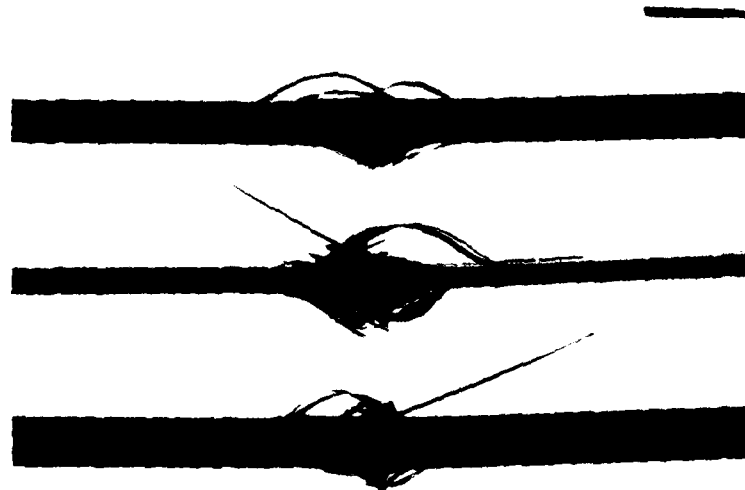
AA-4
 $N_f = 2,060$



BB-12
 $N_f = 2,460$



CA-4
 $N_f = 100$



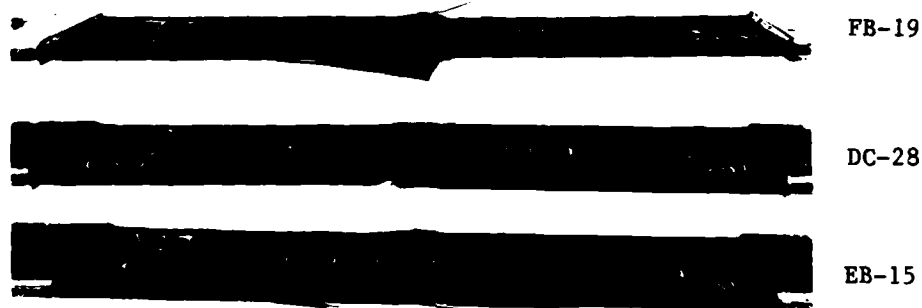
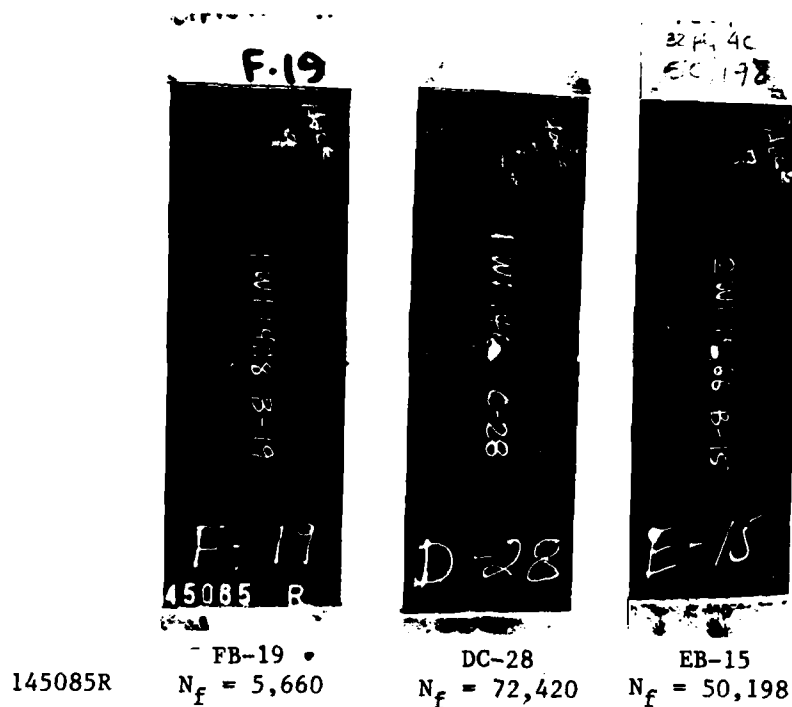
AA-4

BB-12

CA-4

143 172R

Figure 99: Fracture Appearances of 24-Ply Specimens Tested in Fatigue at 180° F (82° C), Case C



145084R

Figure 100: Fracture Appearances of 32-Ply Specimens Tested in Fatigue at 180°F (82°C), Case C

Typical examples of damage growth characteristics for cases A, B, and C, respectively are presented in Figures 101 - 106.

7.3 RESIDUAL STRENGTH RESULTS

Based upon the above limited fatigue life distribution data, three cyclic N values were selected and six replicates per laminate per condition (A, B, or C) were then fatigue cycled to this N level after which three were tested in static tension and three in compression. Residual strength results are presented in Table XXXVI and summarized in Table XXXVII. Typical examples of damage sizes are given in Appendix E.

For Case A, both the tension and compression residual strengths increased slightly over the baseline values for the 24-ply laminate but remained essentially unchanged for the 32-ply laminate. The longitudinal damage growth in the 24-ply laminate induced by the Case B, $R = -0.3$ loading reduced the notch acuity significantly resulting in considerable increase in tensile residual strength with increasing numbers of cycles completed and little change in compression residual strength. Similarly, the reduced notch acuity in the 32-ply laminate resulting from the Case B loading produced a comparable increase in tension residual strength with perhaps a very slight reduction in compression strength. Despite the severity of its effect under fatigue loading, residual strength values of specimens which survived the 180°F (82°C) cycling were not adversely affected.

Representative failed specimens are displayed in Figures 107 - 110. Note the more extensive delamination exhibited by specimens previously fatigue cycled at $R = -0.3$.

TABLE XXXVI
RESIDUAL STRENGTH RESULTS

Test Variable	24-PLY LAMINATE			32-PLY LAMINATE		
	No. of Cycles Completed	Tension Strength ksi	Compression Strength ksi	No. of Cycles Completed	Tension Strength ksi	Compression Strength ksi
A.						
4-Bar Buckling Support	4,000	81.2	45.2	1,000	39.5	35.0
		82.3	50.1		40.6	35.0
		78.0	51.7		40.2	33.7
	8,000	77.8	52.5	10,000	42.5	31.7
		75.4	51.4		43.9	33.6
		81.5	54.1		40.6	38.4
	12,000	77.2	52.5	20,000	43.5	33.7
		79.5	44.8		46.3	35.6
		80.5	63.9		44.9	32.3
	B.					
	4,000	77.1	44.3	20,000	50.8	32.2
		86.6	52.7		50.2	38.7
82.1		54.7	47.6		32.9	
40,000	96.0	50.3	250,000	57.3	30.9	
	96.2	47.4		54.7	29.8	
	92.5	43.8		51.0	29.1	
250,000	102.1	46.7	10 ⁶	51.5	27.1	
	95.8	54.1		56.8	31.0	
	101.7	49.9		51.7	28.8	
R=-0.3	2 x 10 ⁶ (item 4B)	107.3 ^a	--	2 x 10 ⁶ (item 4B)	55.8 ^a	--
		113.3 ^a	--		58.9 ^a	--
		--	--		57.5 ^a	--

a = Run outs from item 4B

TABLE XXXVI (Cont.)
RESIDUAL STRENGTH RESULTS

Test Variable	24-PLY LAMINATE			32-PLY LAMINATE		
	No. of Cycles Completed	Tension Strength ksi	Compression Strength ksi	No. of Cycles Completed	Tension Strength ksi	Compression Strength ksi
C. 180°F	50	80.2	45.0	1,000	39.5	33.4
		73.9	50.1		42.7	39.4
		75.2	47.3		41.5	34.0
	300	70.5	43.0	4,000	43.9	32.8
		76.0	47.2		44.6	32.9
		74.4	47.1		43.5	32.2
	1,000	78.0	53.6	8,000	44.1	33.4
		76.5	49.1		40.6	32.4
		75.9	46.7		44.0	31.9

TABLE XXXVII
RESIDUAL STRENGTH DATA SUMMARY

24-Ply

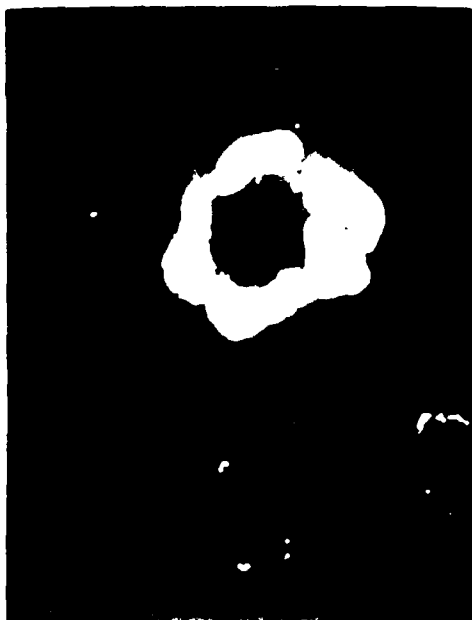
TEST VARIABLE	NO. OF CYCLES COMPLETED	AVERAGE TENSION STRENGTH (KSI)	AVERAGE COMPRESSION STRENGTH (KSI)
A. 4-BAR SUPPORT	4,000	80.5	49.0
	8,000	78.2	52.7
	12,000	79.1	53.7
B. R = -0.3	4,000	81.9	50.6
	40,000	94.9	47.2
	250,000	99.9	50.2
	2×10^6	110.3	--
C. 180°F	50	76.4	47.4
	300	73.6	45.8
	1,000	76.8	49.8
BASLINE	0	70.8	46.5

32-Ply

TEST VARIABLE	NO. OF CYCLES COMPLETED	AVERAGE TENSION STRENGTH (KSI)	AVERAGE COMPRESSION STRENGTH (KSI)
A. 4-BAR SUPPORT	1,000	40.1	34.6
	10,000	42.3	34.6
	20,000	44.9	33.9
B. R = -0.3	20,000	49.5	34.6
	250,000	54.3	29.9
	10^6	53.3	29.0
	2×10^6	57.4	--
C. 180°F	1,000	41.2	35.6
	4,000	43.9	32.6
	8,000	42.9	32.6
BASLINE	0	40.0	35.7



N = 0



N = 1,000



N = 5,000



N = 10,000

Figure 101a: Damage Growth Characteristics of the 24-ply Laminate for
Fatigue Condition A, 4-Bar Support (Table XXV) Specimen
BC-23, ($N_f = 62,710$)

→ 0°



N = 20,000



N = 30,000



N = 45,000



N = 60,000

Figure 10lb: Damage Growth Characteristics of the 24-ply Laminate for
Fatigue Condition A, 4-Bar Support (Table XXIV) Specimen
No. 12, $N_f = 62,710$

↑



N = 0



N = 45,000



N = 90,000



N = 225,000

Figure 102a: Damage Growth Characteristics of the 24-ply Laminate for Fatigue Condition B, $R = -0.3$ (Table XXXV) (Specimen BC-24 completed 2×10^6 without failure)



$N = 1 \times 10^6$



$N = 2 \times 10^6$

Figure 102b: Damage Growth Characteristics of the 24-ply Laminate for Fatigue Condition B, $R = -0.3$ (Table XXXV) (Specimen BC-24 completed 2×10^6 without failure)

→ 0°



N = 0



N = 500



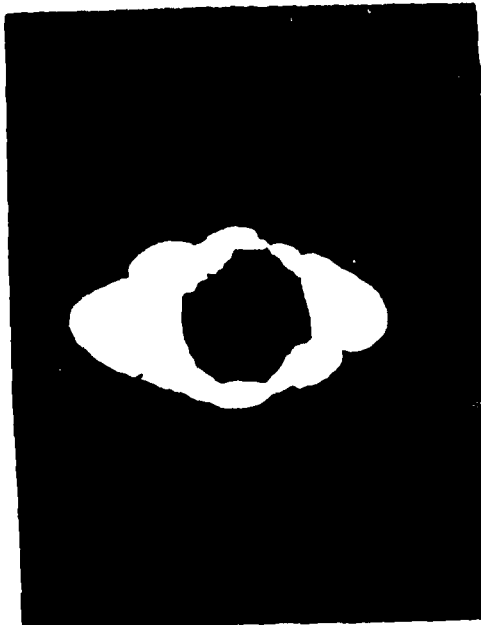
N = 1,000



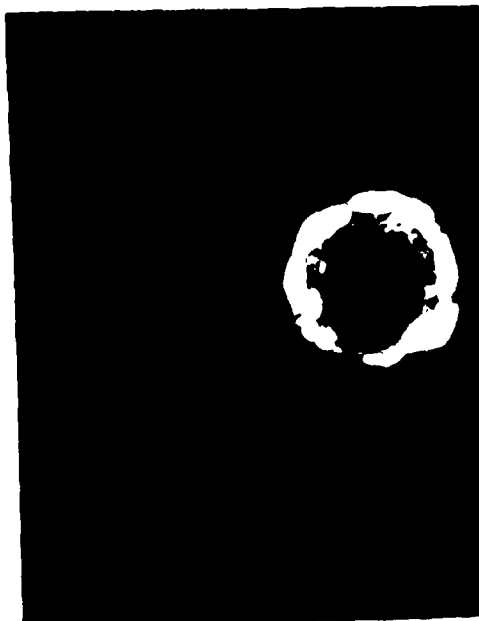
N = 2,000

Figure 103: Damage Growth Characteristics of the 24-ply Laminate for Fatigue Condition C, 180°F (82°C) (Table XXV) (Specimen AA-4, $N_f = 2060$)

→ 0°



N = 500



N = 0



N = 1,000

Figure 104a: Damage Growth Characteristics of the 32-1 V₂O₅ Cathode for
Fatigue Condition A, 4-Bar Support (Table IV, p. 150, line 10)
FA-8, $N_f = 48,789$)



$N = 5,000$



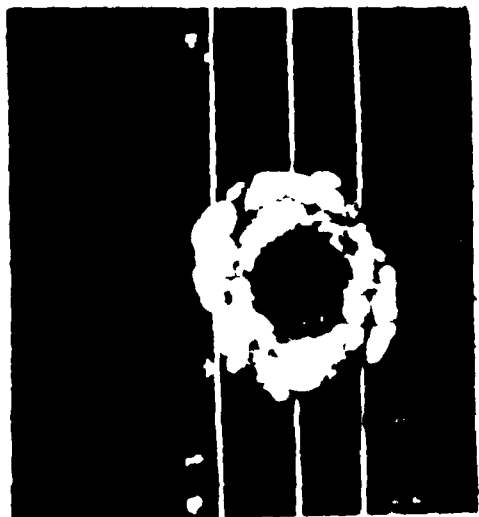
$N = 10,000$

Figure 104b: Damage Growth Characteristics of the 32-ply Laminate for Fatigue Condition A, 4-Bar Support (Table XXXV) (Specimen FA-8, $N_f = 48,789$)

→ 0°



N = 0



N = 100,000



N = 250,000



N = 500,000

Figure 105a: Damage Growth Characteristics of the 32-ply Laminate for Fatigue Condition B, $R = -0.3$ (Table XXV) (Specimen FC-30 completed 2×10^6 without failure)



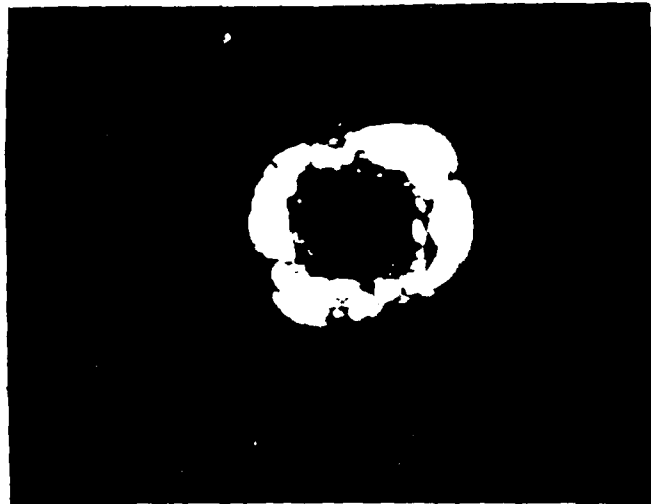
$N = 1,000,000$



$N = 2 \times 10^6$

Figure 105b: Damage Growth Characteristics of the 32-ply Laminate for Fatigue Condition B, $R = -0.3$ (Table XXXV) (Specimen FC-30 completed 2×10^6 without failure)

→ γ^0



N = 0



N = 5,000

Figure 106a: Damage Growth Characteristics of the 32-ply Laminate for Fatigue Condition C, 180°F (82°C) (Table XXXV) (Specimen EB-15, $N_f = 50,198$)

→ 0°

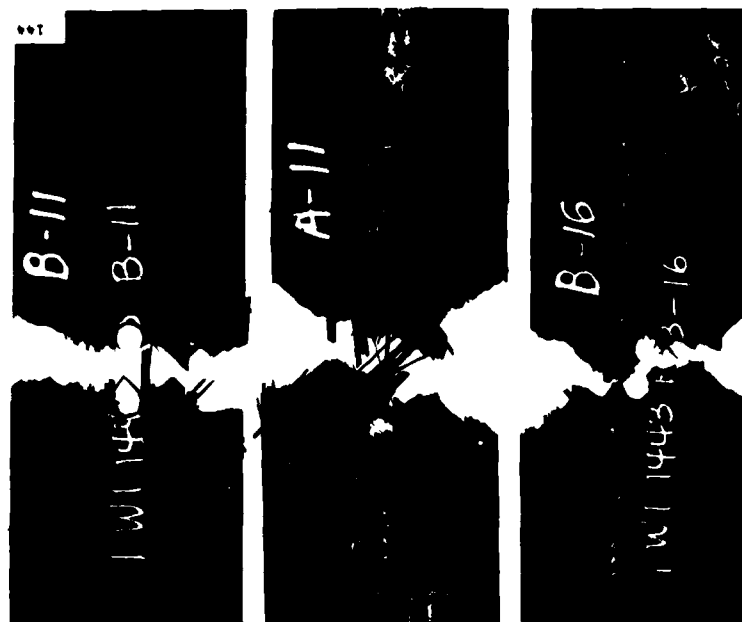


N = 10,000



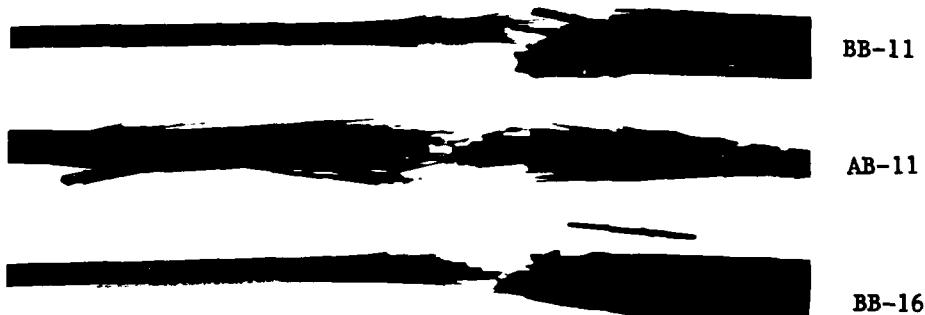
N = 20,000

Figure 106b: Damage Growth Characteristics of the 32-ply Laminate for Fatigue Condition C, 180°F (82°C) (Table XXXV)(Specimen EB-15, $N_f = 50,198$)



144 198

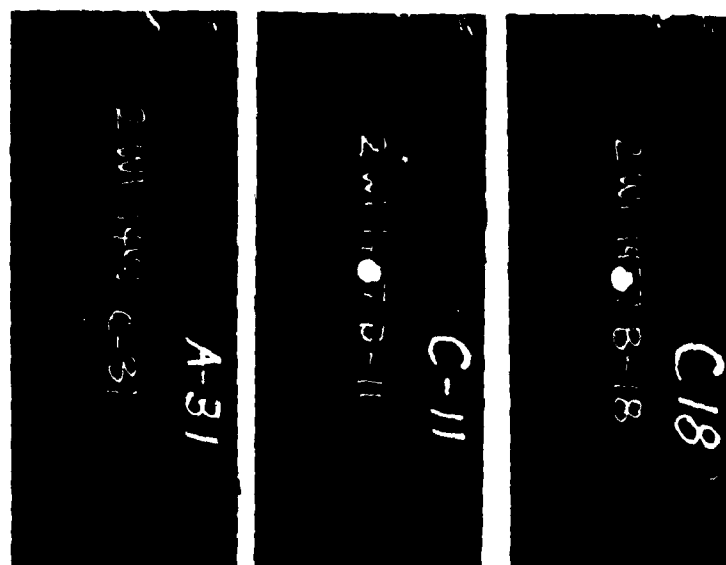
BB-11	AB-11	BB-16
Case A: 4 Bar	Case B: $R = -0.3$	Case C: 180°F (82°C)
$N = 12,000$	$N = 2 \times 10^6$	$N = 1,000$



144 201

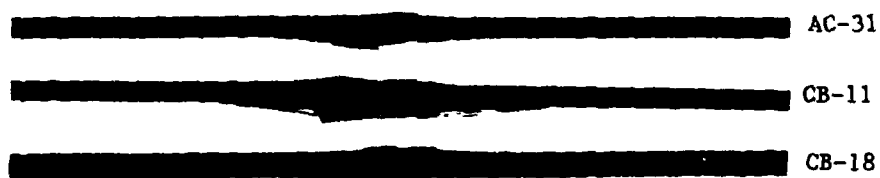
144 201a

Figure 107: Typical Residual Tension Fracture Appearances for 24-Ply Laminate Specimens Tested Under Fatigue Condition A, B, or C of Table XXXV.



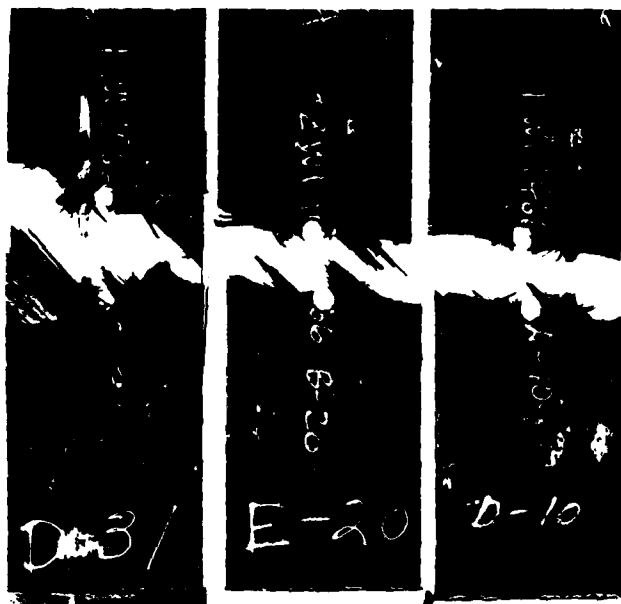
144 199

AC-31	CB-11	CB-18
Case A: 4 Bar	Case B: $R = -0.3$	Case C: 180°F (82°C)
$N = 12,000$	$N = 250,000$	$N = 1,000$



144 203

Figure 108: Typical Residual Compression Fracture Appearances for 24-Ply Laminate Specimens Tested Under Fatigue Conditions A, B, or C of Table XXXV.



144 193

DC-31
Case B:
 $R = -0.3$
 $N = 2 \times 10^6$

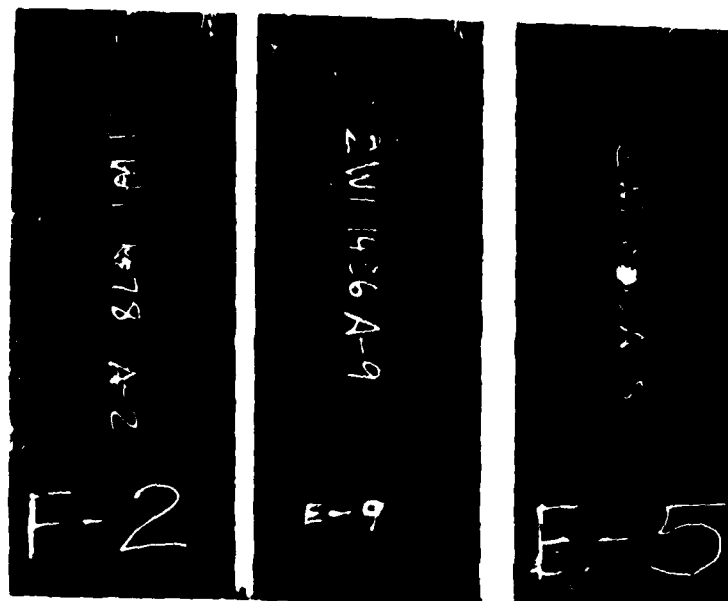
EB-20
Case A:
4 Bar
 $N = 20,000$

DA-10
Case C:
 180°F (82°C)
 $N = 8,000$



144 204

Figure 109: Typical Residual Tension Fracture Appearances for 32-Ply Laminate Specimens Tested Under Fatigue Conditions A, B, or C of Table XXXV.



FA-2
Case A:
4 Bar
N = 20,000

EA-9
Case B:
R = -0.3
N = 250,000

EA-5
Case C:
180°F (82°C)
N = 8,000

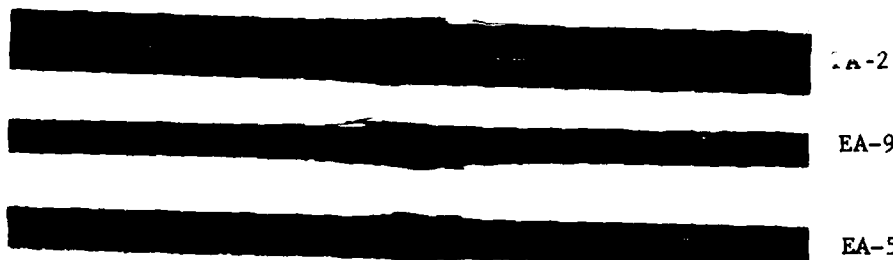


FIG. 110: Typical Residual Compression Fracture Appearances for 32-Ply Laminate Specimens Tested Under Fatigue Conditions A, B, or C of Table XXXV.

SECTION 8

DAMAGE CHARACTERIZATION

In order to determine how accurately damage recorded by the Holscan ultrasonic unit corresponded to damage actually present in the specimens, destructive examination of selected specimens was undertaken as part of Task II.

Of the triplicate specimens of each laminate fatigued to each of the five cycle intervals, one of each group was metallographically sectioned longitudinally (parallel to the 0° fiber) in 0.1 inch increments through the damage region and examined by optical microscopy to ascertain: 1) the delamination location and extent; 2) matrix cracking; and 3) 0° fiber breakage. The second specimen underwent a deplying burn-out procedure to remove the matrix material and separate plies. Each ply was examined for damage zone characteristics which were marked by the metallic residue which had been infused prior to the burn out. An attempt was made to section the third specimen in layers parallel to the surface using a microtome. This technique has been successful for the determination of through-the-thickness moisture distributions ⁽¹⁰⁾. However, for the latter purpose samples were sectioned between two similarly oriented plies. Attempts to slice between plies of different orientations resulted in splintering and fiber losses. Also, since the delaminations existed at multiple levels and were not continuous along any one ply interface, the knife blade tended to slice through several layers, obliterating any damage which may have been present originally. Therefore, no results are reported for this method. This test method was replaced with DIB enhanced radiography of the deply specimens prior to burn-out.

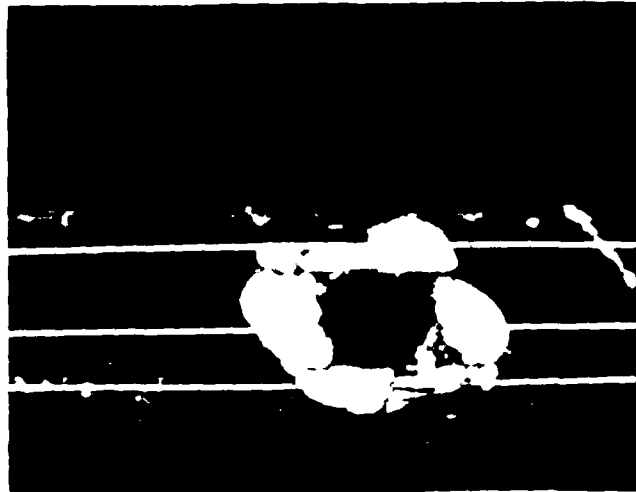
Procedures are detailed in Section 4. Additional data are available in Volume III, Appendixes G, H, and I.

8.1 METALLOGRAPHIC EXAMINATION

The damage region as recorded by the Holscan and the locations at which B-scans were recorded for specimen DB-19 after 12,000 fatigue cycles are shown in Figure 111. Metallographic sections were taken near locations 1 and 2 and are shown compared to the B-scans in Figures 112 and 113. Location of the damage through the thickness appears to be indicated quite well by the Holscan equipment. Moreover, a comparison of the damage measurements obtained from the two techniques (Table XXXVIII) also indicates that the actual delamination length present in the specimens is not significantly different from that recorded by the Holscan unit. In addition, DIB penetrant enhanced x-ray techniques were also employed and compared to the Holscan C-scan records. Typical examples are presented in Figures 114 - 116 indicating good agreement between these two methods. Note in these prints of radiographs that no delaminations or matrix cracking are evident away from the damage region. In fact, enhanced radiographs were made of the entire specimen and no edge delamination or cracking were observed other than that confined to the region surrounding the hole, which was also confirmed by the micrographs.

8.2 EXAMINATION BY BURN-OUT AND DEPLYING

This procedure permitted the evaluation of all plies except those laid up as parallel layers of like orientation. Thus, only 17 laminae were separated for 24-ply samples and 25 laminae for 32-ply samples. Plies which contained damage in the specimens examined are listed in Table XXXIX. The number of plies containing damage generally increased as the number of cycles completed increased. Damage extent within each ply appearing as light regions marked by the dye is evident for the two specimens fatigue

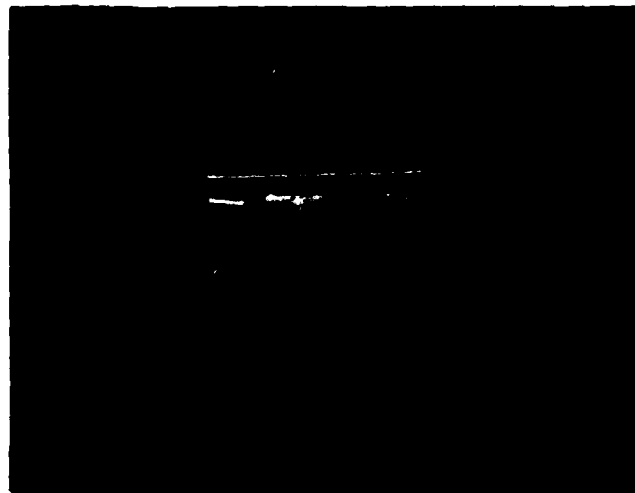


1

2

3

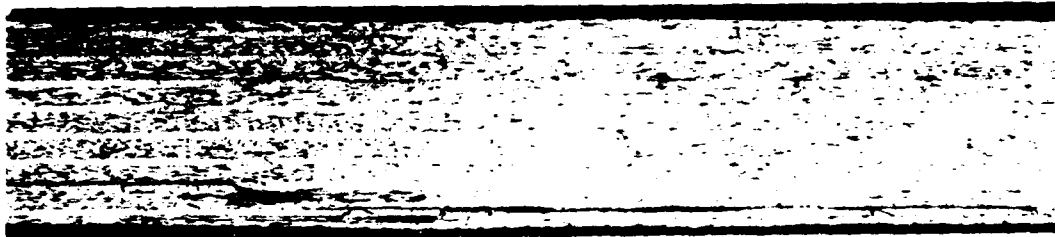
C-SCAN



CUMULATIVE B-SCAN

SPEC: BB-19 $N_3 = 12,000$ CYCLES

Figure 111: Damage as Recorded by Holscan Indicating Locations at Which B-scans Were Obtained.



D19-1-1

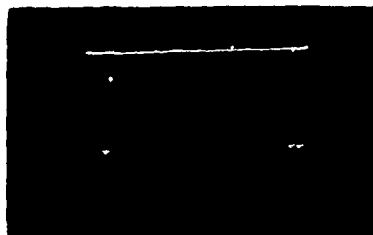
10x



D19-1-2

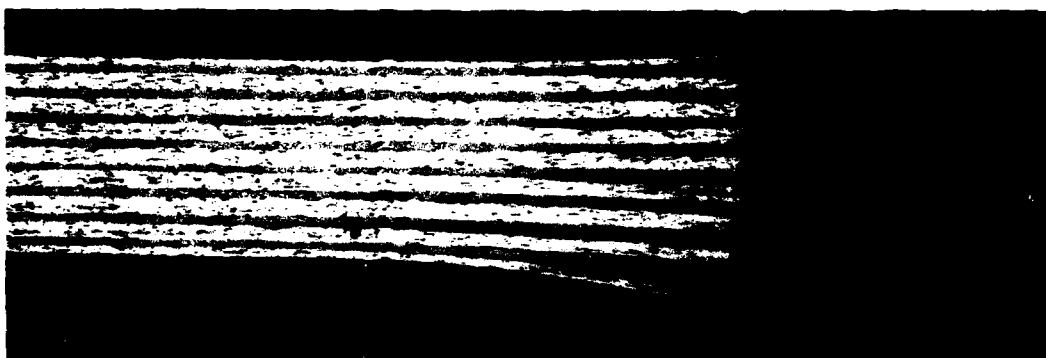
25x

LOCATION: 1.15 IN. DAMAGE LENGTH: 0.859 IN.



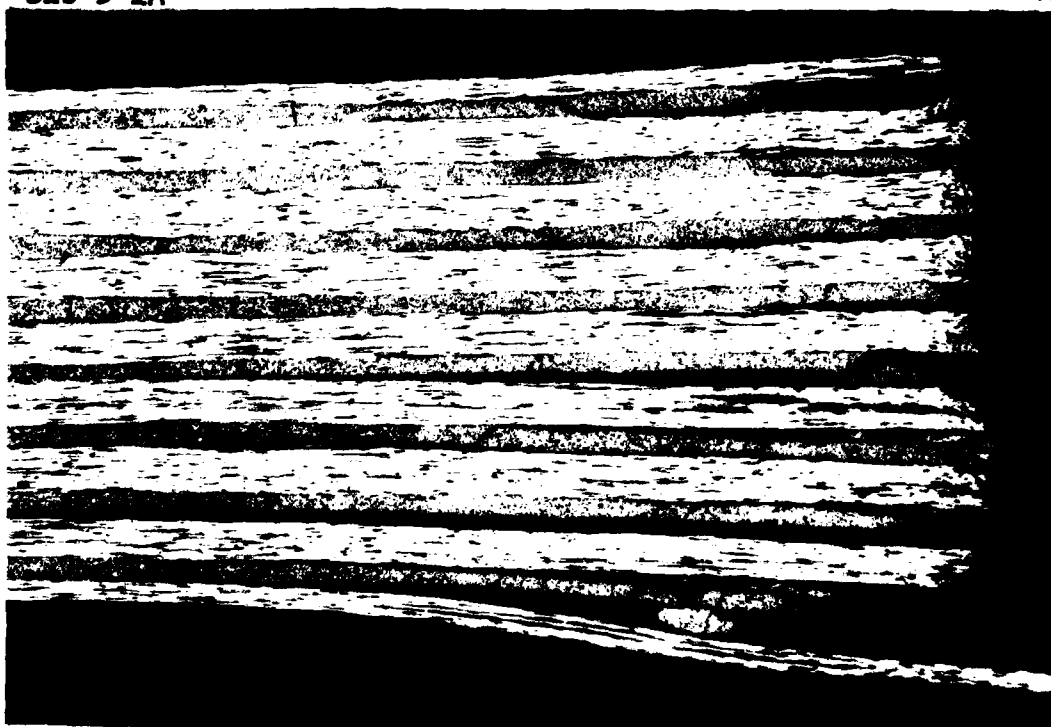
1.04%
1.15 IN.

Figure 112: Comparison of Damage as Determined by Metallographic Sectioning and Holsen Ultrasonic B-scan at Location No. 1 (See Figure 111).



D19-5-1A

10x



D19-5-2A

25x

LOCATION: 1.55 IN. DAMAGE LENGTH: 0.988 IN.

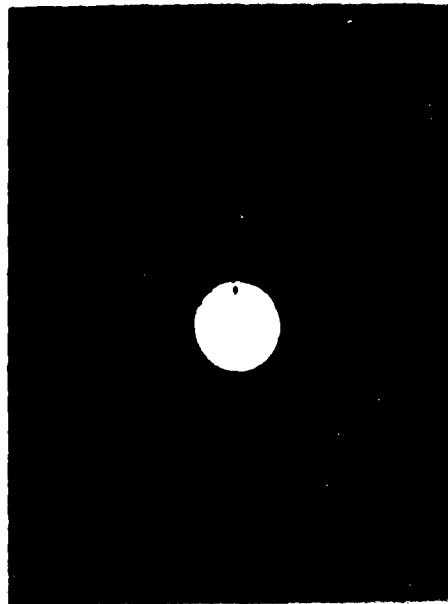


B-SCAN
@ 1.5 IN.

Figure 113: Comparison of Damage as Determined by Metallographic Sectioning And Heliscan Ultrasonic B-scan at Location No. 2 (See Figure 111)

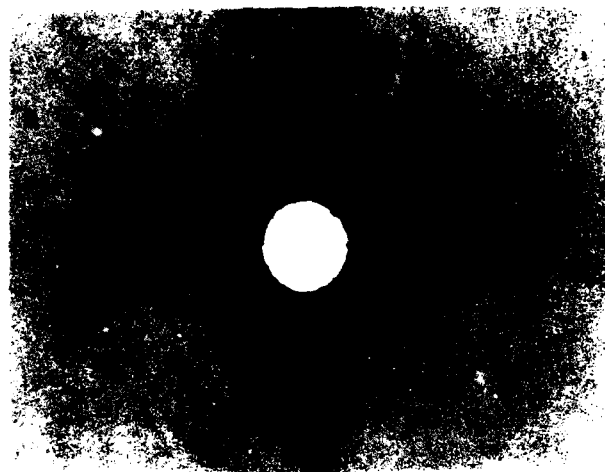
TABLE XXXVIII
COMPARISON OF DAMAGE LENGTHS AS
DETERMINED BY HOLSCAN AND METALLOGRAPHY

Laminate Type	Specimen No.	No. of Cycles	Holscan Length @ Center		Location		Metallography Length	
			in.	mm	in.	mm	in.	mm
24-Ply 67°-0° 33°-+45°	CB-11	4 k	1.04	26.4	1.52	38.6	0.903	22.94
	DB-19	12 k	1.04	26.4	1.45	36.8	1.007	25.58
	IB-12	20 k	1.12	28.4	1.48	37.6	0.997	25.32
	EC-30	40 k	1.45	36.8	1.55	39.4	1.317	33.45
32-Ply Quasi- Isotropic	MC-23	1 k	0.86	21.8	1.53	38.9	0.806	20.47
	MC-22	5 k	0.84	21.3	1.49	37.8	0.780	19.81
	RC-23	10 k	0.94	23.9	1.51	38.4	0.926	23.52
	NB-19	20 k	1.01	25.7	1.48	37.6	0.918	23.32
	JC-30	28 k	0.94	23.9	1.54	39.1	0.850	21.59



SPECIMEN NO. JB-14 N = 20,000 CYCLES

Figure 114: Comparison of Damage as Determined by Holscan Ultrasonic C-scan and DIB Penetrant Enhanced X-ray for 32-Ply Specimen JB-14.



SPECIMEN NO. KA-2 N = 10,000 CYCLES

Figure 115: Comparison of Damage as Determined by Holscan Ultrasonic C-scan and DIB Penetrant Enhanced X-ray for 32-ply Specimen KA-2.



SPECIMEN NO. SC-22 N = 5,000 CYCLES

Figure 116: Comparison of Damage as Determined by Holscan Ultrasonic C-scan and DIB Penetrant Enhanced X-ray For 32-Ply Specimen SC-22.

TABLE XXXIX
PLIES CONTAINING DAMAGE IN DEPLIED
24 AND 32-PLY SPECIMENS

LAMINATE TYPE	SPECIMEN NO.	TOTAL NO. OF LAMINAE	DAMAGED LAMINAE	N _x CYCLES
24-PLY 67%, 0°, 33% ±45°	IA-5	17	1-4, 11-17	N ₁ 4K
	FA-6	17	1-3, 10-17	N ₂ 8K
	HA-8	17	1-5, 13-17	N ₃ 12K
	GC-23	17	1-5, 12-17	N ₄ 20K
	BB-15	17	1 thru 17	N ₅ 40K
32-PLY QUASI-ISOTROPIC	QA-4	25	1-10, 14, 24	N ₁ 1K
	SC-22	25	1/8, 17-24	N ₂ 5K
	PC-21	25	1-4, 21-24	N ₃ 10K
	JB-14	25	1-9, 14-24	N ₄ 20K
	SC-31	25	1 thru 25	N ₅ 28K

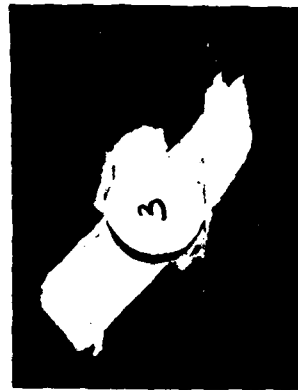
cycled to N_5 presented in Figures 117 and 118 for the 24-ply and 32-ply specimens, respectively. Note the differences in the direction and extent of damage on the various layers which undoubtedly contributed to the large scatter in damage size when measured for a projected area. By careful examination the shape of the delaminations on individual layers can be discerned in the photos of Figures 119 and 120 which display the delamination zone as determined by Holscan and enhanced radiography. Agreement between damage determined by this deply technique and the x-ray photographs is quite good.



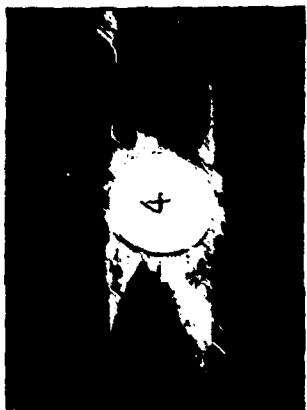
PLY 1, 0°



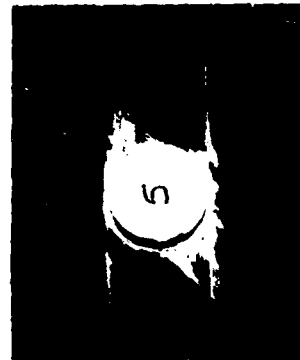
PLY 2, 45°



PLIES 3 & 4, 0°



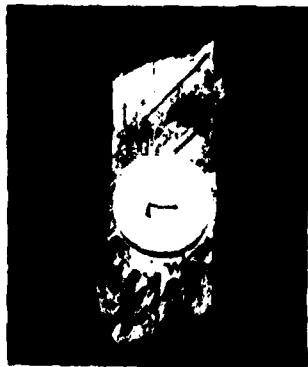
PLY 5, -45°



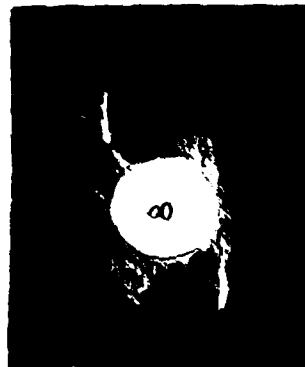
PLIES 6 & 7, 0°



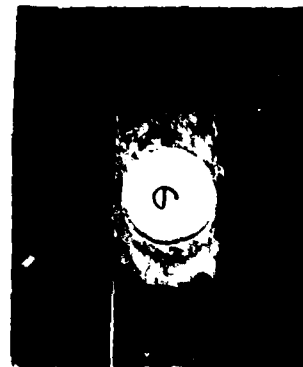
PLY 8, 45°



PLIES 9 & 10, 0°

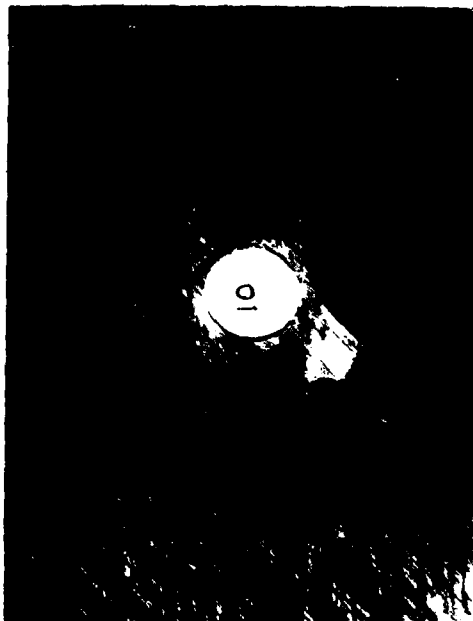


PLY 11, 0°



PLIES 12 & 13, 0°

Figure 117a: Deplied 24-Ply Specimen BB-15 After 40,000 Fatigue Cycles
(Plies 1 - 13)



PLY 14, -45°



PLIES 15 & 16, 0°



PLY 17, 45°



PLIES 18 & 19, 0°

Figure 117b: Deplied 24-Ply Specimen BB-15 After 40,000 Fatigue Cycles
(Plies 14 - 19)

AD-A115 184

LOCKHEED-CALIFORNIA CO BURBANK

F/G 11/4

ADVANCED RESIDUAL STRENGTH DEGRADATION RATE MODELING FOR ADVANC--ETC(U)

JUL 81 K N LAURAITIS, J T RYDER, D E PETTIT

F33615-77-C-3084

UNCLASSIFIED

LR-28360-19

AFWAL-TR-79-3095-VOL-2

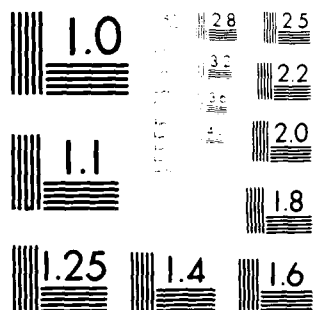
NL

4 OF 4

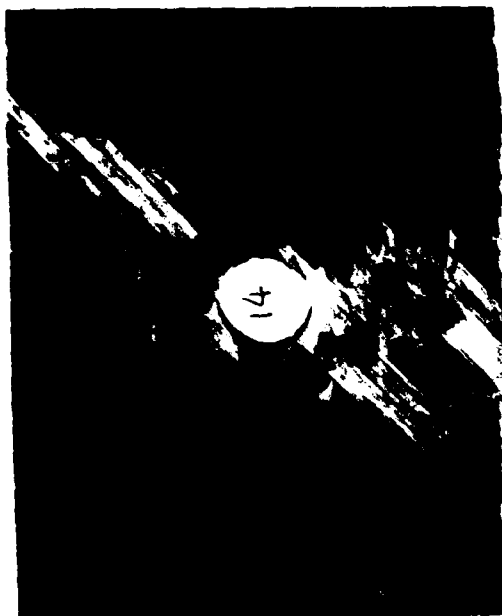
4115 184



END
DATE
FILMED
09:82
DTIC



MICROCOPY RESOLUTION TEST CHART
NATIONAL BUREAU OF STANDARDS-1963-A



PLY 20, -45°



PLIES 21 & 22, 0°

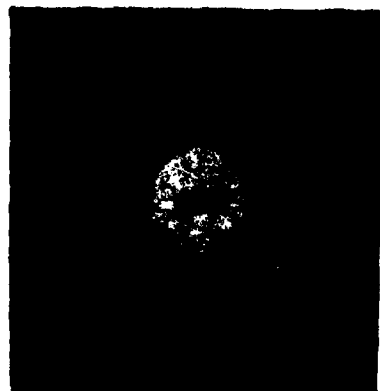


PLY 23, 45°



PLY 24, 0°

Figure 117c: Deplied 24-Ply Specimen BB-15 After 40,000 Fatigue Cycles
(Plies 20 - 24)



PLY 1, 0°



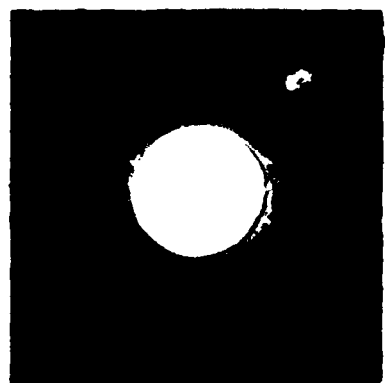
PLY 2, 45°



PLY 3, 90°



PLIES 4 & 5, -45°

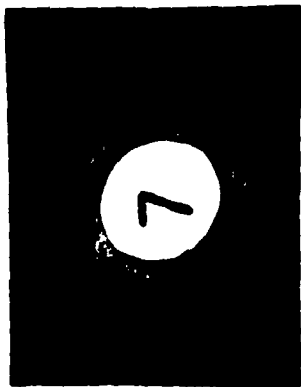


PLY 6, 90°

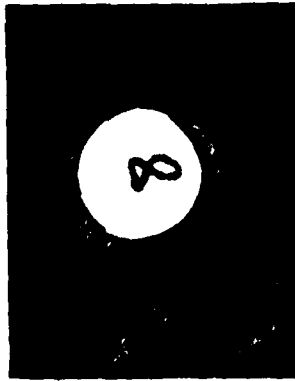


PLY 7, 45°

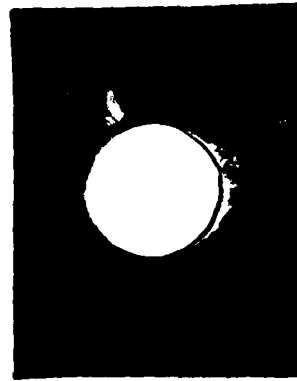
Figure 118a: Deplied 32-Ply Specimen SC-31 After 28,000 Fatigue Cycles
(Plies 1 - 7)



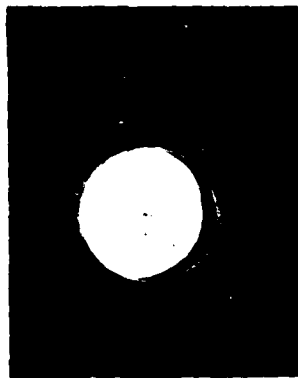
PLIES 8 & 9, 0°



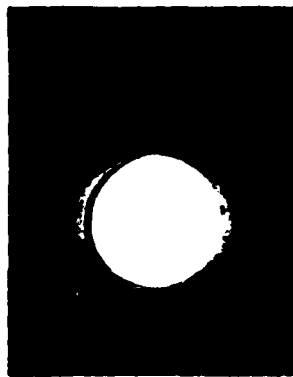
PLY 10, 45°



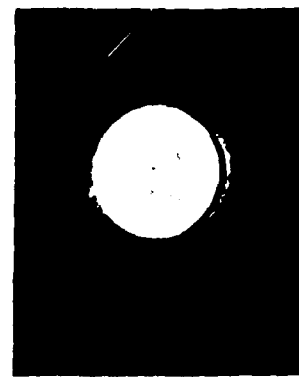
PLY 11, 90°



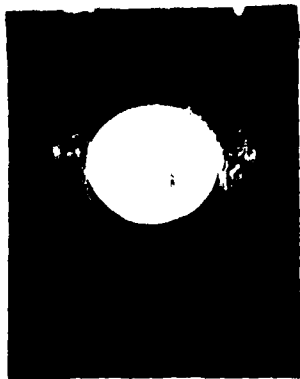
PLIES 12 & 13, -45°



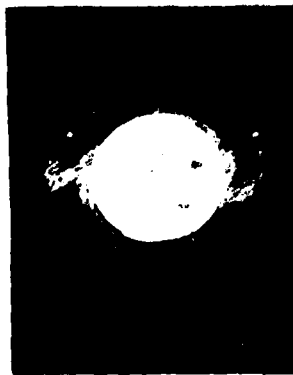
PLY 14, 90°



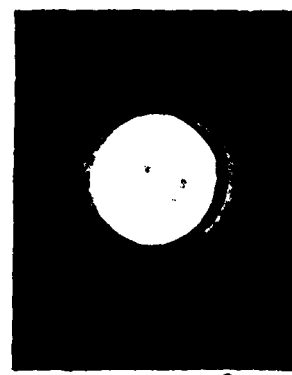
PLY 15, 45°



PLIES 16 & 17, 0°



PLY 18, 45°

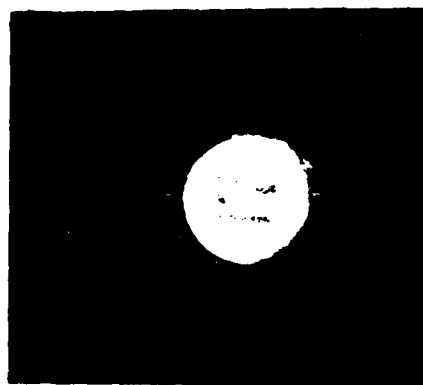


PLY 19, 90°

Figure 118b: Deplied 32-Ply Specimen SC-31 After 28,000 Fatigue Cycles
(Plies 8 - 19)



PLIES 20 & 21, -45°



PLY 22, 90°



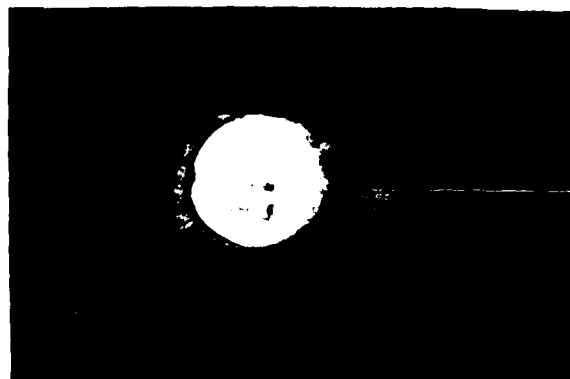
PLY 23, 45°



PLIES 24 & 25, 0°

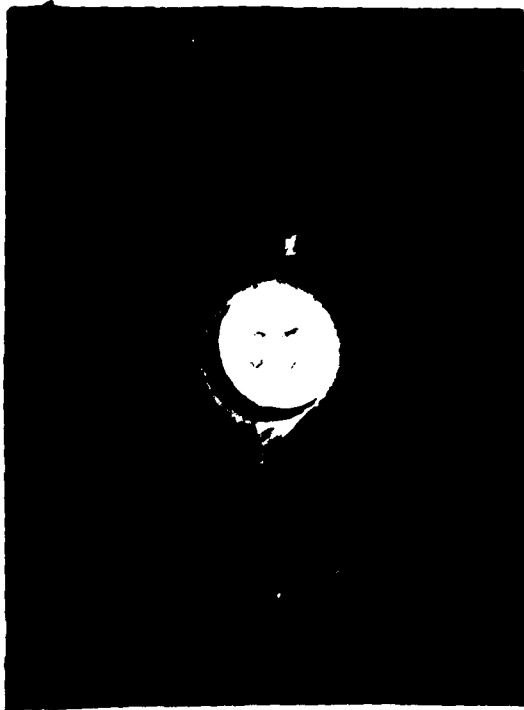


PLY 26, 45°

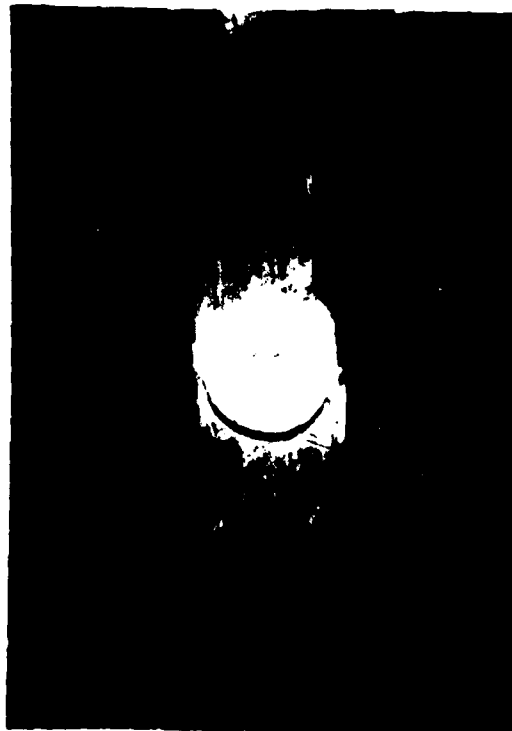


PLY 27, 90°

Figure 118c: Deplied 32-Ply Specimen SC-31 After 28,000 Fatigue Cycles
(Plies 20 - 27)



PLIES 28 & 29, -45°



PLY 30, 90°

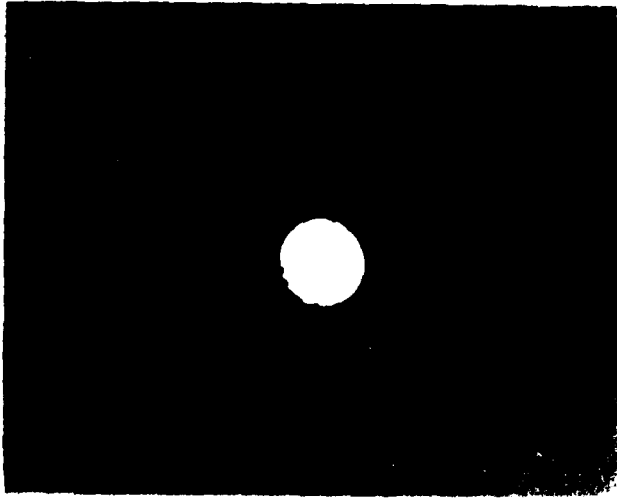


PLY 31, 45°



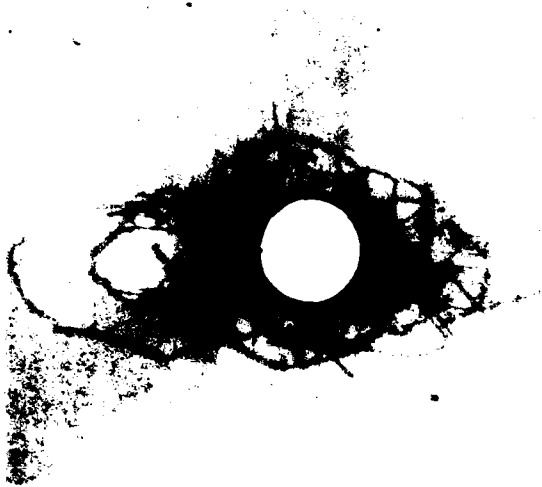
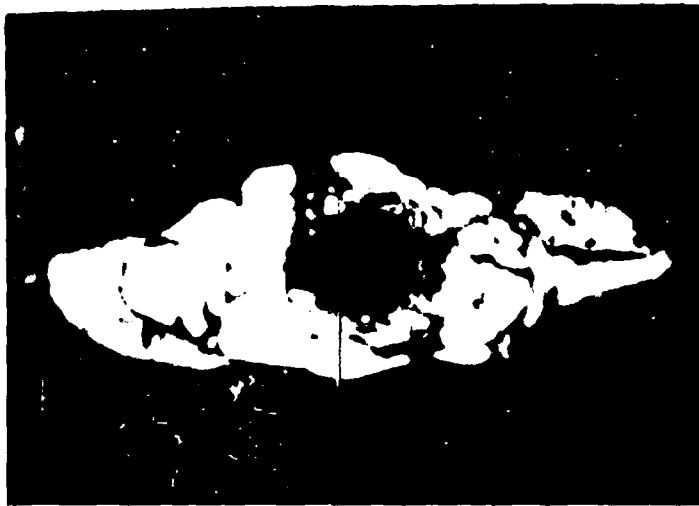
PLY 32, 0°

Figure 118d: Deplied 32-Ply Specimen SC-31 After 28,000 Fatigue Cycles
(Plies 28 - 32)



SPECIMEN NO. BR-15 N = 40,000 CYCLES

Figure 119: Comparison of Damage as Determined by Holscan Ultrasonic C-Scan and DIB Penetrant Enhanced X-Ray for 24-Ply Specimen BR-15.



SPECIMEN NO. SC-31 N = 28,000 CYCLES

Figure 120: Comparison of Damage as Determined by Holscan Ultrasonic C-Scan and DIB Penetrant Enhanced X-Ray for Specimen SC-31

SECTION 9

ANALYSIS OF RESULTS

Throughout this program emphasis was placed upon obtaining mechanical data, residual strength and stiffness, and upon documentation of correlative data, damage state and cycles to failure. These data were collected in a manner which would permit the development of relationships between the mechanical data and the associated correlative data. One purpose of collecting the data was to meet the desire of the Air Force to develop a quantitative, mathematical model to predict residual strength degradation based upon knowledge of damage state and also to predict the growth of that damage and the associated remaining fatigue life. This section addresses that desire.

9.1 DATA ASSESSMENT

The results of this program, presented in previous sections, clearly show for the specimen geometry, laminate types and damage condition evaluated that, under both monotonic tension or compression load, residual strength remained unchanged or increased, sometimes significantly, as the number of fatigue cycles completed increased. Despite the limitations of measurement procedure employed, the evidence is strong that stiffness of the overall composite coupons did not significantly change prior to failure under fatigue load. Further, the characteristics of the damage region which were measured were not found to correlate to residual strength or to be directly indicative of remaining fatigue life. These observations require explanation.

A possible reason for the lack of correlation between observed damage and

mechanical properties is that some of the damage was not detected. There are three principle types of damage which can occur within these laminated composites: intraply matrix cracking; interply matrix delamination, and fiber breakage. Other types of damage simply consist of changes in exent or load at which the three principle types of damage occur except, possibly, for creep within the matrix which is not of importance in the temperature range examined here.

During the fatigue testing of these notched coupons, the maximum load was necessarily restricted to approximately 20% and 30% of the respective 24 and 32-ply laminate undamaged tensile strengths. These loads are at a level that no significant matrix cracking could occur away from the notch region and edge delamination could not develop. Lack of these types of damage was verified by x-ray and photomicrographs of coupon cross sections. These facts combined with the experimental observation that failures occurred through the notch means that only damage around the hole is of interest. However, as shown in Section 8, the extent and location of matrix delamination around the hole was accurately documented. Thus, any improvement in correlation between mechanical data and correlative data must center upon matrix cracking and fiber fracture and/or buckling in the region of the notch.

Intraply matrix cracking was found by photomicrographs to be prevalent only in the near vicinity of the hole, as expected. Matrix cracking, however, does not directly lead to coupon fracture but, instead, results in changes in ply constraint and transfer of load to plies oriented in a load direction. Failure of these coupons under fatigue or monotonic compression loading is due to local buckling instability which is dependent on delamination state and extent of load transfer due to matrix cracking. Delamination extent and location are related to local buckling instability, but not directly because of internal ply and external geometric constraints. Failure under monotonic tension load is also related to

matrix cracking and delamination state, but again not directly. Fracture in this case is due to fiber breakage which occurs only near failure. Successful correlation of damage state to strength, stiffness, and fatigue life thus requires relating the interactional effects of matrix microcracking and delamination as well as accounting for ply and geometric constraints and probability distributions of fiber breakage or fiber bundle buckling instability. The mechanics of fracture in these notched coupons will be described in more detail as an aid to understanding the experimental results.

9.1.1 Mechanics of Fracture in Notched Coupons

Consideration of the mechanics of coupon fracture for notched coupons reveals many similarities to that which occurs in the unnotched case and yet significant differences exist. The principal manifestation of internal material changes remain, namely; matrix cracking, delamination, and fiber breakage. However, in the case of a coupon with a center hole, as in this program, the maximum tensile stress remote from the hole never exceeds about 50% of the unnotched strength for holes of realistic sizes (greater than approximately ten percent of the coupon width). This stress limitation results from the notch acuity effect ⁽¹¹⁾. Maximum fatigue loads are thus always less than 50% of the unnotched tensile strength. As a consequence, matrix cracking and edge delamination are usually limited or non-existent remote from the hole. Thus damage develops primarily in the hole region in the manner described in Sections 6.2 and 7.2. No significant changes in stiffness can occur remote from the hole since matrix cracks, required for displacement changes under constant amplitude fatigue load, are limited in number.

At the hole, matrix cracking and delamination occur and concentrate at first in the high stress regions on either side. If there is a compression load excursion in the fatigue cycle, out-of-plane buckling of the

delaminated plies can eventuate resulting in growth of the delamination region perpendicular to the load as observed in the $R = -1.0$ experiments of this program. Delamination in each ply, however, grows in a direction influenced by the ply orientation. If the compression load excursion is not high enough for significant out-of-plane buckling to occur, delamination can extend parallel to the load direction as in the $R = -0.3$ tests. In either case, notch acuity is decreased due to the redistribution of stress as the delamination region grows. Reduction in notch acuity typically results in an increase in monotonic residual strength,^(9, 12) as observed and discussed in Section 6.3 and 7.3, which may be dramatic if the delamination region grows parallel to the load direction as in the $R = -0.3$ experiments. The fracture event under tensile loading in these notched coupons is due, as in the unnotched case, to the breakage of a small number of fibers in a statistically critical location of weak fibers. Such fiber breakage appears to occur only near the failure event^(13, 14).

The mechanics of the damage process in these notched laminated composites dictates the types of possible correlations that can be found. Stiffness, for example, can not, in general, be a practical measure of damage. As mentioned, stiffness remote from the hole remains unchanged as damage grows. The initial stiffness measured across the hole is lower than the remote stiffness because of the high strains on either side of the notch. As the delaminations around the hole grow, stiffness measured across the hole would, if it changed, increase since the strains on either side can somewhat decrease as loads are redistributed. Thus stiffness measured near the hole can not correlate well to remaining fatigue life while stiffness measured over a large gage length which includes the hole remains essentially unchanged except just prior to the fracture event. The latter result was experimentally observed in this program as documented in Section 6.3. The lack of stiffness change has also been verified by Whitcomb⁽¹⁴⁾ who recorded slight changes (<5%) in the stiffnesses of a few coupons under residual tensile loading, but the changes were increases as expected from

this discussion. Coupons loaded in residual compression also revealed no stiffness change except in a few cases where stiffness decreased due to local buckling.

Whitcomb ⁽¹⁴⁾, as well as Ratwani ⁽¹⁵⁾, has verified that delamination growth is primarily due to high interlaminar shear stress and can occur even in the presence of a compressive stress. Importantly, Whitcomb also confirmed the lack of fiber breakage around the hole up to at least 80% of the notched tensile strength despite the development of extensive delamination.

A correlation for these notched coupons between damage defined as interply matrix cracking (delamination) and such properties as fatigue life and residual strength is not feasible. Matrix cracking begins to saturate as delamination occurs in the adjacent interply region ^(16, 17, 18) and thus the number of matrix cracks cannot be directly related to fatigue life or residual strength. Fiber breakage or instability also cannot be used as a convenient measure of damage in any general sense because such events principally occur at or near the failure event. Because of inherent difficulties of using stiffness, matrix cracking, or fiber breakage/buckling as measures of damage in these notched coupons, delamination was used as a measure of damage. This program has demonstrated such a measure of damage does not correlate, in the usual sense, with residual strength or stiffness, because these properties either increased or remained unchanged, and only indirectly correlates with fatigue life. The question naturally follows from this discussion as to what is actually meant by the word damage.

9.1.2 Assessment of Damage

In actual practice, damage is the term applied when a material changes in a manner which we do not like. Thus, marks left by rubbing on a fine piece

of furniture or a tire that goes flat on a bicycle are both termed damage. These two examples, while illustrating the difference between cosmetic and structural damage, demonstrate the principle that these are material conditions we do not like. In contrast, defective is a term applied when the original material state is one which is not desired.

In this program, primary focus is on the evaluation of damage and the correlation of that damage with mechanical property data for notched laminated graphite/epoxy composites. The effect of damage is traditionally measured in terms of stiffness change, residual strength degradation, or amount of remaining fatigue life. However, in this study such traditional measures were demonstrated not to correlate with damage if it is quantified by delamination growth. Further other measurements such as intraply matrix cracking or extent of fiber breakage or buckling can be seen to be unrealistic in any practical sense. Hence, the question arises as to whether the delamination which occurs at the notch can be called damage.

Clearly, the existence of the delamination meets our definition of cosmetic damage. However, the material change as measured by delamination does not necessarily constitute structural damage. The delamination/hole region can only be termed structural damage in the sense that as the delaminated area increases, the probability of failure increases and that fracture/failure will occur in the delaminated area. However, in relation to residual strength or stiffness, delamination does not constitute damage until the actual failure event. The reason for this situation is simply that the damage region is not a self similar, crack like defect such as occurs in metals. The damage region instead acts like a macrosized inelastic field much like a yield zone in metals. Thus, the delaminated region is damage just as a yield zone can be labeled damage. However, the situation is different than that occurring in a metal in that little or no general stiffness change remote from, but including the damage region, is associated with the inelastic region.

9.2 ANALYSIS/CORRELATIVE METHODOLOGY

This program was conducted with the intention of supporting the structural integrity policy of the Air Force which requires that a structure have a minimum residual strength at the end of a specified period of service usage. In order to meet this overall objective, the residual strength of the structure could conceivably be related to the service induced damage if any eventuates. If such a relationship is not developed, durability requirements could alternatively be met by tracking damage accumulation through changes in residual strength. Procedures which attempt to track damage in this manner are variously known as forms of wear-out models. They have the disadvantage that each laminate and structural geometry combination must be independently evaluated and they thus require extensive data accumulation. A direct relationship between damage and residual strength in theory avoids the necessity of obtaining as much data, but requires instead the development of accurate non-destructive examination procedures capable of detecting and monitoring damage growth. This subsection analyzes the question of using the data obtained in this program for developing a general relationship between damage and residual strength. The relationship of the data to wear-out models will be considered first and that between residual strength and damage second.

There are a number of statistically formulated procedures found in the technical literature ⁽¹⁹⁻²⁴⁾ designed to monitor damage accumulation by tracking changes in residual strength. Some of these procedures are known as wear-out models. The wear-out model concept was developed because of the perceived need to relate residual strength to damage state. At the time of the inception of this program, this approach was the only available one and to a great extent this remains true today. For this reason, the applicability of the models for correlating the data of this program was analyzed. In the analysis discussion of this subsection all of the various

statistically formulated procedures will be considered to be wear-out models since they are all fundamentally but slightly different numerical formulations of the same idea.

As originally proposed ⁽²⁴⁾, the mathematics and statistics of the model were derived from physical principles based on the assumption that the damage which developed during loading could be considered as fracture mechanics type defects. This assumption led to a deterministic set of equations for relating residual strength and fatigue life distributions which required statistical formulation. The deterministically derived model is, however, quite inadequate for correlating the data of this program because the model implicitly assumes that notch acuity increases as damage grows and thus that residual strength always decreases. The data of this program clearly show the inadequacy of the original physical assumption because residual strength either did not change or, instead, increased since the notch acuity decreased.

Other types of wear-out approaches were formulated with a recognition of the difficulties of a deterministically based approach ⁽¹⁹⁻²³⁾. Instead these approaches assume that if the statistical distributions of the monotonic strength and fatigue populations can be formulated, the physics of the failure process can be deduced. This approach was undertaken because the failure modes of composites are often believed to be considerably more complex than those of metals ⁽²³⁾. The derivation of the general statistically formulated wear-out model has been put on a rigorous basis by Hahn ⁽²³⁾. In this procedure, the mathematical description is derived in a manner analogous to the failure process description often derived for metals. Yang and Jones ⁽²²⁾ have shown how all of the various mathematical approaches are related. The analytical approaches were found to differ only in their choice of the numerical values for the mathematical exponents which, in turn, were selected based upon the expected form of the relationships among the variables. In addition, and equally important,

Yang and Jones⁽²²⁾ showed that the final formulation derived by Halpin⁽²⁴⁾ from physical assumptions is a variation of those obtained using an approach which begins by mathematically representing the failure distributions followed by inferring the physical mechanics.

The reason for the similarity in the final formulations of the various approaches was found^(7,9) to be due to the fact that all such statistical formulations make (whether explicitly or implicitly,) the same basic assumptions. The explicit assumptions are that: 1) The distribution of observed phenomena can be represented by an exponential equation (this is usually chosen as a two parameter Weibull equation); 2) change in strength can be represented by a power law; 3) fatigue life and global stress are related by a power law; 4) there is a one-to-one relationship between residual strength and fatigue life. There are also two implicit physical assumptions. The first, is that the damage state at failure of a coupon under monotonic load without prior fatigue loading is assumed to be of the same type as that which eventuates under fatigue load. Mathematically this assumption is known as path independence. Second, notch acuity is assumed to increase, and thus residual strength decrease, as fatigue life increases. These two implicit assumptions are the same as⁽⁹⁾ the explicit assumptions made in the physically based approach.

The applicability of statistically based wear-out models is naturally dependent upon the accuracy of the assumptions. The assumption of load path independence, is apparently not true in any general sense. The results of this and other investigations^(7,9) show that the coupon damage state just prior to fracture during a monotonic load residual strength test is not necessarily the same as the state which develops just prior to failure under fatigue load. At best, therefore, the fourth explicit assumption, that of one-to-one relationship between residual strength and fatigue life is not true. The second implicit assumption, residual strength degrades as fatigue cycles increase, is also not generally true.

Most of the data obtained in this program show no change in residual strength with either fatigue cycles or damage extent. This lack of any significantly measurable change occurs despite the fact the coupons fail under fatigue loading. The remaining data displayed an increase, not a decrease in residual strength as fatigue life increased. This latter result is not uncommon (9,12).

This analysis of wear-out type models and the residual strength data obtained in this and other research programs (7,9,12,25) was used to reach the conclusion that wear-out models are inadequate to represent changes in residual strength for practical applications. The reason for the conclusion is the same regardless of the approach used to derive the mathematical representation. In either case, the results of the experiments were used to infer that the two physical assumptions made, explicitly or implicitly, in all approaches are incorrect. Therefore, no attempt was made to mathematically quantify the parameters of any of the various wear-out models using the data obtained in this program. The analysis of such models as discussed in this program dictates that such a quantification is meaningless since residual strength either did not change or increased.

9.2.1 Methodology for Relating Damage to Residual Strength and Fatigue Life

Having analyzed the applicability of wear-out type models to represent the residual strength data and shown their inadequacy, the question of developing a different methodology for relating residual strength to damage can be considered. There are two different relations, among the pertinent variables, to model. The first, relating damage to residual strength, is a monotonic load cycle problem requiring one failure criterion, while the second, relating damage to remaining fatigue cycles, is a dynamic problem and requires a different failure criterion. The methodology for developing the relationships can be either empirically based or be one of a more

purely mathematical physical representation. The potential of each methodological approach for modeling the relationship between damage and residual strength or fatigue life will be discussed.

All empirical approaches are obtained by curve fitting a mathematical expression to experimentally obtained damage, residual strength, and life data. Such fits are inherently of little value for any other laminate, geometric configuration, or loading condition without a suitable transfer function. These functions allow differences in experimental results for different conditions to be related in such a manner that the curve fit for one data set is accurately adjusted for another. For isotropic materials there are two such transfer functions: The notch acuity concept, normally used for low cycle fatigue, and the stress intensity concept often used for high cycle fatigue. Both of these transfer functions work to a limited extent because of the isotropic nature of the materials for which they are used. For anisotropic materials, such concepts as notch acuity and stress intensity factor can not work as transfer functions in the same manner that they are used for metals unless the damage zone is large compared to the scale of the plies. This is not to say that fracture mechanics, for instance, can not be used as a tool for analyzing composites, but only that it provides an inadequate laminate/geometry load transfer function.

There are, therefore, two reasons why an empirically based methodology for relating damage to residual strength or fatigue life could not be, and, was not performed in this program. The first is that data for one set of test conditions are not directly related to those obtained for another. In order to relate the data suitable transfer functions are required. These transfer functions are not available for laminated composites and will probably not be of the same type as presently used for isotropic materials. Second, the residual strength test results obtained in this program evidenced either no change in strength due to fatigue loading or an increase. These two facts left one with the possibility of developing only a

mathematical/theoretical methodology based on physical principles concerning the nature of the damage accumulation process.

The development of a detailed theoretically based methodology for relating damage to residual strength or to remaining fatigue life is a formidable task. Such an approach requires refinement of the few presently available techniques and probably the creation of entirely new ones. A quantitative representation of the geometry, loading and plies is needed. This is met to some extent by a few finite element representations of laminates. The model must be capable of quantitatively anticipating both matrix cracking and matrix delamination. This requires a dynamic model which can not only anticipate matrix cracking onset and saturation levels, but which also can anticipate the sequence of events which accompanies either monotonic load increase or fatigue cycling. Representations of fiber bundle instability and local buckling instabilities are needed for compression load and of fiber bundle fracture for tension load. All of this requires detailed modeling of the sequence of events which constitute damage accumulation. Only the barest bits and pieces of this formidable task of modeling have been explored. The dynamic portion, requiring experimentally obtained rate data, probably in terms of strain energy, G , has only recently been evaluated ⁽²⁶⁾ and is not generally available.

The necessary data to support such theoretical/physical development were not obtained in this program. The degree of sophistication required for this type of model is considerably beyond, in terms of time and money, that anticipated at the inception of this program. Therefore no attempt was made to formulate such a model; in fact, the program was not structured in a manner which would allow its development. Instead, the program was designed to obtain a large statistical strength and fatigue life data base, hopefully for use in model development, rather than to detail micromechanical phenomena.

SECTION 10

SUMMARY AND CONCLUSIONS

This section summarizes the experimental observations and conclusions which issued from the Task II and III efforts. Statements concerning experimental results are in reference to relatively narrow coupons containing a poorly drilled hole for the two laminate types (quasi-isotropic and $67\frac{1}{2}-0^{\circ}$) evaluated in this research program. Numbers in parentheses at the end of each item reference the particular subsection of the report wherein additional information or support for the statement can be located.

INTRODUCTION

- o The logic for the design of the experimental program followed directly from the desired goal of developing a methodology for predicting the residual strength and its rate of change as a function of fatigue loading and damage size.
- o The overall objectives were aimed at determining whether observed changes in the material due to fatigue loading relate to the mechanical response in a quantifiable manner; determining the extent and range of the relationship; indicating the direction for design and formulation of structural integrity requirements.
- o Program was composed of three major phases:
 - Task I - preliminary screening

- Task II - damage growth and residual strength degradation prediction
 - Task III - effect of fatigue loading/environment perturbations
- o This report documents the work conducted in Tasks II and III and summarizes the Task I results (1.2).
 - o A detailed discussion of the rationale for selection of material, specimen design and damage type, description of the specimen randomization procedure and outlines of the test matrices for Tasks II and III are presented in Section 2.
 - o Laminates evaluated in this study were a 24-ply 67%-0° fiber laminate and a 32-ply quasi-isotropic laminate having the following stacking sequences, respectively:
 - (0/45/0₂/-45/0₂/45/0₂/-45/0)_s
 - (0/45/90/-45₂/90/45/0)_{2s}
 - o Specimens were 3" x 14" (76mm x 356mm) with a 9-inch (229mm) test section and contained a centered poorly drilled 3/8 inch (10mm) hole (2.1).

MATERIAL CHARACTERIZATION

- o The selected material Narmco T300/5208 conformed to all requirements of the Quality Control Plan (3.1).
- o Resin content of batch used for Tasks II and III was comparable

to that for Task I, however fiber strength was 7.5% higher (3.1).

- o Average manufactured panel properties were: Resin Wt. % = 27.9, fiber vol. % = 65, void content << 1%, density = 1.577 (3.2).

STATIC LOADING RESULTS

- o Extensometer data were obtained for the QC specimens but load vs. stroke data were recorded for the primary 3" (76mm) wide coupons. Section 5 presents a discussion of the validity of these data.
- o The Task II and III 24-ply QC specimens had a higher average strength than those of Task I due to the higher fiber strength of the material batch used for Task II and III (5.1).
- o For the 32-ply QC specimens results from all three tasks were within $\pm 10\%$. No effect of the higher fiber strength was evident (5.1).
- o Tension stress-strain records for the damaged laminates differed from those obtained for the undamaged QC specimens for the 24-ply laminates but were similar for the 32-ply specimens (5.2, 5.3).
- o For the 24-ply laminate, damaged tension strength decreased over 50% from the undamaged. An additional 40% drop from the damaged tension results was observed for the damaged compression specimens (5.2).
- o The effect of the higher fiber strength evident in the unnotched Task II 24-ply data nearly disappeared for the damaged compression case (5.2, 5.7).

- o Damaged tension strength of the 32-ply laminates decreased by 50% from the undamaged with an additional reduction of 15% for compression loading (5.3).
- o Decreases in tension and compression strength on the order of 10 to 15% were observed for the damaged 24-ply laminate at the higher strain rate (5.2).
- o The higher strain rate produced a decrease of approximately 14% in the compression strength of the damaged 32-ply laminate while the tension strength remained unaffected (5.3).
- o Damage growth studies under static loading revealed no significant change in the final failure properties as compared to baseline tests for either laminate. However, some damage growth occurred in the 24-ply specimens at stress levels above 56 ksi (386 MPa) in tension and 34 ksi (234 MPa) compression. Damage growth in 32-ply specimens was observed above 34 ksi (234 MPa) in tension and 25 ksi (172 MPa) compression (5.4).
- o Elevated temperature produced an increase in tensile strength of the damaged laminates due to a reduction in notch acuity while compressive strength decreased due to the greater propensity towards buckling (5.5).
- o High strain rates at elevated temperatures either did not affect the strength or produced a slight drop (5.5).
- o For both undamaged laminates, compression strength increased at the higher strain rate while tension strength was unaffected for the 32-ply laminate and reduced for the 24-ply laminates (5.6).

- o Population sample sizes of 10 or less for some static tests were too small to accurately represent the actual distribution functions (5.7). This was especially true for the high strain rate tests where the sample size was five (5.2, 5.3).

FATIGUE LOADING RESULTS

- o Under $R = -1$ fatigue loading data dispersion was over 2.5 orders of magnitude for the 24-ply specimens and slightly more than one order of magnitude for the 32-ply specimens (6.1, 6.3).
- o The 20 specimen sample size was not adequate for accurately representing the 24-ply fatigue life distribution (6.3).
- o Failures occurred during the compressive load excursion due to instability (6.2).
- o Delamination extension for $R = -1$ occurred almost entirely in the width (X) direction for the 32-ply laminate but in both directions for the 24-ply laminate although the major growth was also in the X direction (6.2).
- o Considerable dispersion was evident in the damage growth data for both laminates. Except for the scatter, the general shapes of the damage vs. N curves were similar to a vs. N curves obtained for metals (6.2).
- o No direct relationship between damage size and life was evident for either laminate except for a generally higher probability of failure as damage grows (6.2).
- o The 4-bar constraint condition produced fatigue lives within the

scatter band of the data obtained with the platen supports (7.2).

- o Under $R = -0.3$ loading all specimens of both laminates completed 2 million cycles without failure.
- o Damage development under the $R = -0.3$ condition differed significantly from the $R = -1$ case (7.2).
 - For the 24-ply laminate no growth in the width direction was evident but extensive growth occurred in the length direction.
 - For the 32-ply laminate primary growth was also in the length direction accompanied by slight growth in the width direction.
 - Change in direction was due to an alteration of the stress state in the vicinity of the notch.
- o There appeared to be an order of magnitude decrease in life due to the 180°F (82°C) temperature exposure during cycling for the 24-ply laminate (7.2).
- o The elevated temperature shortened the life of the 32-ply laminate but not as severely (7.2).

RESIDUAL STRENGTH RESULTS

- o After $R = -1$ cycling of the 24-ply laminate tensile residual strengths increased as the number of cycles completed increased, as much as 17% after 40,000 cycles. The increase was due both to a screening effect and reduction in notch acuity (6.3).

- o There was no decrease in compression residual strength for the 24-ply laminate after $R = -1$ loading (6.3).
- o Residual static properties of the 32-ply laminate were essentially unaffected by $R = -1$ fatigue cycling up to $P_{.80}$ (6.3).
- o No relationship between damage size and residual strength was evident (6.3).
- o $R = -0.3$ loading reduced the notch acuity significantly resulting in considerable increase in tensile residual strength with increasing number of cycles completed and little change in compression residual strength for both laminates (7.3).
- o Despite the severity of the elevated temperature cycling, residual strengths of specimens which survived the cycling were not adversely affected (7.3).

DAMAGE CHARACTERIZATION

- o Holscan determined damage sizes compared well with results obtained by metallography and DIB enhanced x-ray (8.1).
- o No cracking or delamination away from the damage region surrounding the hole was observed (8.1).
- o Use of a burn-out (deply) technique revealed that the number of plies containing damage increased as the number of cycles completed increased (8.2).
- o The deply method also indicated that delamination differed in extent and direction on different layers (8.2).

ANALYSIS OF RESULTS

- o Failure under fatigue or monotonic compression loading is due to local buckling instability (9).
- o Delamination extent and location are not directly related to local buckling instability because of internal ply and external geometric constraints (9).
- o Successful correlation of damage state to strength, stiffness and fatigue life requires relating of the interactional effects of matrix microcracking to delamination as well as accounting for ply and geometric constraints and probability distributions of fiber bundle buckling instability (9).
- o The delamination damage region does not behave like a self similar, crack-like defect acting instead like a macroscale inelastic field much like a yield zone (9.1).
- o Wear-out models which involve the implicit assumption that residual strength will decrease with fatigue cycling are not applicable to the data (9.2)
 - Residual strength remained unchanged or increased, at times significantly.
 - Coupons failed in fatigue (in some cases as many as 50%) while remaining coupons increased in residual strength.
 - These models do not account for the mechanics of the failure process which results in reduced notch acuity.

- o Empirical curve fits are of little value for any other laminate without a suitable transfer function (9.2).
- o Neither the concept of notch acuity and strain/life nor one of stress intensity for a crack like defect can be used as transfer function for composites which would permit the curve for one data set to be adjusted accurately for another set of conditions (9.2).

REFERENCES

1. Pettit, D.E., Lauraitis, K.N., and Cox, J.M. "Advanced Residual Strength Degradation Rate Modeling For Advanced Composites Structures, Volume I, Task I: Preliminary Screening", AFWAL-TR-79-3095, Vol. I, Air Force Wright Aeronautical Laboratories Wright-Patterson AFB, August, 1979.
2. Pipes, R. Byron and Pagano, N.J., "Interlaminar Stresses in Composite Laminates Under Uniform Axial Extension," J. Comp. Materials, Vol. 4, (1970), p. 538.
3. Wang, A.S.D., and Crossman, F.W., "Some New Results on Edge Effect in Symmetric Composite Laminates," J. Comp. Materials, Vol 11 (1977), p. 92.
4. Whitney, J.M., and Nuismer, R.J., "Stress Fracture Criteria for Laminated Composites Containing Stress Concentrations," J. Comp. Materials, Vol. 8, (1974), p. 253.
5. Daniel, I.M., Rowlands, R.E., and Whiteside, J.B., "Effects of material and Stacking Sequence on Behavior of Composite Plates with Holes," Experimental Mechanics, Vol. 14 (1974), p.1.
6. Test Report T15756, Delsen Testing Laboratories, Inc., Glendale, California, August 10, 1979.
7. Ryder, J.T., and Walker, E.K., "Ascertainment of the Effect of Compressive Loading on the Fatigue Lifetime of Graphite Epoxy Laminates for Structural Applications," AFML-TR-76-241, Air Force Materials Laboratory, Wright-Patterson AFB, Dec. 1976.
8. Pettit, D.E., "Characterization of Impact Damage in Composite Laminates," Nondestructive Evaluation and Flaw Criticality for Composite Materials, ASTM STP 696, R. B. Papis, Ed., American Society for Testing and Materials, 1979, pp. 101-124.
9. Ryder, J.T. and Walker, E.K., "The Effect of Compressive Loading on the Fatigue Lifetime of Graphite/Epoxy laminates", AFML-TR-79-4128, Air Force Materials Laboratory, Wright-Patterson AFB, October, 1979.

10. Lauraitis, K.N., and Sandorff, P.E., "The Effect of Environment on the Compressive Strengths of Laminated Epoxy Matrix Composites", AFML-TR-79-4179, Air Force Materials Laboratory, Wright-Patterson AFB, December, 1979.
11. Nuismer, R.J., and Whitney, J.M., "Uniaxial Failure of Composite Laminates Containing Stress Concentrations", Fracture Mechanics of Composites, ASTM STP 593, American Society for Testing and Materials, 1975, pp. 117 - 142.
12. Reifsnider, K.L., Stinchcomb, W.W., and O'Brien, T.K., "Frequency Effects on a Stiffness-Based Fatigue Failure Criterion in Flawed Composite Specimens", Fatigue of Filamentary Composite Materials, ASTM STP 636, K.L. Reifsnider and K.N. Lauraitis, Eds., American Society for Testing and Materials, 1977, pp. 171-184.
13. Ryder, J.T., and Wadin, J.R., "Acoustic Emission Monitoring of a Quasi-Isotropic Graphite/Epoxy Laminate Under Fatigue Loading", presented at the ASNT Spring Conference, April 2 - 5, 1979, San Diego, California, published in the Conference Proceedings.
14. Whitcomb, J.D., "Experimental and Analytical Study of Fatigue Damage in Notched Graphite/Epoxy Laminate", Fatigue of Fibrous Composite Materials, ASTM STP 723, American Society for Testing and Materials, 1981, pp. 48 - 63.
15. Ratwani, M.M., and Kan, H.P., "Compression Fatigue Analysis of Fiber Composites", NADC-78049-60, September 1979.
16. Ryder, J.T., "Nondestructive Monitoring of Damage in Composites: Mechanics Of The Damage Process", Lockheed-California Company Report LR 29773, 1981.
17. Kim, R.Y., "Experimental Assessment of Static and Fatigue Damage of Graphite/Epoxy Laminates", Advances in Composite Materials, Proceedings of the Third International Conference on Composite Materials, Paris, France, 26 - 29 August, 1980, pp. 1015 - 1028.
18. Reifsnider, Kenneth, "Fatigue Behavior of Composite Materials", International Journal of Fracture, Vol. 16, No. 6, December, 1980, pp. 563 - 583.
19. Hahn, H.T., and Kim, R.Y., "Proof Testing of Composite Materials", Journal Of Composite Materials, Volume 9, July 1975, pp. 297 - 311.
20. Chow, P.C. and Croman, R., "Degradation and Sudden-Death Models of Fatigue of Graphite/Epoxy Composites," Composite Materials: Testing

- and Design (Fifth Conference), ASTM STP 674, S.W. Tsai, Ed., American Society for Testing and Materials, 1979, pp. 431 - 454.
21. Yang, J.N. and Liu, M.D., "Residual Strength Degradation Model and Theory of Periodic Proof Tests for Graphite/Epoxy Laminates", Journal of Composite Materials, Volume 11, April 1977, pp. 176 - 203.
 22. Yang, J.N. and Jones, D.L., "Load Sequence Effects on Statistical Fatigue of Composite Materials", ASTM STP 723, Fatigue of Fibrous Composite Materials, American Society for Testing and Materials, 1981, pp. - 213 - 232.
 23. Hahn, H.T., "Fatigue Behavior and Life Prediction of Composite Laminates", Composite Materials: Testing and Design (Fifth Conference), ASTM STP 674, S.W. Tsai, Ed., American Society for Testing and Materials, 1979, pp. 383 - 417.
 24. Halpin, J.C., Waddoups, M.E., and Johnson, T.A., "Kinetic Fracture Models and Fracture Stability", International Journal of Fracture Mechanics, Volume 8, 1972, pp. 465 - 468.
 25. Ryder, J.T. and Lauraitis, K.N., "Effects of Load History on Fatigue Life", Air Force Materials Laboratory, Wright-Patterson Air Force Base, To be published in September, 1981.
 26. Wilkins, R.J., Presentation at ASTM D-30.04 and E9.03 Subcommittee Meetings in Phoenix, Arizona, May, 1981.
 27. Gumbell, E.J., Statistics of Extremes, Columbia University Press, New York, 1958.
 28. Burington, R.S. and May, D.C., Handbook of Probability and Statistics with Tables, 2nd Edition, McGraw-Hill, New York, New York, 1970.

FILME
9-8